

COMSAT

Technical Review

Volume 20 Number 2, Fall 1990

Advisory Board Joel R. Alper
Joseph V. Charyk
John V. Evans
John. S. Hannon
Willard R. Nichols

Editorial Board Richard A. Arndt, *Chairman*
S. Joseph Campanella
Dattakumar M. Chitre
William L. Cook
Calvin B. Cotner
Allen D. Dayton
Russell J. Fang
Ramesh K. Gupta
Michael A. Hulley
Ivor N. Knight
Alfred A. Norcott
Hans J. Weiss
Amir I. Zaghloul

Past Editors Pier L. Bargellini, 1971–1983
Geoffrey Hyde, 1984–1988

Editorial Staff MANAGING EDITOR
Margaret B. Jacocks
TECHNICAL EDITOR
Barbara J. Wassell
PRODUCTION
Barbara J. Wassell
Virginia M. Ingram
N. Kay Flesher
CIRCULATION
Merilee J. Worsey

COMSAT TECHNICAL REVIEW is published twice a year by the Communications Satellite Corporation (COMSAT). Subscriptions, which include the two issues published within a calendar year, are: one year, \$20 U.S.; two years, \$35; three years, \$50; single copies, \$12; article reprints, \$3. Overseas airmail delivery is available at an additional cost of \$18 per year. Make checks payable to COMSAT and address to Records Department, Communications Satellite Corporation, 22300 Comsat Drive, Clarksburg, MD 20871-9475, U.S.A.

ISSN 0095-9669

© COMMUNICATIONS SATELLITE CORPORATION 1990
COMSAT IS A TRADE MARK AND SERVICE MARK
OF THE COMMUNICATIONS SATELLITE CORPORATION

COMSAT TECHNICAL REVIEW

Volume 20 Number 2, Fall 1990

v FOREWORD
J. D. Hampton AND I. Goldstein

229 EDITORIAL NOTE
S. B. Bennett AND G. Hyde

INTELSAT VI: The Communications System

231 THE PROCESS FOR SUCCESS—INTELSAT VI
E. I. Podraczky AND W. R. Schnicke

247 INTELSAT VI SYSTEM PLANNING
L. B. Perillan, W. R. Schnicke AND E. A. Faine

271 INTELSAT VI COMMUNICATIONS PAYLOAD PERFORMANCE
SPECIFICATIONS
B. A. Pontano, A. I. Zaghloul AND C. E. Mahle

309 SPECIFYING THE SPACECRAFT BUS
G. P. Cantarella AND G. Porcelli

335 SS-TDMA SYSTEM CONSIDERATIONS
S. J. Campanella, G-P. Forcina, B. A. Pontano AND J. L. Dicks

373 INTELSAT VI TRANSMISSION DESIGN AND ASSOCIATED COMPUTER
SYSTEM MODELS FOR FDMA SERVICES
**M. P. Brown, Jr., R. W. Duesing, L. N. Nguyen, W. A. Sandrin
AND J. A. Tehrani**

Non-INTELSAT VI Papers

401 CTR NOTE: OFFSET-QPSK MODULATION FOR MARITIME SATELLITE
COMMUNICATIONS
L-N. Lee AND S. Rhodes

419 TRANSLATIONS OF ABSTRACTS
FRENCH 419 SPANISH 422

425 PAPERS SCHEDULED FOR PUBLICATION IN THE CTR INTELSAT VI
SERIES



John D. Hampton
Acting Director General
INTELSAT

Irving Goldstein
Chairman and Chief
Executive Officer,
COMSAT



Foreword

The dynamic telecommunications environment of the past few decades has provided INTELSAT and COMSAT with many challenges. Since the inception of services over "Early Bird" (INTELSAT I) in 1965, significant changes have occurred in spacecraft and earth station technology, as well as in the telecommunications environment. These include explosive growth in traffic (and its changing character), large-scale use of digital technologies, and the appearance of competing systems.

Each new generation of satellites has marked a step forward in meeting the needs of this changing environment. The INTELSAT VI spacecraft and system certainly represented a very large step forward in this progression. In the decade since the decision was made to procure INTELSAT VI, it has gone from concept to reality. Today, INTELSAT VI satellites are supporting major elements of the global communications requirements. INTELSAT VI is uniquely equipped to adapt to the needs of the INTELSAT community into the 21st century.

Realization of this satellite would not have been possible without the dedicated efforts of a team of people from INTELSAT, Hughes Aircraft, COMSAT, and other organizations. Their cooperation and their commitment to excellence have overcome long distances and disparate cultures to produce a satellite that will serve the diverse telecommunications needs of the global community for many years to come. The importance of this work to INTELSAT and COMSAT make it fitting that the details of this satellite's conception, design, implementation, testing, and initial use be preserved. It is, therefore, appropriate to dedicate this and upcoming issues of the *COMSAT Technical Review* to this purpose.

Editorial Note

S. B. BENNETT, Guest Editor, INTELSAT
G. HYDE, Associate Guest Editor, COMSAT

The INTELSAT VI dedicated issues of *COMSAT Technical Review* (CTR)* break new ground in a number of respects. Because of the importance and complexity of the INTELSAT VI satellite and its associated system operation, three volumes of CTR will be needed to fully document the process leading to its very successful implementation. These volumes will cover the subject from concept, through design and test, to in-orbit operation. Related fourth and fifth volumes will address system applications and the implementation of satellite-switched time-division multiple access (SS-TDMA). This compilation is a joint effort of COMSAT and INTELSAT, including co-editors from each organization.

This first volume focuses on the early stages of the evolution of the INTELSAT VI satellite system. The first paper deals with the process followed by INTELSAT in defining, procuring, and monitoring the manufacture, testing, and early operation of the satellite. The second paper details the system planning considerations underlying the specifications and discusses the evolution of the INTELSAT system and its impact on the use of the satellite. The next three papers describe in detail the derivation of the satellite specifications in three critical areas: the communications payload, the spacecraft bus, and the SS-TDMA system. The last paper discusses INTELSAT VI transmission design and modeling for frequency-division multiple access (FDMA) service. These papers are also intended to set the stage for papers in subsequent volumes.

The second volume will describe in detail the design of the INTELSAT VI spacecraft. The third volume will cover a wide range of topics, from measures taken to ensure a reliable satellite; the launch, deployment, and in-orbit testing phases; and the operation of the satellite in orbit. Presented in a related fourth volume on the INTELSAT system and applications will be papers on earth station considerations, and on digital, video, and other modulation and coding techniques used in the INTELSAT VI era. The fifth volume will be devoted to describing all aspects of the SS-TDMA system, which was first used for commercial purposes on INTELSAT VI.

The editors trust that this comprehensive treatment of the INTELSAT VI system will prove useful to future system planners. The papers in this and

* Refer to pages 425 through 429 of this issue for a listing of the INTELSAT VI-related papers scheduled for publication in this series. Note that papers on other research topics will continue to be provided as well.

subsequent volumes are the result of a major effort by a large group of authors from COMSAT, INTELSAT, and Hughes Aircraft Corporation, and we congratulate them on their substantial achievement.



Simon B. Bennett received a B.E.E. from City College of New York in 1959 and an M.E.E. from New York University in 1961. His career, which spans the entire history of communications satellites, began with work on the first TELSTAR satellite program at Bell Telephone Laboratories from 1959 to 1963. He continued in this field at COMSAT from 1961 to 1974, where he contributed to the success of satellite programs from Early Bird to INTELSAT IV. Since 1974 he has been at INTELSAT, where he has been manager of spacecraft programs, directed systems planning studies, and managed the operation of

INTELSAT's 15-satellite fleet (including the INTELSAT VI series). He is currently Assistant to the Senior Director of Engineering.

Geoffrey Hyde received a B.A.Sc. in engineering physics and an M.A.Sc. in electrical engineering from the University of Toronto in 1953 and 1959, respectively, and a Ph.D. in electrical engineering from the University of Pennsylvania, Philadelphia, in 1967. Prior to joining COMSAT Laboratories in July 1968, he worked on antennas, microwaves, and propagation at RCA, Moorestown, NJ, and at Avro Aircraft Company and Sinclair Radio Labs in Canada.

At COMSAT prior to 1974, Dr. Hyde was concerned with the development of the torus antenna, a general antenna analysis computer program (GAP), and related areas of endeavor. In February 1974 he became Manager of the Propagation Studies Department, where his work included a wide variety of efforts in propagation measurement and analysis. In 1980 he joined the staff of the Director, COMSAT Laboratories, and in 1984 became Assistant to the Director. His duties included coordination of the COMSAT R&D programs, coordination of ITU activities at COMSAT Laboratories, and editorship of the COMSAT Technical Review. In June 1989 he retired, and is currently a consultant to COMSAT Laboratories.

Dr. Hyde is a member of URSI Commissions B and F, and the AIAA, and is a Registered Professional Engineer in Ontario, Canada. His honors include David Sarnoff Fellowships (1965 and 1966), Fellow of the IEEE (1987), and the IEEE G-AP award for best paper, 1968 (jointly with Dr. Roy C. Spencer).



Index: communication satellites, INTELSAT, procurement management, project management

The process for success—INTELSAT VI

E. I. PODRACZKY AND W. R. SCHNICKE

(Manuscript received March 1, 1991)

Abstract

The various stages of the INTELSAT VI provisioning process are described, from the initial task of defining the mission requirement in terms of user traffic, to the final stages of the actual procurement. The timetable for the various aspects of the process is presented, along with a discussion of the major participants and process dynamics.

Introduction: INTELSAT system evolution

Since its inception in 1964, INTELSAT has provided the commercial geosynchronous satellite capacity to match the rapid growth in demand for international communications services. Increased capacity has been achieved through a combination of added locations in the orbital arc, reuse and exploitation of the existing and expanded frequency spectrum, and the application of technology to optimize bandwidth efficiency.

INTELSAT services over the years have grown in diversity, complexity, and volume [1],[2]. The services meet a variety of user needs, from simple trunk telephony to the integrated services digital network (ISDN); from trunk switching to thin-route business communications; and from point-to-point TV to broadcasting and direct distribution to a wide user community. For example, INTELSAT's first spacecraft, "Early Bird," was designed to carry either 240 channels of telephony or one TV channel and had a planned operational life measured in months. In contrast, the INTELSAT VI spacecraft is capable of carrying 120,000 channels of telephony (assuming the use of digital circuit multiplication) and four TV channels simultaneously. It can support trunk public-switched network services (including ISDN), business services to user premises,

and TV distribution to small receive-only terminals, and has the stationkeeping ability to operate for at least 13 years.

To meet the growing market demand, INTELSAT plans and implements periodic increases in space segment capacity, with concomitant additions of earth segment by INTELSAT Signatories and system users. The nominal capacity of the space segment increases in discrete steps each time the number of operating satellites is increased or an operating satellite is replaced by one of higher capacity. With the introduction of each new generation of satellites, INTELSAT system planners have a unique opportunity to lower costs, improve the quality of services, and meet new market demands.

The INTELSAT VI spacecraft owes much of its success to the well-developed and thorough planning and procurement process followed by INTELSAT in developing the architecture and spacecraft designs for its system evolution. The INTELSAT VI program provides an excellent case study of this process.

INTELSAT VI satellites were a turning point in the planning process. The first five generations of spacecraft, bought before 1982, presented a technical and operational challenge. Technical innovation and development had to be managed to meet the rapid growth of analog international telephony services, while minimizing operational changes that might increase earth station costs. Each new generation of INTELSAT spacecraft has provided greater capacity by reusing and expanding the frequency spectrum, while maintaining transmission power levels sufficient to link large earth stations in efficient bandwidth-limited operation. Each succeeding generation has introduced new technology, been larger in mass and power, provided significantly more capacity, and utilized larger launch vehicles. INTELSAT VI is no exception.

INTELSAT VI satellites have been planned to support the growth of conventional services without the need for additional orbital slots. The spacecraft also incorporate capabilities to meet new market demands. Additional bandwidth is provided in orbit by introducing new spectrum and by adding reuses of existing spectrum. Compared to their predecessors, the INTELSAT VI series spacecraft have longer lifetimes (a design life of 10 years, with stationkeeping for 13 years), are more reliable, allow the use of smaller and less expensive earth stations for new services, provide better coverage for domestic services, and provide for more efficient digital services. The risks involved include increased spacecraft complexity, more complicated transitions from previous generations, more expensive launchers, the introduction of extensive new technology, greater investment per satellite and, above all, more market uncertainty due to longer time horizons. Specifically, the basic INTELSAT VI procurement decision was taken in 1981, and the satellite will be operational at least until the year 2006.

The satellite planning cycle

The satellite planning cycle comprises the following elements:

- Agreement on a mission for the satellite system (*i.e.*, the traffic requirements).
- Establishment of the system concept, including the number of satellites in each ocean region, the modulation and processing techniques to be used, frequency bands to be used (and the reuse of each), and the technologies available for inclusion on the satellite.
- Convergence on the specific satellite design.
- Development of the procurement specification.
- Solicitation and evaluation of bids.
- Contractor selection and negotiation.
- Fabrication of the spacecraft, with INTELSAT oversight.
- Launch and operation of the spacecraft.
- Traffic management or operational planning.

The first three elements are discussed briefly below. An overview of the planning cycle is presented in the form of a timeline in Figure 1 and indicates how the cycle for one generation of spacecraft overlaps the timeline for its predecessors and successors. Note the coincidence of the start of operations on INTELSAT V and the release of the RFP for INTELSAT VI in March 1981.

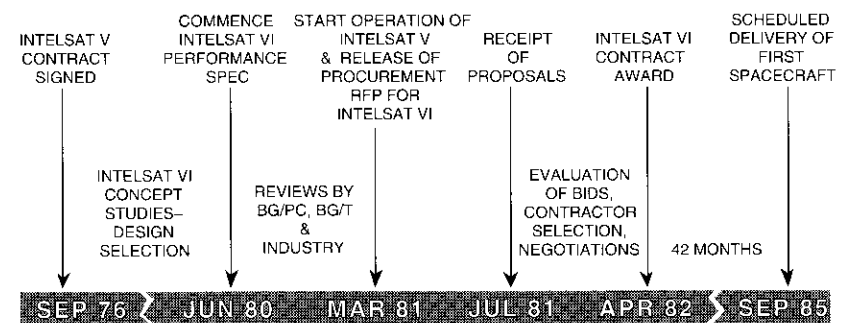


Figure 1. Timeline for INTELSAT VI Program

Spacecraft mission

The first step in the planning cycle is to define the mission to be served by the satellite. This requires specifying the planning horizon and estimating the nature and level of the service requirements to be met by the satellite. In the case of INTELSAT VI, the planning horizon was taken as the year 1999, which corresponds to the projected end of use of the spacecraft—13 years after its original planned launch date of 1986. The service requirements are derived from the INTELSAT Traffic Database, a compilation of worldwide traffic requirements to be met by INTELSAT, as provided and bilaterally agreed upon by the system users at an annual gathering of forecasters known as the Global Traffic Meeting. INTELSAT may be unique as a commercial service provider in that it relies primarily on the service projections of its users for planning. These projections are adjusted, usually downward, by the INTELSAT staff based on past experience to produce the “Director General’s Forecast.”

At this early stage in the planning process, the timeline for procurement and use of the satellites, as well as the traffic requirements, is subject to review by the INTELSAT Board of Governors’ Advisory Committee on Planning (BG/PC) which critically evaluates work prepared by INTELSAT staff and provides guidance to both the staff and the Board of Governors. The BG/PC is composed of representatives from all interested Signatories of INTELSAT, and typically convenes 15 to 25 planning specialists from around the world in a quarterly meeting.

System concept

Planners next postulate a series of alternative system concepts, each including an assumed number of satellites for each ocean region serving the needs of INTELSAT’s users; modulation and signal processing technologies such as compression and interpolation techniques, frequency bands to be used, and the number of frequency reuses of each; and the technologies available for inclusion in the spacecraft. The selection of these parameters is reviewed by both the BG/PC and the Board’s Advisory Committee on Technical Matters (BG/T). The latter is composed of technical experts from organizations designated by interested Signatories of INTELSAT.

Satellite alternatives

Alternative spacecraft concepts are formulated for use within each system concept. The spacecraft concepts must provide capacity matched to the requirements of each orbital slot, and this capacity typically will vary with the

system concept assumed. Spacecraft concepts, in particular, must be based on the technologies expected to be available for incorporation in the design at the time the spacecraft is to be procured and fabricated. Each spacecraft/system alternative is evaluated against a set of agreed-upon criteria, which may include cost, service quality, flexibility, compatibility with predecessor generations, impact on the worldwide ground segment, and technical/schedule risk, among other factors. In this way, a preferred spacecraft is selected for procurement (as discussed in greater detail in a companion paper by Perillan *et al.* [1]). The process then moves on to the preparation of the performance specification.

Development of the performance specification

Having selected a spacecraft design to meet mission requirements, INTELSAT commences preparation of the performance specifications, which form the basis for requirements in the procurement Request for Proposal (RFP). These specifications are discussed in detail by Cantarella and Porcelli [3] and Pontano *et al.* [4]. The specification details the performance required by INTELSAT to meet its projected communications needs; for example, isolation between spacecraft beams, or the linearity of traveling wave tube amplifiers (TWTAs). In order to allow industry to propose their best designs, which take advantage of the most attractive technologies, INTELSAT deliberately does not specify a design in detail. However, to capitalize on experience gained from previous satellite procurements, INTELSAT does specify some aspects of the design where previous experience has shown difficulty.

INTELSAT’s draft specification then undergoes a thorough review and revision in a series of critical steps. First, the INTELSAT Signatories, which have technical capabilities that bolster and complement the skills available in-house at INTELSAT, review the draft specifications in the BG/T. The Committee’s initial review typically results in a revised draft specification, which is then shared with the spacecraft industry to ensure that the performance criteria set forth are indeed reasonable and feasible at realistic cost and with known technology. Industry feedback, along with a second intensive review by the BG/T, is then cycled into a final specification to be released with the RFP.

The INTELSAT VI procurement process

After the INTELSAT VI performance specification for the RFP was reviewed and modified by the BG/T and BG/PC, the Director General submitted the full RFP to the Board of Governors for approval. After making some modifications to the Terms and Conditions, the Board approved the RFP for release to

potential bidders. The RFP was released on March 26, 1981, and required that bidders submit their proposals by close of business on July 24, 1981.

INTELSAT wanted to avoid "auctioning off" the INTELSAT VI contract, since it believed that doing so could lead to the construction of an unreliable spacecraft. The RFP required that the Price/Cost and Technical and Management proposals be presented separately, to Price Waterhouse and INTELSAT Headquarters, respectively, to allow their separate evaluation. On July 24, 1981, proposals were received from Ford Aerospace and Communications Corporation (FACC)* and Hughes Aircraft Corporation (HAC).

Communications between potential bidders and INTELSAT and Signatory personnel were restricted during the bidding and subsequent evaluation process. Clarification questions from potential bidders had to be submitted in writing, and the questions and answers were provided to all bidders.

Proposal evaluation

The technical evaluation was conducted at INTELSAT Headquarters. The staff participating in the evaluation were selected on the basis of their technical knowledge, and consisted of both Executive Organ and Technical Services Contractor (COMSAT) personnel. The evaluation team was organized into seven groups, each addressing subsystems in their area of expertise. The overall technical evaluation was based on a rating system which took into account both the significance of the subsystems and the maturity and feasibility of the solution proposed.

This evaluation led to several questions related to the design choices made by the bidders. Both the FACC and HAC designs had deficiencies, with the HAC design having a particularly high number of design risks as well. INTELSAT held discussions with both bidders, which led them to propose improvements to their original proposals.

In the final comparative evaluation, the FACC technical approach was rated superior to that of HAC. The most significant aspects leading to this rating were the superiority of the FACC communications payload and antenna design, the simpler in-orbit operation of their body-stabilized design (which was also judged to be less costly), the simpler and lower risk initial deployment sequence of the antennas and solar arrays, a better mass margin, and a greater ability to accommodate payload changes without a major redesign. The BG/T reviewed the Director General's evaluation and agreed with his preference for the FACC Technical and Management proposal, but with a less pronounced

preference than that expressed by the Director General. The BG/T also recommended that some of the TWTAs in the FACC design be replaced by solid-state power amplifiers, as provided for in an option by FACC. The final evaluation also concluded that both designs were feasible, even though higher schedule and performance risks were associated with the HAC design.

Terms and conditions

Both proposals were generally compliant with the Terms and Conditions contained in the RFP model contract (which provides the bidder with the terms and conditions desired by INTELSAT). HAC had taken fewer and less substantive exceptions to this model contract than had FACC. After discussions were held with the bidders, FACC removed many exceptions; however, the preference for HAC's proposed terms and conditions remained.

The final evaluation concluded that the proposals of both companies could serve as an adequate base for finalization of an INTELSAT VI contract.

Financial comparison

After the technical and contractual evaluations of the proposals were completed, the Director General began the financial evaluation. In order to fairly compare proposals which had different rates of progress and in-orbit incentive payments, the payment figures were converted into present values using a discount rate of 14 percent (the INTELSAT rate of return). The analysis was performed for two basic scenarios: the purchase of five spacecraft, and the purchase of an initial five spacecraft and a later buy of seven more. Comparison of the two proposals showed a consistent price advantage for the HAC design.

In his final financial evaluation, the Director General further adjusted these prices to reflect the operational and technical differences of the two designs, as determined by the technical evaluation. Adjustments were made to account for the higher operational cost and costlier modifications for growth of the HAC design, and for the additional cost associated with the FACC solid-state amplifier option. Even with these adjustments, the cost advantage of the HAC proposal prevailed.

Other features of the HAC financial proposal were also deemed superior. These related to the level of periodic in-orbit incentive payments over time, with the payment being made by the contractor in case of failure in the initial 180 days in orbit, and better late delivery penalties.

Overall, the HAC financial proposal was deemed significantly better than the one submitted by FACC.

* Now Space Systems/Loral (SS/L).

Overall evaluation

INTELSAT was in the difficult situation of having received only two proposals—one superior technically and the other financially. In the RFP cover letter, INTELSAT had stated that it would not accept price changes that were unrelated to technical modifications. Considering that both proposals were basically technically acceptable, the financial advantage carried considerable weight. Accordingly, the Director General recommended to the Board of Governors that he be authorized to begin negotiations with HAC for an initial buy of five spacecraft. The negotiations would cover the elimination of unwarranted contingencies and duplication of effort, appropriate terms for a 10-year spacecraft design life,* the amounts to be paid as in-orbit incentives, and an improved partial-progress payment plan. Should these negotiations fail to achieve the desired results, the Director General would initiate negotiations with FACC.

The Board of Governors, at their 49th Meeting, concurred with the Director General's recommendations. Negotiations with HAC were successful and included improvements in a number of areas which were intended to reduce risk and improve the usefulness of the satellite. The Director General submitted the negotiated contract for Board approval at its 50th Meeting. With Board concurrence, the contract was signed on April 7, 1982.

Contract monitoring

The INTELSAT experience, particularly the reliability and longevity achieved in orbit, indicates the value of careful monitoring of the design and production of a sophisticated satellite. A spacecraft contractor working to a fixed-price contract, even with in-orbit incentives, is under constant pressure to minimize his current cost. This often can lead to differences in judgment with regard to the adequacy of the design or test program. In addition, the detailed interpretation of performance specifications for hardware design could lead to misunderstandings. Thus, INTELSAT has over the years developed a method of close monitoring which is accomplished by a group of specialists addressing all the major disciplines involved in the design, construction, and testing of the spacecraft. Some of these specialists are located near the contractor facility for the duration of the contract; others only participate at design reviews or special meetings called to review problems or anomalies in testing.

* The period of time for which in-orbit incentives are paid; also an input to various reliability analyses and design criteria.

In addition, the resident staff is charged with assessing contractor performance against progress payment milestones.

Concurrent with the procurement process, INTELSAT began addressing the aspects of program management. The structure proposed took into account prior experience on other programs and the availability of experienced personnel. Experience on earlier programs indicated an expenditure level for the monitoring approaching 10 percent of the value of the contract. Considering the maturity of the industry and the strong in-orbit incentives embedded in the contract, a lower level of monitoring expenditure was deemed appropriate for INTELSAT VI (on the order of 7 percent of the value of the contract).

The structure developed involved establishing an INTELSAT Spacecraft Program Office (ISPO) near the contractor location. Due to extensive subcontracting by HAC, another office was established in Europe near a major subcontractor. INTELSAT also contracted for extensive support with the Technical Assistance Contractor (TAC), COMSAT Corporation. Additional contracts were signed with quality control inspectors, and specialists were brought in as required when problems arose in disciplines not covered by the existing staff.

The monitoring program made a significant contribution to the success of the INTELSAT VI program, as discussed in a companion paper by Johnson *et al.* [5]. Even in the early stages of the program, problems were discovered which had not been identified during the evaluation process. Two of these discoveries led to contract amendments. Also, the staff involved in the monitoring were able to perform a beneficial independent audit of contractor designs. Participation by INTELSAT satellite system operations staff in the acceptance testing of the spacecraft provided the familiarity and experience needed for subsequent in-orbit operation.

Launch, testing, operation, and in-orbit monitoring

The ability to gainfully use the satellite is critically dependent upon the success of the launch, in-orbit testing, and the subsequent phases of operation and performance monitoring.

Launch

INTELSAT adopted a strategy of contracting with two launch service contractors to ensure the availability of launches if one of the programs was grounded. Accordingly, the INTELSAT VI contract required that the spacecraft be compatible for launch on both the Space Shuttle Transportation System (STS) and the Ariane 4 expendable launch vehicle. The Launch Vehicle

Program Office (LVPO) was made responsible for ensuring that this compatibility was achieved. All interface documents and specifications were reviewed by this office, which also ensured that proper launch dynamics analysis and tests were performed to the satisfaction of the suppliers of both the launch vehicle and the spacecraft. Further details of the work performed by this office are given in the companion paper by Cantarella and Porcelli [3].

After the unfortunate STS failure in 1986, it became apparent that NASA would not be able to perform INTELSAT VI launches in a timely way. In accordance with its dual-sourcing philosophy, INTELSAT then contracted with Martin Marietta Corporation for TITAN III launch services. The LVPO was involved in evaluating and negotiating the spacecraft and launch vehicle contracts. It participated at the design review meetings and at the interface testing of the spacecraft and launch vehicles. The LVPO also planned the launch campaigns in Kourou, French Guiana, and Cape Canaveral, Florida.

The first launch took place on October 27, 1989, in Kourou on an Ariane 4 launch vehicle [6]. The success of that launch attests not only to the performance of the Ariane, but also to the professionalism and dedication of the LVPO staff. The launch vehicle placed the spacecraft in a transfer orbit with its apogee at geostationary altitude. The spacecraft was also given a low spin rate to ensure dynamic stability.

After the injection into transfer orbit, the INTELSAT Satellite Control Center (SCC) took over control of the satellite. This center was staffed by a combination of experts, including the regular in-orbit operation staff, personnel associated with monitoring spacecraft construction, and specialists from HAC. The task of this team was to circularize the orbit by successive firings of the liquid apogee motor, adjust the spacecraft to the required spin rate, and eventually perform all of the deployment functions. This process required several days of careful tracking, monitoring, and commanding the spacecraft at odd hours of the day. The team performed extremely well and the spacecraft was placed at a temporary orbital location, suitable for testing, on November 1, 1989. Further details are provided in Virdee *et al.* [6] and Smith [7].

Testing

The in-orbit testing of the satellite [8] was a very critical function which not only served to validate that the contractor had met the performance specifications, but also provided a database for subsequent operation of the spacecraft. The testing again involved special teams. Satellite functional and dynamic testing was performed at the SCC partly during the deployment phases of the launch. The team consisted of the same personnel used during the deployment phase.

Communications performance testing took place at a specially equipped earth station—the In-Orbit Testing (IOT) station. A special team involving the Satellite Operations Department, the Communications Engineering Department, the TAC, and the Satellite Engineering Department spent several weeks carefully measuring satellite performance. The testing indicated that the satellite was in good working order and met all of the essential specifications [8].

Operation and in-orbit monitoring

With the deployment and testing successfully completed, the satellite was allowed to drift to its final operating position over the Atlantic Ocean. The Operations Division began the transfer of traffic in accordance with a carefully developed plan. The Satellite Operations Department undertook the routine monitoring and commanding of the satellite, which are highly computerized functions. A complex set of software was developed during the spacecraft construction phase which permitted effective operation of the satellite with a minimum of personnel [5]. Spacecraft telemetry was received by tracking, telemetry, command, and monitoring (TTC&M) earth stations and forwarded to the SCC in Washington, D.C. Further details on the INTELSAT VI TTC&M system implemented for later launches are given in Skroban and Belanger [9].

Computers at the TTC&M sites and at the SCC alert operating personnel to any anomalies in satellite operation. Special procedures were written to overcome many of the possible anomalies. For unexpected events, a special on-call group of personnel was assigned which consisted of specialist engineers covering all the disciplines involved in satellite operations. Since anomalies can occur at any time of the day, members of the group have special telephone lines and computers in their homes to access the SCC database for diagnostic purposes. Decisions on correcting an anomaly require commands which are transmitted to, and executed by, the SCC personnel on duty. For more routine operations such as orbital corrections, eclipse-related actions, and the switching of transponders or communications paths, computer-generated commands are transmitted by the SCC staff at the required times.

The database obtained from the satellite telemetry and from routine communications parameter measurements by the IOT station is also used for trend analysis. The Satellite Operations Department maintains detailed tracking of critical performance parameters. The most important of these is the amount of propellant remaining for orbital control. Ground calibration reference for the thrusters, tank pressures, temperature of the propellants, and impulses provided to the satellite can be used to calculate the amount of fuel and oxidizer expended. This approach, supplemented by less-accurate gauges in the tanks, is the primary method of estimating the satellite's propulsion lifetime.

Other parameters tracked involve monitoring of the batteries, the solar array output power, and many communications parameters.

This operational setup has been successful in achieving an extremely high continuity of service. Significantly more than 99.9-percent path availability (earth station to satellite to earth station) has been demonstrated over many years of operation.

Traffic management

The final phase of the planning cycle involves actual use of the satellite to accommodate system needs. During this phase, which lasts 13 to 15 years (or even longer if inclined-orbit operation is used), the planning responsibility conveys to the system traffic planners and managers [10]. A typical satellite will serve in an initial in-orbit role for the early part of its lifetime, and will later be relocated to a less demanding role, perhaps in a different ocean region, as traffic requirements grow and replacement spacecraft become available.

Adaptability to a changing environment

An important feature of the INTELSAT VI design is its ability to adapt to changes in the composition and geographic distribution of traffic requirements, as well as to revised plans for deployment and use of the satellite. First and foremost, the INTELSAT VI beam coverage areas [11] include two broad hemispheric C-band beams in the east and west, in addition to dual-polarized global coverage beams. Approximately 400 MHz of bandwidth is available in each hemispheric beam, and up to 298 MHz in the global beams. Such broad area coverage beams provide a high degree of flexibility in assigning traffic from a variety of geographic sources.

Another element of flexibility is reflected in the satellite's use of a switchable beam-forming network for the C-band zone beams. Selected by ground command, an RF distribution network excites those feed horns needed to obtain each of three separate sets of coverage patterns tailored to the geographic distribution of traffic demand in the three ocean regions, as shown in Figure 2.

A third element of flexibility lies in the steerability of the K-band spot beams [11]. These two cross-polarized beams are independently steerable over the earth's northern hemisphere. In fact, in initial deployment, the Atlantic spare satellite at 332.5°E has both east and west spot beams pointed over Europe to meet the demand for domestic distribution of TV service in the U.K.

Finally, INTELSAT VI incorporates an 8 x 8 dynamic switch matrix for operation of satellite-switched time-division multiple access (SS-TDMA) in channels (1-2) and (3-4) [12]. The dynamic switch allows easy in-orbit re-

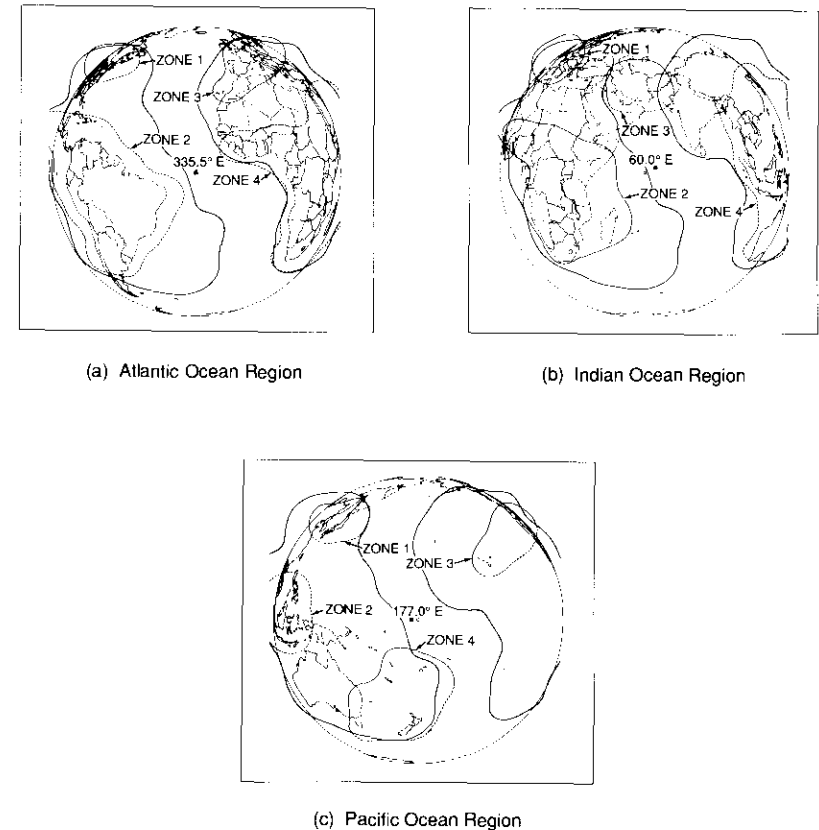


Figure 2. Three-Ocean C-Band Coverage Patterns for INTELSAT VI

assignment of the time slots allocated to each possible beam-to-beam connectivity. As the actual traffic demand between two beam coverage areas changes, the length of the TDMA burst and the length of time the switch is set in the appropriate connectivity are adjusted via ground command. This results in an excellent capability to reconfigure SS-TDMA capacity in orbit [13],[14].

The flexibility to launch on more than one launch vehicle provides a hedge against delays in the availability of one launch system, and has already proved to be an important feature, as mentioned earlier.

The perigee kick motor (PKM) for INTELSAT VI was conceived to provide growth margin in the event that additional capabilities requiring greater launch mass were later incorporated into the design. The PKM provided for a payload

growth of approximately 10 percent. This capability was later used when the coverage areas of the K-band spot beams, as well as the K-band effective isotropically radiated power (e.i.r.p.) levels, were increased after initial contract to cater to evolving market trends.

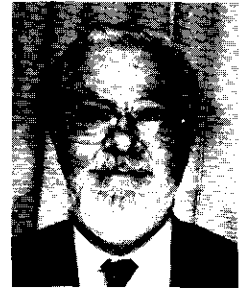
Conclusions

The INTELSAT VI design, procurement, and deployment process was quite successful, owing much to the thorough nature of the INTELSAT mechanism for system planning, as well as to the teams involved. Each stage of the process enjoys a well-developed and time-tested sequence of activities, which have been described in detail.

References

- [1] L. B. Perillan, W. R. Schnicke, and E. A. Faine, "INTELSAT VI System Planning," *COMSAT Technical Review*, Vol. 20, No. 2, Fall 1990, pp. 247-269 (this issue).
- [2] J. V. Evans, "Twenty Years of International Satellite Communication," *Radio Science*, Vol. 21, No. 4, July-August 1986, pp. 647-664.
- [3] G. P. Cantarella and G. Porcelli, "Specifying the Spacecraft Bus," *COMSAT Technical Review*, Vol. 20, No. 2, Fall 1990, pp. 309-333 (this issue).
- [4] B. A. Pontano, A. I. Zaghloul, and C. E. Mahle, "INTELSAT VI Communications Payload Performance Specifications," *COMSAT Technical Review*, Vol. 20, No. 2, Fall 1990, pp. 271-308 (this issue).
- [5] C. Johnson *et al.*, "Ensuring a Reliable Satellite," scheduled for publication in *COMSAT Technical Review*, Vol. 21, No. 2, Fall 1991.
- [6] L. Virdee *et al.*, "INTELSAT VI Launch Operations, Deployment, and Bus In-Orbit Testing," scheduled for publication in *COMSAT Technical Review*, Vol. 21, No. 2, Fall 1991.
- [7] G. Smith, "INTELSAT Satellite Operations," scheduled for publication in *COMSAT Technical Review*, Vol. 21, No. 2, Fall 1991.
- [8] G. Rosell *et al.*, "In-Orbit RF Test of an INTELSAT VI Spacecraft," scheduled for publication in *COMSAT Technical Review*, Vol. 21, No. 2, Fall 1991.
- [9] R. J. Skroban and D. J. Belanger, "TT&C Earth Station Operations," scheduled for publication in *COMSAT Technical Review*, Vol. 21, No. 2, Fall 1991.
- [10] M. Wheeler, "INTELSAT Communications Operations," scheduled for publication in *COMSAT Technical Review*, Vol. 21, No. 2, Fall 1991.
- [11] R. R. Persinger *et al.*, "The INTELSAT VI Antenna System," scheduled for publication in *COMSAT Technical Review*, Vol. 21, No. 1, Spring 1991.
- [12] R. K. Gupta *et al.*, "SS-TDMA On-Board Subsystem Design," scheduled for publication in *COMSAT Technical Review*, Vol. 21, No. 1, Spring 1991.
- [13] S. J. Campanella *et al.*, "SS-TDMA System Considerations," *COMSAT Technical Review*, Vol. 20, No. 2, Fall 1990, pp. 335-371 (this issue).
- [14] J. A. Lunsford *et al.*, "SS-TDMA System Design," scheduled for publication in *COMSAT Technical Review*, Vol. 22, No. 1, Spring 1992.

Emeric I. Podraczky received a Masters degree in electrical engineering from the Polytechnic University of Budapest in 1955, where he also completed many of the postgraduate courses toward a Ph.D. He has been involved in the field of communications satellites since 1959. At RCA Victor Company, Ltd., he was responsible for design of the communications repeater on the NASA "Relay" satellite launched in 1962. He joined COMSAT in 1963, where he played a leading role in the definition and design of the INTELSAT I, II, and III satellites and their transmission systems. As Director of the System Laboratory, he had a profound influence on the evolution of the INTELSAT system.



In 1974, Mr. Podraczky joined the newly formed INTELSAT organization as Director of Engineering. As the key technical person at INTELSAT, he was responsible for the INTELSAT V and VI satellite programs, earth stations and transmissions standards, and the TT&C and TDMA programs. His responsibilities also included specifications for RFPs, proposal evaluation, contract negotiation, launch and in-orbit deployment of the satellites, and their operation in orbit. He also was involved in formulating INTELSAT policies, negotiating bilateral agreements with Signatories and non-Signatories, and relationships with other international organizations.

In 1985, Mr. Podraczky founded Space Systems Engineering Corporation, Bethesda, MD, which is engaged in space systems studies, including advising on system design and implementation, policy issues, and international relationships.

William R. Schnicke holds an M.B.A. in finance and accounting from the University of Maryland, an M.S. in electrical engineering from the University of Pennsylvania, and a B.S. in electrical engineering from the Massachusetts Institute of Technology. As Senior Director, Systems Engineering and Planning for COMSAT's INTELSAT Satellite Services (now COMSAT World Systems), he was responsible for directing COMSAT's participation in advisory committees related to technical and planning matters for the INTELSAT global communications satellite system. He collaborated in developing the concept and design of INTELSAT's fifth, sixth, and seventh generations of spacecraft, and was instrumental in developing additional high-power, Ku-band satellite capacity for television service between North and South America and Europe. Mr. Schnicke is currently a Senior Scientist at Hughes Aircraft Corporation in Los Angeles, California.



Index: communication satellites, earth stations, INTELSAT, networks, planning, time division multiple access

INTELSAT VI system planning

L. B. PERILLAN, W. R. SCHNICKE, AND E. A. FAINE

(Manuscript received April 25, 1991)

Abstract

The planning of the INTELSAT VI spacecraft, the world's largest operational communications satellite, is described in detail. Various INTELSAT system considerations influenced the spacecraft design, as did the marketplace, which defines users' needs, including new services. The external environment, with its nascent separate satellite systems and emerging fiber optic undersea cables, also influenced INTELSAT service offerings and INTELSAT VI spacecraft design criteria. The decision-making process that led to the technology incorporated in the INTELSAT VI design is explained, including the alternative satellite concepts and technologies considered.

Introduction

The INTELSAT system evolved from 1965 to 1980 through five generations of spacecraft, each providing enhanced technology, capability, lifetime, and service offerings, as summarized in Table I. Three features—spectrum utilization or bandwidth, lifetime, and spacecraft mass—best illustrate the dramatic evolution of the system from INTELSAT 1 ("Early Bird") to INTELSAT V. As shown in the table, bandwidth increased 50-fold (from 50 to 2,480 MHz), lifetime increased fivefold (from 1.5 to 7 years), and spacecraft mass increased 30-fold (from 68 to 2,140 kg). The large increase in spectrum utilization was due to the introduction of twofold frequency reuse at C-band (6/4 GHz) on INTELSAT IV-A, followed by fourfold frequency reuse at C-band and twofold reuse at Ku-band (14/11 GHz) on INTELSAT V.

TABLE 1. EVOLUTION OF

| CHARACTERISTIC | INTELSAT I "EARLY BIRD" 1964-1965 | INTELSAT II 1966-1967 | INTELSAT III 1968-1970 |
|----------------------------------|---|---|--|
| Service/Development | <ul style="list-style-type: none"> INTELSAT created; starts commercial operations First live trans-oceanic TV | <ul style="list-style-type: none"> Multipoint communications Two-ocean network: Atlantic, Pacific | <ul style="list-style-type: none"> Global network Multiservices (TV, telephony, telex, data) |
| Spectrum Utilization | | | |
| C-Band | 50 | 130 | 300 |
| Ku-Band | - | - | - |
| Bandwidth (MHz) | 50 | 130 | 300 |
| Coverage/e.i.r.p. (dBW) | Omni squinted north/11.5 | Omni/15.5 | Global/23.0 |
| Communications Key Technology | Spin-stable Geosynch orbit | Static switch | Despun antennas |
| Launch Vehicle | Thor-Delta | Thor-Delta | Thor-Delta |
| Orbital Design Life (yr) | 1.5 | 3 | 5 |
| Communications Payload Mass (kg) | 13 | 36 | 56 |
| S/C Transfer Orbit Mass (kg) | 68 | 126 | 293 |

INTELSAT SPACECRAFT

| INTELSAT IV 1971-1975 | INTELSAT IV-A 1975-1985 | INTELSAT V 1980-1995 | INTELSAT V-A 1985-2000 | INTELSAT VI 1990-2010 |
|--|--|---|--|---|
| <ul style="list-style-type: none"> Spot network Lower costs Domestic services | <ul style="list-style-type: none"> Rapid telephony growth | <ul style="list-style-type: none"> IBS Full-time TV | <ul style="list-style-type: none"> INTELFNET Digital communications Competition | <ul style="list-style-type: none"> New services Full digital Competition |
| 480 | 720 | 1,480 | 1,680 | 2,560 |
| - | - | 800 | 800 | 960 |
| 480 | 720 | 2,280 | 2,480 | 3,520 |
| Global/25.5 Spot/33.7 | Global/22.0 Hemi/29 Zone/29 | Global/23 Hemi/29 Zone/29 K-Spot/41 | Global/23 Hemi/29 Zone/29 C-Spot/33 K-Spot/41 | Global/23 Hemi/31 Zone/31 K-Spot/44.7 |
| Steerable antennas | Twofold frequency reuse (C-band) | Fourfold frequency reuse (C-band); twofold reuse (Ku-band) | Expanded Ku-band Steerable C-Spots | Antenna farm SS-TDMA SSPAs Sixfold frequency reuse (C-band) |
| Atlas Centaur | Atlas Centaur | Atlas Centaur Ariane | Atlas Centaur Ariane | Ariane 4 STS Titan |
| 7 | 7 | 7 | 7 | 10 |
| 185 | 190 | 235 | 260 | 687 |
| 1,385 | 1,469 | 1,946 | 2,140 | 4,226 |

This paper describes the planning of the INTELSAT VI spacecraft, commencing with a brief description of the telecommunications environment in 1980 and proceeding step-by-step through the various phases of the planning process. The planning exercise was challenged by the long time frame from concept formulation to the projected end of service in orbit, a period spanning more than 25 years, and by the dynamic and rapidly growing international telecommunications market and the changing institutional environment. The rationale leading to the ultimate selection of the INTELSAT VI design is described, and a retrospective of the INTELSAT VI design decision is provided in light of actual developments during the 1980s. The overall process is described in a companion paper by Podraczky and Schnicke [1].

The INTELSAT planning environment in 1980

In 1980, the INTELSAT planning environment was characterized by a changing international telecommunications structure, portended by U.S. domestic developments such as the emergence of MCI as a public-switched telephone network (PSTN) service competitor to AT&T. Also, the increased likelihood of the availability of fiber optic undersea cable systems and separate (from INTELSAT) satellite systems promised to provide additional capacity in large quantities at highly competitive rates. At that time, commercial satellite technology was dominated by U.S. vendors.

The introduction into orbit of the first of the INTELSAT V/V-A series of spacecraft had marked the first use of dual polarization at C-band to achieve fourfold frequency reuse; the first use of Ku-band by INTELSAT; and the introduction of Ku-band spot beams to accommodate high-density traffic streams (e.g., North America to Europe). This was combined with steady projected growth of traffic requirements to be met by INTELSAT. At the same time, commercial satellite technology had matured to the point where new organizations could enter the marketplace with separate (from INTELSAT) satellite systems if they possessed the necessary capital and an orbital slot. The INTELSAT organization, meanwhile, had grown into a fully self-managing entity following implementation of definitive agreements from 1976 through 1979.

The planning challenge

Figure 1 depicts the INTELSAT VI planning challenge, including the various planning elements that were taken into account in designing the INTELSAT VI spacecraft. To meet projected user requirements driven by different markets, each subject to varying degrees of competition, INTELSAT planners had

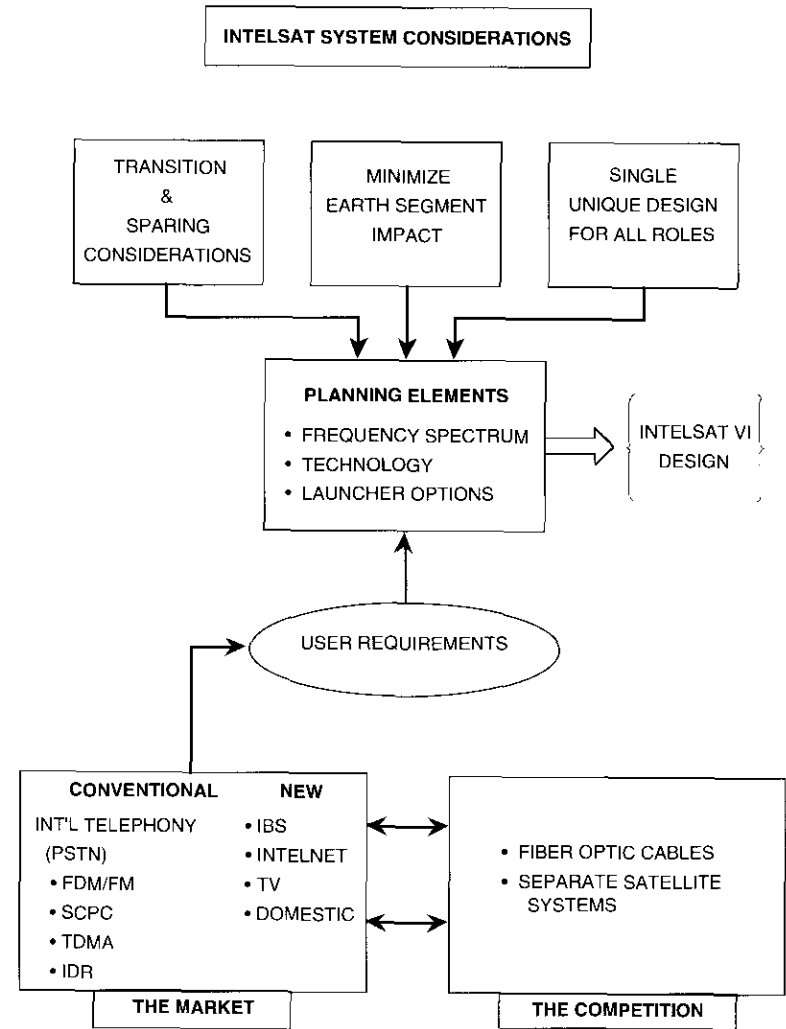


Figure 1. The INTELSAT Planning Challenge

variables such as spacecraft technology, frequency spectrum, and launcher options available to meet conditions forged by the evolution of the INTELSAT system.

User requirements

The first step in designing a new INTELSAT spacecraft is to define the mission to be served, based on the system users' traffic requirements over the planning horizon. In the case of INTELSAT VI, the planning horizon was taken as 1996 to 1999, which corresponds to the projected end of life of the spacecraft—10 to 13 years after its original planned launch dates in 1985 and 1986.

INTELSAT annually convenes a meeting of traffic forecasting experts from each user country in a forum known as the Global Traffic Meeting (GTM). The output of the GTM is a 15-year forecast of bilateral user traffic requirements for all services offered on the INTELSAT system. INTELSAT services are partitioned into three ocean regions (Atlantic, Indian, and Pacific), and a demand forecast by type of service is generated for each. A summary of demand forecasts by service category and ocean region, which resulted from the GTM process in 1979, is provided in Table 2. As can be seen from the table, INTELSAT planners were faced with a potential 14-fold increase in traffic requirements over the planning period.

At the time that INTELSAT VI was being planned, the dominant user requirement was voice traffic carried on the PSTN. This requirement was accommodated on the INTELSAT system by using analog frequency-division multiplexing (FDM)/FM transmission. Thin-route traffic needs were typically met with single-channel-per-carrier (SCPC) digital transmissions, which formed the second major component of the GTM forecasts in 1979. INTELSAT also carried international television (mostly occasional-use service ordered on a

minute-by-minute or hour-by-hour basis) and domestic services utilizing leased transponders.

Although INTELSAT transmissions were predominantly analog when INTELSAT VI was being planned, major plans existed in 1980 to introduce digital services using the time-division multiple access (TDMA) technique [2],[3]—which promised higher capacity per unit of satellite bandwidth—in conjunction with the more conventional quadrature phase shift keying/frequency-division multiple access (QPSK/FDMA) modulation/access method, which was soon to become known as intermediate data rate (IDR) service. This trend toward digital transmission was a major factor in the INTELSAT VI satellite design.

Evolving user requirements and projected increased competition demanded an ever-expanding set of new service offerings from INTELSAT. International Business Service (IBS) and INTELNET were developed to provide integrated digital services, with no distinction made among specific applications. The services were to be offered using both Ku- and C-band frequencies, and were characterized by digital transmission, small earth stations, and low cost. These needs led to an INTELSAT VI satellite design which provided higher power than the preceding INTELSAT V/V-A series.

INTELSAT competitive environment

The 1980s saw the emergence of serious competitors for INTELSAT, and this competition will certainly continue throughout the INTELSAT VI era. Undersea fiber optic cables have emerged as a major force in the North Atlantic and North Pacific, while separate satellite systems, including domestic, regional, and private systems, have also been established.

UNDERSEA TRANSOCEANIC CABLES

In 1980, plans for the last major analog transatlantic undersea cable, TAT-7, were being finalized. TAT-7 was to provide approximately 4,200 bearer circuits between the U.S. and Europe, with a mid-1983 service date. Shortly thereafter, serious planning for the first digital fiber optic undersea cable began in earnest, leading to an agreement to build TAT-8, which would provide some 7,000 to 8,000 64-kbit/s bearer circuits between the U.S. and Europe. An undersea branch point was integral to the design, providing direct links to both the U.K. and France from the same undersea system. TAT-8 was planned for service in late 1988 and actually entered service in 1989. With circuit multiplication, TAT-8 capacity could grow to some 40,000 voice circuits—amounting to several times the in-service cable capacity between the U.S. and Europe in

TABLE 2. SUMMARY OF INTELSAT DEMAND FORECAST: HALF-CIRCUITS (SOURCE: INTELSAT 1979 GLOBAL TRAFFIC MEETING)

| OCEAN REGION | END 1979 | | END 1993 | | END 1996 | |
|--------------|----------|-------|----------|--------|----------|--------|
| | FDM/FM | SCPC | FDM/FM | SCPC | FDM/FM | SCPC |
| Atlantic | 22,318 | 946 | 179,740 | 4,890 | 276,478 | 5,281 |
| Indian | 8,766 | 583 | 51,440 | 3,818 | 87,658 | 4,810 |
| Pacific | 3,648 | 258 | 22,424 | 1,540 | 37,371 | 2,056 |
| Total | 34,732 | 1,787 | 253,604 | 10,248 | 401,507 | 12,147 |

1980. Clearly, satellites' share of traffic on the dense North Atlantic routes was destined to decline from its 1980 levels of over 60 percent, a factor which was taken into account in sizing the INTELSAT VI spacecraft.

COMPETITIVE SEPARATE SATELLITE SYSTEMS

In 1980, satellite technology had matured to the point where the use of separate (from INTELSAT) satellite systems for regional and domestic services was becoming quite common. In the early 1980s, the following regional and domestic systems outside the U.S. and Canada were either in service or planned:

- EUTELSAT, to serve intra-European telecommunications needs
- PALAPA, to serve the domestic needs of Indonesia and the regional needs of the ASEAN nations
- INSAT, to serve the domestic needs of India
- MORELOS, to serve the domestic needs of Mexico
- BRAZILSAT, to serve the domestic needs of Brazil.

In addition, a variety of systems, such as the Condor system for the Andean nations in South America and Arabsat for the Middle East, were in earlier stages of planning. Clearly, INTELSAT was facing a changing environment wherein at least a portion of its services would be subject to some form of competition from other satellite systems during the in-orbit time frame of INTELSAT VI.

INTELSAT system considerations

The changing INTELSAT environment has given rise to changing considerations in planning INTELSAT satellite systems. The impact of these considerations is discussed below.

GROWTH NEEDS OF THE INTELSAT SYSTEM

During INTELSAT's first few years, commencing in 1964, satellites were added in quick succession to provide service first over the Atlantic, then over the Pacific, and finally over the Indian Ocean in 1971. While three ideally spaced geosynchronous satellites are sufficient to provide international global coverage, additional satellites were introduced to interconnect communications points over the widely dispersed, irregularly spaced and shaped geographical land masses of the world in order to meet traffic growth requirements of some

25 percent per year and to diversify large traffic streams. Moreover, traffic growth and the need for mid-ocean high-connectivity satellites serving the widest possible community of users led to the need for larger, more sophisticated and higher-capacity satellites.

The mid-ocean connectivity satellite in the Atlantic Ocean Region, known as the "Primary" satellite, served as the point of entry for new system users desiring the widest range of connectivity from one ground antenna, and carried more traffic than any other satellite in the system. Thus, the Atlantic Primary satellite was the pacing satellite in terms of sizing and timing of the new generation of INTELSAT VI spacecraft.

TRANSITION AND SPARING CONSIDERATIONS

As would be expected, the INTELSAT VI design was influenced by the design and capabilities of its predecessor INTELSAT V/V-A satellites and their operational configurations. The desire to easily transition traffic from INTELSAT V/V-A to INTELSAT VI with minimal disruption of services and reconfiguration of traffic carriers significantly influenced the design of INTELSAT VI. Moreover, two generations of satellites are typically served by a common in-orbit spare, preferably the more recent satellite generation having the greater capacity. In the rare event of an in-orbit failure, the ability to point-over from an INTELSAT V/V-A to an INTELSAT VI spare satellite without a major service disruption or traffic carrier reconfiguration is highly desirable. These considerations led to an INTELSAT VI design that could emulate the INTELSAT V/V-A capabilities as closely as possible.

MINIMIZING EARTH SEGMENT INVESTMENT

As with all predecessor satellites, the design objectives for INTELSAT VI were to maximize operational capacity while minimizing the impact on the earth segment. Although ever-increasing traffic demands are usually handled by investment in both the earth and space segments, minimizing earth segment investment is a major planning criterion. An INTELSAT VI satellite that employs new technologies to handle manyfold increases in traffic demand through the satellite alone should minimize changes to operational earth stations and reduce the need for new ones.

These criteria for minimizing earth segment investment led to maximum digitalization (use of TDMA and IDR services), introduction of satellite-switched TDMA (SS-TDMA), and minimum expansion of new frequency bands (to minimize both retrofitting cost and the number of earth stations involved), all of which will be discussed in subsequent papers [1],[4]-[6].

SINGLE UNIQUE DESIGN FOR ALL ROLES

Following past INTELSAT practice, the INTELSAT VI spacecraft was based on a single satellite design tailored first and foremost to the Atlantic Primary role. Since this role presented the most stringent and demanding service requirements, it was assumed that a satellite designed for this role would be more than adequate for the requirements of all other roles for which INTELSAT VI would be suitable. INTELSAT VI was also designed to be compatible with the projected needs of the Primary and Major Path roles in the Indian region and the Major Path role in the Atlantic region—for a total of five spacecraft, with one more for in-orbit sparing purposes. It was further assumed that five or six *additional* INTELSAT VI spacecraft might be needed, not only to serve the Pacific region, but also to serve new roles in the Atlantic and Indian regions. Overall then, it was generally thought that a grand total of 10 to 12 INTELSAT VI spacecraft might ultimately be procured. Most importantly, it was assumed that a single unique or generic design for all roles was an appropriate response to the marketplace of the future.

One advantage of the generic design approach is that nonrecurring costs associated with the spacecraft manufacturing process are spread over a large number of spacecraft, reducing the per-unit cost to a minimum. Although valid for the early 1980s, this hypothesis is becoming less and less valid as the number of satellite roles increases and the marketplace becomes more competitive and specialized.

SATELLITE DESIGN ALTERNATIVES

The INTELSAT VI spacecraft design evolved from a thorough exploration of options, which commenced shortly after the INTELSAT V spacecraft contract was completed in 1977. Referred to as the INTELSAT V Follow-On System, the INTELSAT VI design options included six broad classes of spacecraft, each of which relied on a different approach for expanding system capacity, as set forth below:

- *Class A.* Spacecraft relying on increased bandwidth in frequency bands allocated to the fixed satellite service.
- *Class B.* Spacecraft relying on more efficient use of the existing bandwidth achieved by implementing advanced modulation/multiple-access techniques.
- *Class C.* Spacecraft relying on the distributed primary concept of connecting two satellites by an intersatellite link.

- *Class NB.* Spacecraft relying on implementation of new frequency bands not yet allocated to the fixed satellite service and used by the INTELSAT system.
- *Class T.* Trunk spacecraft for operation in Major Path roles to serve high-density traffic routes with small-size, lower gain-to-noise temperature ratio (G/T) earth stations.
- *Class AV.* Spacecraft based on advanced modifications to INTELSAT V for the purpose of extending system capacity.

Within each class of spacecraft, a range of designs (in some classes as many as six distinct spacecraft concepts) was postulated and evaluated in terms of their ability to meet system requirements cost-effectively. Among other features, the spacecraft differed in the number of frequency reuses of the 6/4- and 14/11-GHz bands, the complexity of the beam coverages and associated antenna systems, the bandwidth and power levels of each transponder, the complexity of their interconnectivity and associated on-board switching capabilities, the total bandwidth and capacity provided by each, the potential use of new bands such as 30/20-GHz, and their degree of reliance on advanced ground segment transmission/access techniques to achieve necessary system capacities. Differing numbers of spacecraft were involved to meet the projected needs in each ocean region. Further, mixed deployments (*e.g.*, three Class A spacecraft in the most demanding roles, coupled with two or three Class AV spacecraft in the less demanding roles) were also considered.

Compatibility with more than one existing or planned launch system was another factor in postulating the alternative designs. The ability to launch the spacecraft on more than one launch system (launcher diversity) was an important design criterion to hedge against a delay in spacecraft in-orbit delivery due to an unexpected problem in one launch system.

The most promising spacecraft concepts within each class were selected for more detailed development and evaluation. Eventually, a preferred design based on all options was selected for preparation of a detailed performance specification, which would form the basis for a procurement Request for Proposal (RFP).

The INTELSAT V Follow-On System was planned for initial deployment in either 1985 or 1986, depending on whether system saturation (*i.e.*, all growth capacity fully utilized) or the end-of-life of the predecessor INTELSAT V/V-A spacecraft paced the timing. In the event that an advanced INTELSAT V spacecraft (Class AV) was chosen as an interim solution to meet growth needs, initial deployment of the actual INTELSAT VI spacecraft might be delayed

several years beyond 1986, and hence a different procurement timetable would apply. The timeline set for the INTELSAT VI program in the early 1980s is shown in Figure 2. Further information on the procurement process is provided in a companion paper [1].

By 1980, three basic system options had been evaluated on a cost/benefit basis:

- *Alternative 1.* Procurement of six Class AV-type INTELSAT V-A spacecraft (in addition to the eight INTELSAT V spacecraft already under procurement) to meet international and domestic service requirements during the 1984 to 1985 period. These would be followed by an INTELSAT VI series of spacecraft to be deployed commencing at year-end 1985. A total of 10 to 12 INTELSAT VI spacecraft would be required during the period 1986–1992.
- *Alternative 2.* A high-capacity Class AV-type advanced INTELSAT V satellite introduced in the Indian Ocean Region in 1984 and in the Atlantic region in 1985; followed by a number of INTELSAT VI spacecraft to be introduced in the 1987 to 1989 time frame.
- *Alternative 3.* A new class of “small” all-6/4-GHz satellites (referred to as “hybrid” spacecraft in recognition of the fact that INTELSAT would for the first time plan its deployments around the use of distinct new spacecraft for the Pacific region, and possibly for domestic purposes as well) would be procured to meet Pacific international and domestic service requirements through year-end 1988. In addition, an INTELSAT VI spacecraft would be introduced in the Atlantic Ocean Region in 1985.

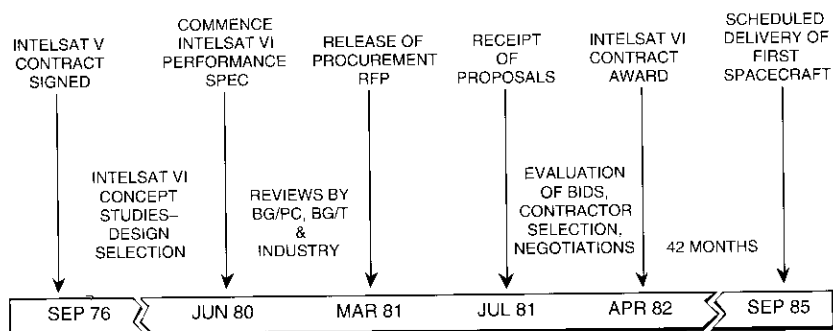


Figure 2. Timeline for the INTELSAT VI Program: Original Planning Schedule

Early economic analyses using net present value (NPV) as the criterion concluded that alternative 2 would be 20 percent more expensive than alternative 1, while alternative 3 would be 4 percent less expensive.

By mid-1980, concept studies had progressed to the point of clearly identifying the following three spacecraft options:

- *Hybrid Spacecraft.* An all-6/4-GHz spacecraft designed for Pacific Ocean Region service. A program involving development of competing designs by qualified bidders under contract to INTELSAT was envisioned, leading to receipt of firm proposals by year-end 1980. An expedited delivery program was believed feasible for these relatively simple spacecraft.
- *INTELSAT VI/B7.* An attractive INTELSAT VI design alternative employing eightfold reuse of the C-band via dual-polarized northeast, northwest, southeast, and southwest zone beams in 160 MHz—the lower channels (1-2) and (3-4)—with sixfold reuse of the C-band in 240 MHz—the upper channels (5-6), (7-8), and (9-10)—via two hemispheric coverage beams overlaid by four orthogonally polarized zone beams. An 8×8 dynamic SS-TDMA switch would be used in the lower channels to achieve system interconnectivity. This design was compatible only with NASA's Shuttle Transportation System (STS). Compatibility with the Titan/Centaur launch system may have been possible; however, this system was not offered for commercial launch service when the INTELSAT VI design was selected.
- *INTELSAT VI/L1.* A variant of the B7 concept described above, but limited to sixfold reuse of the C-band in 360-MHz—lower and upper channels (1-2), (3-4), (5-6), (7-8), and (9)—resulting in a much simplified antenna design, lower mass and volume requirements and, most importantly, compatibility with both the STS and the planned Ariane III launch systems and retention of a 6×6 dynamic SS-TDMA switch to achieve system interconnectivity. This design concept ultimately formed the basis for the INTELSAT VI performance specification [4],[7]–[9].

Throughout the systems planning process, the major creative work and analyses were conducted by INTELSAT in-house staff, with assistance from expert contractors as needed. Progress reports on the effort were reviewed periodically by the Signatories, who participated in the Board of Governors Advisory Committee on Planning (BG/PC). The advice and comments of the BG/PC were helpful and influential in selecting the spacecraft design best suited to meet INTELSAT's future traffic requirements.

INTELSAT VI planning elements

Previous sections have described the user requirements, external environment, and internal dynamics leading to selection of the technology, frequency spectrum, and launchers that influenced the final INTELSAT VI satellite design. This section discusses these key planning elements in more detail.

Frequency spectrum

The use and reuse of C- and Ku- frequency bands on the INTELSAT VI spacecraft was dictated by the evolution of the INTELSAT system to ensure maximum compatibility and ease of transition from the predecessor INTELSAT V/V-A satellites. The connectivity between the bands—referred to by INTELSAT as cross-strap operation—was needed to link large users who can access the Ku-band capacity with smaller users who can access only C-band, in a manner that makes effective use of the total satellite capability. INTELSAT VI uses more Ku-band bandwidth (a total of 1,000 MHz) than did INTELSAT V/V-A, in part to deliver new services to developed countries and in part to increase INTELSAT VI capacity.

The total bandwidth incorporated on INTELSAT VI at both C- and Ku-band was driven by international telephony PSTN requirements. The volume and geographic distribution of telephony traffic demand determined the number of transponders and the beam coverage requirements. Figure 3 depicts the PSTN traffic volume (in percent) and distribution projected in the early 1980s for the mid-1990s for both the Atlantic and Indian regions. The four main geographical regions are the Americas; Europe, the Mediterranean, and Africa; the Middle East; and East Asia, South Asia, and Australia.

Several observations are pertinent. The Atlantic region traffic projections account for approximately 75 percent of the total system traffic, with the main source being traffic between Europe and North America (33 percent). North America and Europe are also the source of a major percentage of traffic toward southern countries in the Americas and Africa. These factors call for a large proportion of bandwidth over North America and Europe, which leads to the use of both C- and Ku-band frequencies in both regions.

Interregional traffic ranged from a minimum of 1 percent for countries on the East Indian Ocean to 14 percent among the Americas, Europe, and Africa. The projected traffic distribution in the Atlantic region was more balanced than in the Indian region. This traffic imbalance in the Indian region was not of great concern at the time because, should it materialize, it would result in excess capacity that could be used for other services such as domestic and business services.

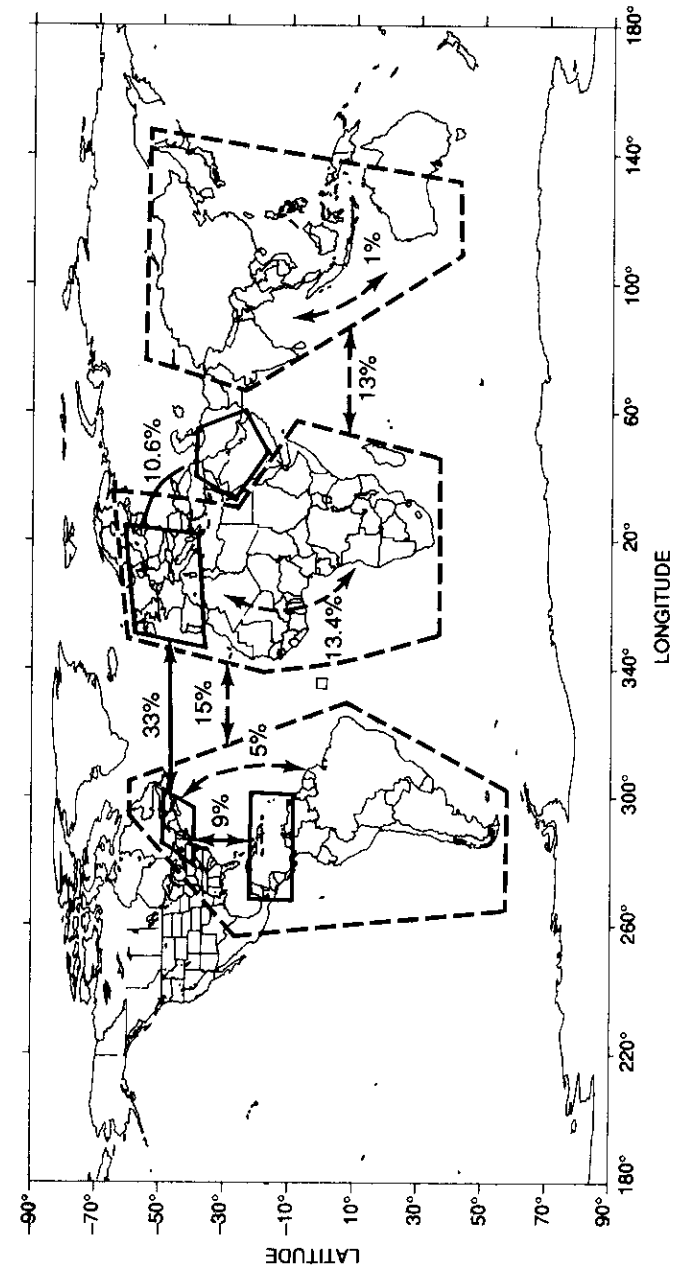


Figure 3. Regional Traffic Plans

Given the user requirements, the INTELSAT VI spacecraft were required to accommodate a threefold increase in traffic relative to their predecessor INTELSAT V/V-A satellites. A capacity of some 60,000 bearer channels per spacecraft was seen to be sufficient to carry the Primary and Major Path roles in the Atlantic and Indian regions forward some 10 to 13 years—the expected spacecraft lifetime. The capacity increase was accomplished through sixfold reuse of the spectrum at 6/4 GHz, in conjunction with a significant increase in bandwidth use efficiency using SS-TDMA and IDR along with conventional FDMA/FM. Traffic distribution patterns in the most demanding roles, as well as limitations in spacecraft antenna technology, dictated frequency reuse to six times over 360 MHz of the 500-MHz bandwidth allocated to the fixed satellite service, with two hemispheric coverage beams in one polarization and four geographical zone beams over major sources of traffic in the other. Global coverage was provided with twofold frequency reuse over 120 MHz. These coverages provided 2,560 MHz of usable bandwidth at 6/4 GHz, with an additional 960 MHz derived from twofold reuse of the 14/11-GHz band for the traffic sources with the highest density.

The INTELSAT VI spacecraft was designed to carry a communications payload consisting of an antenna farm capable of providing the above-mentioned coverages, along with 46 transponders (channel 9 having a maximum of six reuses) with bandwidths of 72, 36, 41, and 159 MHz (see Figure 4). Even with this increase in bandwidth, the capacity required to meet demand was only achieved by increasing the efficiency of bandwidth utilization through the introduction of SS-TDMA into the system for international PSTN traffic.

Technology

Technology has been the driver in previous INTELSAT satellite series because the type, quality, and quantity of service have been limited by technology in almost every respect. While technology per se remains a significant driver for INTELSAT VI, it is also a major driver of cost-effectiveness, which is all-important in the competitive environment.

SPACECRAFT TECHNOLOGY

INTELSAT continuously monitors the status of spacecraft technology. It conducts a vigorous research and development (R&D) program in its own right, and the various signatories to INTELSAT also conduct R&D in the satellite communications field. Finally, the industry itself is constantly pushing forward the capabilities of spacecraft and satellite communications technology. In addressing alternatives for the INTELSAT VI design, INTELSAT knew which technologies were feasible to implement in the time frame of the INTELSAT VI

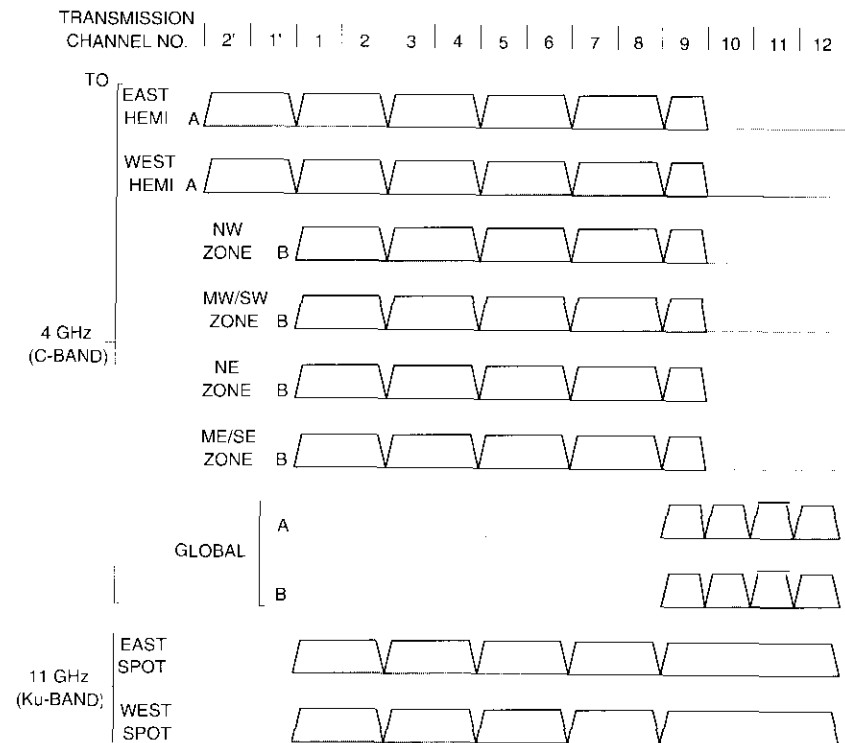


Figure 4. INTELSAT VI Transponder Plan

program. The INTELSAT VI procurement specification was written so that requirements could be met with available technology.

For INTELSAT VI, the following key technologies pushed the state of the art of spacecraft design:

- *SS-TDMA Switch*. A dynamic switch providing rapid beam-to-beam switching capability to achieve full connectivity and efficient bandwidth usage for INTELSAT VI transponders [9].
- *Sixfold Frequency Reuse at C-Band*. Two hemispheric coverage beams and four zone beams covering northeast, northwest, southeast, and southwest areas provided two more reuses of C-band than the predecessor INTELSAT V/V-A satellites [10].
- *C-Band Solid-State Power Amplifiers (SSPAs)*. Judged available for commercial service up to 10 W based on successful in-orbit experience of a U.S. domestic spacecraft with 8.5-W SSPAs [11].

- *Bipropellant Fuel System.* Used for the first time by INTELSAT for both apogee boost and stationkeeping, it allowed a greater share of the spacecraft mass to be used for the communications payload [12].
- *Contiguous Channel Multiplexing at Ku-Band.* Allowed INTELSAT to accommodate the full 500 MHz of available Ku-band spectrum with a single Ku-band transmit antenna [11].

These evolving technologies permitted INTELSAT to specify a 10-year design life and to carry stationkeeping fuel sufficient for 13 years of fully station-kept life—compared to a 7-year design life and 9-year fuel life for the INTELSAT V/V-A series spacecraft. The longer design lifetime resulted from the use of SSPAs and increased confidence in the reliability of C-band traveling wave tube amplifiers (TWTAs) based on experience with the highly successful INTELSAT IV/IV-A program, as well as from the use of enhanced TWTA redundancy at Ku-band (*i.e.*, 2-for-1 redundancy vs 3-for-2 on INTELSAT V/V-A).

EARTH SEGMENT TECHNOLOGY

The digitalization of the INTELSAT system required the introduction of complementary technology to both the space segment (*i.e.*, INTELSAT VI satellites, from filters to SS-TDMA), and the earth terminals. Two digital alternatives were specified—TDMA terminals [13] and IDR carriers—both greatly assisted by the development of digital circuit multiplication equipment (DCME) [14]. It was anticipated in the early 1980s that INTELSAT would introduce 32-kbit/s low-rate encoding with digital speech interpolation and allow for some 4-to-1 capacity enhancement as measured in derived (or virtual) voice circuits. This technology would maintain circuit quality and yield a very low cost per telephone circuit.

Recognizing the trend toward the use of smaller earth stations, INTELSAT introduced new earth station standards which complemented the conventional ones (*i.e.*, A, B, and C), some of which allowed users to access the satellites directly from an antenna located on or very close to the user's premises without relying on extensive terrestrial connecting facilities. The range of earth stations now available for use on INTELSAT satellites allows each user to choose the network architecture best suited to its own needs. Three types of earth station facilities were planned for use with INTELSAT VI [5]:

- *User Gateway.* Characterized by the use of small earth stations, 3.5-m (Standard E1) to 5.5-m (Standard E2) antennas in Ku-band, or 5-m (Standard F1) to 7-m (Standard F2) antennas in C-band, with very short and inexpensive terrestrial interconnect lines to business

customers. Each of these small earth stations could serve a single large business user, or could be shared by a community of smaller users.

- *Urban Gateway or Teleport.* Based on medium-size earth stations having antennas from 5.5 m (Standard E2) to 8/9 m (Standard E3) in Ku-band, or from 9 m (Standard F3) to 11 m (Standard B) in C-band. These urban gateways or teleports are located in a city or its outskirts to minimize terrestrial interference and terrestrial coordination problems. Traffic from customer premises is routed via local terrestrial digital networks.
- *Country Gateway.* Continued use of existing or planned national gateways having antennas from 16 to 30 m (Standard A) in C-band and 11 to 18 m (Standard C) in Ku-band. The use of this concept in the future will depend on the availability and economy of a wideband national digital network.

The most important criteria controlling the design of these earth stations are related to cost, since there are potentially a large number of standard earth stations involved in the user gateway and urban gateway concepts. Therefore, not only are small antennas (less than 9 m) chosen by users, but some reasonable constraints are also placed on other cost-sensitive elements of the earth stations. For example, up-link power control is not used for these earth stations unless very high-quality service is needed, and tracking is not necessary when antennas are smaller than 5 m. In addition, earth stations are equipped with relatively low-power high-power amplifiers and high-temperature low-noise amplifiers. Rate 1/2 or 3/4 forward error correction (FEC) coding is employed to trade off bandwidth for satellite power, with reasonable state-of-the-art FEC codes installed on these earth stations. Furthermore, standards development has led to optimal flexibility, equipment availability from numerous manufacturers in several countries, manufacturer competition, and cost reductions for procurement and maintenance of earth segment equipment.

Launch vehicles

Launch systems represented a significant consideration in the design of the INTELSAT VI spacecraft. The INTELSAT VI design options had to be compatible with the U.S. STS and the emerging European Ariane launch systems. Further discussion of launcher systems in relation to the INTELSAT VI program can be found in companion papers [1],[8],[15],[16].

Retrospective

While INTELSAT VI was designed for compatibility with a large number of in-orbit roles in all three ocean regions, the initial procurement was limited to five spacecraft for use in the most demanding system roles, namely the Atlantic and Indian Primary and Major Path satellites and the Atlantic Spare role. This limited procurement was influenced by what turned out to be conservative traffic projections and a concern that emerging fiber optic cables coupled with advanced modulation/access/voice compression techniques would limit the demand for satellite bandwidth. In retrospect, demand has increased beyond expectations, in part due to the emergence of a variety of new services that required vast amounts of bandwidth (such as full-time video leases and digital services into small earth station antennas) and in part due to the demand resulting from the emergence of competing international telecommunications carriers in the U.S. and elsewhere, in particular AT&T, MCI, and Sprint in the U.S. Had traffic projections in the mid-1980s reflected the increased demand that actually materialized in the late 1980s, it is likely that INTELSAT would have procured additional INTELSAT VI spacecraft to supplement the initial procurement.

On the other hand, and also in retrospect, the limited procurement might have worked to INTELSAT's advantage because of the increasingly accepted notion that a single unique or generic design cannot possibly meet the needs of all ocean regions and all roles within an ocean region. Due to the limited procurement of INTELSAT VI spacecraft, further system expansion in the 1990s will be carried forward by the next-generation INTELSAT VII spacecraft, augmented by non-generic or specialized spacecraft.

Conclusions

INTELSAT VI spacecraft were planned as the largest communications satellites ever built, to meet the traffic growth needs of the INTELSAT system. They also had to be sufficiently flexible to accommodate the changing levels and geographic distribution of demand, as well as new service needs, some of which were unforeseen when the spacecraft design was finalized. The INTELSAT VI spacecraft was sized to meet the most demanding roles in the INTELSAT system, and the procurement was limited to filling five main roles in the Atlantic and Indian ocean regions. Cost efficiency and quality improvements flowed from the introduction of digital transmission, whereby satellite bandwidth was used more efficiently. The introduction of SS-TDMA further enhanced this trend and provided connectivity that allowed greater use of available capacity. Increasing the useful in-orbit lifetime also contributed to

the lower annualized cost for INTELSAT VI spacecraft. The expansion of C-band usage to sixfold reuse was largely driven by growing conventional service needs, while new services and the proliferation of smaller earth stations called for wider beam coverage patterns and higher e.i.r.p. levels. At the same time, new services and competition brought full use of the Ku-band, with steerable beams and higher-e.i.r.p. transponders.

Acknowledgments

The authors would like to acknowledge the contributions and efforts of the INTELSAT planning staff, as well as planning experts from the various member Signatories to INTELSAT.

References

- [1] E. I. Podraczky and W. R. Schnicke, "The Process for Success—INTELSAT VI," *COMSAT Technical Review*, Vol. 20, No. 2, Fall 1990, pp. 231–246 (this issue).
- [2] *COMSAT Technical Review*, Vol. 15, No. 2B, Fall 1985, Special Issue on INTELSAT TDMA: Part I.
- [3] *COMSAT Technical Review*, Vol. 16, No. 1, Spring 1986, Special Issue on INTELSAT TDMA: Part II.
- [4] S. J. Campanella *et al.*, "SS-TDMA System Considerations," *COMSAT Technical Review*, Vol. 20, No. 2, Fall 1990, pp. 335–371 (this issue).
- [5] M. P. Brown *et al.*, "INTELSAT VI Transmission Design and Associated Computer System Models for FDMA Services," *COMSAT Technical Review*, Vol. 20, No. 2, Fall 1990, pp. 373–399 (this issue).
- [6] M. P. Brown, F. A. S. Loureiro, and M. Stojkovic, "Earth Station Considerations for INTELSAT VI," scheduled for publication in *COMSAT Technical Review*, Vol. 21, No. 2, Fall 1991.
- [7] B. A. Pontano, A. I. Zaghoul, and C. E. Mahle, "INTELSAT VI Communications Payload Performance Specifications," *COMSAT Technical Review*, Vol. 20, No. 2, Fall 1990, pp. 271–308 (this issue).
- [8] G. P. Cantarella and G. Porcelli, "Specifying the Spacecraft Bus," *COMSAT Technical Review*, Vol. 20, No. 2, Fall 1990, pp. 309–333 (this issue).
- [9] R. K. Gupta *et al.*, "SS-TDMA On-Board Subsystem Design," scheduled for publication in *COMSAT Technical Review*, Vol. 21, No. 1, Spring 1991.
- [10] R. R. Persinger *et al.*, "The INTELSAT VI Antenna System," scheduled for publication in *COMSAT Technical Review*, Vol. 21, No. 1, Spring 1991.
- [11] G. Horvai *et al.*, "INTELSAT VI Communications Subsystem Design," scheduled for publication in *COMSAT Technical Review*, Vol. 21, No. 1, Spring 1991.
- [12] L. I. Slafer and V. L. Seidenstucker, "Attitude and Payload Control System for the INTELSAT VI Communications Satellite," scheduled for publication in *COMSAT Technical Review*, Vol. 21, No. 1, Spring 1991.

- [13] J. A. Lunsford *et al.*, "SS-TDMA System Design," scheduled for publication in *COMSAT Technical Review*, Vol. 22, No. 1, Spring 1992.
- [14] M. Onufry *et al.*, "DCME in the INTELSAT VI Era," scheduled for publication in *COMSAT Technical Review*, Vol. 21, No. 2, Fall 1991.
- [15] L. R. Dest *et al.*, "INTELSAT VI Spacecraft Bus Design," scheduled for publication in *COMSAT Technical Review*, Vol. 21, No. 1, Spring 1991.
- [16] L. Virdee *et al.*, "INTELSAT VI Launch Operations, Deployment, and Bus In-Orbit Testing," scheduled for publication in *COMSAT Technical Review*, Vol. 21, No. 2, Fall 1991.



Luis B. Perillan received an M.E.E. in 1966 and a Ph.D. in telecommunications in 1975 from Madrid Polytechnic University, and a M.S. in digital communications from George Washington University in 1973. He joined INTELSAT in 1977, and for 7 years worked in the R&D and Planning Division, leading the system studies team responsible for the INTELSAT V-A and VI satellite definitions. He also led the feasibility studies for the IBS and INTELNET services. In 1984, Dr. Perillan joined the Business and Service Development Division and is currently the Regional Director for Latin America and the Caribbean. Prior to joining INTELSAT, he worked on electronic instrumentation at Hewlett-Packard, on satellite transmission impairments modeling and antennas at COMSAT Laboratories, and on international network operations and engineering at the Spanish Telephone Company.



William R. Schnicke holds an M.B.A. in finance and accounting from the University of Maryland, an M.S. in electrical engineering from the University of Pennsylvania, and a B.S. in electrical engineering from the Massachusetts Institute of Technology. As Senior Director, Systems Engineering and Planning for COMSAT's INTELSAT Satellite Services (now COMSAT World Systems) he was responsible for directing COMSAT's participation on advisory committees related to technical and planning matters for the global communications satellite system, INTELSAT. He collaborated in developing the concept and design of INTELSAT's fifth, sixth, and seventh generations of spacecraft, and was instrumental in developing additional high-power, Ku-band satellite capacity for television service between North and South America and Europe. Mr. Schnicke is currently a Senior Scientist at Hughes Aircraft Corporation, Los Angeles, California.

Edward A. Faine received a B.S.E.E. from Ohio State University in 1963 and an M.S.E.E. from the State University of New York at Buffalo in 1969. He has been with COMSAT since 1973, and is now Director of International Systems Planning with COMSAT World Systems.

Mr. Faine collaborated on the conceptual design and evaluation of three generations of INTELSAT spacecraft, (INTELSAT V, VI, and VII) and their various modifications. He was also instrumental in demonstrating the viability of innovative new technologies such as tracking C-band VSATs, HDTV, and TMTV, as well as services such as disaster relief and distance learning on the INTELSAT system. He has been a member of the Advisory Committee on Planning to the INTELSAT Board of Governors for the past 8 years.



INTELSAT VI communications payload performance specifications

B. A. PONTANO, A. I. ZAGHLOUL, AND C. E. MAHLE

(Manuscript received May 24, 1991)

Abstract

The INTELSAT VI satellite is currently the world's largest commercial communications satellite, incorporating many advanced technologies. For at least the next decade, it is expected to be the mainstay of the INTELSAT system in the Atlantic and Indian Ocean Regions. This paper describes the development of the performance specifications used for the INTELSAT VI payload and discusses many of the key considerations, tradeoffs, and data that formed the basis for these specifications.

Introduction

The INTELSAT VI satellite design provides a significant increase in telephone channel capacity over that of the previous satellite series, INTELSAT V—24,000 circuits for INTELSAT VI (up to 120,000 with digital circuit multiplication equipment), compared to 15,000 circuits on INTELSAT V. This enhanced capacity was achieved by increasing the satellite's usable bandwidth with additional allocated frequency spectrum, and by increasing the number of frequency reuses. This paper describes the development of performance specifications for the INTELSAT VI communications payload, and the technical considerations from which the specifications were derived.

The most notable extension from the INTELSAT V design is the addition of two southern zone beams which, together with the two northern zone and two hemispheric beams, provide an increase in the number of frequency reuses at C-band from fourfold to sixfold. To efficiently utilize the sixfold reuse

bandwidth, dynamic switching in the form of satellite-switched time-division multiple access (SS-TDMA) is incorporated in transponder channel banks (1-2) and (3-4) to dynamically interconnect up-link to down-link beams.

Additional spectrum bandwidth made available by the 1979 World Administrative Radio Conference (WARC '79) is added by including two transponder channels (1'-2') below channels (1-2) in the hemispheric beams. Global beam capacity is approximately doubled over that provided by INTELSAT V by adopting dual-polarized global beams.

Since a large portion of the traffic is expected to be carried by TDMA, many performance characteristics have been developed and optimized for TDMA operation, including those for group delay, gain flatness, differential* group delay and gain flatness, differential* path length, bit error rate (BER) performance, and on-board local oscillator stability. The rationale for specifying each of these parameters will be described later.

INTELSAT VI is the first INTELSAT satellite to employ solid-state power amplifiers (SSPAs). The specification gave bidders the option of using either traveling wave tube amplifiers (TWTAs) or SSPAs. However, the performance specifications for the SSPA are more stringent than for the TWTA, resulting in improved transmission performance, especially for multicarrier operation. This, together with the potentially greater reliability of SSPAs, led to their inclusion in the specification.

This paper describes all major INTELSAT VI payload specifications, including beam coverages, transponder channelization, beam connectivity, link performance (e.g., effective isotropically radiated power [e.i.r.p.], gain-to-noise temperature ratio $[G/T]$, beam isolation, and saturation flux density), and nonlinear performance. Factors leading to the specified characteristics are also described. The specified values are those released in the Request for Proposals (RFP); an attempt is made to indicate where these specifications were changed during the course of the implementation contract. The design and resulting performance of the INTELSAT VI spacecraft are described in companion papers [1]-[5] in this and subsequent volumes of the *COMSAT Technical Review* dedicated to INTELSAT VI.

Beam coverages and antenna requirements

To increase the satellite's usable frequency bandwidth within the constraints of the allocated bandwidth, frequency reuse through multiple beams

* "Differential" indicates a specification regarding the difference between group delay, gain flatness, or path length on co-frequency transponders or adjacent transponders.

was first introduced in INTELSAT IV-A. Two C-band hemispheric beams with spatial isolation of 27 dB provided twofold frequency reuse. This was followed by INTELSAT V, which produced fourfold frequency reuse through polarization and spatial isolation. This was achieved at C-band with the addition of two smaller spatially isolated, cross-polarized coverage zones overlaid on the two hemispheric beams. To further increase traffic-carrying capacity, Ku-band spot beam antenna coverage was included for high-traffic regions.

The INTELSAT VI system further increased satellite capacity by adding six-fold frequency reuse in C-band. This is achieved by increasing the number of spatially isolated zones to four and making them orthogonally polarized with respect to the two hemispheric beams. All C-band beams employ circular polarization. The coverages of the four zones are defined separately for the Atlantic, Pacific, and Indian Ocean Regions and are specified in terms of a set of earth station locations. The two hemispheric beams, much broader in coverage, have the same coverage in each ocean region. The zone coverages can be switched by ground command.

Figure 1 shows the coverage requirements in the three ocean regions as they appear from primary satellite locations. For comparison, the figure also illustrates the coverages for INTELSAT V, showing how the angular separation of the zones decreased with INTELSAT VI. Table 1 lists the spacings (in satellite coordinates) between the zones in the three ocean regions, and between the common hemispheric beams.

The choice of design parameters for the C-band hemi/zone antenna is described by Zaghloul *et al.* [6]. The minimum interzone spacing, σ in degrees, is the key parameter which determines the minimum antenna aperture diameter, D [2]. The minimum interzone spacing is represented in terms of the

TABLE 1. INTELSAT VI INTERZONE SPACINGS, σ (deg)

| ZONES | ATLANTIC OCEAN REGION | INDIAN OCEAN REGION | PACIFIC OCEAN REGION |
|--------------------|-----------------------|---------------------|----------------------|
| Z1 to Z2 | 2.5 | 3.2 | 2.6 |
| Z1 to Z3 | 5.3 | 2.2 | 7.4 |
| Z1 to Z4 | 6.5 | 9.5 | 8.1 |
| Z2 to Z3 | 7.5 | 3.0 | 11.0 |
| Z2 to Z4 | 3.7 | 7.6 | 4.4 |
| Z3 to Z4 | 2.2 | 3.3 | 6.6 |
| E. Hemi to W. Hemi | 3.0 | 3.0 | 3.0 |

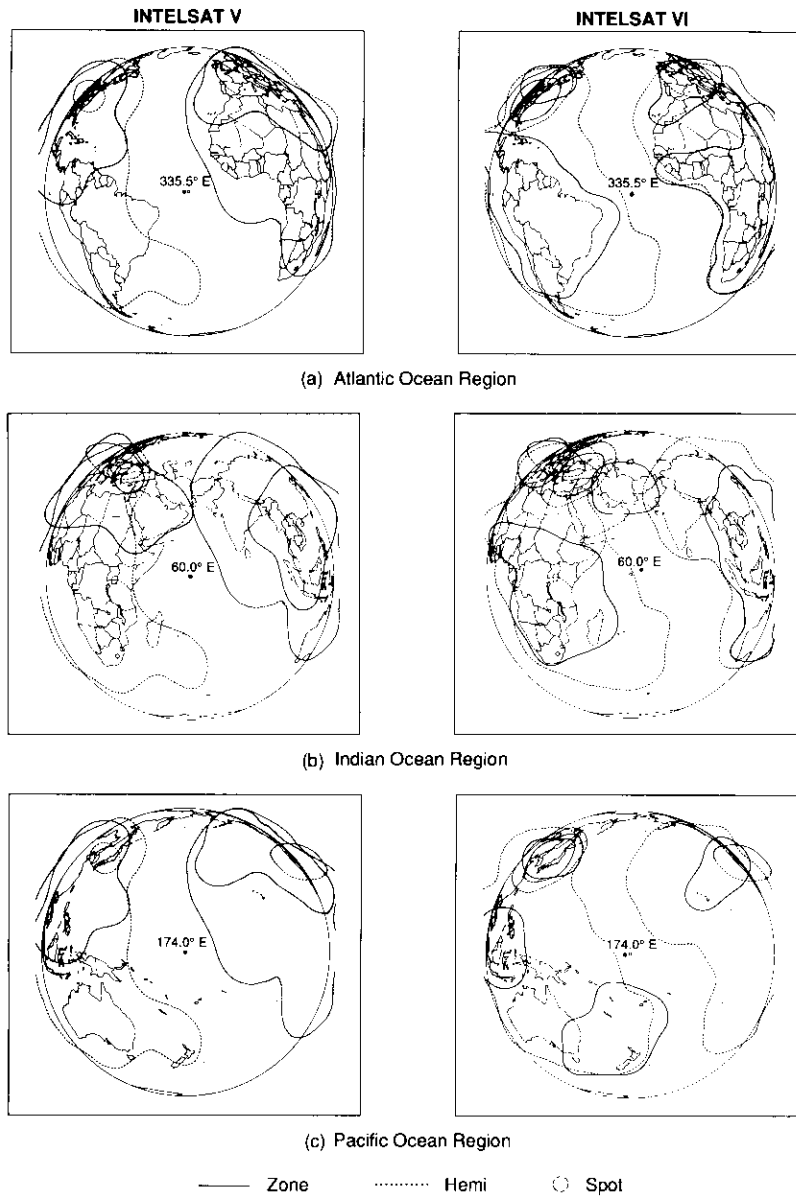


Figure 1. *INTELSAT V and VI Coverage Requirement Comparison*

beamwidth generated by individual feeds (component beams), as shown in Figure 2, and is about 1.4 times the 3-dB component beamwidth, for copolarization isolation of about 27 dB between the shaped beams. Based on previously developed INTELSAT satellite antennas, the empirical relationship $D > \alpha\lambda/\sigma$ sets the lower bound on the reflector diameter, where α ranges from 80 to 100. The maximum aperture of a solid reflector is limited by launch vehicle constraints. Bearing in mind the available launch vehicles, a minimum interzone spacing can be determined which aids in defining realistic zone coverages.

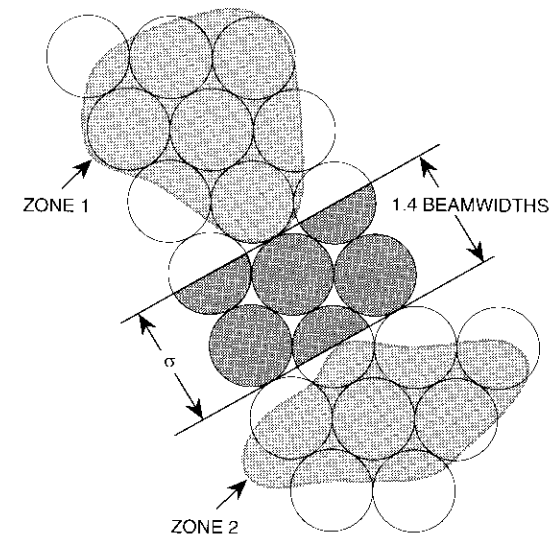


Figure 2. *Definition of the Minimum Interzone Spacing, σ*

The focal length to aperture diameter ratio, f/D , is the other parameter in the antenna reflector design which affects overall antenna size. It too is constrained by the launch vehicle envelope. The ratio f/D is related to the offset height and to f/D_p , where D_p is the diameter of the "parent" paraboloid from which the offset parabolic section is taken. The relationship to the offset height results from the maximum feed array size that offers blockage-free design. The variation of f/D_p and feed array size with f/D is illustrated in Figure 3 for a global field of view. Increasing f/D , or simply increasing f , results in a larger feed array, which also increases the offset height and consequently the overall size. On the other hand, lowering f/D reduces the array

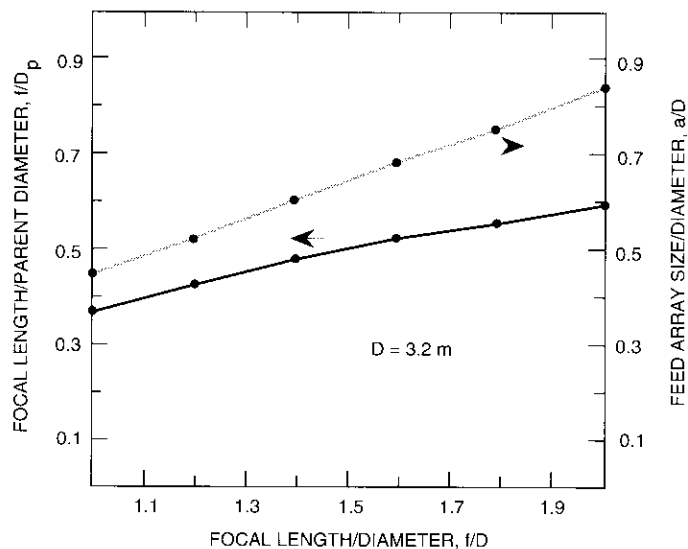


Figure 3. Local Length/Parent Reflector Diameter and Feed Array Size/Reflector Diameter vs Focal Length/Reflector Diameter

size (and thus the element aperture), introducing coupling effects which result in polarization degradation. An f/D value in the range of 1.0 to 1.4 defines the practical limits for overall size and polarization degradation.

For optimal performance, a large f/D_p is desirable because it produces lower cross polarization in a linear polarization system, less beam squint in a circular polarization system, and less beam distortion as the beam is scanned to the earth's edge. Figure 4 illustrates the changes in the 4-dB pattern contours for the eight component beams scanning from the boresight to beyond the global edge view angle for $f/D = 0.9$ to $f/D = 1.4$. Note that the crossover level as a function of scan is more uniform for $f/D = 1.4$, and that the shape of beam 8 is maintained. The effect of f/D on scan loss for the first eight component beams is shown in Figure 5. From this figure, it is apparent that an f/D of 1.3 is a reasonable value for eight beamwidths of scan. Further increasing f does not significantly reduce the scan loss.

The complexity of the feed array, its overall size, and the size of the individual feed are the next factors to be considered in specifying the shapes of the different beams and the isolation between them. The feed horn size controls the crossover levels between adjacent component beams, and thus plays an important role in the beam-shaping process. The optimum range of

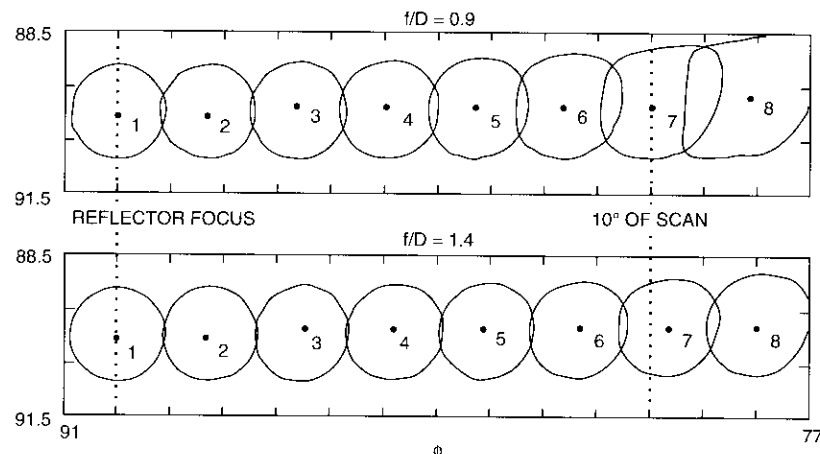
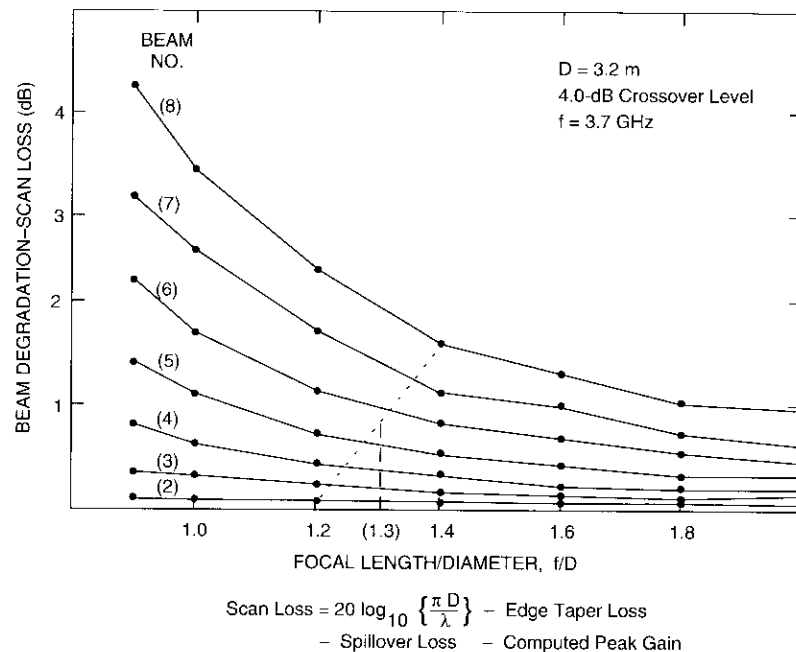


Figure 4. Component Beams for Two Values of f/D



$$\text{Scan Loss} = 20 \log_{10} \left\{ \frac{\pi D}{\lambda} \right\} - \text{Edge Taper Loss} - \text{Spillover Loss} - \text{Computed Peak Gain}$$

Figure 5. Beam Degradation vs Focal Length/Diameter

crossover levels, considering both gain and spatial isolation, is 2.5 to 4.0 dB below the beam peak. This range also offers greater amplitude and phase control, and thus better control over the beam shape for the specific coverage region. The higher crossover values (lower pattern levels) are obtained by increasing the size of the horns. A diameter exceeding 1.4 wavelengths would also allow the use of a multimode, which has the properties of low cross polarization and negligible mutual coupling between horns. Again, the choice of feed horn dimensions must satisfy both the crossover requirements and the cross-polarization specifications.

In addition to C-band hemi/zone antenna coverage, INTELSAT VI is required to provide two Ku-band spot beams in high-traffic regions, similar to INTELSAT V. The spot beams mostly serve the northern hemisphere, are steerable anywhere on the visible portion of the earth, and operate in two orthogonal linear polarizations. The two beams cover elliptical areas with a major axis of 2.8° and a minor axis of 1.4° , as seen from the satellite, with the major axes tilted 22.9° clockwise and 37° counterclockwise from the equator for the east spot and west spot beams, respectively.

Two more beams covering the whole earth operate at C-band. With two orthogonal circular polarizations, these beams provide global service and are separated from the hemi/zone beams by frequency. Table 2 provides a summary of the coverage beams in the 6/4-GHz C-band and the 14/11-GHz Ku-band and gives the polarization requirements [7].

The performance of the INTELSAT VI antennas is specified by the performance parameters of e.i.r.p., G/T , gain slope within the beam coverage area, and spatial and cross-polarization isolation. The e.i.r.p. and G/T requirements are discussed in the sections that follow. The beam isolation requirements are summarized in Tables 3a, 3b, and 3c for the C-band hemi/zone beams, C-band global beams, and Ku-band spot beams, respectively. Details of the design and achievable performance of the INTELSAT VI spacecraft antenna system are provided in a companion paper by Persinger *et al.* [2].

Transponder channelization plan

A transmission channel is established within the satellite repeater by connecting a receiver accessible from one receive coverage area at either 6 or 14 GHz to a transmitter associated with any transmit coverage area at either 4 or 11 GHz. This enables a user transmitting in any up-link coverage area to have their traffic routed to the appropriate down-link coverage area. Each frequency segment within the allocated 500 MHz defines a transmission channel. The transponder channelization plan (Figure 6) is subdivided into 12

TABLE 2. INTELSAT VI COVERAGE BEAMS AND POLARIZATION PERFORMANCE

| FREQUENCY BAND (GHz) | COVERAGE | POLARIZATION ^a | |
|-------------------------|----------|---------------------------|-----------|
| | | UP-LINK | DOWN-LINK |
| 6/4 ^b | Global A | LHCP | RHCP |
| | Global B | RHCP | LHCP |
| | W. Hemi | LHCP | RHCP |
| | E. Hemi | LHCP | RHCP |
| | Zone 1 | RHCP | LHCP |
| | Zone 2 | RHCP | LHCP |
| | Zone 3 | RHCP | LHCP |
| | Zone 4 | RHCP | LHCP |
| 14/11 | E. Spot | Linear ^c | Linear |
| | W. Spot | Linear | Linear |

^a LHCP is left-hand circular polarization, and RHCP is right-hand circular polarization.

^b Polarization performance (voltage axial ratio for transmit and receive beams) is ≤ 1.05 , global; and ≤ 1.09 , hemispheric and zone.

^c Polarization of east spot coverage will be orthogonal to that of west spot coverage.

nominal 40-MHz segments numbered 1 through 12. When a channel extends over more than one of these segments, this is indicated by multiple channel numbers, for example, (1-2). Channel (1'-2') falls outside the frequency band used by previous-generation INTELSAT satellites and provides the extended C-band capacity made possible by WARC '79.

There are five banks of 72-MHz transponders at C-band—(1'-2') and (1-2) through (7-8). Transponders (1'-2') have twofold frequency reuse via two hemi beams, and transponders (1-2) through (7-8) have sixfold frequency reuse through the combination of two hemi and four zone beams, giving a total of twenty-six 72-MHz C-band transponders. C-band transponder banks (1-2) and (3-4) are intended to carry INTELSAT 120-Mbit/s TDMA and have special channel and switching characteristics that will be described later. All other transponders are intended to carry frequency-division multiple access (FDMA) FM or digital phase shift keying (PSK) traffic. Global beam transponders normally will carry a variety of traffic, including analog FM video transmissions for occasional-use TV, and single channel per carrier (SCPC) telephone traffic.

TABLE 3. TRANSMIT AND RECEIVE ANTENNA BEAM ISOLATION (dB)

(a) 4- and 6-GHz Hemi and Zone Beams

| OCEAN REGION | ZONE 1 | ZONE 2 | ZONE 3 | ZONE 4 | E. HEMI | W. HEMI |
|-----------------|--------|--------|--------|--------|---------|---------|
| Atlantic | | | | | | |
| Zone 1 | - | 27 | 27 | 30 | 30 | 27 |
| Zone 2 | 27 | - | 30 | 27 | 30 | 27 |
| Zone 3 | 27 | 30 | - | 27 | 27 | 30 |
| Zone 4 | 30 | 27 | 27 | - | 27 | 30 |
| E. Hemi | 30 | 30 | 27 | 27 | - | 27 |
| W. Hemi | 27 | 27 | 30 | 30 | 27 | - |
| Indian | | | | | | |
| Zone 1 | - | 27 | 27 | 30 | 30 | 27 |
| Zone 2 | 27 | - | 27 | 30 | 30 | 27 |
| Zone 3 | 27 | 27 | - | 27 | 27 | 27 |
| Zone 4 | 30 | 30 | 27 | - | 27 | 30 |
| E. Hemi | 30 | 30 | 27 | 27 | - | 27 |
| W. Hemi | 27 | 27 | 27 | 30 | 27 | - |
| Pacific | | | | | | |
| Zone 1 | - | 27 | 30 | 30 | 30 | 27 |
| Zone 2 | 27 | - | 30 | 27 | 30 | 27 |
| Zone 3 | 30 | 30 | - | 30 | 27 | 30 |
| Zone 4 | 30 | 27 | 30 | - | 27 | 27 |
| E. Hemi | 30 | 30 | 27 | 27 | - | 27 |
| W. Hemi | 27 | 27 | 30 | 27 | 27 | - |

(b) 4- and 6-GHz Global Beams

| COVERAGE | ISOLATION (dB) |
|----------------------|----------------|
| Global A to Global B | 32 |

(c) 11- and 14-GHz Spot Beams

| ANGLE BETWEEN BEAM CENTERS, θ | ISOLATION (dB) |
|--|----------------|
| $3.5^\circ \leq \theta \leq 6.5^\circ$ | 25 |
| $6.5^\circ < \theta < 8.0^\circ$ | 27 |
| $8.0^\circ \leq \theta$ | 33 |

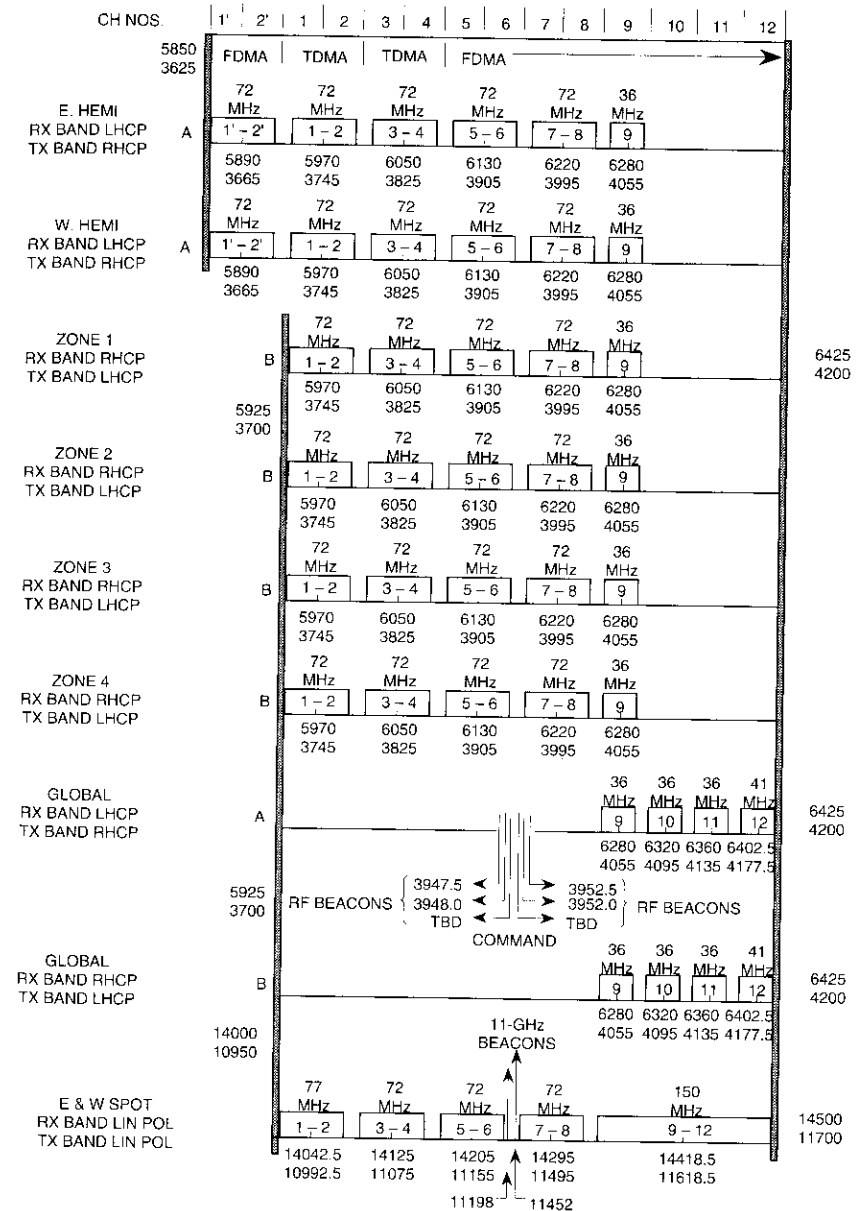


Figure 6. Transponder Center Frequencies, Bandwidths, and Polarizations

Transponder (9) can be configured by static switches into one of two modes, to provide either sixfold frequency reuse through the hemi and zone beams or twofold reuse through the cross-polarized global beams. The remaining 36- and 41-MHz transponders—(10), (11), and (12)—are permanently assigned to the global beams.

At Ku-band, there are four 72-MHz transponder banks, each having two-fold frequency reuse (eight transponders), and one 150-MHz transponder bank (two transponders). The 72-MHz transponders can be interconnected (cross-strapped) to the C-band transponders, as will be described later.

The transponder plan and channel bandwidths used in the INTELSAT VI satellite evolved from previous generations of INTELSAT satellites. This evolutionary process minimized the impact of the new satellite design on earth station owners in terms of carrier frequencies, and on system planners in terms of transition plans.

Transponder interconnectivity

Switching requirements

Receive coverage areas and transmit coverage areas are interconnected on a transponder-by-transponder basis using either static or dynamic switching. The simplified signal flow diagram of Figure 7 shows the beam connections that are achievable with the INTELSAT VI spacecraft. The diagram illustrates the connectivity possible for each transponder, and whether the switching is static or dynamic. A $k \times k$ static switch is a device with k inputs and k outputs. The switch, by ground command, can connect each input to any one output, with no two inputs connected to the same output port.

As can be seen, most transponders use static switching to interconnect up-link to down-link beams. These connections can be set based on projected traffic patterns. The settings will differ from satellite to satellite, depending on orbital position. Once in operation, the switch connections on a given satellite can be changed to match actual traffic growth. Table 4 summarizes the static connections that are possible with INTELSAT VI.

Transponder banks (1-2) and (3-4) at C-band provide dynamic switching via a microwave switch matrix (MSM) for operation with TDMA. Dynamic switching is performed cyclically according to a controllable sequence of connections (switch states) over a 2-ms TDMA frame period. TDMA operation with dynamic switching leads to better transponder utilization than that obtainable with static switching [8]. TDMA operating with dynamic switching is referred to as satellite-switched TDMA (SS-TDMA). Table 5 gives the dynamic interconnection requirements for INTELSAT VI. The dynamic switch can provide both point-to-point and broadcast connections.

TABLE 4. STATIC INTERCONNECTION REQUIREMENTS FOR 6-GHZ UP-LINKS

| RECEPTION | | | TRANSMISSION | |
|-----------|----------------------|--|-----------------|----------------------|
| COVERAGE | FREQUENCY BAND (GHz) | VIA CHANNELS | COVERAGE | FREQUENCY BAND (GHz) |
| Global A | 6 | (9), (10), (11), (12) | Global A | 4 |
| Global B | 6 | (9), (10), (11), (12) | Global B | 4 |
| E. Hemi | 6 | (1'-2'), (1-2), (3-4), (5-6), (7-8), (9) | E. or W. Hemi | 4 |
| | 6 | (1-2), (3-4), (5-6), (7-8) | E. or W. Spot | 11 |
| | 6 | (1-2), (3-4), (5-6), (7-8), (9) | Zone 1, 2, 3, 4 | 4 |
| W. Hemi | 6 | (1'-2'), (1-2), (3-4), (5-6), (7-8), (9) | E. or W. Hemi | 4 |
| | 6 | (1-2), (3-4), (5-6), (7-8) | E. or W. Spot | 11 |
| | 6 | (1-2), (3-4), (5-6), (7-8), (9) | Zone 1, 2, 3, 4 | 4 |
| Zone 1 | 6 | (1-2), (3-4), (5-6), (7-8), (9) | E. or W. Hemi | 4 |
| | 6 | (1-2), (3-4), (5-6), (7-8), (9) | Zone 1, 2, 3, 4 | 4 |
| | 6 | (5-6), (7-8) | E. or W. Spot | 11 |
| Zone 2 | 6 | (1-2), (3-4), (5-6), (7-8), (9) | E. or W. Hemi | 4 |
| | 6 | (1-2), (3-4), (5-6), (7-8), (9) | Zone 1, 2, 3, 4 | 4 |
| | 6 | (5-6), (7-8) | E. or W. Spot | 11 |
| Zone 3 | 6 | (1-2), (3-4), (5-6), (7-8), (9) | E. or W. Hemi | 4 |
| | 6 | (1-2), (3-4), (5-6), (7-8), (9) | Zone 1, 2, 3, 4 | 4 |
| | 6 | (5-6), (7-8) | E. or W. Spot | 11 |
| Zone 4 | 6 | (1-2), (3-4), (5-6), (7-8), (9) | E. or W. Hemi | 4 |
| | 6 | (1-2), (3-4), (5-6), (7-8), (9) | Zone 1, 2, 3, 4 | 4 |
| | 6 | (5-6), (7-8) | E. or W. Spot | 11 |

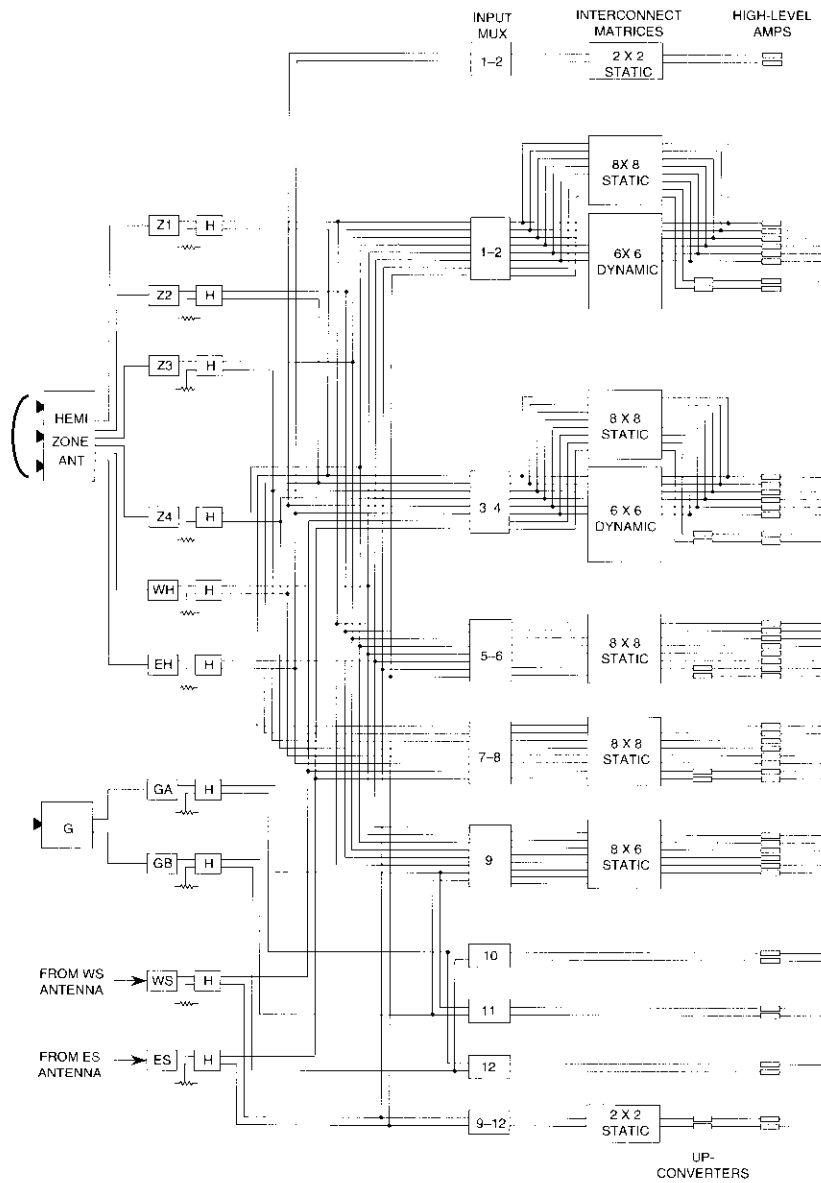
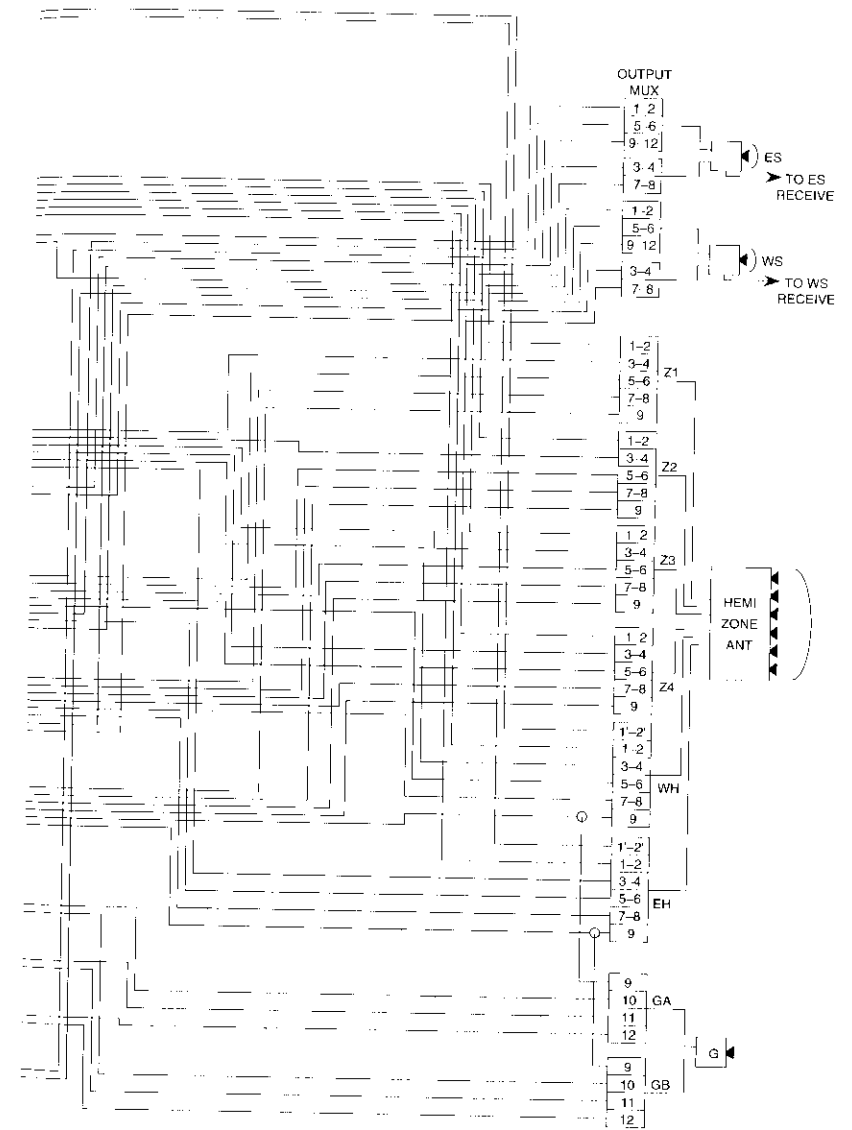


Figure 7. INTELSAT VI Simplified



Signal Flow Diagram

TABLE 5. DYNAMIC INTERCONNECTION REQUIREMENTS FOR 6-GHz UP-LINKS

| RECEPTION | | | TRANSMISSION | |
|-----------|----------------------|--------------|-----------------------|----------------------|
| COVERAGE | FREQUENCY BAND (GHz) | VIA CHANNELS | COVERAGE | FREQUENCY BAND (GHz) |
| E. Hemi | 6 | (1-2), (3-4) | E. or W. Hemi | 4 |
| | | | Zone 1 or 2 or 3 or 4 | 4 |
| | | | Broadcast, 2-6 beams | 4 |
| W. Hemi | 6 | (1-2), (3-4) | E. or W. Hemi | 4 |
| | | | Zone 1 or 2 or 3 or 4 | 4 |
| | | | Broadcast, 2-6 beams | 4 |
| Zone 1 | 6 | (1-2), (3-4) | E. or W. Hemi | 4 |
| | | | Zone 1 or 2 or 3 or 4 | 4 |
| | | | Broadcast, 2-6 beams | 4 |
| Zone 2 | 6 | (1-2), (3-4) | E. or W. Hemi | 4 |
| | | | Zone 1 to 2 or 3 or 4 | 4 |
| | | | Broadcast, 2-6 beams | 4 |
| Zone 3 | 6 | (1-2), (3-4) | E. or W. Hemi | 4 |
| | | | Zone 1 or 2 or 3 or 4 | 4 |
| | | | Broadcast 2-6 beams | 4 |
| Zone 4 | 6 | (1-2), (3-4) | E. or W. Hemi | 4 |
| | | | Zone 1 or 2 or 3 or 4 | 4 |
| | | | Broadcast, 2-6 beams | 4 |

Dynamic switch requirements

The INTELSAT VI SS-TDMA system [3] comprises three major on-board components: the dynamic MSM, the distribution and control unit (DCU), and the timing unit (TU). Figure 8 is a block diagram of the on-board configuration. Each of two switching units [for channel (1-2) and channel (3-4)] consists of its own MSM, a 2-for-1 DCU, and a 3-for-1 common TU. The MSM provides the RF interconnections between the receive beams and the transmit beams. The DCU stores the sequence of beam interconnections and implements it cyclically in accordance with a 2-ms TDMA frame period by controlling the FM cross-connect points of the MSM. The TU provides a common timing signal to both switching units. Further details on the MSM, DCU, and TU are given in Gupta *et al.* [4].

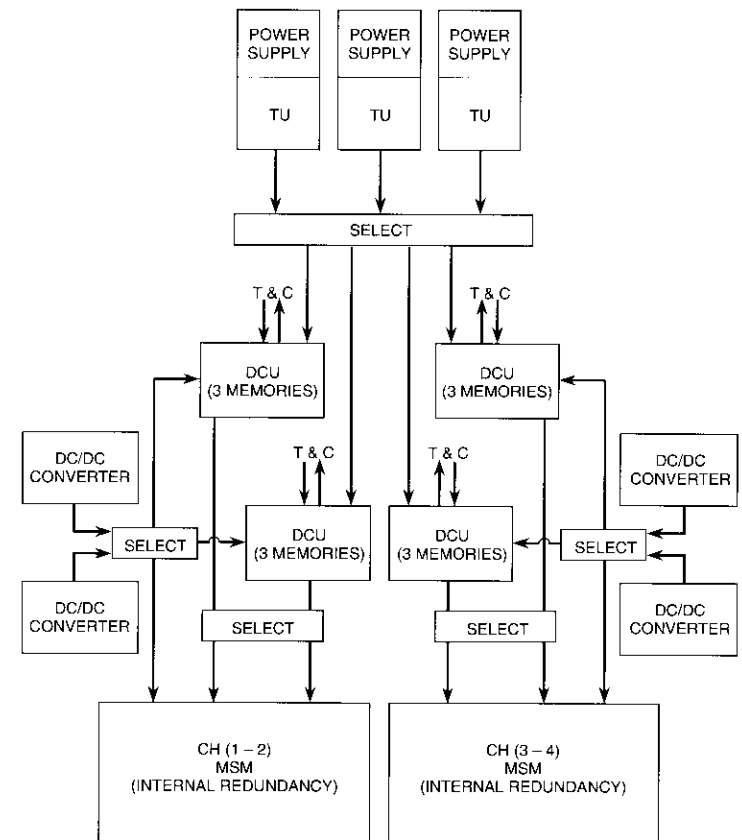


Figure 8. Dynamic Switch Functional Redundancy

The MSM associated with each transponder bank must interconnect each of the six C-band receive beams with one or more of the six transmit beams, thus necessitating a switch that has six input ports and six output ports. A crossbar switch architecture was assumed in order to provide a broadcast state, enabling one input to be connected to all six outputs. Although a broadcast state was not believed to be essential for the provision of traffic data, its use appeared very desirable for disseminating control and timing information from the reference stations to the traffic stations. Such a switch would require $6 \times 6 = 36$ electronic switching elements. To increase the reliability of the MSM, additional switching elements were added to the array. Figure 9 shows that the reliability of the MSM is improved as additional elements are added.

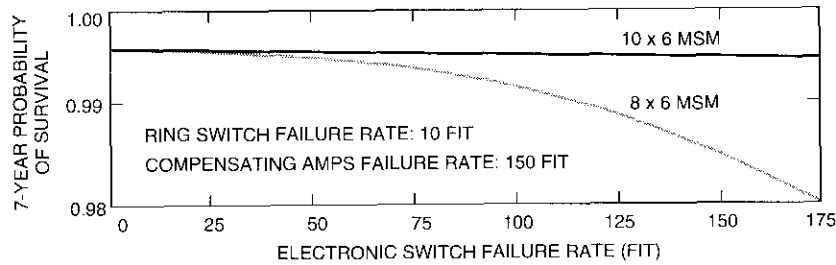


Figure 9. MSM Configuration Reliability vs Electronic Switch Failure Rates

Figure 10 depicts the MSM configuration selected for the INTELSAT VI satellite. The selected configuration is a 10×6 MSM, and therefore requires 60 electronic switching elements. This configuration in effect provides the MSM with four redundant rows of switching elements. Only six of the input ports and corresponding rows of switching elements are used at any given time. The input ports and their associated rows are selected through the electromechanical redundancy switch. If any switching element fails, whether it be in the open or short position, the use of that complete row of switch elements will be discontinued and replaced by one of the four redundant rows of switching elements.

Each MSM set of connections is called a switch state. The maximum number of switch states that must be stored in the DCU memories and executed in a single TDMA frame period is 48. Theoretically, it can be shown that for an $N \times N$ matrix where $N = 6$, the number of switch states, S , needed to optimally accommodate traffic is 26, obtained from [9]

$$S = N^2 - 2N + 2 \quad (1)$$

Since six additional switch states are required for the distribution of synchronization information, a total of 32 states is required. In practice, the requirement to minimize earth station equipment, along with other operational constraints, would not permit the use of optimum slot assignments. Therefore, the theoretical value of 32 was increased by 50 percent to 48 in the specification (and ultimately to 64 in the spacecraft implementation) to provide sufficient margin to accommodate any connectivity requirements which may develop in the future.

Each redundant DCU contains three memories which will store the switch state patterns. Each memory is selectable by ground command to be either on-

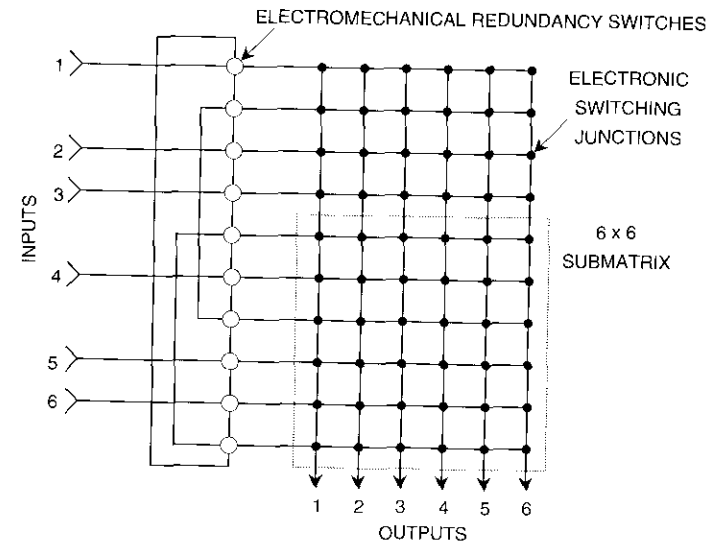


Figure 10. 10×6 MSM Configuration

line, off-line, or standby. The switch states contained in the on-line memory control the MSM; the off-line memory is used to load new switch state patterns for implementing the next burst time plan change. The standby memory provides redundancy and will replace either of the other two memories in case of failure.

The TU provides the basic clock rate needed to cycle the DCU through the stored switch states at the frame rate. Since the SS-TDMA terrestrial interface is designed to operate in accordance with International Telegraphy and Telephony Consultative Committee (CCITT) recommendations pertaining to plesiochronous operation, the on-board clock can exhibit an uncertainty of no more than one part in 10^{11} over the satellite lifetime. This accuracy is not achievable by an on-board clock without the use of ground correction. The following three methods of frequency correction were examined in developing the specification:

- On-board demodulation of the unique word of the reference burst operating off a high-stability source.
- An on-board clock phased-locked to a high-stability clock sent from the ground.
- An on-board digitally controlled clock periodically adjusted from the ground.

Although all three methods were believed to be technically feasible, method (c) was selected because of its simplicity of implementation. Additional information on this implementation is provided in Maranon *et al.* [5]. Details of the SS-TDMA systems are given in companion papers by Campanella *et al.* [3], Gupta *et al.* [4], Maranon *et al.* [5], and Lunsford *et al.* [10].

Link and performance analysis

A detailed link and performance analysis for both FDMA and TDMA transmission formed the basis for developing the specified values of spacecraft e.i.r.p., saturation flux density, and interbeam isolation. The analysis considered both TWTAs and SSPAs.

Figure 11 shows transponder capacity as a function of satellite saturation e.i.r.p. for the case of FDMA transmissions. This capacity analysis uses the characteristics of the INTELSAT Standard-A earth station in use at the time of the INTELSAT VI procurement (*i.e.*, 32-m earth stations with $G/T = 40.7$ dB/K). Although INTELSAT has revised its Standard-A specifications to 35 dB/K (15- to 18-m antennas), a large number of 32-m earth stations are still in use. The figure shows that a reduction of 3 dB in satellite e.i.r.p., from 32 to 29 dBW, results in a capacity reduction of about 9 percent for zone-to-zone links and 12 percent for hemi-to-hemi links. Figure 12 shows that such a reduction would significantly reduce the TDMA link margins for hemi-to-hemi

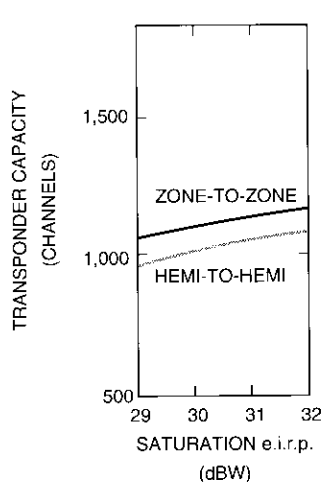


Figure 11. FDMA Capacity vs Satellite e.i.r.p.

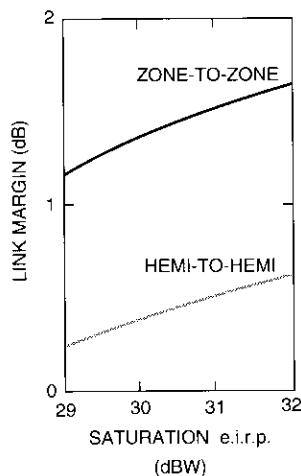


Figure 12. TDMA Margin vs Satellite e.i.r.p.

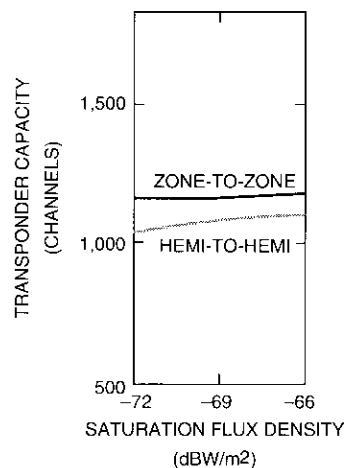


Figure 13. FDMA Capacity vs Saturation Flux Density

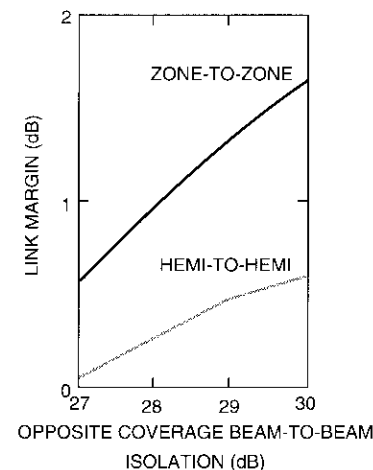


Figure 14. TDMA Margin vs Opposite Coverage Beam-to-Beam Isolation

connections from about 0.6 to 0.2 dB. However, a reduction to 31 dBW would result in only a 0.1-dB reduction in TDMA link margin and less than 3-percent reduction in FDMA capacity; therefore, 31 dBW was selected as the baseline value for the 72-MHz C-band transponders.

A saturation flux density of about -69 dBW/m² seems to be near-optimal for the hemi and zone beams to reduce up-link thermal noise, as seen from Figure 13, for FDMA transmissions operating with the low-gain setting. The final value selected for the specification for this case is -67.1 dBW/m² \pm 2 dB.

For TDMA transmissions which operate with a high gain setting, a saturation flux density was selected that balanced up-link noise performance against earth station e.i.r.p. The selected value for the high-gain setting case is -77.6 dBW/m² \pm 2 dB. With an input transponder backoff of 2 dB, this would correspond to an earth station e.i.r.p. of less than 84 dBW.

Examination of the sensitivity of the interbeam isolation showed that, for the FDMA case, a 3-dB reduction in beam-to-beam isolation (from 30 to 27 dB) would result in a capacity reduction of about 4 to 8 percent. For FDMA links, the capacity was affected more by satellite e.i.r.p. than by isolation reduction. The TDMA links were found to be sensitive to variations in interbeam isolation, as shown in Figure 14. As seen from the above, it was necessary to control the satellite's antenna gain and isolation variations. Peak-to-peak gain variation is held to 3 dB for the zone beams and 2 dB for the hemispheric beams.

Performance parameters

The major performance parameters of the communications subsystem are G/T , saturation e.i.r.p., saturation flux density, transponder filter characteristics, gain flatness, differential path length, and nonlinearity characteristics. The rationale used for specifying these parameters is described below.

G/T performance

Table 6 gives the assumed values of beam edge antenna gains, expected losses, and estimated noise figures, which were used in the analysis and which led to the specified values of satellite G/T . The planned receiver performance was based on the use of field-effect transistor (FET) low-noise amplifiers. The 6-GHz receivers were assumed to be about 0.5 dB better than those used on INTELSAT V-A, and the 14-GHz receiver specification was taken to be similar to that being implemented on the Satellite Business System satellite.

TABLE 6. G/T PERFORMANCE

| COVERAGE | ANTENNA GAIN (dBi) | LOSSES (dB) | EST. NOISE FIGURE OF RECEIVER AND TRANSPONDER (dB) | NOISE TEMP. (dB/K) | SPEC. G/T^* (dB/K) | MARGIN (dB) |
|----------|--------------------|-------------|--|--------------------|----------------------|-------------|
| Global A | 16.0 | 1.5 | 3.0 | 27.6 | -15.0 (-14.0) | 1.9 |
| Global B | 16.0 | 1.5 | 3.0 | 27.6 | -15.0 (-14.0) | 1.9 |
| E. Hemi | 21.9 | 1.5 | 3.0 | 27.6 | -8.5 (-9.2) | 1.3 |
| W. Hemi | 21.3 | 1.5 | 3.0 | 27.6 | -8.5 (-9.2) | 0.7 |
| Zone 2 | 23.3 | 1.5 | 3.0 | 27.6 | -7.0 | 1.2 |
| Zone 4 | 23.5 | 1.5 | 3.0 | 27.6 | -7.0 | 1.4 |
| Zone 1 | 32.8 | 1.5 | 3.0 | 27.6 | -1.0 (-2.0) | 4.7 |
| Zone 3 | 29.2 | 1.5 | 3.0 | 27.6 | -1.0 (-2.0) | 1.1 |
| E. Spot | 33.6 | 2.0 | 5.0 | 29.6 | 1.0 | 1.0 |
| W. Spot | 37.5 | 2.0 | 5.0 | 29.6 | 4.3 (1.7) | 1.6 |

* Numbers in parentheses are the revised specification values agreed to during the course of the implementation program.

Saturation e.i.r.p.

Tables 7 and 8 give the amplifier outputs, expected losses, and beam edge antenna gains that were used to develop the specified e.i.r.p. values. These values, and the resulting margins, are shown for the hemi, zone, and spot beams. The expected losses (including switches, output multiplex filters, and waveguide) were determined based on experience with INTELSAT V. Losses due to beam-forming networks are included in the antenna gain values.

Seven different power amplifier sizes were considered for INTELSAT VI. SSPAs were considered to be well within the state of existing technology for the 1.3- and 2.5-W amplifiers. Their use was also believed to be feasible for the 5.0- and 8.5-W amplifiers, since a 6-W FET amplifier had been developed

TABLE 7. HEMISPHERIC AND ZONE BEAM e.i.r.p.

| COVERAGE | AMPLIFIER OUTPUT (W) | EXPECTED LOSSES* (dB) | ANTENNA GAIN, INCL. FEED ** (dBi) | SPEC. e.i.r.p. (dBW) | MARGIN (dB) |
|----------|----------------------|-----------------------|-----------------------------------|----------------------|-------------|
| W. Hemi | | | | | |
| 80 MHz | 16.0 | 1.7 | 21.3 | 31.0 | 0.6 |
| 40 MHz | 8.5 | 1.7 | 21.3 | 28.0 | 0.9 |
| E. Hemi | | | | | |
| 80 MHz | 16.0 | 1.7 | 21.9 | 31.0 | 1.2 |
| 40 MHz | 8.5 | 1.7 | 21.9 | 28.0 | 1.5 |
| Zone 1 | | | | | |
| 80 MHz | 2.5 | 1.7 | 32.8 | 31.0 | 4.1 |
| 40 MHz | 1.3 | 1.7 | 32.8 | 28.0 | 4.2 |
| Zone 2 | | | | | |
| 80 MHz | 10.0 | 1.7 | 23.3 | 31.0 | 0.6 |
| 40 MHz | 5.0 | 1.7 | 23.3 | 28.0 | 0.6 |
| Zone 3 | | | | | |
| 80 MHz | 2.5 | 1.7 | 29.2 | 31.0 | 0.5 |
| 40 MHz | 1.3 | 1.7 | 29.2 | 28.0 | 0.6 |
| Zone 4 | | | | | |
| 80 MHz | 10.0 | 1.7 | 23.5 | 31.0 | 0.8 |
| 40 MHz | 5.0 | 1.7 | 23.5 | 28.0 | 0.8 |

* Expected losses due to switches, output multiplex filters, and waveguide.

** Antenna gains include losses due to the beam-forming network and are based on lowest gain for the beam in any ocean region.

TABLE 8. SPOT BEAM e.i.r.p.

| COVERAGE | AMPLIFIER OUTPUT (W) | EXPECTED LOSSES* (dB) | ANTENNA GAIN** (dBi) | SPEC e.i.r.p. (dBW) | MARGIN (dB) |
|----------|----------------------------|-----------------------------|----------------------------|------------------------|----------------|
| E. Spot | 10 | 2.0 | 33.6 | 41.1 | 0.5 |
| W. Spot | 10 | 2.0 | 37.5 | 44.4 | 1.1 |

* Expected losses due to switches, output multiplex filters, and waveguide.

** Antenna gain scaled from INTELSAT V.

under INTELSAT contract with RCA. The TWTAs identified for each power level were either off-the-shelf or derivatives of off-the-shelf amplifiers, and it was assumed that they would be depressed multicollector designs for improved efficiency. The actual TWTAs used in the design and implementation of the INTELSAT VI spacecraft are identified in a companion paper by Horvai *et al.* [1].

Saturation flux density

Due to improved G/T performance, it was possible to increase the satellite sensitivity (*e.g.*, decrease the flux density required to achieve saturation) without increasing the up-link thermal noise. The flux density at the high-gain setting is established based on the performance of the hemi-to-hemi links operating with TDMA. Over the satellite lifetime, the flux density specifications permit a variation of ± 2 dB. Therefore, the worst-case condition occurs when the satellite is at the low limit of saturation flux density. Table 9 presents the link budgets for the TDMA case for a range of saturation flux densities. The minimum margin for a BER of 1×10^{-6} occurs at a saturation flux density of -79.6 dBW/m² and requires an earth station e.i.r.p. of 83.1 dBW. The high-gain specification was therefore selected to be -77.6 ± 2 dBW/m².

The saturation flux density at the low-gain setting is governed by the performance of the hemi-to-hemi links operating with multicarrier FDMA. The link budgets based on representative transponder loading plans (Table 10) demonstrate that the capacity per transponder should be approximately equal to that for INTELSAT V and V-A, for a low-gain saturation flux density of -67.1 dBW/m². In addition, a commandable $+4.5$ -dB gain step is incorporated in each channel receiver to allow an "ultra-high-gain" mode of operation, facilitating access by small earth stations. The corresponding saturation flux density is -82.1 dBW/m².

TABLE 9. TDMA LINK ANALYSIS AS A FUNCTION OF SATURATION FLUX DENSITY

| PARAMETER | SATURATION FLUX DENSITY (dBW/m ²) | | | | |
|---|--|-------|-------|-------|-------|
| | -81.6 | -80.6 | -79.6 | -78.6 | -77.6 |
| Up-Link | | | | | |
| Input Backoff (dB)* | 1.0 | 1.0 | 1.0 | 1.0 | 1.0 |
| G/T , Satellite (dB/K) | -8.5 | -8.5 | -8.5 | -8.5 | -8.5 |
| Path Loss (dB) | 200.7 | 200.7 | 200.7 | 200.7 | 200.7 |
| C/N , Thermal (dB) | 22.7 | 23.7 | 24.7 | 25.7 | 26.7 |
| C/I , Frequency Reuse (dB) | 19.2 | 19.2 | 19.2 | 19.2 | 19.2 |
| C/I , External Systems (dB) | 32.2 | 32.2 | 32.2 | 32.2 | 32.2 |
| $C/(N+I)$, Up-Link (dB) | 17.5 | 17.7 | 18.0 | 18.1 | 18.3 |
| Down-Link | | | | | |
| Saturation e.i.r.p. (dBW) | 31.0 | 31.0 | 31.0 | 31.0 | 31.0 |
| Output Backoff (dB) | 0.1 | 0.1 | 0.1 | 0.1 | 0.1 |
| Path Loss (dB) | 197.2 | 197.2 | 197.2 | 197.2 | 197.2 |
| G/T , Earth Station (dB/K) | 40.7 | 40.7 | 40.7 | 40.7 | 40.7 |
| C/N , Thermal (dB) | 25.2 | 25.2 | 25.2 | 25.2 | 25.2 |
| C/I , Frequency Reuse (dB) | 20.0 | 20.0 | 20.0 | 20.0 | 20.0 |
| C/I , External Systems (dB) | 32.2 | 32.2 | 32.2 | 32.2 | 32.2 |
| $C/(N+I)$, Down-Link (dB) | 18.7 | 18.7 | 18.7 | 18.7 | 18.7 |
| Link Degradations | | | | | |
| Adjacent Channel (dB) | 0.5 | 0.5 | 0.5 | 0.5 | 0.5 |
| Δ e.i.r.p. (dB) | 0.5 | 0.5 | 0.5 | 0.5 | 0.5 |
| Total $C/(N+I)$ (dB) | 14.0 | 14.2 | 14.3 | 14.4 | 14.5 |
| Total E_p/N_o (dB) | 11.0 | 11.2 | 11.3 | 11.4 | 11.5 |
| Margin w. FEC (dB) (BER = 1×10^{-6}) | 0.2 | 0.4 | 0.5 | 0.6 | 0.7 |
| Earth Station e.i.r.p. (dBW) | 81.1 | 82.1 | 83.1 | 84.1 | 85.1 |

* Minimum input backoff is taken as 1.0 dB.

TABLE 10. FDMA LINK ANALYSIS AS A FUNCTION OF SATURATION FLUX DENSITY (HEMI-TO-HEMI)

| PARAMETER | SATURATION FLUX DENSITY (dBW/m ²) | | | | | |
|-----------------------------------|--|-------|-------|-------|-------|-------|
| | -67.1 | -68.1 | -69.1 | -70.1 | -71.1 | -72.1 |
| Up-Link | | | | | | |
| <i>G/T</i> , Satellite (dB/K) | -8.5 | -8.5 | -8.5 | -8.5 | -8.5 | -8.5 |
| Input Backoff (dB) | 10.0 | 10.0 | 10.0 | 10.0 | 10.0 | 10.0 |
| Path Loss (dB) | 200.7 | 200.7 | 200.7 | 200.7 | 200.7 | 200.7 |
| <i>C/N</i> , Thermal Noise (dB) | 27.9 | 26.9 | 25.9 | 24.9 | 23.9 | 22.9 |
| <i>C/I</i> , Frequency Reuse (dB) | 20.7 | 20.7 | 20.7 | 20.7 | 20.7 | 20.7 |
| <i>C/(N + I)</i> , Up-Link (dB) | 19.9 | 19.7 | 19.5 | 19.3 | 19.0 | 18.6 |
| Intermodulation | 18.0 | 18.0 | 18.0 | 18.0 | 18.0 | 18.0 |
| Down-Link | | | | | | |
| Saturation e.i.r.p. (dBW) | 31.0 | 31.0 | 31.0 | 31.0 | 31.0 | 31.0 |
| Output Backoff (dB) | 5.6 | 5.6 | 5.6 | 5.6 | 5.6 | 5.6 |
| Path Loss (dB) | 197.2 | 197.2 | 197.2 | 197.2 | 197.2 | 197.2 |
| <i>G/T</i> , Earth Station (dB/K) | 40.7 | 40.7 | 40.7 | 40.7 | 40.7 | 40.7 |
| <i>C/N</i> , Thermal Noise (dB) | 19.4 | 19.4 | 19.4 | 19.4 | 19.4 | 19.4 |
| <i>C/I</i> , Frequency Reuse (dB) | 20.2 | 20.2 | 20.2 | 20.2 | 20.2 | 20.2 |
| <i>C/(N + I)</i> , Down-Link (dB) | 16.8 | 16.8 | 16.8 | 16.8 | 16.8 | 16.8 |
| Total <i>C/(N + I)</i> (dB) | 13.3 | 13.2 | 13.2 | 13.1 | 13.1 | 13.0 |
| Misc. Losses (dB) | 0.5 | 0.5 | 0.5 | 0.5 | 0.5 | 0.5 |
| Available <i>C/(N + I)</i> (dB) | 12.8 | 12.7 | 12.7 | 12.6 | 12.6 | 12.5 |

Filter Characteristics

The nominal 40-MHz transponder was originally developed for the INTELSAT IV system. At that time, an optimization [11] was performed to achieve the best possible utilization (maximize the communications capability) of the available 500 MHz of satellite bandwidth. Tradeoff parameters included the transponder guard band (a development program reduced the transponder guard band to 10 percent of the transponder bandwidth [12]), the transmitter TWT power, and the payload mass. The traffic assumed at that time

was predominantly frequency-division multiplexing (FDM)/FM telephony. The nonlinear channel characteristics, in conjunction with the in-band and out-of-band attenuation specifications, determine the intelligible crosstalk performance [13]. Since the nonlinear performance of the transmitter is usually given and cannot easily be modified, the intelligible crosstalk was controlled by the input multiplexer specifications. The use of linearizers on INTELSAT VI was considered, but not pursued because the behavior of linearized TWTAs with aging was not well understood at that time. In addition, consideration was given to adjacent transponder multipath, which influences the channel's amplitude and group delay characteristics. To minimize this effect—by keeping carriers located at the transponder's band edge from "leaking" through the adjacent transponder and being recombined with the original carrier with an arbitrary phase relation—the input multiplexer design requires stringent adjacent channel rejection. These factors resulted in a filtering distribution between the input and output multiplexers heavily weighted toward the input and less toward the output. The input multiplexer characteristics specified for INTELSAT VI could be met with an eight-pole elliptic function filter, with an output multiplexer having six poles or less.

The input multiplexers were assumed to be implemented at 4 GHz with the odd-even method of multiplexing (the method that had previously been used on INTELSAT V). All filters in the input multiplexers were assumed to be dual-mode, elliptic-function filters with an estimated eight poles. Input transponder group delay requirements for the 72-MHz C-Band channels are given in Figure 15. The input group delay is defined as the group delay measured between the input to the transmission channel (including the receive antenna) and the input of the final transmitter.

All 4-GHz output multiplexers were assumed to be of the contiguous-band type employing six poles, as used on INTELSAT V. Total transponder group delay requirements for the 72-MHz C-band channels are given in Figure 16. Total group delay is defined as the group delay measured between the input and output of the transmission channel (including the receive and transmit antennas).

Special requirements were placed on the amplitude and group delay characteristics for the signal paths through the SS-TDMA switching units of channels (1-2) and (3-4) to simplify the equalization of amplitude and group delay at the receiving earth station. Since TDMA bursts may originate in any of six up-link beams but may be switched into any down-link beam, the input multiplexer filter characteristics must be held within the tolerances shown in Table 11. This will enable the receiving earth station to use a single equalizer setting for all received bursts, regardless of the originating beam. Computer

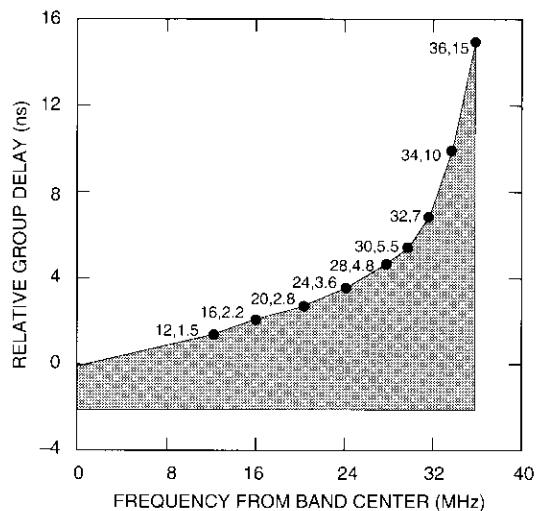


Figure 15. *Input Group Delay for 80-MHz Channels*

simulations were performed to examine the effect of worst-case variations in the amplitude and group delay. At a BER of 1×10^{-6} , a degradation of about 0.5 dB was observed over that obtained under nominal link conditions. This amount of degradation was considered acceptable, since a 1-dB margin was assumed in the modem specifications for imperfect equalization.

Gain flatness

The e.i.r.p. of any transmission channel is specified to vary by not more than 1.5 dB peak-to-peak over 90 percent of the usable transponder bandwidth for 80-MHz channels, and by no more than 1.3 dB peak-to-peak for 40-MHz channels. This specification is based on INTELSAT V experience; a tighter specification was judged to be impractical. Computer simulations of TDMA performance indicated that such a specification would cause only about 0.2 dB of degradation at a BER of 1×10^{-6} , with no compensating amplitude equalization. When amplitude equalization was used as specified in the TDMA specification, no degradation in performance was found. Consequently, this relaxation in the gain flatness specification was accepted.

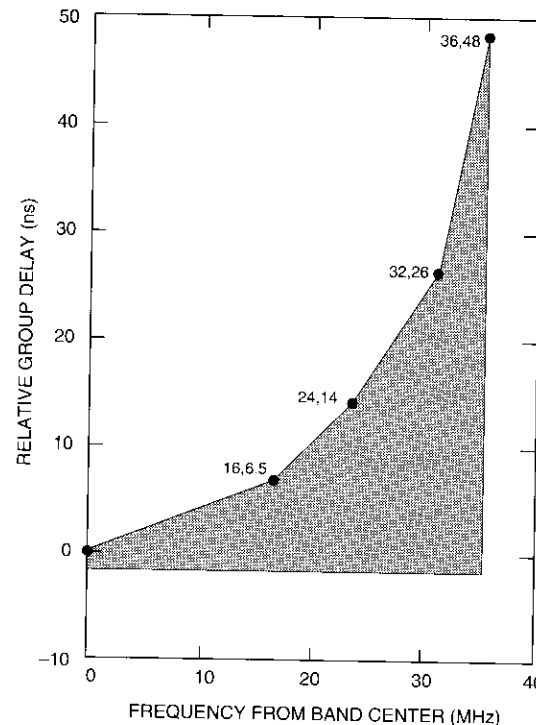


Figure 16. *Total Group Delay for 80-MHz Channels Transmitted at 4 GHz*

TABLE 11. PERCENT OF USABLE BANDWIDTH CENTERED ON CHANNEL CENTER FREQUENCY

| USABLE BANDWIDTH (%) | VARIATION IN GAIN/FREQUENCY RESPONSE (dB, p-p) | VARIATION IN GROUP DELAY RESPONSE (ns, p-p) |
|----------------------|--|---|
| 70 | 0.3 | 1.0 |
| 80 | 0.5 | 2.0 |
| 90 | 0.7 | 4.0 |
| 100 | 1.5 | 12.0 |

Differential path length variation

Differential path length variation through all paths of the SS-TDMA switching units must be held within a specified tolerance so that TDMA bursts originating from different input paths are not significantly offset in time from their target position with respect to one another. The specification for the peak-to-peak path length variation from any receive antenna input to the input of the dynamic switch shall not exceed 16 ns. To account for the possibility of transponder-hopping of the TDMA terminal, an additional requirement is placed on the differential path length variation which limits the peak-to-peak variation from any antenna input through the dynamic switch to the output of a transmit antenna to a tolerance not to exceed 32 ns. This value corresponds to slightly less than two TDMA symbols.

Nonlinear channel performance

INTELSAT VI is the first of the INTELSAT satellites to employ SSPAs. Although their use was not explicitly required in the specification, the potential for improved performance was recognized. In order not to prejudice the technical design, INTELSAT provided two sets of nonlinear specifications—one for TWTAs and the other for SSPAs—and bidders were given a choice of which to propose. Because performance with SSPAs was expected to be better than with TWTAs, the SSPA specification was tighter. The specifications for the TWTA channels were taken from the INTELSAT V specifications (Tables 12 through 14).

TABLE 12. OUTPUT TRANSMITTER PHASE SHIFT

| RELATIVE FLUX DENSITY* (dB) | MAXIMUM PHASE SHIFT (deg) | |
|--------------------------------|------------------------------|------|
| | TWTA | SSPA |
| 0 | 46 | 20 |
| 3 | 38 | 14 |
| 6 | 28 | 7 |
| 9 | 18 | 3 |
| 12 | 12 | 1 |
| 14 | 9 | 1 |

TABLE 13. AM-PM TRANSFER COEFFICIENT

| RELATIVE FLUX DENSITY* (dB) | AM-PM TRANSFER COEFFICIENT (°/dB) | |
|--------------------------------|--------------------------------------|------|
| | TWTA | SSPA |
| 0 | 8 | 2 |
| 3 | 9 | 2 |
| 6 | 9 | 2 |
| 9 | 8 | 2 |
| 12 | 5 | 1 |
| 14 | 3 | 1 |
| >14 | 3 | 1 |

* Measured below the flux density that produces single-carrier saturation.

TABLE 14. INTERMODULATION PRODUCT VALUES

| RELATIVE FLUX DENSITY PER CARRIER* (dB) | MAXIMUM CI/1** (dB) | |
|---|------------------------|------|
| | TWTA | SSPA |
| 3 | -10 | -12 |
| 10 | -15 | -25 |
| 17 | -26 | -38 |

* Flux density illuminating the spacecraft for each of two equal-amplitude carriers, below the flux density which produces single-carrier saturation.

** Maximum level of third-order intermodulation product relative to the level of each RF carrier, measured at the output of each transmission channel.

Definition of saturation

Figure 17 shows that the saturation level of an SSPA may not be as well defined as that of a TWTA. This is most pronounced in the SSPA built by Ford Aerospace Corporation (FAC) for which, as the input power is increased, the output power increases and reaches a plateau. Although there is no unique saturation point for the TWTA, there is a knee in the transfer curve beyond which further increase in input power yields very little or no increase in output power. Both SSPAs saturate and then fall off, although the saturation points are

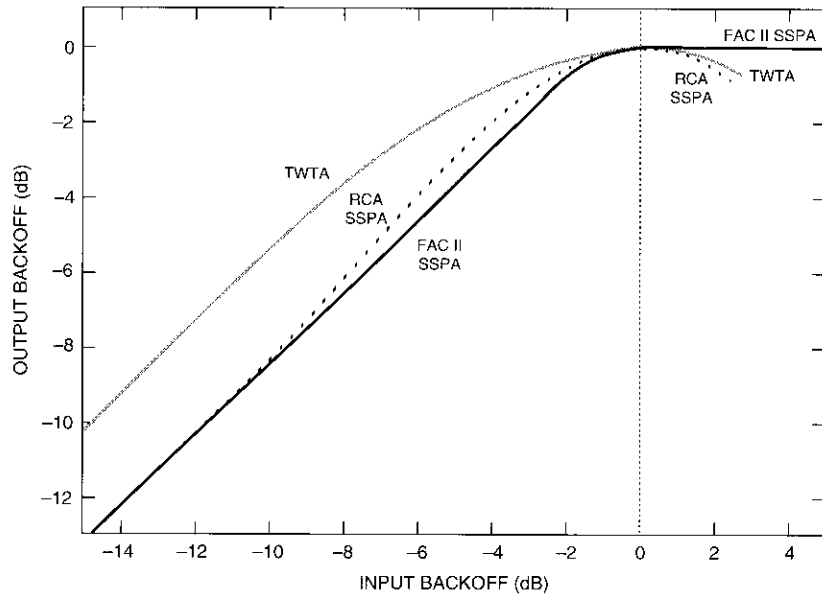


Figure 17. SSPA and TWTA Transfer Curves

approached quite slowly and are not graphically well defined. A reference point was defined for the SSPA which yields an output level nearly equal to the maximum output power, without overdriving the amplifier to a point that can cause unnecessary nonlinearity. The following definition was adopted and seems to meet this intent: "Saturation illumination for transmission channels using SSPAs is that illumination level which, when decreased by 1.5 dB, results in a decrease in e.i.r.p. of 0.25 dB." Figure 17 shows the application of this definition to the two SSPAs.

SSPA nonlinear characteristics

Table 15 derives a maximum phase shift specification which is easily met with designs similar to either the RCA or FAC SSPAs. Comparison with the TWTA performance given in Table 12 reveals that SSPA performance is significantly better.

Tables 16 and 17 show how the AM-PM transfer coefficient and carrier-to-intermodulation (C/I) ratio specifications were derived for the SSPA. Again, these specifications are significantly better than the corresponding TWTA specifications, as can be seen by comparison with Tables 13 and 14.

TABLE 15. MAXIMUM PHASE-SHIFT SPECIFICATION WITH SSPAs

| RELATIVE FLUX DENSITY* | MAXIMUM PHASE SHIFT | | SPEC. (deg) |
|------------------------|---------------------|--------|-------------|
| | RCA | FAC II | |
| 0 | 16.0 | 13.5 | 20 |
| 3 | 11.0 | 6.0 | 14 |
| 6 | 5.5 | 3.5 | 7 |
| 9 | 2.0 | 2.0 | 3 |
| 12 | 0.75 | 0.5 | 1 |
| 14 | 0.5 | 0.25 | 1 |

* Measured below the flux density that produces single-carrier saturation.

TABLE 16. AM/PM TRANSFER COEFFICIENT WITH SSPAs

| RELATIVE FLUX DENSITY* | AM-PM TRANSFER COEFFICIENT | |
|------------------------|----------------------------|--------------|
| | RCA | SPEC. (%/dB) |
| 0 | 1 | 2.0 |
| 3 | 1 | 2.0 |
| 6 | 1 | 2.0 |
| 9 | 1 | 2.0 |
| 12 | 0.5 | 1.0 |
| 14 | 0.2 | 1.0 |
| >14 | 0.2 | 1.0 |

* Measured below the flux density that produces single-carrier saturation.

TABLE 17. C/I SPECIFICATIONS WITH SSPAs

| RELATIVE FLUX DENSITY* | MAXIMUM C/I (dB) | | SPEC. |
|------------------------|------------------|--------|-------|
| | RCA | FAC II | |
| 3 | -13 | -15 | -12 |
| 10 | -28 | -32 | -25 |
| 17 | -41 | -41 | -38 |

* Measured below the flux density that produces single-carrier saturation.

Additional communications requirements

In addition to the communications parameters discussed above, there are numerous additional repeater characteristics which are essential for proper transmission performance of the satellite communications carriers. Some of these are discussed here.

Frequency stability

The stability of frequency translation between up- and down-link frequencies is an important design parameter for the receiver and up-converter local oscillators. The parameter is a compromise between complexity in the satellite and cost in the earth stations. The stability characteristics are usually grouped into long-term and short-term specifications. The long-term stability specifications are listed in Table 18.

These specifications were developed to have the earth station receive the satellite down-link signal in a predetermined frequency interval independent of the up- or down-link band used. The short-term frequency stability requirements result from the desire to keep phase noise contributions due to the satellite local oscillator to a negligible amount for any type of signal. Both short- and long-term specifications can be met with a local oscillator consisting of an overtone crystal followed by a multiplier chain.

TABLE 18. FREQUENCY STABILITY

| TRANSLATION (GHz) | STABILITY (parts) |
|--------------------------------------|----------------------|
| Long-Term* | |
| 6/4 | ± 10 in 10^6 |
| 6/11 | ± 4 in 10^6 |
| 14/4 | ± 2 in 10^6 |
| 14/11 | ± 7 in 10^6 |
| Over 1 mo., Excluding Eclipse | |
| 6/4 | ± 10 in 10^7 |
| 6/11 | ± 4 in 10^7 |
| 14/4 | ± 2 in 10^7 |
| 14/11 | ± 7 in 10^7 |

* Stability over lifetime, including initial tolerance and eclipse effects.

Spurious emissions

Spurious emissions from the satellite may interfere with its own communications signals, with other satellite communications services, with terrestrial services, or with other space-related activities such as radio astronomy. The maximum allowable power density (e.i.r.p.) for spurious emissions is -55 dBW in any 1-MHz band and -65 dBW in any 4-kHz band for any frequency within the transmit band at the input to each transmit antenna. It was assumed that these specifications would be met with filtering by the output multiplexer, complemented by a multioctave harmonic filter which prevents emissions above the communications bands.

Repeater isolation

In the repeater at 4-GHz, a channel frequency may be reused up to six times. The repeater isolation specification addresses interference between these paths. The worst isolation is likely to occur in the static and dynamic switch matrices. A specification of 50 dB has been set between statically switched channels, and 47 dB for dynamically switched channels.

Summary and conclusions

This paper has attempted to describe the performance characteristics of the INTELSAT VI satellite and give some insight into the technical considerations that formed the basis for development of the satellite performance specifications. As described, many new technologies were factored into the design and resulting specifications in order to maximize the satellite's capacity and performance while minimizing payload mass and power. Some of the new technologies ultimately employed in the implementation of INTELSAT VI include SS-TDMA, SSPAS, an expanded frequency band at C-band, sixfold frequency reuse at C-band, and dual-polarized global beams. It is anticipated that the INTELSAT VI series of satellites will prove to be quite successful.

Acknowledgments

The development of the INTELSAT VI payload performance specifications was the work of many, including contributors from the INTELSAT Executive Organ, the INTELSAT Board of Governors Technical Advisory Committee, and COMSAT Laboratories. The successful development of these specifications would not have been possible without the dedicated efforts of these individuals.

References

- [1] G. Horvai *et al.*, "INTELSAT VI Communications Subsystem Design," scheduled for publication in *COMSAT Technical Review*, Vol. 21, No. 1, Spring 1991.
- [2] R. R. Persinger *et al.*, "The INTELSAT VI Antenna System," scheduled for publication in *COMSAT Technical Review*, Vol. 21, No. 1, Spring 1991.
- [3] S. J. Campanella *et al.*, "SS-TDMA System Considerations," *COMSAT Technical Review*, Vol. 20, No. 2, Fall 1990, pp. 335-371 (this issue).
- [4] R. K. Gupta *et al.*, "SS-TDMA On-Board Subsystem Design," scheduled for publication in *COMSAT Technical Review*, Vol. 21, No. 1, Spring 1991.
- [5] C. L. Maranon *et al.*, "Timing Source Oscillator Control," scheduled for publication in *COMSAT Technical Review*, Vol. 22, No. 1, Spring 1992.
- [6] A. I. Zaghoul, R. R. Persinger, and D. F. DiFonzo, "Design Optimization Procedures for Multi-Feed Satellite Shaped-Beam Antennas," 11th European Microwave Conference, Amsterdam, The Netherlands, September 1981, *Proc.*, pp. 540-545.
- [7] A. Ghais *et al.*, "Summary of INTELSAT VI Communications Performance Specifications," *COMSAT Technical Review*, Vol. 12, No. 2, Fall 1982, pp. 413-429.
- [8] S. J. Campanella, B. A. Pontano, and J. L. Dicks, "Advantages of TDMA and Satellite-Switched TDMA in INTELSAT V and VI," *COMSAT Technical Review*, Special Issue on TDMA: Pt. 2, Vol. 16, No. 1, Spring 1986, pp. 207-238.
- [9] T. Inukai, "An Efficient SS/TDMA Time Slot Assignment Algorithm," *IEEE Transactions on Communications*, Vol. COM-27, No. 10, October 1979, pp. 1149-1155.
- [10] J. A. Lunsford *et al.*, "SS-TDMA System Design," scheduled for publication in *COMSAT Technical Review*, Vol. 22, No. 1, Spring 1992.
- [11] P. L. Bargellini, ed., "The INTELSAT IV Communications System," *COMSAT Technical Review*, Vol. 2, No. 2, Fall 1972, pp. 437-572.
- [12] A. E. Williams, "A Four-Cavity Elliptic Waveguide Filter," *IEEE Transactions on Microwave Theory and Techniques*, Vol. MTT-18, No. 12, December 1970, pp. 1109-1114.
- [13] A. L. Berman and C. E. Mahle, "Nonlinear Phase Shift in Travelling-Wave Tubes as Applied to Multiple Access Communications Satellites," *IEEE Transactions on Communication Technology*, Vol. COM-18, No. 1, February 1970, pp. 37-48.



Benjamin A. Pontano received a B.S.E.E. from Carnegie Institute of Technology in 1965, and an M.S.E.E. and Ph.D. from the Pennsylvania State University in 1967 and 1970, respectively. He has been with COMSAT Laboratories for 10 years and is currently Executive Director of the Network Technology Division, where he directs research and development activities in the area of advanced network systems. In this capacity, he was responsible for the development of NASA's Advanced Communications Technology Satellite (ACTS) TDMA terminal equipment. He has also been involved with numerous technical and economic studies on advanced communications satellite systems.

Dr. Pontano was previously with INTELSAT for 10 years, where he was actively involved in development of the INTELSAT TDMA system and system design of the INTELSAT VI communications payload. He has written more than 40 papers in the field of satellite communications, and holds patents in the area of interference measurement and cancellation. He has taught graduate-level courses in the field of communications systems at the George Washington University. Dr. Pontano is a Senior Member of IEEE and a member of AIAA and Sigma Xi.

Amir I. Zaghoul received a B.Sc. from Cairo University, Egypt, in 1965, and an M.A.Sc. and Ph.D. from the University of Waterloo, Canada, in 1970 and 1973, respectively, all in electrical engineering. He also received an MBA from the George Washington University in 1989. Prior to joining COMSAT Laboratories in 1978, he held faculty positions at the University of Waterloo and Toronto, Canada, and at Aalborg University in Denmark. At COMSAT Laboratories, he has been a member of the Microwave Technology and Systems Division, where he is presently Manager of the Satellite Systems Department.



His responsibilities have included the study, design, and development of microwave integrated circuits, microwave switch matrices for SS-TDMA systems, multibeam antennas, phased-array systems, microstrip antennas, reflector antenna systems, and future satellite systems. He has also been involved in study and support efforts for several satellite programs. Dr. Zaghoul is a Senior Member of IEEE; a Senior Member of AIAA; a Member of the Electromagnetics Academy; past Chairman of the Washington, D.C., Chapter of the IEEE Antennas and Propagation Society; and recipient of the 1986 H. A. Wheeler Applications Prize Award for best applications paper in IEEE Transactions on Antennas and Propagation. He is also a co-recipient of the 1986 COMSAT Laboratories Research Award, and of COMSAT's Exceptional Invention Award in 1990.



Christoph E. Mahle received the Dipl. Ing. and Dr. S.C. Tech. degrees from the Swiss Federal Institute of Technology in 1961 and 1966, respectively. He joined COMSAT Laboratories in 1968 as a Member of the Technical Staff in the Transponder Department. In 1983, he was appointed Executive Director of the Microwave Technology Division, where he directed R&D in areas such as high-technology microwave circuits for satellites and earth stations, MMICs, satellite transponder performance, antennas, microwave systems, optical communications, and wave propagation. He also served as Acting Director of the newly formed Micro-

electronics Division, which was set up to combine COMSAT's efforts in analog and digital GaAs integrated circuits.

Dr. Mahle is currently Executive Director of the Satellite Technologies Division at COMSAT Laboratories, directing R&D in such areas as spacecraft bus technologies, microwave circuits for satellites and earth stations, analysis and verification of satellite transponder performance, microwave systems, and radio wave propagation. He designed and evaluated communications transponders for the INTELSAT IV, IV-A, and COMSTAR programs, and was responsible for the design, development, and testing of the transponder orbited on ATS-6 as part of the COMSAT Propagation Experiment. In addition, he advanced the state of the art of automated satellite in-orbit measurements. He is a Fellow of IEEE, has published numerous papers, and has been awarded several U.S. patents.

Index: communication satellites, INTELSAT, propulsion, feasibility analysis, spacecraft configuration

Specifying the spacecraft bus

G. P. CANTARELLA AND G. PORCELLI

(Manuscript received October 12, 1990)

Abstract

This paper describes how specifications for the INTELSAT VI spacecraft bus were generated. In early 1980, a conceptual design was developed to verify the feasibility of implementing the INTELSAT VI mission requirements within the lift-off mass and volume constraints of the launch vehicles being considered. A second goal was to generate specifications that were not only realistic, but also more general than those applicable solely to the baseline design.

Introduction

The INTELSAT VI spacecraft, as originally conceived [1],[2], relied on launch by the Space Transportation System (STS) as early as 1985. However, due to STS schedule slippage and uncertainties regarding the availability of a sufficient number of STS launches in the post-1985 time frame, INTELSAT decided to consider the use of Titan/Inertial Upper Stage (IUS) and Ariane 4 as alternative launch vehicles. Consequently, the INTELSAT VI spacecraft design had to be compatible with all three launch vehicles.

To assess the technical feasibility of implementing the INTELSAT VI mission requirements within the lift-off mass and volume constraints of the three launch vehicles, and in order to generate realistic performance specifications for INTELSAT VI, INTELSAT initiated a feasibility study of this spacecraft in early 1980 with the support of COMSAT Laboratories. A body-stabilized spacecraft configuration similar to INTELSAT V was selected. Initial mass model predictions for INTELSAT VI using INTELSAT V technology resulted in a spacecraft mass too high for some of the launch systems being considered. To alleviate this problem, the application of advanced technologies in various subsystems was examined.

Even though the feasibility study considered only a three-axis-stabilized spacecraft, the performance specifications in the INTELSAT VI Request for Proposal (RFP) were more general than the conceptual design and covered the requirements of both spin-stabilized and body-stabilized spacecraft. Two proposals were received in response to this RFP. The proposal submitted by Ford Aerospace Corporation offered a three-axis-stabilized spacecraft configuration, while Hughes Aircraft Company (HAC) offered a spin-stabilized configuration. Proposal evaluation is discussed by Podraczky and Schnicke [1]. The contract was eventually awarded to HAC.

Mass, volume, and size assessments

The mass of the spacecraft was driven primarily by the requirements of the payload (the antenna and the communications subsystems) and by its operational life. Volume and size were determined based on the constraints of the available launch vehicles. This section gives details regarding these design drivers.

Antenna coverage and beam isolation requirements

The antenna coverage requirements at 6/4-GHz in the Atlantic Ocean Region (AOR), the Indian Ocean Region (IOR), and the Pacific Ocean Region (POR) were assumed to be met by the following:

- Two hemispheric beams operating in one polarization (left-hand circular)
- Four zone beams operating in the orthogonal polarization (right-hand circular)
- One dual-polarized global beam.

The antenna coverages at 14/11 GHz were assumed to be obtained by means of two spot beams, identical to those of INTELSAT V, operating in single polarization. Traffic and coverage requirements development is discussed by Perillan *et al.* [2] and by Pontano *et al.* [3]. Reference 3 also provides details on antenna tradeoffs and specifications.

Antenna subsystem design

The INTELSAT VI antenna design considered in the feasibility study was a relatively straightforward extrapolation of the INTELSAT V design. The hemi/zone antenna configuration consisted of two offset parabolic reflectors, with combined hemi and zone feed networks.

Analysis of the coverage requirements showed that the minimum separation between two adjacent zone beams occurred in the AOR for the primary orbital location (335.5°E). The two beams involved, shown in Figure 1, were the northeast zone beam and the middle-east/southeast zone beam. The pair of earth stations for which minimum separation occurred were Fucino, Italy, and Arbaniyeh, Lebanon, for a nominal separation of 2.15°. The actual separation, taking into account spacecraft pointing errors ($\pm 0.25^\circ$ in pitch and roll, and $\pm 0.5^\circ$ in yaw) was 1.65°. This minimum separation dictated the reflector diameter. Assuming a 27-dB spatial isolation requirement between zone beams, the reflector diameter at 3.7 GHz was estimated to be approximately 4.5 m.

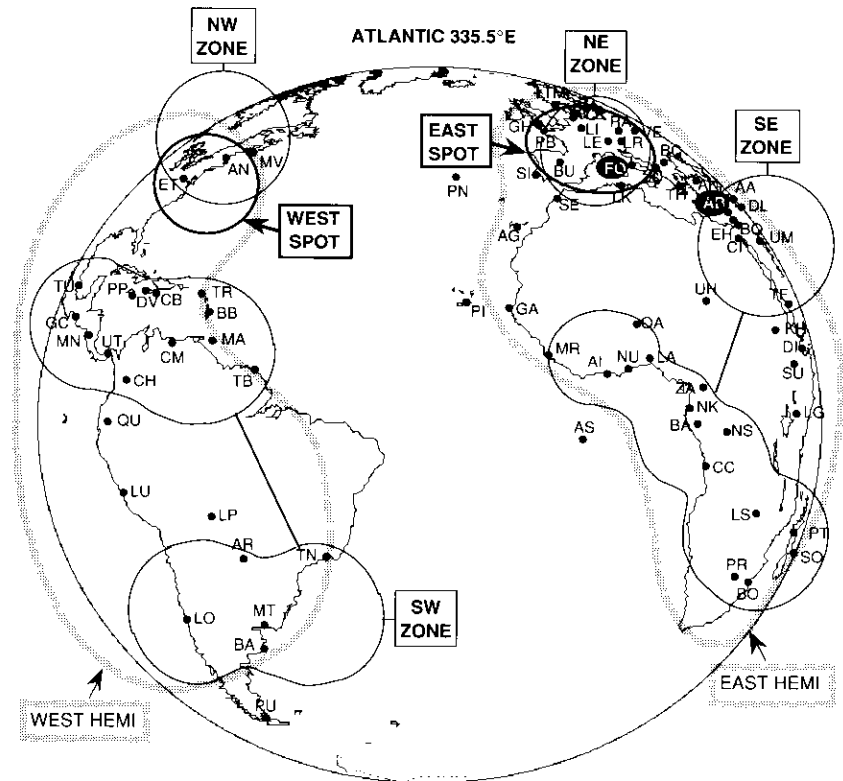


Figure 1. Coverage Requirement at 335.5°E

The elemental beam width was assumed to be 2° , and the total number of feeds required to generate the hemi/zone coverage was estimated at approximately 150 feeds per reflector. The hemi/zone antenna geometry is shown in Figure 2.

The estimated dimensions of the 6/4-GHz hemi/zone antenna and the 14/11-GHz east spot/west spot antenna are given in Table 1. The overall mass of the antenna subsystem, excluding the supporting tower, was estimated to be approximately 150 kg. The design of the antenna systems is discussed in a companion paper by Persinger *et al.* [4].

TABLE 1. ANTENNA DIMENSIONS

| ANTENNA | D (m) | h (m) | f (m) | θ | α | a (m) |
|---------------------|------------|------------|------------|------------|------------|------------|
| 4-GHz Hemi/Zone | 4.5 | 1.5 | 4.5 | 43° | 10° | 1.8 |
| 6-GHz Hemi/Zone | 2.75 | 0.9 | 2.75 | 41° | 10° | 1.0 |
| 14/11-GHz East Spot | 1.0 | 0.62 | 1.0 | 39° | 10° | — |
| 14/11-GHz West Spot | 1.6 | 0.44 | 1.6 | 41° | 10° | — |

Transponder subsystem mass and power estimates

The salient features of the INTELSAT VI transponder channelization plan assumed in the feasibility study, and shown in Figure 3, are as follows:

- Sixfold frequency reuse at 6/4 GHz in transmission channels 1 through 9.
- Dual-polarized global coverage in transmission channels 10, 11, and 12.
- 80-MHz channelization of the 14/11-GHz band in transmission channels 1 through 8. (Transmission channels [9–12] were not partitioned due to the mass constraints of the then-unproven Ariane 4.)
- Satellite-switched time-division multiple access (SS-TDMA) implementation at 6/4 GHz in transmission channels (1–2) and (3–4).

The overall mass of the INTELSAT VI transponder subsystem was estimated at approximately 345 kg, and its power requirement at 1,400 W. Details regarding transponder and SS-TDMA specification development are provided in Pontano *et al.* [3].

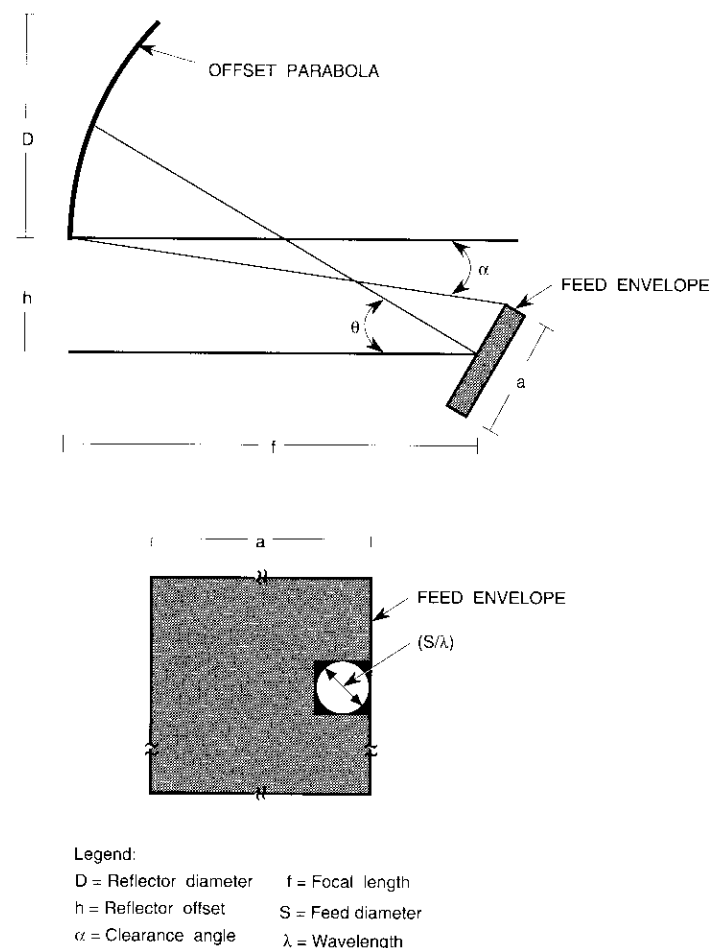
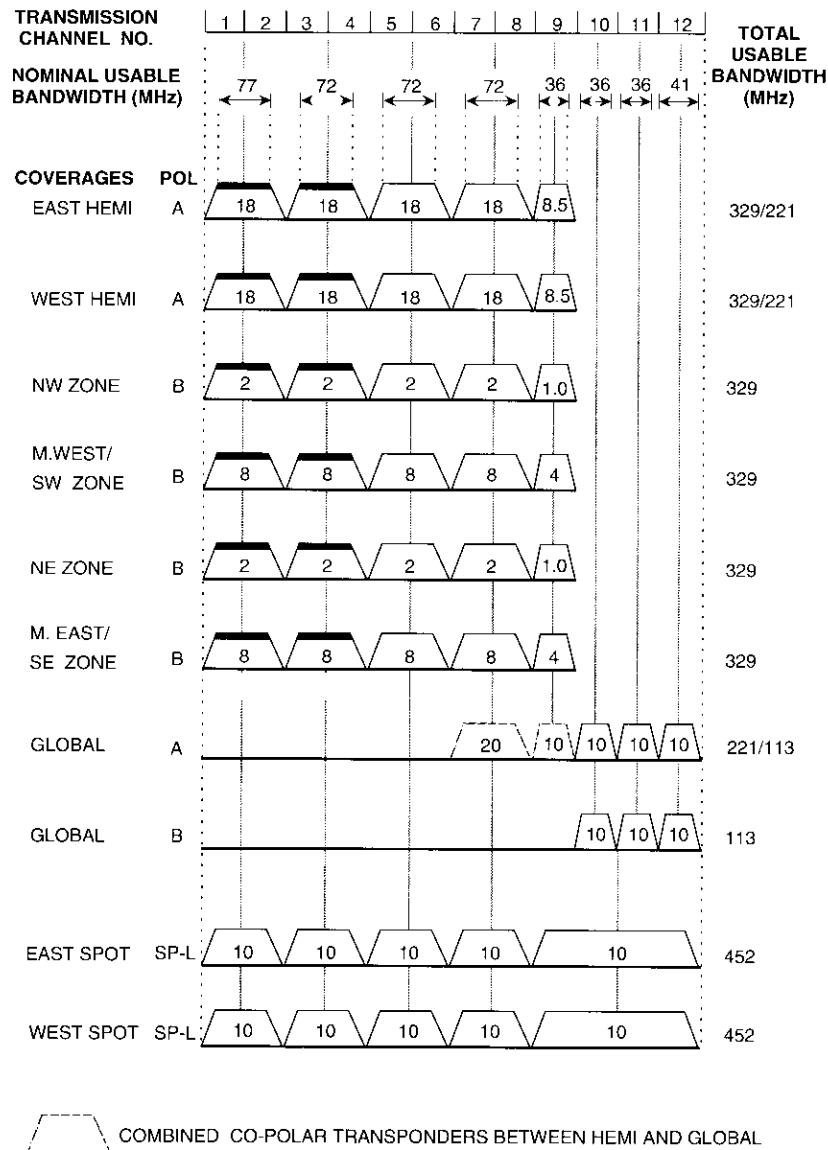


Figure 2. Hemi/Zone Antenna Geometry

Dry spacecraft mass

The INTELSAT satellite mass and power prediction model was used initially to estimate the requirements of individual subsystems and to provide the overall dry spacecraft mass, which totaled approximately 1,400 kg.



Note: Figures shown within transponders are output power levels in watts.

Figure 3. INTELSAT VI Transponder Plan

Launch vehicle considerations

At the time of the feasibility study (March–April 1980), system requirements dictated that INTELSAT VI be on-station in the 1985 to 1990 time frame. In that time frame, the choice of launchers was at best uncertain. The STS launch planned for this period had encountered numerous problems and its availability was in question. Until the first four test flights of the STS were successfully flown, the availability of such a new concept had to remain open. If major problems developed in the future with the STS, it was conceivable that expendable launchers would have to continue to serve launch vehicle requirements into the later 1980s.

The Ariane expendable launcher program was somewhat ahead of the STS, having had its first successful launch in December 1971. This first of four test flights due to be completed in 1980 would lead to operational flights of Ariane 1 beginning in 1981. Development of Ariane 2/3 began in 1980 and the vehicle was planned to become operational in 1982/1983, while long-range plans called for Ariane 4 to be available in 1984.

The launch vehicles considered for the INTELSAT VI spacecraft were Ariane 4, Titan/IUS, STS/IUS, and STS/perigee kick motor (PKM). The fairing dimensions and geosynchronous orbit payload capabilities of the various launch vehicles are given in Table 2. A review of the capabilities of these launch vehicles indicates that the Ariane 4 fairing dimensions determined the spacecraft volume constraints, whereas the mass constraints were imposed by the Titan/IUS launcher.

TABLE 2. INTELSAT VI LAUNCH VEHICLES

| SYSTEM | FAIRING DIAMETER (STATIC ENVELOPE) (m) | DELIVERED PAYLOAD (kg) | |
|-----------|--|------------------------|----------------|
| | | TRANSFER ORBIT | GEO SYNC ORBIT |
| Ariane 4 | 3.65 | 3,300–3,500 | NA* |
| Titan/IUS | 3.7 | NA | 1,741 |
| STS/IUS | 4.6 | NA | 2,268 |
| STS/PKM | 4.6 | Open | Open |

*Not applicable.

Ariane 4 and Titan/IUS configurations

The goal of the spacecraft design was to meet the Ariane 4 volume constraints. The size of the hemi/zone antenna reflectors, and the required focal length ($f/D = 1$), lead to a design that used deployable reflectors and a tall feed tower to provide the necessary view angles. Compounding the view angle situation were the large feed structures necessary for the 6/4-GHz antenna. The 4.57-m-diameter reflector also presented a stowage problem, since the diameter of the Ariane 4 fairing was only 3.65 m. An unfurlable antenna design concept used by previous spacecraft, including ATS-6, was selected to resolve this dilemma.

In order to reduce the height of the antenna tower so that it could fit into the Ariane 4 fairing, the 4-GHz hemi/zone reflector was envisioned to be attached at the side of the spacecraft body. This configuration resulted in relocation of the east-west thrusters to reduce plume impingement on the antenna reflector.

The spot beam reflectors were also envisioned to be mounted on the antenna tower structure. Both 14/11-GHz (Ku-band) reflectors had to be stowed for launch and deployed in orbit in order to clear the large feed array associated with the 3.7-GHz antenna. The solar array was assumed to be stowed on the north and south faces of the main spacecraft body.

STS/IUS and STS/PKM configurations

Figure 4 shows a conceptual design of INTELSAT VI, together with the IUS, installed in the STS cargo bay. The structure supporting the spacecraft and IUS within the cargo bay would also eject the spacecraft-IUS combination at the appropriate time. A similar arrangement would be required for the spacecraft-PKM combination.

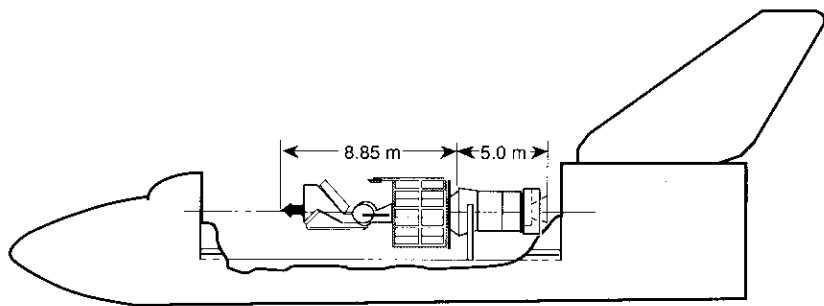


Figure 4. Spacecraft With IUS Installed in STS

Geosynchronous orbit configuration

In the conceptual design, the difference between the launch configuration and the geosynchronous orbit configuration lay in the way the solar array and antennas were deployed. The main body was a box-shaped structure, 1.88 × 3.14 × 2.4 m. The total height of the spacecraft was 8.68 m, including 5.70 m for the antenna tower. Each wing of the solar array had a yoke and two empty panels to avoid shadowing of the 4-GHz antenna by the solar array. The need to reduce the antenna tower height due to Ariane fairing limitations was the primary driver for placing the 4-GHz antenna on the east panel. The antenna tower height could have been decreased further, but this would have increased the antenna offset and the length of the reflector support arm.

The total spacecraft power requirement for geosynchronous orbit was estimated at 2,226 W. The solar array was designed for a 2.7-kW end-of-life (EOL), and the batteries were designed to provide a maximum of 1,785 W during eclipse. The total dry spacecraft mass was estimated at 1,348 kg.

Propulsion studies

The propulsion requirements for INTELSAT VI were derived from two primary requirements. The first was spacecraft compatibility with the Titan/IUS launcher, whose geosynchronous orbit payload delivery capability was assessed at 1,741 kg. The second was a 7-yr minimum life on-station.

Baseline and alternatives

The baseline design used monopropellant hydrazine for all low-thrust phases, either in transfer orbit (when applicable) or in final orbit, and a solid propellant apogee motor for final orbit insertion. Two alternative design approaches were evaluated in terms of potential weight reduction: a bipropellant system for all low-thrust phases, with a solid propellant apogee motor, and an all-bipropellant system for both the low-thrust phases and the apogee orbit insertion. The propulsion systems were analyzed for compatibility with the following launch vehicles:

- Titan/IUS (1,741 kg in geosynchronous orbit)
- STS/PKM
- Ariane 4 (3,300 kg in geosynchronous transfer orbit).

Extensive analyses were conducted to determine the propellant requirements and to select the apogee kick motor (AKM)—or alternatively to assess the liquid propellant required for geosynchronous orbit insertion. Because the

analyses were based on the weight-limiting payload delivery capability of the Titan/IUS, the propellant requirements for boosters such as the STS/PKM or Ariane 4 were computed for the spacecraft mass relative to Titan/IUS, incremented by the burn-out weight of the AKM (or by the additional tankage weight of an all-liquid system), plus the extra propellant required by the greater EOL weight. Iterations were performed to refine the estimates.

Although the final choice for INTELSAT VI was a spin-stabilized spacecraft configuration, it is relevant to note that all the preliminary analyses were based on a three-axis configuration. Thus a 16-thruster positioning and orientation propulsion system (POPS) configuration similar to that of INTELSAT V was assumed.

One concern regarding this spacecraft design was to locate the thruster for minimum interference between the thruster plumes and the large and obstructively located antenna reflectors. Plumes impinging on these surfaces

TABLE 3. MONOPROPELLANT SUBSYSTEM COMPONENTS

| ITEM | NUMBER | UNIT MASS (kg) | TOTAL MASS (kg) |
|---|--------|-------------------|--------------------|
| POP Thruster | 16 | 0.3 | 5.0 |
| Propellant Tanks (Internal diameter = 74 cm) | 4 | 10.5 | 42.0 |
| Valves | | | |
| Latch | 4 | 0.35 | 1.4 |
| Fill/Drain | 4 | 0.1 | 0.4 |
| Filters | 2 | 0.2 | 0.4 |
| Transducers | 2 | 0.2 | 0.4 |
| Plumbing | | | 3.0 |
| Bracket and Alignment | | | <u>7.0</u> |
| | | | 59.6 |
| Pressurant (N ₂) | | | 6.0 |
| Residuals (approx. 0.5% of tank volume) | | | <u>4.0</u> |
| | | | 10.0 |

Monopropellant Hydrazine: Mass = 430 kg; Volume = 0.43 m³
Tank Volume: 0.86 m³

would cause pressure and drag, producing disturbance torques and reducing the effective thrust, which in turn would require increased thruster firings and propellant consumption. Also, heat transfer from the plume would heat the structures impinged upon. Thermal failures were not expected, but distortion was a concern. Means of alleviating the problem of impingement on the large antenna, such as splitting the function of the eastward-firing thruster into two thrusters located on the edges of the east side of the spacecraft in the roll-yaw plane, were considered. (Augmented electrothermal hydrazine thrusters were not considered in the baseline due to uncertainties in development.)

Estimates of components and masses for the POPS in the baseline and the two alternative configurations mentioned above are given in Tables 3, 4, and 5, respectively. The scheme for a POPS in the all-liquid propellant alternative is provided in Figure 5.

TABLE 4. BI-PROPELLANT POPS COMPONENTS

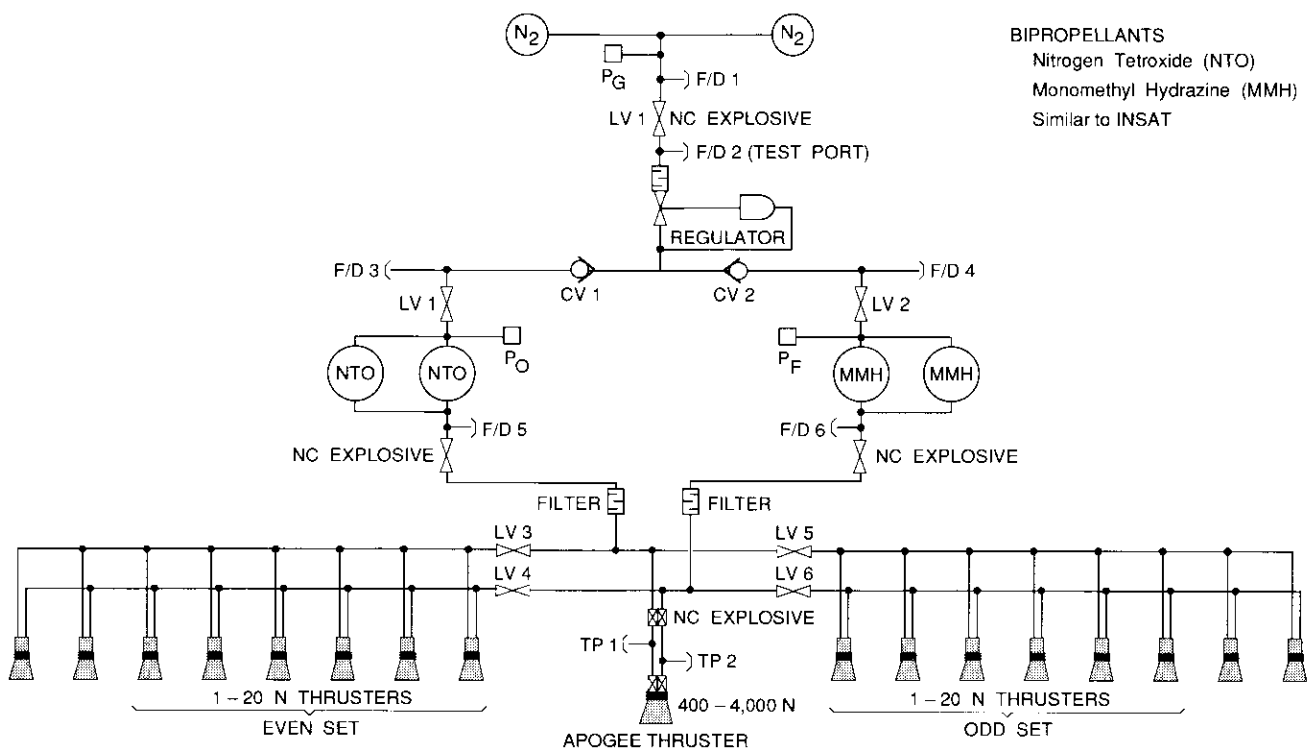
| ITEM | NUMBER | UNIT MASS (kg) | TOTAL MASS (kg) |
|---|--------|-------------------|--------------------|
| Propellant Tanks (Internal diameter = 66 cm) | 4 | 7.50 | 30.0 |
| Thrusters (20 N) | 16 | 0.56 | 9.0 |
| Valves | | | |
| Latch | 8 | 0.35 | 2.8 |
| Fill/Drain | 4 | 0.1 | 0.4 |
| Filters | 4 | 0.2 | 0.8 |
| Transducer | 4 | 0.2 | 0.8 |
| Plumbing | | | 8.0 |
| Brackets and Alignment | | | 8.0 |
| | | | 59.8 |
| Pressurant (N ₂) | | | 4.0 |
| Residuals (2%) | | | 6.0 |
| | | | 10.0 |

Total Propellant Mass, $M_p = 340$ kg
Oxidizer Mass, $M_{OX} = 209$ kg
Fuel Mass, $M_f = 131$ kg
Oxidizer Volume, $V_{OX} = 0.16$ m³
Fuel Volume, $V_f = 0.16$ m³

TABLE 5. COMBINED APOGEE AND POPS COMPONENTS

| ITEM | NUMBER | UNIT MASS (KG) | TOTAL MASS (KG) |
|---|--------|----------------|-----------------|
| Pressurant Tank | 2 | 12.5 | 25.0 |
| Valves | | | |
| Fill/Drain | 6 | 0.1 | 0.6 |
| Pyroactuated | 5 | 0.18 | 0.9 |
| Check | 2 | 0.1 | 0.2 |
| Regulator | 1 | 1.3 | 1.3 |
| Filter | 3 | 0.3 | 0.9 |
| Transducer | 3 | 0.2 | 0.6 |
| Latch | 10 | 0.35 | 3.5 |
| Thruster | | | |
| Apogee (3 kN) | 1 | 6.0 | 6.0 |
| AOC (20 N) | 16 | 0.56 | 9.0 |
| Propellant Tanks (Internal diameter = 96 cm) | 4 | | 93.0 |
| Plumbing | | | 141.0 |
| Brackets and Alignment | | | 10.0 |
| Pressurant (N ₂) = $\rho \times V \times P_f$ | | | 9.0 |
| Residuals (1%) | | | 160.0 |
| | | | 14.0 |
| | | | 19.0 |
| | | | 33.0 |

AOC: Attitude and orbit control
 Total Propellant Mass, $M_p = 1,856$
 Oxidizer Mass, $M_{ox} = 1,142$ kg
 Fuel Mass, $M_f = 714$ kg
 Oxidizer Volume, $V_{ox} = 0.875$ m³
 Fuel Volume, $V_f = 0.875$ m³
 $\rho = N_2$ density = 1.25 kg/m³
 $V =$ Propellant tank vol. = 1.86 m³
 $P_f =$ EOL tank pressure = 6 atm



BIPROPELLANTS
 Nitrogen Tetroxide (NTO)
 Monomethyl Hydrazine (MMH)
 Similar to INSAT

Figure 5. Combined Apogee and POPS

While the baseline design was motivated by conservatism, the alternatives, particularly the all-liquid approach, were gaining favor due to the significant mass/life advantages accruing from the higher performance of the bipropellants. In the bipropellant/solid AKM alternative, the Thiokol Star-48 solid rocket motor, having a burnout weight lower than the estimated corresponding bipropellant system EOL weight, appeared to offset the advantage of the higher bipropellant performance, I_{sp} , as described later.

A preliminary analysis of the velocity increments required for the INTELSAT VI mission is summarized in Table 6.

Results of a propulsion system weight tradeoff are presented in Table 7. The tradeoff indicated that the best weight savings would be obtained by using bipropellant for all low-thrust functions and a solid AKM for the apogee boost. This was in part the result of relatively higher inert weights estimated in the all-liquid system, and in part due to the availability of an efficient AKM (the original design of the Star-48).

The bipropellant/solid AKM also offered the advantage of avoiding the potentially critical effects of large amounts of liquid propellant on the stability of the spacecraft in transfer orbit, if apogee insertion were to be performed in the spin mode.

TABLE 6. ESTIMATED VELOCITY INCREMENT REQUIREMENTS

| FUNCTION | VELOCITY INCREMENT (m/s) |
|--------------------------------------|--------------------------|
| Apogee Insertion | |
| Shuttle/PKM | 1,738.0* |
| Ariane 4 | 1,487.4** |
| Dispersion Correction | |
| Shuttle/PKM | 81.1 |
| Ariane 4 | 57.9 |
| Titan/IUS | 16.0 |
| 1st Repositioning (BOL) at 2°/day | 11.6 |
| N-S Stationkeeping (1987-1993, 7 yr) | 336.5 |
| E-W Stationkeeping (7 yr) | 12.8 |
| 2nd Repositioning (FOL) at 2°/day | 11.6 |
| Final De-Orbiting (+185 km) | 6.7 |

*Based on 300 x 36,900 km, 27.0° transfer orbit.

**Based on 185 x 35,788 km, 8.5° transfer orbit.

TABLE 7. PROPULSION SYSTEM MASS TRADEOFF (kg)

| PROPULSION SYSTEM | TITAN/IUS | STS/PKM | ARIANE 4 |
|--------------------------|-----------|---------|----------|
| Monopropellant/Solid AKM | | | |
| Hydrazine | 321.8 | 436.8 | 417.4 |
| Dry Mass | 60.0 | 60.0 | 60.0 |
| Pressure + Residual | 10.0 | 10.0 | 10.0 |
| Solid Propellant | - | 1,619.0 | 1,314.0 |
| AKM Burnouts | - | 83.0 | 83.0 |
| Total (baseline) | 391.8 | 2,208.8 | 1,884.4 |
| Bipropellant/Solid AKM | | | |
| Bipropellant | 247.2 | 316.0 | 321.3 |
| Dry Mass | 60.0 | 60.0 | 60.0 |
| Pressure + Residual | 10.0 | 10.0 | 10.0 |
| Solid Propellant | - | 1,522.3 | 1,315.9 |
| AKM Burnouts | - | 83.0 | 83.0 |
| Total | 317.2 | 1,991.3 | 1,790.2 |
| Mass Saving | 74.6 | 217.5 | 94.2 |
| All-Liquid | | | |
| Bipropellant | - | 1,808.7 | 1,603.5 |
| Dry Mass | - | 160.0 | 160.0 |
| Pressure + Residual | - | 33.0 | 33.0 |
| Total | - | 2,001.7 | 1,796.5 |
| Mass Saving | - | 207.1 | 87.9 |

AKM selection

The AKM selected for the INTELSAT VI baseline design, and for the alternative using a solid propellant apogee motor, was the Thiokol Star-48 motor in its original spherical design (*i.e.*, prior to a 6-inch case stretching requested by McDonnell Douglas Astronautics Company for the Payload Assist Module Program). The original design was selected because it was much closer in mass to the INTELSAT VI requirements. (The stretched version would have required off-loadings in the range of 22 to 38 percent, while the original design required them in a range of 7.6 to 26 percent.)

The mass, component, and performance characteristics of the fully loaded motor are presented in Tables 8, 9, and 10, respectively. Figure 6 is an assembly diagram showing the dimensions of the motor configuration, while Figure 7 shows the predicted thrust profile.

The design of the INTELSAT VI spacecraft bus is described in detail by Dest *et al.* [5].

TABLE 8. STAR-48 MASS SUMMARY

| COMPONENT | MASS (kg) |
|-----------------------------|-----------|
| Case | 47.0 |
| Insulation | 19.9 |
| Liner | 0.5 |
| Nozzle and Igniter Assembly | 24.5 |
| Initiator | 0.4 |
| Misc. Hardware | 0.7 |
| Total Mass | 93.0 |
| Propellant | |
| Grain | 1,682.0 |
| Igniter | 0.4 |
| Total Mass | 1,775.4 |
| Predicted Expended Mass | |
| Inerts | 10.4 |
| Propellant | 1,681.8 |
| Total Mass Expended | 1,692.2 |

TABLE 9. STAR-48 MOTOR CHARACTERISTICS

| COMPONENT | CHARACTERISTIC |
|------------|---------------------|
| Case | Titanium |
| Insulation | EPDM* |
| Propellant | TP-H-3340 |
| Grain | Radial-Slotted Star |
| Igniter | Aft-End Toroidal |
| Nozzle | Carbon/Carbon |

*Ethylene propylene diene monomer.

TABLE 10. STAR-48 PERFORMANCE CHARACTERISTICS

| PARAMETER | PERFORMANCE |
|--------------------------------------|--|
| Expansion Ratio | 50.1 |
| Maximum Pressure, psi (atm) | 633 (44.6) |
| Average Pressure, psi (atm) | 554 (39) |
| Burn Time (s) | 85.37 |
| Action Time (s) | 86.38 |
| Maximum Thrust, lbf (N) | 15,230 (67,912) |
| Average Thrust, lbf (N) | 12,510 (55,783) |
| Total Impulse, lb*s (N*s) | 1,087 x 10 ⁶ (4,847 x 10 ⁶) |
| I_{sp} Propellant, lbs/lb (N*s/kg) | 293.8 (2,882) |
| I_{sp} Effective | 292 (2,865) |

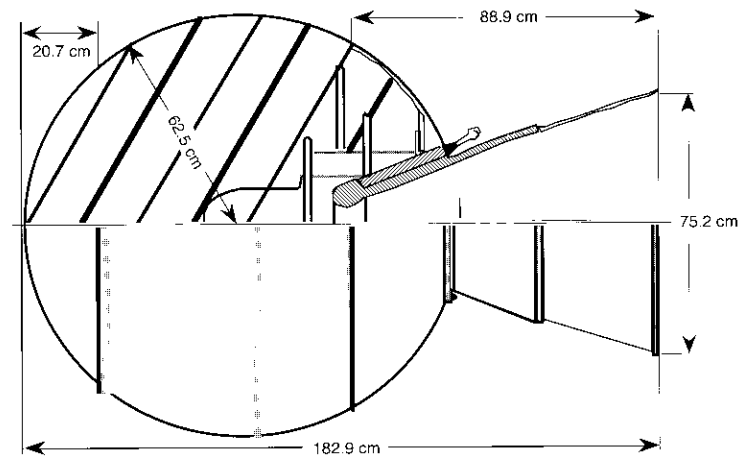


Figure 6. Star-48 Assembly Diagram

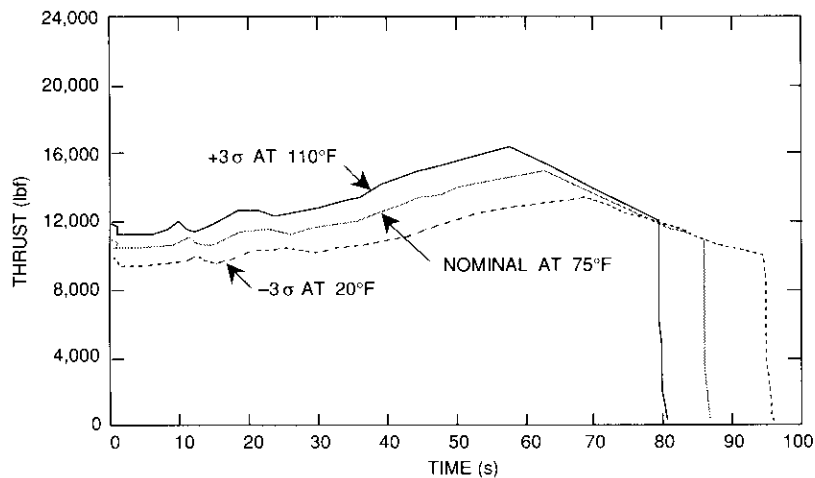


Figure 7. Star-48 Thrust vs Time

Antenna beam-pointing accuracy

The specification of beam-pointing accuracy is driven by two elements: avoidance of interference with other systems, and attainment of specified communications system performance. For the spacecraft designer, the definition of beam-pointing accuracy is a primary input into a spectrum of possible choices which involve the spacecraft bus and its configuration, the design of structures, the choice of materials, the attitude control system (ACS) concept, the selection of critical components, the spacecraft propulsion system, the thermal control system, the orbit control tolerance (stationkeeping accuracy), and other elements specific to each of these areas.

For the satellite operator, the attainment and maintenance of the pointing accuracy to which the spacecraft has been designed requires implementation of the appropriate operation plan and careful monitoring of telemetry data, which normally can only be considered as an indirect indication of beam-pointing error. Direct measurement of this error would require the use of ground-based equipment capable of determining the location of the ground intersection with the axis of maximum radiation of the satellite-based antenna beam. More practically, error could be determined by measuring signal strength variations at a number of stations properly located around the periphery of the beam.

In defining beam-pointing accuracy, it has become customary to identify the antenna boresight axis with the beam axis. Having reduced the problem of beam pointing to that of pointing the boresight axis of a satellite antenna, the following subsections review the various error sources, the available technology, and the performance attainable with a reasonable expenditure of resources.

The error budget

Errors which contribute to the mispointing of an antenna boresight axis can be conveniently subdivided into four classes: constant, seasonal or long-term, daily, and short-term. Much of the contribution of the various error sources depends on what is assumed as a pointing reference, what control system craft is maintained around its nominal orbital station.

For geostationary satellites, the orientation of the satellite as a rigid body, as well as the orientation of its antenna boresight axes, are normally referred to an orthogonal orbiting set of coordinate axes centered at the satellite, of which one axis (yaw) is directed toward the geocenter and another (pitch) is perpendicular to the orbit plane. The third axis (roll) is perpendicular to the other two and is normally oriented in the forward direction of motion. The orbital coordinate axes, in turn, are referenced by appropriate translations and rotations to the nominal coordinate axes, which are centered at the nominal geostationary location of the satellite. The nominal yaw and roll axes are located in the equatorial plane and are oriented respectively to the geocenter and to the instantaneous east position. The nominal pitch axis is parallel to the earth's axis of rotation.

The spacecraft is built around an orthogonal set of coordinate axes to which all spacecraft components are referred. Controlling the orientation of the spacecraft in orbit so that the spacecraft axes align themselves precisely with respect to the orbiting axes, and controlling the parameters of the orbit actually occupied by the spacecraft so that the orbiting axes align themselves and coincide with the nominal axes, are necessary conditions for holding constant the orientation of the various spacecraft components with respect to any point on the earth's surface. The yaw axis is the most common reference axis for antenna boresight pointing, since it is also the optical axis of earth-center-seeking sensors.

Mechanical alignment errors and tolerances within the sensor itself, the sensor mounting plate, the master alignment cube, the spacecraft frame, the antenna structure, and the deployment mechanisms, as well as errors in gravity-compensation fixtures, all contribute to a constant error. In earth-oriented spacecraft of the spin-stabilized type, or those containing a fixed

momentum storage device (wheel), the spin axis of the wheel or spacecraft rotor must be aligned with the orbit normal to prevent continuous expenditure of precessional effort. Thus, any misalignment of the spin axis with regard to the spacecraft pitch axis introduces another component into the constant error.

Compensation of some of the above component errors is not readily achievable from an operational standpoint. For example, misalignment of a pitch wheel or rotor spin axis with regard to the spacecraft pitch axis cannot be compensated without propellant expenditure, except in the case where a wheel is gimballed. The same is true, in part, for earth sensor misalignment—only the pitch component can be compensated in a biased momentum spacecraft concept. If a spacecraft has more than one antenna, then compensating for the misalignment of one antenna (if feasible) can aggravate the pointing error of the others if their mechanical alignment errors have opposite sense, unless each antenna is independently steerable. A further contributor to a constant error is the effect of such factors as long-term variation in sensor characteristics, material properties, or material “creep.”

Seasonal errors are typically due to seasonal variations in earth radiance and satellite orientation to the sun. These variations induce seasonal fluctuations in infrared earth sensor characteristics, thermally induced variations in control electronics, and deformations in structures. Another component of long-term error can be the triaxial drift of the spacecraft in its longitudinal deadband.

Errors in daily period arc due partly to effects similar to those of the seasonal class, and partly to the daily orbital motion of the satellite within its stationkeeping tolerances (eccentricity librations in longitude, and latitude oscillations due to orbit inclination). The pitch and roll mispointing induced by fluctuation of the satellite position within its longitude and latitude deadband varies approximately between zero and one-sixth of the angular longitude/latitude excursion of the satellite, depending on the ground location of the station to which the antenna beam points. Specifically, a $\pm 0.1^\circ$ stationkeeping tolerance would contribute $\pm 0.0178^\circ$ to the daily pointing error at the subsatellite point. However, yaw error coupling from orbit inclination is in the ratio 1/1. Finally, short-term errors are caused by various sources within the ACS electronics and components, and by disturbance torques due to orbital maneuvers (stationkeeping).

Because of the statistically independent nature of these various error terms, the expected total error is normally estimated by the root sum square (rss) method, applied within each class, and by the sum of the subtotals of each class. A worst-case absolute error sum is viewed as overly conservative.

Options

Various options are available to the spacecraft designer to meet given beam-pointing requirements. Options exist in the areas of spacecraft configuration, structural design, material selection, control system configuration, and component selection, as well as for various other elements such as operational modes and procedures. To achieve the stringent pointing accuracies required in modern communications satellites, an optimized design is necessarily the result of complex techno-economic tradeoffs that can push the limits of technology.

The spacecraft configuration, the design of pertinent structures (*e.g.*, antenna reflector, support structure, deployment mechanism, and spacecraft main structure), and material selection can all have a significant impact on beam-pointing error. An optimum design is one that minimizes the effects of structural misalignments, mechanical tolerances, and thermo-mechanical deformations, thus ensuring a minimal contribution to some of the error classes previously defined. A sophisticated spacecraft bus design can be used with a relatively unsophisticated ACS, whereby the pointing accuracy of the various antenna beams is related to the accuracy and stability of the orientation of the entire spacecraft. This approach, which could be called the “traditional” technique, relies on independently minimizing each of the four classes of errors rather than eliminating some of them.

In parallel with refinement of the spacecraft configuration, structural design, and material selection, refinement of the ACS technology can also help reduce the error budget. The performance of a traditional ACS can be refined by the appropriate selection of key elements such as sensors, actuators, and control laws. For earth-oriented geostationary communications satellites, the earth sensor is fundamental to ACS performance. The current state of the art in earth sensor technology offers null accuracies in the range of 0.02° to 0.05° , depending on sensor design, while advances in reaction or momentum wheel technology have made available actuators with minimum torque noise. Advances in spacecraft propulsion technology (specifically in the areas of catalytic and hypergolic low-thrust thrusters, thrust-level accuracy, and minimum pulsewidth) have resulted in actuators whose contribution to spacecraft attitude error can be contained within a small fraction of the error budget. Continued efforts in advancing the state of the art of ACS component technology (sensors and actuators) can further improve performance and reduce the ACS error contribution to the pointing error budget. However, as long as the other independent pointing error sources remain, it is not advantageous to reduce the ACS contribution alone, particularly if this requires expensive new technology.

An alternative to the traditional technique is offered by a spacecraft bus design that employs a control system concept capable of compensating or eliminating some component errors altogether. A possible choice is a multi-loop control system in which the basic ACS orients and stabilizes the spacecraft as a rigid body, while the antennas are independently steered and pointed to their respective stations by auxiliary tracking loops operated by ground-based RF beacons. By directly tracking a ground beacon, the pointing error of an antenna can be freed of most of its structure-dependent portion (a significant portion of the constant, seasonal, and daily components).

Control systems of this type are being employed on current or planned satellites; however, adherence to stringent design factors is necessary to ensure adequate performance. These requirements result from the complex nature of the sensor, which includes the reflector, the feed system, and the ground beacon. The sensor characteristics are sensitive to the orientation of the beacon relative to the antenna boresight axis; to thermal effects on the reflector, support structures, feed system, and filters; and to reflector deflections produced by the antenna-pointing control loops in response to error signals. Beacons located toward the edge of the antenna coverage tend to produce strongly nonlinear characteristics. Additional practical difficulties in implementation occur when a spacecraft needs to operate at different longitudes, as in the INTELSAT system. The difficulty lies in the availability of ground stations (for the location of a beacon) that satisfy the same geometrical relationship to the spacecraft at the different longitudes.

The design of the ACS ultimately used on INTELSAT VI is described in the companion paper by Slafer and Seidenstucker [6].

INTELSAT VI specifications

In view of the above considerations, INTELSAT VI beam-pointing accuracy was specified [7] as follows:

The spacecraft design shall be such that the range of boresight variations of each antenna beam does not exceed the values shown in Table [11] at any time during the ten year operational life of the spacecraft under all modes of operation.

The Contractor shall perform a detailed antenna pointing error analysis, accounting for all the sources of error which are involved, and demonstrating that the antenna pointing error specifications will be met. Table [12] presents a list of some of the principal factors which shall be addressed by the analysis and whose contributions shall be included in the pointing error budget.

The Contractor shall analyze the time behavior of the various error sources and shall add the individual contributions which make up the pitch, roll, and

TABLE 11. MAXIMUM ALLOWABLE ANTENNA POINTING ERROR

| | C-BAND | KU-BAND |
|-------|--------|---------|
| Roll | 0.12° | 0.12° |
| Pitch | 0.12° | 0.12° |
| Yaw | 0.15° | 0.15° |

yaw errors, and combine the effects of pitch, roll, and yaw in a manner which accounts for the worst case expected conditions. Additionally, margins shall be allocated and identified to reflect the uncertainty of the estimates. In certain cases, if the Contractor can provide a detailed justification for the validity of the approach, INTELSAT may accept addition of certain error contributors using the root sum square (rss) approach; otherwise worst case linear addition shall be used.

If the antenna beam-pointing accuracy specification is satisfied by mechanically repositioning the spacecraft reflectors or feeds, based on pointing data obtained through ground measurements (RF or otherwise) of the satellite performance in orbit, such repositioning shall not be required more than once during the spacecraft orbital design life.

Summary

This paper has summarized the issues that played a major role in the design of the INTELSAT VI spacecraft bus, and reported on some of the in-house study results obtained preliminary to the RFP. The payload requirements and the spacecraft life determined the mass of the satellite, while the limiting constraints of the available launch vehicles determined its configuration, size, and volume. The requirements for beam-pointing accuracy had a significant bearing on the design of the attitude and position control system, as well as on the formulation of the spacecraft's operational plan.

References

- [1] E. I. Podrazzky and W. R. Schnicke, "The Process for Success—INTELSAT VI," *COMSAT Technical Review*, Vol. 20, No. 2, Fall 1990, pp. 231–246 (this issue).
- [2] L. B. Perillan, W. R. Schnicke, and E. A. Faine, "INTELSAT VI System Planning," *COMSAT Technical Review*, Vol. 20, No. 2, Fall 1990, pp. 247–269 (this issue).
- [3] B. A. Pontano, A. I. Zaghoul, and C. E. Mable, "INTELSAT VI Communications Payload Performance Specifications," *COMSAT Technical Review*, Vol. 20, No. 2, Fall 1990, pp. 271–308 (this issue).

TABLE 12. ERROR SOURCES

- | TABLE 12. ERROR SOURCES | |
|-------------------------------------|--|
| A. Geometric Factors | |
| 1. | Orbital inclination of up to 0.02° |
| 2. | Spacecraft location in longitude about the nominal station $\pm 0.10^\circ$ |
| 3. | Actual location in orbital arc |
| 4. | Antenna mechanical boresight misalignment |
| 5. | Antenna RF boresight misalignment |
| 6. | Antenna deployment error |
| 7. | Control sensor misalignment |
| 8. | Attitude sensing cross-coupling effects |
| 9. | Geometric axis relative to principal axis misalignment |
| 10. | Attitude drift between correction maneuvers |
| 11. | Bearing mount wobble |
| 12. | Effects on North-South stationkeeping maneuvers resulting in orbit plane changes as large as 0.04° |
| B. Control Electronics Factors | |
| 1. | Resolution and granularity |
| 2. | Thermal effects, drift, aging, radiation effects |
| 3. | Control sensor inaccuracy and bias |
| C. Disturbance Factors | |
| 1. | Thermal distortion |
| 2. | Control sensor noise |
| 3. | Change in control sensor mode |
| 4. | Effect of stationkeeping maneuvers and thruster firings (inclination maneuvers resulting in plane changes of up to 0.04° shall be accounted for) |
| 5. | Center of mass uncertainty and variations |
| 6. | Propulsion thrusters thrust vector misalignment |
| 7. | Structural flexure |
| 8. | Solar and magnetic torques |
| 9. | Gravity gradient torques |
| 10. | Control mode transition |
| 11. | Plume impingement |
| 12. | Bearing torque disturbance |
| D. RF Boresight Calibration Factors | |
| 1. | Resolution and granularity of antenna positioning mechanisms |
| 2. | Thermal effects |
| 3. | Orbital effects |
| 4. | Sensor inaccuracies and biases |
| 5. | Antenna RF null misalignment |
| 6. | Software and algorithm inaccuracies |

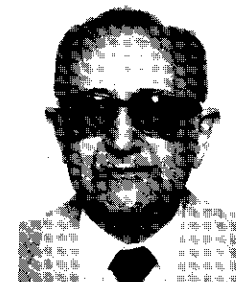
- [4] R. R. Persinger *et al.*, "The INTELSAT VI Antenna System," scheduled for publication in *COMSAT Technical Review*, Vol. 21, No. 1, Spring 1991.
- [5] L. Dest *et al.*, "Spacecraft Bus Design," scheduled for publication in *COMSAT Technical Review*, Vol. 21, No. 1, Spring 1991.
- [6] L. I. Slafer and V. L. Seidenstucker, "Attitude and Payload Control System for the INTELSAT VI Communications Satellite," scheduled for publication in *COMSAT Technical Review*, Vol. 21, No. 1, Spring 1991.
- [7] Private communication.



Gian Paolo Cantarella graduated in electrical engineering, Summa Cum Laude, from the University of Rome, Italy, in 1962. Prior to joining INTELSAT in 1978, he was employed as a Communications System Analyst by the European Space Agency (1969–1978), the Boeing Company (1966–1969), and Selenia (1963–1966). Since joining INTELSAT, he has worked primarily on the technical planning and operations of the INTELSAT system. He is currently Manager of the Intersystem Coordination Office in the INTELSAT Operations Plans Division.

Giacomo Porcelli graduated from the University of Naples in industrial engineering, and then took an M.S.E.E. and a Ph.D.E.E. at the University of Pennsylvania on a Fulbright scholarship. He worked for various industrial organizations, including the General Electric Company/Missile and Space Division, the Westinghouse Astronuclear Laboratories, and the Fairchild Space and Electronics Company, before joining INTELSAT.

Upon his retirement from INTELSAT, Dr. Porcelli rejoined Fairchild Space with responsibilities in the Systems Engineering directorate. His experience in the space industry covers stage vehicles and spacecraft mission analysis, guidance/control/propulsion requirements, definition, design and performance evaluation, trajectory analysis and synthesis, and overall systems engineering. He has published numerous papers in the area of spacecraft attitude control, LEO-GEO transfer via low-thrust liquid rocket propulsion, and various aspects of orbital rendezvous.



SS-TDMA system considerations

S. J. CAMPANELLA, G-P. FORCINA, B. A. PONTANO, AND J. L. DICKS

(Manuscript received February 28, 1991)

Abstract

The INTELSAT VI satellite-switched time-division multiple access (SS-TDMA) system represents completion of the full cycle of the 120-Mbit/s TDMA system design that was first introduced operationally on an Atlantic Ocean Region INTELSAT V satellite in October 1985. The original design was intended for operation with static transponders, but contained all the features needed to graduate to dynamic switched operation. This paper describes how compatibility between static and dynamic switched operation was accomplished through the network control system design (including the SS-TDMA frame structure), acquisition and synchronization between earth and space segments, the structure of the traffic burst time plans, preparations for establishing the switch-state time plans, coordination and synchronization of the changing of the two time plans so that no ongoing traffic is disrupted (hitless time plan change), and plesiochronous interface operation and the related control of the on-board timing oscillator.

Introduction

Satellite-switched time-division multiple access (SS-TDMA) [1] employs a programmable, fast-acting microwave switch matrix (MSM) on board the satellite to route TDMA bursts arriving on various up-link beams to various down-link beams. The switch, comprising a crossbar row-column configuration, is programmed to cyclicly execute a set of switch states, each consisting of

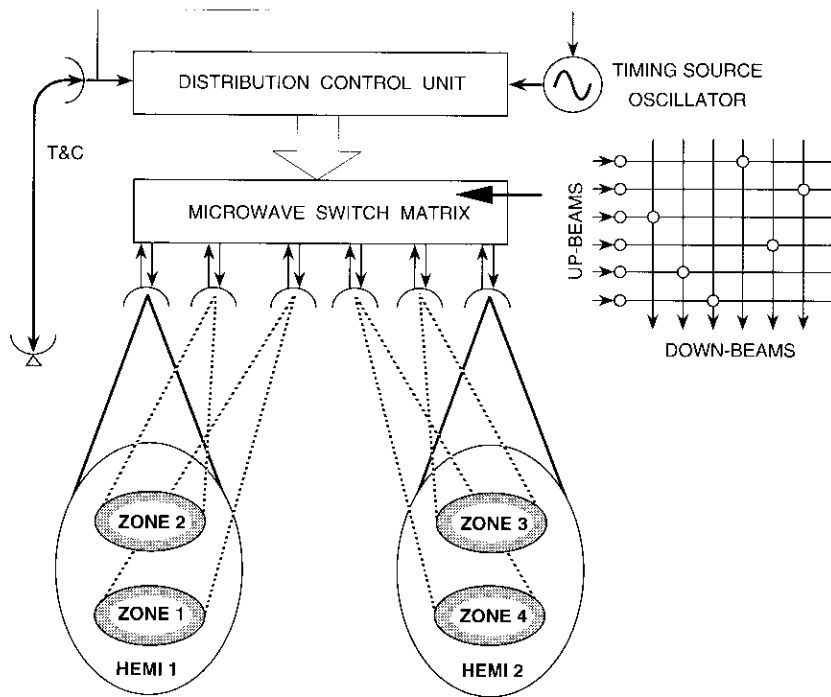


Figure 1. INTELSAT VI SS-TDMA System

connections between the up- and down-zones and the hemi beams, as shown in Figure 1. The connection may be single-point, with only one connection in each row (up-link) or column (down-link) of the matrix; or multipoint (broadcast state), with multiple connections between a row element and a number of column elements. Each state dwells for a time period that is adjusted in length to carry its assigned amount of traffic between the beams [2].

A set of switch states occurring in sequence, as shown in Figure 2, is repeated each TDMA frame to satisfy the traffic requirements of a network. The set consists of a network control (synchronization) field and a traffic field. The network control field includes metric burst (MB) states used to synchronize the earth and space segments, reference burst distribution (RBD) states, traffic terminal acquisition and synchronization (TAS) states, and system test and monitoring states. The traffic field contains a large number of switch states selected to carry the full beam-to-beam traffic. Acquisition and synchronization between the earth and space segments are performed by an

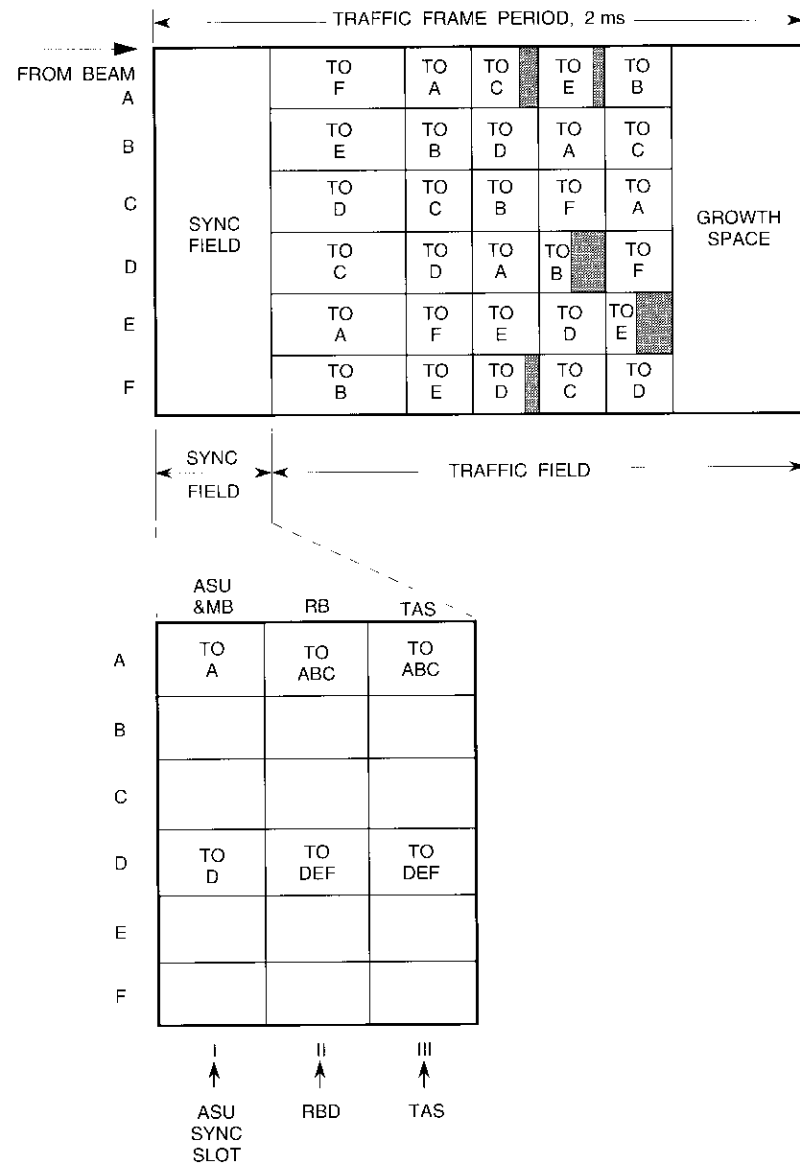


Figure 2. SS-TDMA Switch State Time Plan

acquisition and synchronization unit (ASU) [3],[4], which positions and maintains a special metering burst in the loopback state. The ASU function also provides the precise control of the on-board satellite switch clock necessary for plesiochronous operation of the satellite and terrestrial network [5].

The INTELSAT VI SS-TDMA subsystem

The INTELSAT VI SS-TDMA subsystem [6] (Figure 1) interconnects six beam regions comprising two hemi beams (east and west) and four zone (approximately quarter-earth) beams (northeast, northwest, southeast, and southwest). The system is controlled by two reference stations [7], one in the east and the other in the west. These are designated as the master primary (MPRT) and the secondary (SRT) SS-TDMA reference terminals (SSRTES) and serve master primary and secondary roles in the TDMA frame in the same sense as specified in INTELSAT's BG-42-65 System Specification for the 120-Mbit/s burst rate TDMA system. (While the burst rate is referred to as 120 Mbit/s for convenience, it is actually 120.832 Mbit/s.) The master primary and secondary roles of the two reference stations can be interchanged as needed to meet 120-Mbit/s TDMA operation and maintenance requirements. The flexible beam-to-beam switched connectivities provided in the SS-TDMA system make it possible to eliminate two of the four reference stations required in the INTELSAT V system non-switched 120-Mbit/s TDMA. When appropriate broadcast switch states are introduced into the sequence of states that comprise a switch state time plan (SSTP) [8], two reference bursts will appear in all down-beams, thus providing total compatibility with the 120-Mbit/s TDMA earth stations currently operating in the INTELSAT V system.

The SS-TDMA subsystem on board INTELSAT VI [9] dynamically switches up-beams to down-beams within each TDMA frame according to a preprogrammed sequence of switch states selected to execute a desired connectivity plan. The communications payload is implemented with two MSMS, each operating on a different carrier frequency, using TDMA transmission and quadrature phase shift keyed (QPSK) modulation with a burst rate of 120 Mbit/s at C-band, and interconnecting six 72-MHz transponders that serve both the east and west hemi beam coverages and the four zone beam coverages. Traffic burst transmissions from earth stations in the beams are synchronized to arrive at the satellite in time slots assigned in a 2-ms TDMA frame period, which occurs within a switch state epoch that routes the burst to the down-beam containing the burst's destination stations. The TDMA frames, control multiframe, and switch master frames (SMFs) of the two separate MSMS are locked together, but each executes its own independent SSTP.

The MSM can be programmed to provide any of the following:

- No-connect states.
- Multiple single-up-beam to single-down-beam connect states (*i.e.*, single-row-to-single-column matrix connectivities where rows of the matrix are connected to the up-beams and columns to the down-beams). (See Figure 3 for notation.)
- Partial broadcast connect states (*i.e.*, single-row-to-multiple-column connectivities).
- Full-broadcast connect states (*i.e.*, single-row-to-all-column connectivities).

However, multiple rows (up-beams) cannot be connected to single columns (down-beams).

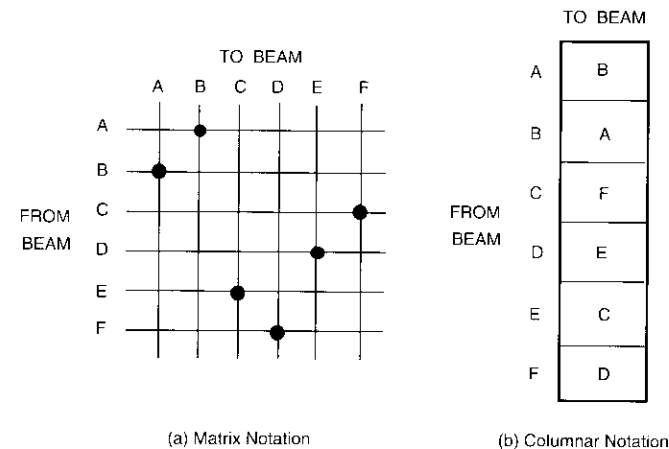


Figure 3. Switch State Notation

Each MSM's switching sequence is controlled by an on-board distribution control unit (DCU) which contains three identical memories, each storing sequences of up to 64 switch states. Each switch state requires 48 bits to identify its connections and address, and each memory may serve as on-line, off-line, or standby. Timing of occurrences of switch states is incremented in 64-symbol steps called frame units (FU). There are 120,832 symbols or 1,888 FU per 2-ms SS-TDMA frame. A triply redundant timing source provides timing signals for the following:

- Frame units (64 symbols)
- SS-TDMA frame (120,832 symbols or 2 ms)
- Switch master frame (8,192 2-ms SS-TDMA frames or 16.384 s).

The SMF is equivalent to the 120-Mbit/s INTELSAT TDMA system superframe.

To change the SSTP executed by an MSM, the off-line memory of the associated DCU is loaded with the new SSTP and a command to rotate the roles of the off-line and on-line memories is given. The DCU is designed to execute this memory role change in synchronism with the start of the next SMF. The standby memory provides a means to store, on board the satellite, a new SSTP which has been sent over the command link. The roles of all three memories rotate during operation. In association with changing the SSTP, changes must be made in the burst time plan (BTP) used by the stations of the network. To ensure that ongoing traffic is not perturbed during the BTP/SSTP change process, the changes in the two time plans are precisely synchronized by the synchronous BTP/SSTP change procedure described later.

Organization of the switch state frame

As illustrated in Figure 4, there are three general types of SS-TDMA frames, which differ in terms of the switch state regions they contain. The first type, called a metric transponder frame, starts with an MB region to support the acquisition and synchronization functions between the TDMA frame clock (TFC) at the SS-TDMA reference stations and the satellite switch frame clock on board the satellite. Metric transponder frames also contain an RBD region, a TAS region, a traffic burst (TFC) region, a switch state verification (SSV) region, and a test switch state (TSS), and terminate in a 4-FU-long no-connect (NC) state that serves as a metric guard boundary for the metric state. The second SS-TDMA frame type, called a non-metric transponder frame, does not have the metric burst, SSV, or no-connect metric guard states. The third type, called a zone beam frame, eliminates the TAS state as well. Brief descriptions of the various regions are given below. The functions of the Metric Burst, Reference Burst, Acquisition and Synchronization, and Traffic regions are described in detail in the subsections that follow.

- *Metric Burst Region.* This region consists of two switch states, with a combined length of 13 FU, assigned at the start of each 2-ms SS-TDMA frame in transponders (called metric transponders) that carry ASU metering bursts. These bursts control SS-TDMA frame and superframe acquisition and synchronization between each SSRTE and the on-board satellite switch. This is accomplished using an ASU which is described

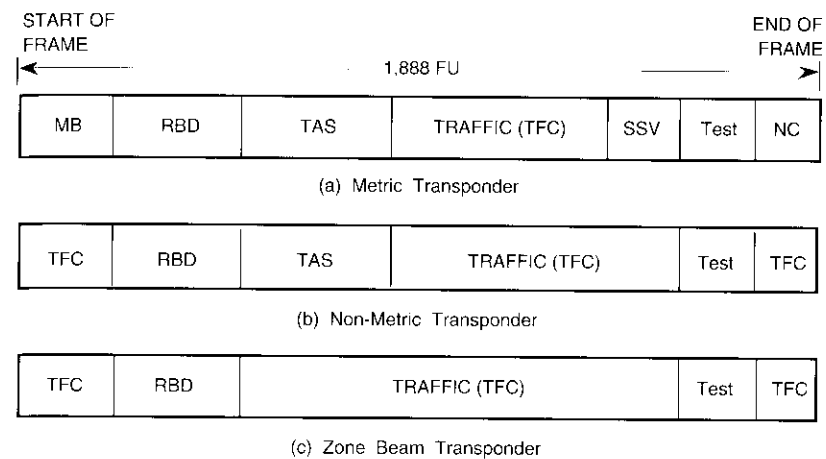


Figure 4. SS-TDMA Frame Types

later. The metric burst region is assigned only in transponders that perform this function; all other transponders are assigned traffic in the epoch of this region.

- *Reference Burst Distribution Region.* The RBD region consists of two broadcast switch states that distribute the reference bursts from both SSRTEs into all beams in each SS-TDMA frame. Each of these states is long enough (6 FU) to pass a reference burst plus its guard time.
- *Terminal Acquisition and Synchronization Region.* The TAS region is reserved for controlled acquisition of terminals entering the system and for continued synchronization of terminals during normal operation. Its maximum length is typically 64 FU for terminal acquisition and 224 FU for terminal synchronization, but can be less depending on the number of acquiring terminals. The TAS region is not used in the zone beam frames because stations in the zones use hemi beam connectivity for acquisition and synchronization.
- *Traffic Region.* The traffic region of the frame carries the traffic bursts. It is divided into a number of switch states that provide interconnectivities among the six beams of each 6×6 -transponder SS-TDMA network. The number of switch states used and their connectivities are governed by the traffic routing matrix. Taking into account that approximately 325 FU are used for the composite of all the synchronization, acquisition, and housekeeping functions, the length of the traffic region is nominally 1,563 FU.

- *Switch State Verification Region.* The SSV region is used to loop back an SSV burst transmitted from and received by the ASU during BTP/SSTP changes. It assists in determining the status of the satellite SSTP during a synchronous change. This burst will occupy a minimum of 4 FU SSV switch states in each metric transponder prior to the test slot. Traffic bursts may be scheduled concurrently in other transponders.
- *Test Switch State.* The TSS is assigned in all transponders to provide a short state, typically 4 FU in length, to support burst-mode link analyzer transmissions and TDMA system monitor measurements. The TSS follows the SSV in metric transponders and the traffic region in other transponders.
- *No-Connect Metric Burst Guard State.* To simplify both the design of the ASU and the burst scheduling algorithm, no-connect metric burst guard states occupy a fixed position at the start of frames. In order for an ASU to locate the metric region, its search procedure requires that the metric burst be preceded by a metric guard state at the end of the preceding frame. The metric guard state is a minimum-duration (4-FU) no-connect state which preserves the duration of the metric loopback switch state. In non-metric transponders, traffic can be assigned during the metric burst guard state epoch as part of longer switch states.

Satellite switch acquisition and synchronization in the metric burst region

Each SSRTE is equipped with an ASU subsystem that acquires and continuously synchronizes with the switch frame and SMF generated at the satellite. Figure 5 shows a block diagram of the ASU and illustrates its relationship to the on-board satellite switch and its timing unit.

The ASU transmits a metering burst to the satellite which is designed to measure and synchronize the position of the burst relative to the end of a special ASU metering state programmed into the on-board switch frame. The measurement is performed by truncating a metering segment of the metering burst that is modulated by a random bit pattern. The segment is truncated when its path through the on-board switch to the down-link of the beam from which it was up-linked is blocked by the end of the metering burst switch state, as depicted in Figure 5. When the truncated metering segment of the burst is received by the ASU, the number of errors occurring during the metering burst is observed. This approach will yield an accurate measure of the location of the metering burst, as illustrated by the following example.

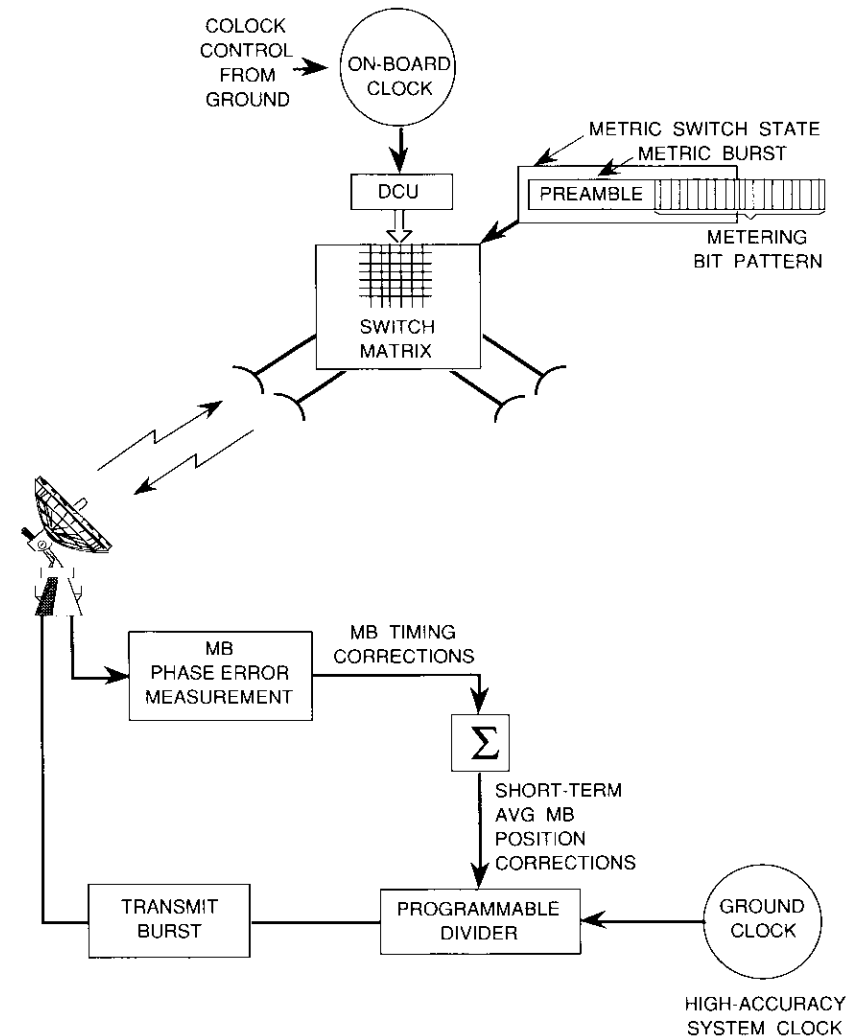


Figure 5. ASU Metering Burst Timing Corrections

Consider that the metering segment contains L bits of a random pattern. These bits are compared with a stored version of the pattern when the signal is returned to the receiver after passage through the satellite switch. If the metering segment is bisected by the truncation, there will be no errors for the first $L/2$ bits received (assuming error-free reception), while an average of $L/4$ bits will be received erroneously for the second $L/2$ bits received (assuming random error), since the metering segment has been truncated and only random noise is received. Thus, bisecting the metering pattern results in an average of $3L/4$ bits of the pattern being received correctly and $L/4$ received in error.

This measure is made once every 2 ms and averaged over a few hundred bursts to provide a sensitive measure of burst position in terms of the average number of bits received. For example, if the pattern contains 64 bits, the number of erroneous bits for the bisected case occurring over 512 frames is 8,192. If the truncation occurs one symbol earlier or later, then the number of errors increases or decreases by 512. Thus the cumulative number of bit errors can be translated directly into timing corrections, in terms of symbol increments. Short-term averaged corrections can be used to keep the metering burst aligned to the TDMA frame on board the satellite and to provide the source of timing for reference burst transmissions. Long-term deviations of the on-board clock, measured by observing the time domain bisector between the instant of transmission of the metering burst and its instant of reception, can be used to measure the drift of, and make corrections to, the on-board clock. This is discussed in greater detail later.

SYNCHRONIZING THE SSRTE TO ON-BOARD SWITCH TIMING

The metric burst region of the SS-TDMA frame contains a loopback connectivity state, terminated by either of two no-connect states, which routes an ASU metric burst through the metric transponder(s). The structure of the ASU metric burst is shown in Figure 6. The first part consists of a 176-symbol-long carrier (CR) and bit timing recovery (BTR) sequence that prepares the demodulator. Next is a 24-symbol unique word (UW) which is used to detect burst arrival time, followed by a 64-symbol bit metric pattern. The degree of truncation of the metric pattern provides a measure of the location of the ASU burst relative to the the start of SS-1. The last 24 symbols of the metering pattern serve as a UW, which is received only at the start of the SMFs due to action of the switch state substitution process which lengthens the loopback state by 1 FU every SMF. This allows the ASU to mark the timing of the SMFs. This process is vital to synchronizing the traffic BTP changes with SSTP changes and is described in greater detail below. Two arrangements of states SS-0, SS-1, and SS-2 define

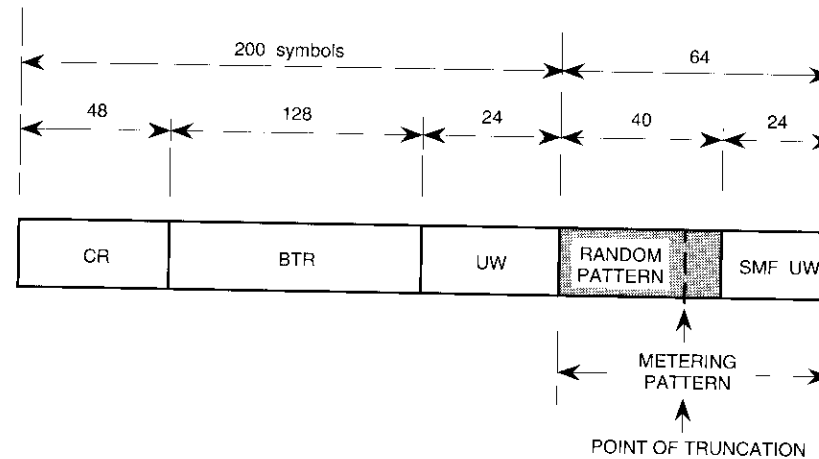


Figure 6. Metric Burst Format

the normal loopback configuration shown in Figure 7 and the extended loopback configuration shown in Figure 8. The difference between these configurations is the result of substituting SS-2 for SS-1 once every superframe.

Initially, the ASU searches for and acquires the position of the metric region state SS-0 by transmitting a continuous sequence of search mode acquisition bursts and detecting the pattern of received bursts as chopped by the duration of SS-0. The normal duration of the metric loopback switch state is 8 FU, which is unique and differentiates it from all other loopback states in the SS-TDMA frame. Once SS-0 is found, the ASU switches to transmission of the metric burst.

The ASU maintains the position of the metric burst such that the metering pattern contained in this burst is truncated by the trailing edge of the normal metric loopback switch state at a predefined position in the metric pattern (typically the bisector of the pattern). Measurement of the cutoff point of the metric pattern, and adjustment of the time of transmission of the metric burst, can be done as frequently as once per second, thus allowing the ASU to be constantly synchronized with the satellite switch frame.

MARKING THE SWITCH MASTER FRAME

To mark the start of SMFs, a 1-FU extension of the loopback interval in the metric region allows the SMF codeword carried at the end of each ASU metric burst to pass through the switch once every SMF. This is accomplished by the switch state substitution feature built into the on-board DCU, which modifies the switch states executed at the start of the SS-TDMA frame that begins each

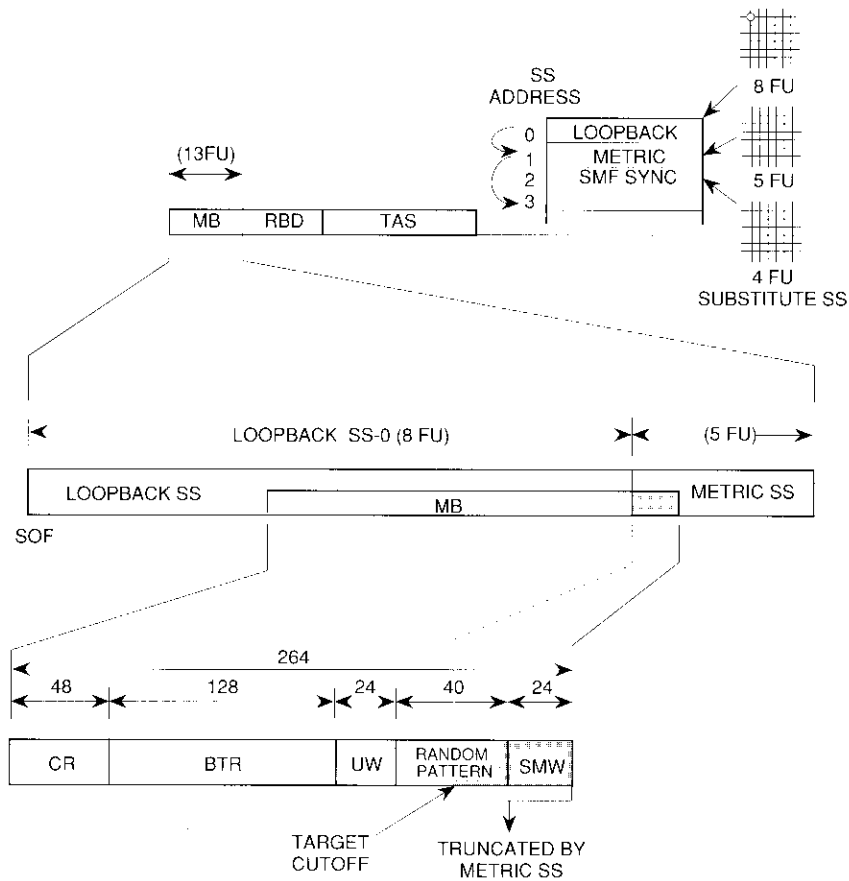


Figure 7. Metric Region: Normal Frames

SMF. This technique is illustrated by the SS sequences shown in Figures 7 and 8. The SS sequence that controls the process at the start of each SS-TDMA frame (shown in the upper right of each figure) comprises a metric burst loopback state of length 8 FU in SS-0, a no-connect state of length 5 FU in SS-1, and another no-connect state of length 4 FU in SS-2. The substitution feature permits no-connect state SS-2 to replace no-connect state SS-1 at the start of each SMF.

Figure 7 shows the situation that results for normal frames. Loopback state SS-0, located at the start of each SS-TDMA frame, permits the ASU metering burst to pass back to its originating beam. The no-connect state SS-1, which

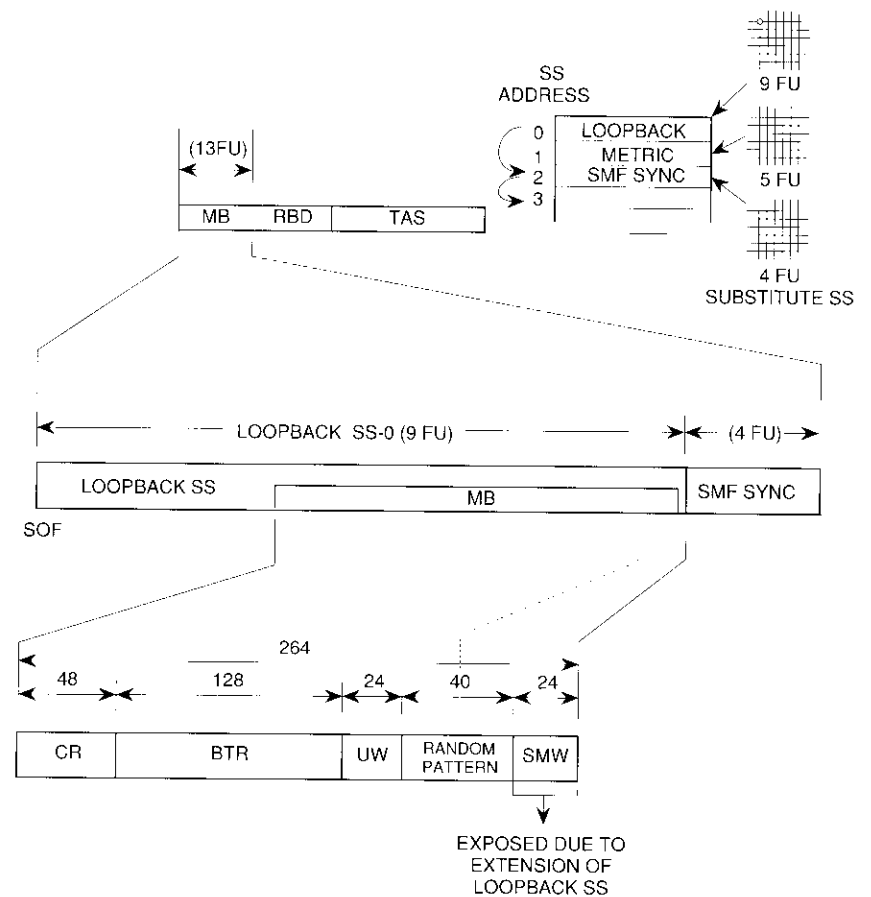


Figure 8. Metric Region: Switch Master Frame

normally follows SS-0, blocks the loopback at 8 FU and truncates the last half of the metering pattern and the following SMF codeword. The ASU metric burst remains in this position as a consequence of the closed-loop tracking action of the ASU.

Figure 8 shows the situation for the first frame at the start of the SMF. No-connect state SS-2 replaces no-connect state SS-1, causing the loopback to block at 9 FU and permitting the normally truncated portion of the metric burst (which contains the rest of the metering pattern, including the SMF codeword) to be looped back to the originating beam. When this normally blocked portion is received at the SSRTE, the beginning of the SMF is marked.

Switch state substitution is controlled by the DCU by means of a substitution state bit. When the DCU encounters a memory word in location N that has the substitution bit set, it will skip execution of the switch state word at location $N + 1$ and execute the switch state word in location $N + 2$. The DCU is designed to set the substitution bit at a location N every SMF. For the operation described above, $N = 0$.

Reference burst distribution

Each SSRTE distributes a maximum of four reference bursts to a maximum of 12 transponders using full- or partial-broadcast RBD switch states in the two 6×6 MSM SS-TDMA systems of an INTELSAT VI satellite. Each RBD region has a length of at least 12 FU to accommodate two reference bursts. These states connect the beam in which a reference station is located to all beams (including the beam containing the reference station) into which reference bursts are to be distributed. The locations of the RBD states in each type of transponder are shown in Figure 4.

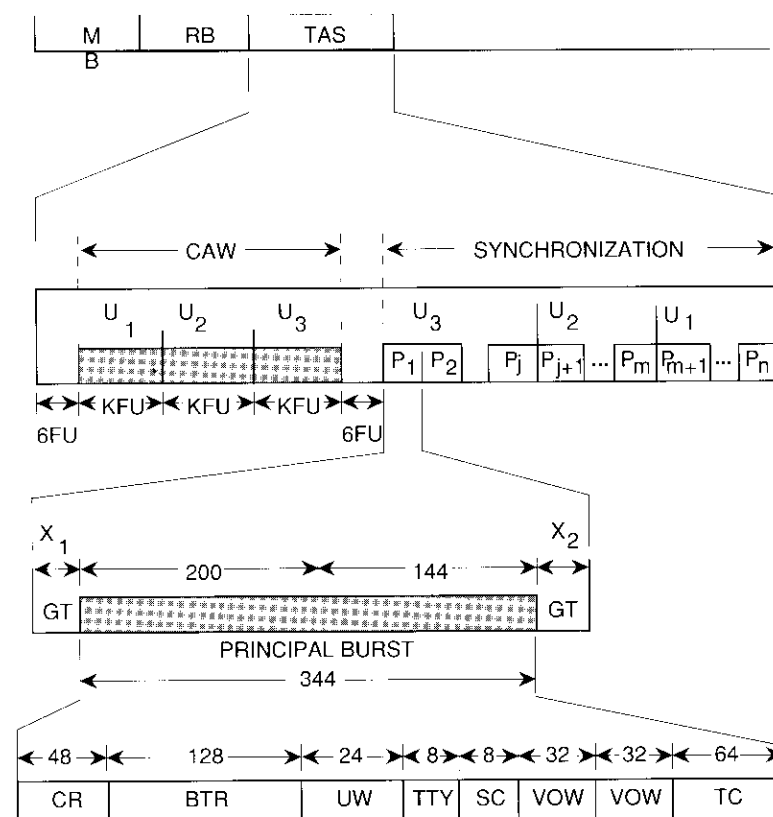
Two reference bursts are needed per TDMA frame in each beam to fulfill the operating requirements of the 120-Mbit/s TDMA system. When reference bursts occur they take precedence over all other bursts—a fact that must be accounted for in scheduling traffic bursts. The RBD states remain fixed during SSTP changes to ensure synchronization continuity. Additionally, the switch states in the RBD region are aligned across all transponders. The RBD states are followed by the TAS region, which is described next.

Terminal acquisition and synchronization

The TAS region supports TDMA terminal acquisition and synchronization in a manner that is compatible with 120-Mbit/s terminals operating on INTELSAT V.

TAS REGION DEFINITION

The SS-TDMA system uses two SSRTEs located in opposite (east and west) coverage areas. Each traffic terminal must have at least one burst under cooperative feedback/position control by each of these SSRTEs. The approach adopted is to set aside a region of the frame—the TAS region—in each down-beam (transponder) received by the SSRTEs, into which traffic terminals transmit a "principal burst" that carries no traffic. This burst is sent to both SSRTEs using a partial-broadcast switch state. The TAS region of the frame (Figure 9) will vary in length according to the number of terminals controlled in a particular beam region. All principal bursts are acquired sequentially.



- U_n = Up-Beam Connectivity
 P_j = Principal Burst Slot j
 FU = Frame Unit
 GT = Guard Time
 VOW = Voice Orderwire
 TCC = Traffic Channel
- $X_1 = 8$ for First Burst in Subsync Region;
 4 for All Other Bursts
 $X_2 = 4$ for all But Last Burst in Subsync Region
 = For Last Burst:
 0 if Even Number of Bursts in Region
 32 if Odd Number of Bursts in Region

Figure 9. TAS Region

Each TAS region is separated into a common acquisition window (CAW) subregion and a synchronization subregion. The CAW region, whose use is described below, occurs first, allowing switch state boundaries within the TAS region to be aligned across all transponders providing the TAS function.

SUPPORT OF TERMINAL ACQUISITION

The sequential method of acquisition support (as defined for the INTELSAT 120-Mbit/s TDMA system) is used, with minor changes to the manner in which terminals are assigned to an acquisition cycle interval (ACI). In order to acquire, a terminal under control of an SSRTE transmits short bursts into time slots of duration K FU assigned in the CAW subregion of the TAS region of the TDMA frames of selected hemi up-beams. The initial location of these bursts in the ACI is controlled by the open-loop method [10], which relies on prediction of the distance to the satellite from the acquiring station. The slot width parameter K must be large enough to permit passage of a 200-symbol short burst plus a reasonable guard time. A value of $K = 4$ is sufficient. Each superframe is divided into four equal ACIs of four control frames each. Each ACI is associated with one of four sequentially acquiring terminals, and up to four terminals can be in serial acquisition. The acquisition control information used by acquiring traffic terminals is carried in the control and delay channel (CDC) data field of each reference burst. The start of each superframe is signaled by the occurrence of terminal short address zero in the CDC. Four terminals may be designated in each reference burst's CDC for sequential acquisition, and all acquiring terminals share the ACIs. Once an ACI is allocated to a terminal, sequential acquisition takes place using the procedure defined for the INTELSAT 120-Mbit/s TDMA system.

Each SSRTE (MPRT and SRT) may acquire terminals whose signals are received from up-links via four switch states, each routing a TAS region with a CAW. Since each CAW will be associated with a CDC (MPRT or SRT), all terminals allocated for acquisition and synchronization in the same TAS region will be controlled in the same CDC. Each SSRTE can simultaneously acquire up to four terminals in the same ACI using all four CAWs in all four transponders. In the next ACI, another four terminals may be acquired, and so on. Since there are four ACIs per superframe per SSRTE, up to 32 terminals can be in acquisition during a superframe.

The SSRTEs maintain a list of non-acquired terminals in each TAS region and allocate them, one at a time, to each ACI. Since both the MPRTs and SRTs share the initial acquisition function, ACI allocations between the two are coordinated from Acquiring Terminal tables that assign terminals to each. To accomplish this, a new service channel message is introduced which contains the ACI number and CDC address of the terminal from each acquiring terminal table to be controlled in this ACI. The ACI assignment message for ACI N is transmitted in the first multiframe of every control frame of ACI $N - 1$.

During acquisition, a terminal N is instructed to transmit a short burst in a particular acquisition window using an initial value of delay compensation,

D_N , which when applied will cause the burst to appear at a location in the frame that is only a few symbols in error from the desired target location. The reference station observes the acquisition burst location, determines the error between this location and the target, and sends a correction to the acquiring station. The correction is applied by the acquiring station, and this time the transmitted burst should be within one or two symbols of the target position. If it is, then the reference station completes the acquisition process by assigning the burst to a principal burst location in the principal burst region of the TAS region. The timing provided by the principal burst is used to locate all traffic bursts transmitted by the station.

The traffic region follows the TAS region and is contiguous in the remainder of the frame.

Traffic region

The previously described functionally orientated regions of the frame establish the operating discipline needed to assign, maintain, and reassign traffic bursts to the traffic region. Approximately 325 FU of the 1,888-FU SS-TDMA frame are used for frames carrying the system control functions, leaving 1,563 FU for assignment to traffic bursts. In frames that do not carry the TAS function, 1,851 FU are available for traffic.

In SS-TDMA, traffic bursts must be assigned to fill a traffic load matrix among the six beam regions interconnected by the 6×6 MSM. The interconnections are expressed in terms of switch states, and a sequence of switch states is required in order to accommodate the total traffic load among the six beams. The total load can be expressed in terms of a 6×6 traffic load matrix of the beam-to-beam traffic demand. Combinatorial theoretical approaches are available that can select a sequence of the least number of switch states with the shortest overall duration to accommodate the traffic load. Application of one such method, known as the Greedy algorithm, is now described [11].

TRAFFIC SWITCH STATES

The satellite switch is programmed to cyclically execute a set of switch states, with each state consisting of a set of connections between the six up-beams and six down-beams and having a duration sufficient to carry the traffic assigned to it. A matrix of the type shown in Figure 3a is an effective representation of the switch state connections. Each of six horizontal lines is connected to one of the up-beams (A through D), and each of the vertical lines to one of the down-beams (A through D). A crosspoint with a dot indicates a connection, while no dot indicates a no-connect state.

An equivalent representation is shown in Figure 3b, where a column is divided vertically into cells in which the letter to the left of the cell designates the up-beam connection (the beam from which the signal comes), and the letter in the cell designates the down-beam connection (the beam to which the signal is destined). A cell with no letter indicates a no-connect state. The columnar representation is the most convenient for illustrating a cascade of switch state sequences (e.g., Figure 2). The width of each column is adjusted to represent the duration of each switch state, which is proportional to the traffic load carried by the state. Selection of the sequence of states comprising the traffic burst region is discussed below.

SELECTING A SEQUENCE OF TRAFFIC SWITCH STATES

The switch states that make up the traffic field are normally of the single-point connectivity type in which only one up-beam is connected to one down-beam. In the matrix representation, only single connections are made between the rows and columns. (It is assumed that no broadcast states are used for traffic.) The number of different single-point switch states is a function of the number of beams interconnected. For an $N \times N$ matrix, the number of possible switch states is $N!$. Thus, for $N = 3$ there are six different states, as shown in Figure 10. For the INTELSAT VI six-beam system, the number of possible states is 720. The traffic planner must select from these the subset of switch states which optimally routes the 6×6 -beam traffic load.

The Greedy algorithm was devised to select a set of switch states that is optimum in that it minimizes the number of switch states and the duration of

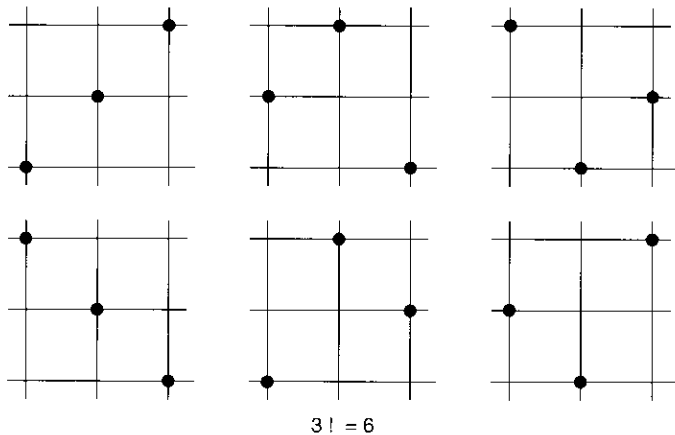
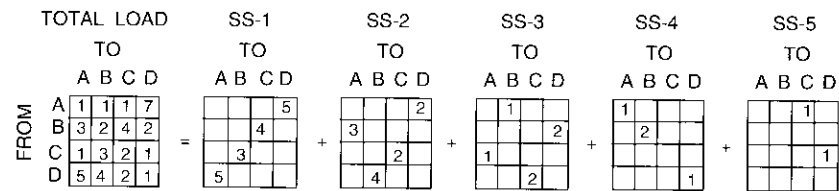


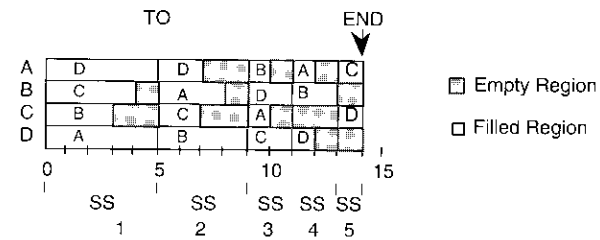
Figure 10. Complete Set of Single-Point 3×3 Switch States

the sequence of switch states needed to serve a given traffic matrix. A general estimate of the upper bound of the number of switch states needed may also be calculated [12].

Briefly, the procedure used in the Greedy algorithm is as follows. First, an $N \times N$ traffic matrix is formed by summing the loads from each of N up-beams to each of N down-beams. This matrix need not be symmetrical. The total load matrix is then broken into a small subset of constituent switch states which are selected from among the 720 possible switch states. The sum of these subsets equals the total load. It is obviously desirable that the least number of switch states be selected and that their composite length be a minimum. Figure 11 shows an example of this type of decomposition, as performed using the Greedy algorithm [11] for $N = 4$. Each switch state is selected to represent the greatest fraction of the load presented at each stage of the selection process. The first switch states selected will thus have the longest duration, with each of their interconnections being assigned an appropriate fraction of the traffic. As the process continues, remainder states occur for which it is no longer possible to completely fill all interconnections. The result of the process is a set of switch states which covers the full traffic load, as shown in the example.



(a) Traffic Matrix Decomposition Into Switch States



(b) SSTP for Above Decomposition

Figure 11. Development of the SSTP

The sequence of occurrence of the selected states forms the SSTP. The ordering of the states within the sequence is selectable by the traffic planner. In general, each arrangement of the sequence will result in a different number of switchings, and that sequence which results in the least number is preferred. An upper bound to the number of switch states that achieves a fill factor of at least 90 percent for an $N \times N$ beam system is given by $N^2 - 2N + 2$ [12]. For $N = 6$, this upper bound is 26 switch states. Additional switch states are needed to distribute reference bursts, support acquisition and synchronization, and perform other monitoring and test functions, as previously described. The on-board DCU for INTELSAT VI has a capacity of 64 switch states, which appears to be entirely adequate.

At the beginning of satellite life, when the system is not filled to capacity, the switch state sequence that satisfies the traffic load will be shorter than the SS-TDMA frame and there will be empty space between the end of the switch state traffic sequence and the start of the next frame. While this space will eventually be needed to support traffic growth, it is not desirable to leave a large segment of the frame empty. A better alternative is to distribute the growth space among all states by lengthening each state as appropriate.

On-board clock correction

Plesiochronous (nearly synchronous) operation of international digital circuits, as recommended in International Telegraphy and Telephony Consultative Committee (CCITT) Recommendation G.811, relies on clocks on each side of an international connection having a long-term accuracy of 1 part in 10^{11} . At a TDMA earth terminal, the clock on the terrestrial side is supplied by the national network and the clock on the satellite side by the TDMA frame periodicity, which is determined by the on-board SS-TDMA frame clock [13]. Thus, the long-term accuracy of the timing source oscillator (TSO) must be 1 part in 10^{11} . It is not reasonable to expect the TSO by itself to have this accuracy. However, it is possible to observe the timing of the TSO via the SSRTE by observing the ASU metering burst timing, comparing this to the timing supplied by a high-accuracy local timing standard (LTS) located in the SSRTE, and feeding back corrections to the TSO. The LTS consists of a high-stability cesium beam oscillator having an accuracy of at least 1 part in 10^{11} . The inherent accuracy of the TSO (without the feedback correction) is 5 parts in 10^{11} per day. Operation of the feedback TSO correction system is discussed below.

Phase difference measurement

It is important to first understand the method used to observe TSO timing. The ASUs at both the MPRT and SRT periodically measure the phase drift of the switch frame relative to the SSRTE LTS, using a technique which inherently eliminates Doppler shift from the measurement. This is accomplished by recognizing that the midpoint of the time difference between the instant of the start of the receive frame (SORF)—which is established by the reception instant of the UW of the TDMA frame reference burst—and that of the start of the transmit frame (SOTF) is independent of the distance to the satellite and hence contains no Doppler shift. This is because the time shift in the SOTF is equal to but opposite that in the SORF, as illustrated in Figure 12. Thus, observation of this midpoint gives a measure of the drift of the on-board TSO timing, uncontaminated by Doppler shift.

Midpoint time observations are used to generate frequency corrections to the TSO by a method similar to that shown in Figure 13. A 60.416-MHz symbol clock derived from the LTS oscillator is provided to the phase measurement circuitry. A flywheel counter, driven by the LTS, provides a reference pulse having TDMA frame periodicity that can be adjusted in phase in one-symbol steps. A measuring circuit, based on observations from the ASU, computes the midpoint between the SORF instant and the SOTF instant (each measured in terms of the end of the UW) and outputs a pulse at the midpoint instant. This midpoint observation can also be obtained by delaying the SORF instant by $D_N/2$. The timing difference between the LTS frame pulse reference and the SOTF-SORF midpoint frame pulse observation is measured by a timing phase difference circuit. At the start of observation, the LTS TDMA frame reference is adjusted to make the difference zero.

In INTELSAT's 120-Mbit/s TDMA system, frame synchronization timing is observed once every multiframe (every sixteen 2-ms TDMA frames), and consequently frame timing is in terms of the start of the receive multiframe (SORMF) and start of the transmit multiframe (SOTMF), rather than SORF and SOTF. This makes no difference in the procedure for midpoint calculation other than exchanging the multiframe measures for frame measures.

Observations are reported for each control frame (every 512 TDMA frames). During each control frame, the phase difference and the accumulated phase change from the last control frame for both the on-line and standby ASUs are reported to the CDC of the reference terminal equipment. The CDC calculates a local cumulative phase value from the values reported by the on-line ASU and

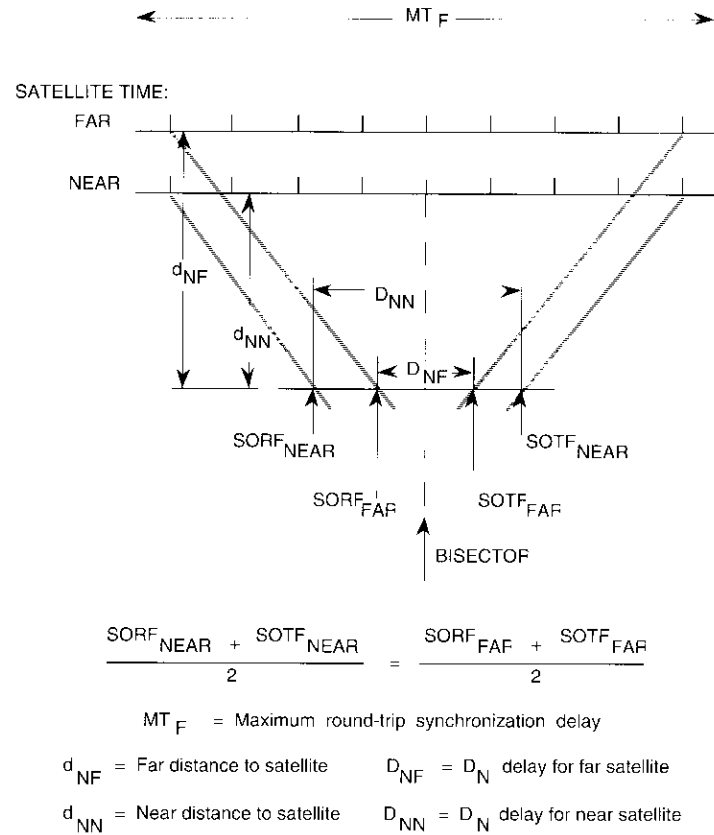
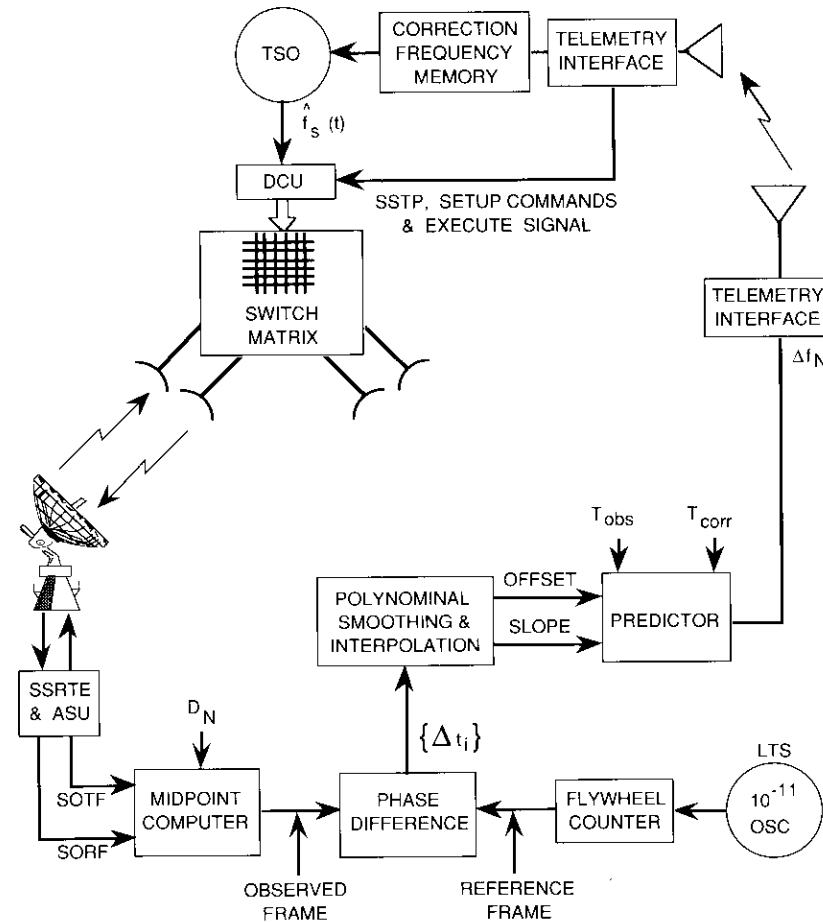


Figure 12. SOTF/SORF Bisector Independent of Distance to Satellite

reports this to the INTELSAT Operations Center TDMA Facility (IOCTF) [14] once each clock phase reporting interval (CPRI). The TSO frequency difference that corresponds to the cumulative phase difference is given by the expression

$$\Delta f_{TSO} = f_{TSO} (\Delta T / T) \tag{1}$$

where f_{TSO} is the TSO frequency and ΔT is the cumulative phase difference expressed in time (the product of the number of symbols of drift and the symbol period) over the accumulation interval of duration T .



- $\{\Delta t_i\}$ = Incremental timing corrections
- T_{corr} = Predictor correction interval
- T_{obs} = Observation interval since last correction

Figure 13. On-Board Clock Control System

Clock correction prediction

The cumulative phase difference values described above are used at the IOCTF to calculate the clock frequency correction for the TSO using the procedure [15] described below.

The IOCTF computes and logs the current cumulative phase difference and oscillator frequency change performance observed in each CPRI. Normally, frequency corrections will be scheduled to occur at times which do not conflict with other scheduled satellite commanding activities. The interval between successive corrections is called the TSO correction interval (TCI). An unscheduled frequency correction will be administered if the cumulative phase exceeds a preset threshold.

When a TCI has elapsed, the IOCTF will execute the TSO drift correction algorithm, which fits a least mean squared error polynomial to the cumulative phase data. Phase is expressed as the time equivalent, Δt , of the phase differential accumulated between the TSO and LTS oscillators as a function of time. Based on this fit, the predicted phase is extrapolated to the end of the next TCI. The incremental frequency correction is computed such that the cumulative phase will become zero at the end of the next TCI in the case of constant frequency differences, or will have minimum peak deviations in the case of constant oscillator drift.

The frequency correction process consists of two parts: a constant frequency offset correction and a constant slope correction. A combination of both will usually be needed to achieve optimum correction. The objective of the process is prevent the time difference over a correction interval from exceeding 500 μ s.

A least mean squared parabolic fit to the time displacement function during an observation interval, T_{obs} , will result in a parabolic estimation function given by

$$\Delta T(t) = \Delta f/f_{LTS}(t-t_o) + (a/2)(t-t_o)^2 \quad (2)$$

The first-order term coefficient, $\Delta f/f_{LTS}$, is the constant offset between the TSO and the TSL oscillators and must be corrected by a constant offset process. The second-order term coefficient, $a/2$, where a is the constant slope frequency drift of the TSO relative to the LTS expressed in parts per day, must be corrected by a constant slope correction process.

The constant offset situation is shown in Figure 14a. A constant frequency offset of Δf_o between the TSO frequency, f_{TSO} , and the LTS frequency, f_{LTS} , observed over an observation interval T_{obs} will result in a time difference in the phase of

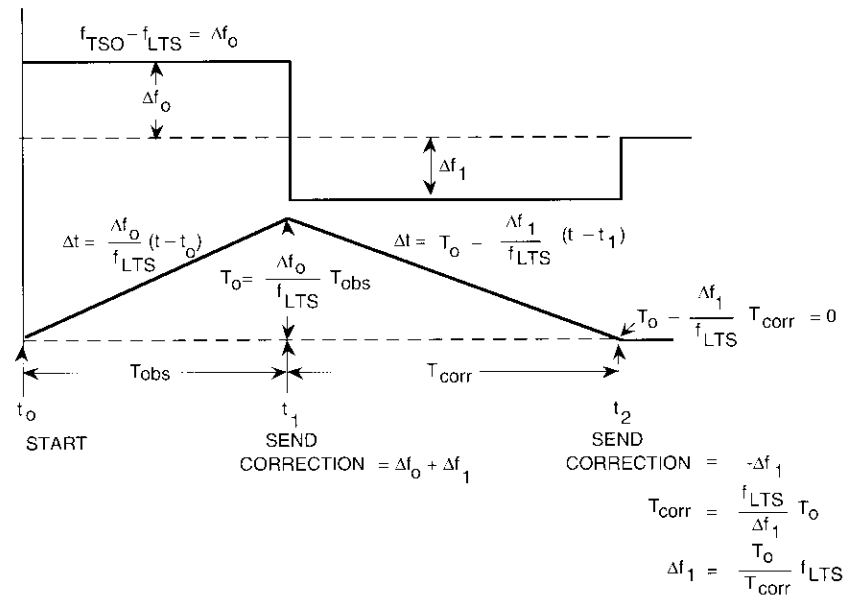
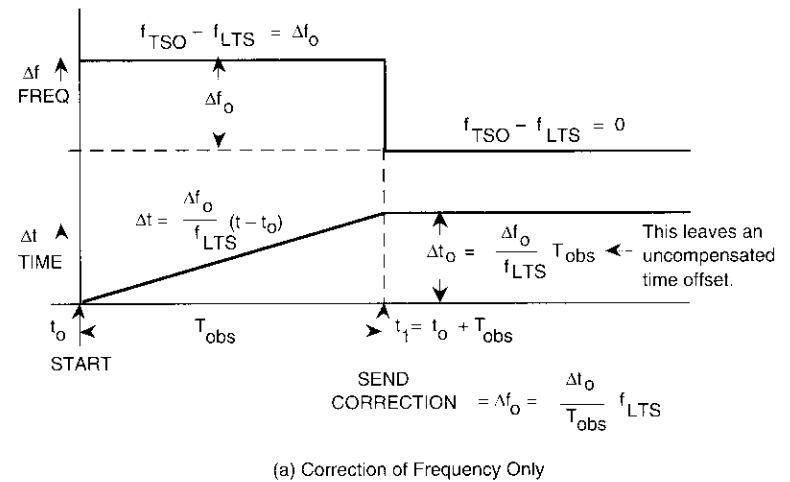


Figure 14. Fixed-Frequency Offset Correction

$$\Delta t_o = (\Delta f_o / f_{LTS}) T_{obs} \quad (3)$$

and requires a correction in the TSO frequency of

$$\Delta f_{corr} = \Delta f_o + \Delta f_o (T_{obs} / T_{corr}) \quad (4)$$

At the end of the correction interval, T_{corr} , a second correction of

$$\Delta f_{corr} = -\Delta f_o (T_{obs} / T_{corr}) \quad (5)$$

must be applied. The resulting time function is illustrated in Figure 14b. Note that an amount, $\Delta f_o (T_{obs} / T_{corr})$, is added at the beginning of the correction interval and subtracted at the end. If this were not done, the time function would be as shown in Figure 14a, where the time offset is not reduced to zero.

The situation for the constant-slope correction process is shown in Figure 15. In this case, it is assumed that a slope of a , expressed in terms of oscillator drift in parts per day, is observed over an observation interval, T_{obs} . Recall that for a constant drift, a , between the TSO and the TSL oscillators, the time difference accumulated over an interval T_x is $aT_x^2/2$. The frequency offset after such an interval would be $\Delta f = aT_x$. Thus, over the observation interval, the frequency offset will be $\Delta f_o = aT_{obs}$. However, if only this value is applied as a correction to the TSO, then the phase offset will continue to diverge indefinitely. To prevent this and to achieve the contained situation shown in Figure 15a, an additional correction of $aT_{corr}/2$ must be applied. This results in the sawtooth frequency function and the periodic parabolic time difference function with period T_{corr} shown in Figure 15a, which is still not optimum. It is considerably better to achieve the situation shown in Figure 15b, where the periodic parabolic function results in equal positive and negative peak deviations of half the peak-to-peak magnitude. This is accomplished by adding a step frequency correction of $a(T_{obs})^2/T_{corr}$ at the start of the first correction interval, and subtracting the same amount at the end.

The algorithm has three modes of operation: cold start, warm start, and normal. Cold start is used at system startup when the frequency difference is expected to be much larger than 5 parts in 10^{11} . Warm start is used when restarting the network after a short failure which has resulted in the loss of phase measurement data. Normal use is as previously discussed. The difference between the three modes of operation lies in the duration of the CPRI (corresponding to T_{obs}) and the TCI (corresponding to T_{corr}). During cold start, the CPRI is short (10 minutes) and the TCI is approximately 1 hour. Warm start uses the normal CPRI (4 to 6 hr) and a relatively short TCI (2 to 4 days). The TCI for normal mode depends on the drift characteristics of the on-line TSO. All parameters can be manually set.

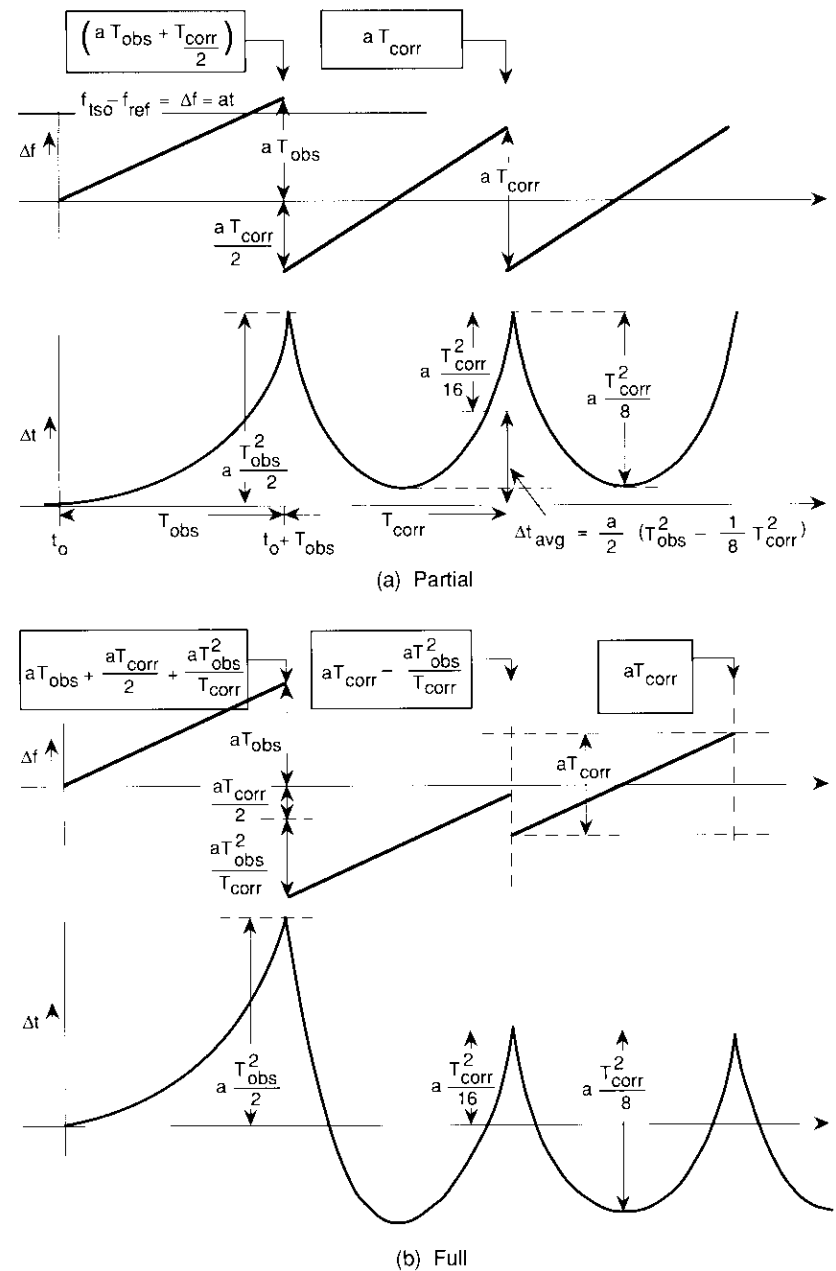


Figure 15. Constant-Slope TSO Frequency Drift Correction

Administering the frequency correction

When a correction is to be administered, the satellite control center (SCC) computes a new frequency correction for the on-line TSO in the spacecraft by adding the incremental correction requested to the sum of all previous corrections since startup. This amount is then added to the nominal oscillator frequency of 5.664 MHz. The characteristic curve (frequency vs control integer) for the specific TSO is then used to determine the value of a control integer that is sent to the TSO over the satellite's command link.

Traffic burst synchronization in the SS-TDMA frame

Proper SS-TDMA operation depends on adjusting traffic burst transmissions from earth stations located in the various beams such that each burst arrives at the satellite in its assigned time slot and switch state without infringing on the time slots of bursts from other stations or the epochs of other switch states [16]. To allow for some error in positioning, each time slot is augmented by an amount referred to as guard time. The timing conditions must be such as to place a burst at its target location in an assigned switch state in the SS-TDMA frame at the satellite.

Each earth station adjusts its burst transmission timing to compensate for the propagation delay between its location and that of the satellite. To accommodate synchronized SSTP changes and traffic BTP changes, this adjustment must be done so that changes executed at all stations of a network occur at the satellite at their assigned locations in the same TDMA frame in which the SSTP change takes place. This requires that the total round-trip delay between the satellite and each station be made equal to a common maximum for all stations, sufficient to accommodate the farthest possible station from the satellite (*i.e.*, one located on the locus of tangency of the line of sight to the satellite with the sphere of the earth). For a satellite in geostationary orbit, this distance is 41,600 km. In addition, the maximum round-trip delay must equal an integer number of synchronization frame periods in order to keep the bursts aligned to their assigned positions in the TDMA frame.

Space-time graph of the synchronization process

The space-time graph [2] of Figure 16 illustrates how time events on the satellite are synchronized with those at the earth station. The horizontal time line at the top of the figure represents events at the satellite, and the time line below it represents events at the earth station. The sloped time lines represent the timing of burst transmissions transiting from satellite to earth

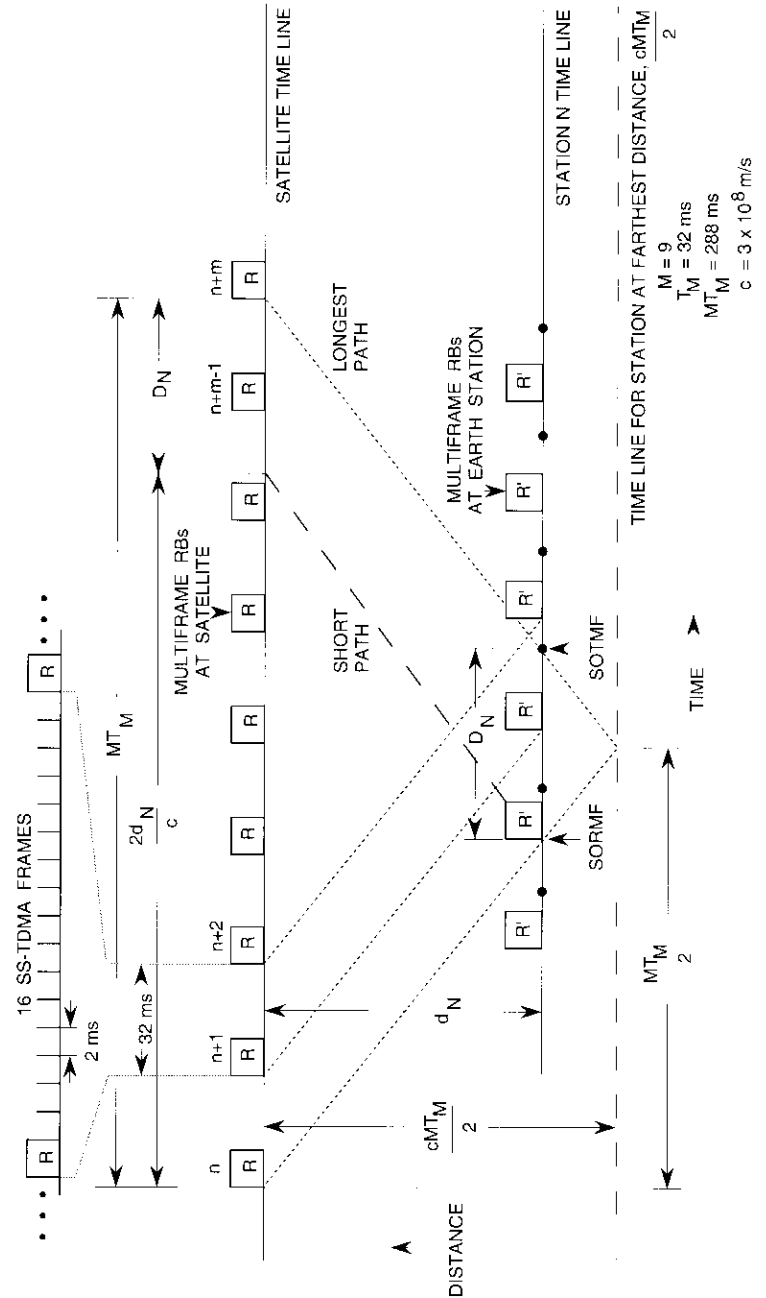


Figure 16. TDMA Synchronization Space-Time Graph

(down-slope) and return (up-slope). The pulses designated R are the multiframe reference bursts, which occur in the reference burst distribution switch states with a TDMA control multiframe period T_M . For the INTELSAT 120-Mbit/s SS-TDMA system, each of these control multiframes contains sixteen 2-ms TDMA traffic frames, each with a reference burst. All traffic bursts at the satellite are timed relative to these reference bursts, and the reference bursts are synchronized to arrive in their assigned time slots in reference distribution switch states at the satellite. The latter timing is accomplished by the ASU located in the SSRTE.

The time reference of a burst occurs at the end of the UW. The UWs of reference bursts mark the beginning of TDMA frames, and specially coded UWs occurring at intervals of 16 TDMA frames mark the start of the control multiframes. As illustrated in Figure 16, at earth station N a time delay D_N is introduced between the time of reception of the SORF and the time of transmission of the SOTF. Both the SORMF and SOTMF are timed in terms of control multiframes. Thus, the total round-trip delay between the satellite and any station N is

$$\text{Round-trip delay} = D_N + 2d_N/c \quad (6)$$

where d_N is the one-way distance between earth station N and the satellite, and c is the speed of light. This round-trip delay must be greater than the round-trip delay to the point of line-of-sight tangency with the sphere of the earth, which for a satellite in geostationary orbit is 277.3 ms (corresponding to a one-way distance of 41,600 km). The requirement that this delay also be an integer number of TDMA synchronization frames (a value equal to MT_M) increases the maximum delay to 288 ms—the duration of nine TDMA control multiframes. The design of the INTELSAT TDMA system adds another three multiframes to this maximum delay to allow margin for processing time. Thus, the expression for D_N becomes

$$D_N = 12T_M - 2d_N/c \quad (\text{ms}) \quad (7)$$

Note that the bottom dashed line in Figure 16 (designated as the maximum range) represents this maximum delay between the satellite and the farthest possible earth station.

Administering the delay correction

An earth station located a distance d_N from the satellite must introduce a delay, D_N , to achieve proper frame synchronization at the satellite. This also

guarantees synchronization of traffic BTP changes among all traffic stations for static-switched 120-Mbit/s TDMA operation, as well as synchronization of the satellite SSTP change with the traffic BTP changes in dynamic SS-TDMA operation. Synchronization of traffic BTP changes with satellite SSTP changes is accomplished in a hitless fashion (*i.e.*, without interruption to ongoing traffic). The means of accomplishing this is discussed later.

To position an individual traffic burst at its assigned location in the frame, the burst delay relative to the start of the frame must be added to D_N , which may also be augmented by an integer multiple of TDMA frames to allow for processing time in the traffic station. D_N is applied in the following manner. A station first determines the SORMF by detecting the instant of correlation of the received reference burst UW pattern with a replica stored in the receive station. Using this instant as the reference, the station adds an amount D_N , plus processing delay, to mark the SOTMF. Traffic bursts are located in the TDMA frame by appending an additional delay to place the station's burst at its assigned location in the TDMA frame. The adjustment is done in terms of multiframes which contain 16 TDMA frames. Burst locations are assigned in the BTP.

Synchronous BTP/SSTP change countdown procedure

The SSTP and BTPs of all earth terminals must change synchronously on the same TDMA frame, as observed on board the satellite. (This is sometimes referred to as an SSBTP change.) The special substitution switch state invoked during the metering region of every 512 multiframes (16.384 s) to mark a superframe is used to synchronize traffic station BTP changes among all participating traffic stations with the SSTP change. Figure 17 is a space-time diagram showing the various phases of synchronization during a superframe.

Using the satellite time line as reference, a superframe begins on board with the occurrence of a substitute switch state, S . This switch state lengthens the switch state connection for the metering burst sent from the ASU at the MPRT so that the entire metering burst is received once every 512 multiframes. The lengthened metering burst is received at the ASU and initiates the following synchronization sequence at the MPRT. The MPRT waits for a time D_N , which is determined by equation (7). This adjusts the round-trip response time between the satellite and any station N , at distance d_N , to be 12 multiframes. The MPRT then waits an additional $456T_M$ and starts a $32T_M$ countdown sequence. All traffic terminals in all beams receive the countdown. Each traffic station N then waits $D_N + 3T_M$ after completion of the countdown and initiates transmission of the new BTP. The station also waits $12T_M$ after

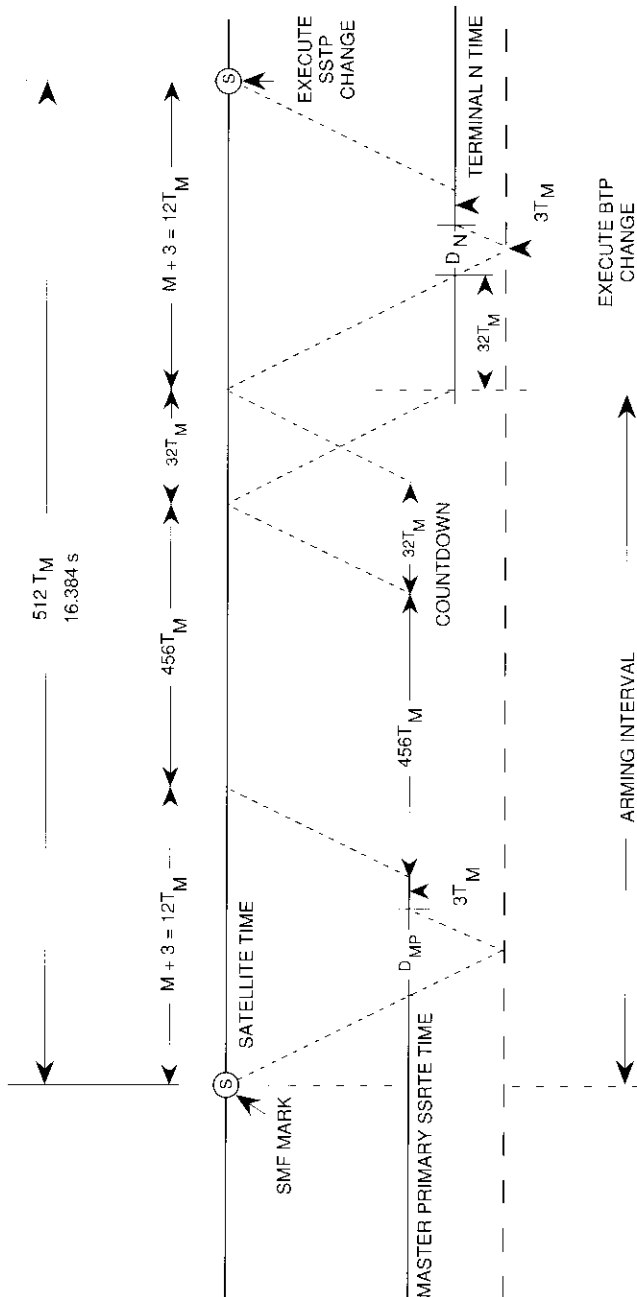


Figure 17. BTP/SSTP Change Synchronization Interval

completion of the countdown to change its receive side to the new BTP. Because the total time to complete the entire sequence of events is adjusted to equal precisely $512T_M$ by selecting an intermediate wait time of $456T_M$, all new traffic bursts of the new time plan are synchronized to arrive at the satellite during the first TDMA frame of the next superframe. Synchronization with the SSTOP is accomplished by invoking the new SSTOP on the next superframe upon receipt of an arming command from the earth, before the end of the same superframe in which the countdown exercise is performed.

The new SSTOP is invoked by rotating the on-line and off-line memories in the DCU. The commanding necessary to rotate the memories consists of setup commands followed by an Execute signal. Since memory rotation takes place on the next SMF boundary after reception of the Execute signal, the signal must be received during the 16.384-s superframe interval during which the countdown procedure occurs. To ensure that the Execute signal is transmitted at the correct time relative to the SSTOP change procedure, the MPRT will calculate the Universal Time Code (UTC) time at which the Execute command should be transmitted. This calculation is based on local knowledge of the time of occurrence of the start of transmit superframe (SOTSF) relative to UTC time at the MPRT. The UTC time at the MPRT will be synchronized to the UTC time at the INTELSAT SCC via reception at the SSRTE of an international time standard signal such as that from the Global Positioning System (GPS). The accuracy of calculation of the Execute time is ± 0.1 s. Execute time can be calculated by the MPRT up to 18 minutes in advance of the actual time, thus permitting manual setup of the command sequence.

After the satellite command (including the Execute signal) has been transmitted, the INTELSAT TDMA Headquarters Subsystem (HQS) [17] will detect from telemetry that the satellite has received the Execute signal. If not, the HQS will then send the "SSTOP change armed message is not received" message to the MPRT, which will suspend the procedure. The procedure can be suspended any time up until completion of the countdown at the MPRT.

Diagnostics and interference protection

To provide near-real-time data for the diagnostics subsystem [18] being implemented as part of the HQS, the ASU subsystem will include a diagnostics receiver. This receiver will detect the presence or absence of all bursts defined in its time plan, with the exception of the metric burst, and report this information to the HQS via the CDC. As a consequence of this passive monitoring capability, and to protect the signal processing equipment from broadcast interference within the traffic region of the frame, the equipment will not

monitor non-principal traffic bursts, and will receive only the RBD and TAS regions of the frame, which are grouped together for this purpose.

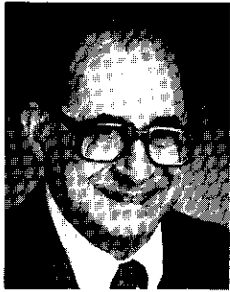
Conclusions

The use of SS-TDMA on the INTELSAT VI satellite represents the most advanced state-of-the-art implementation of a communications satellite system that has ever been attempted in an operational application. It provides an extremely flexible means for achieving efficient, non-blocking connectivity among its six multiple beams which cannot be matched by the static-switched techniques that have traditionally been used for satellite communications. It also brings with it other advantages not possible with static-switched systems, such as a reduction from four to two in the number of reference terminals needed to control TDMA operation, as well as enhanced protection of reference bursts from stray up-link interference. This paper has described many of the key features of the INTELSAT VI SS-TDMA that have made this unique system possible. The aim of this and the other papers on SS-TDMA appearing in these Special Issues of the *COMSAT Technical Review* is to provide a record of the unique features of INTELSAT VI SS-TDMA for use in future extensions of the technology to even more advanced satellite communications payloads.

References

- [1] W. G. Schmidt, "An On-Board Switched Multiple-Access System for Millimeter-Wave Satellites," INTELSAT/IEE Conference on Digital Satellite Communication, London, November 1969, *Proc.*, pp. 399-407.
- [2] S. J. Campanella and R. J. Colby, "Network Control for TDMA and SS-TDMA in Multiple-Beam Satellite Systems," 5th International Conference on Digital Satellite Communications, Genoa, Italy, March 1981, *Proc.*, pp. 335-343.
- [3] R. A. Rapuano and N. Shimasaki, "Synchronization of Earth Stations to Satellite-Switched Sequences," AIAA 4th Communications Satellite Systems Conference, Washington, D.C., April 1972, AIAA Paper No. 72-545.
- [4] S. J. Campanella, "Synchronization of SS-TDMA On-Board Clocks" (Abstract), International Telemetry Conference, San Diego, CA, October 1980.
- [5] G. Forcina and B. A. Pontano, "Network Timing and Control in the INTELSAT VI SS-TDMA System," 6th International Conference on Digital Satellite Communications, Phoenix, AZ, September 1983, *Proc.*, pp. X-9-X-15.
- [6] J. A. Lunsford *et al.*, "SS-TDMA System Design," scheduled for publication in *COMSAT Technical Review*, Vol. 22, No. 1, Spring 1992.
- [7] R. Bedford *et al.*, "SS-TDMA Reference Terminal," scheduled for publication in *COMSAT Technical Review*, Vol. 22, No. 1, Spring 1992.

- [8] S. J. Campanella and T. Inukai, "Satellite Switch State Time Plan Control," 6th International Conference on Digital Satellite Communications, Phoenix, AZ, September 1983, *Proc.*, pp. X-16-X-26.
- [9] R. K. Gupta *et al.*, "SS-TDMA On-Board Subsystem Design," scheduled for publication in *COMSAT Technical Review*, Vol. 21, No. 1, Spring 1991.
- [10] K. Hodson and S. J. Campanella, "Open Loop Acquisition and Synchronization," 4th International Conference on Digital Satellite Communications, Montreal, Canada, October 1978, *Proc.*, pp. 354-357.
- [11] Y. Ito, Y. Urano, T. Muratani, and M. Yamaguchi, "Analysis of a Switch Matrix for an SS/TDMA System," *Proc. IEEE*, Vol. 65, No. 3, March 1977, pp. 411-419.
- [12] T. Inukai, "An Efficient SS/TDMA Time Slot Assignment Algorithm," *IEEE Transactions on Communications*, Vol. COM-27, No. 10, October 1979, pp. 1449-1455.
- [13] C. L. Maranon *et al.*, "Timing Source Oscillator Control," scheduled for publication in *COMSAT Technical Review*, Vol. 22, No. 1, Spring 1992.
- [14] B. A. Pettersson *et al.*, "The Satellite Control Center and Its Role in Testing and Operation of the INTELSAT VI SS-TDMA Payload," scheduled for publication in *COMSAT Technical Review*, Vol. 22, No. 1, Spring 1992.
- [15] T. Inukai and S. J. Campanella, "Optimal On-Board Clock Control," *IEEE Journal on Selected Areas in Communications*, Vol. SAC-1, No. 1, January 1983, pp. 208-213.
- [16] T. Mizuike *et al.*, "Generation of Burst Time Plans for the INTELSAT VI SS-TDMA System," scheduled for publication in *COMSAT Technical Review*, Vol. 22, No. 1, Spring 1992.
- [17] F. H. Luz, D. Sinkfield, and N. Engelberg, "INTELSAT TDMA Headquarters Subsystem," scheduled for publication in *COMSAT Technical Review*, Vol. 22, No. 1, Spring 1992.
- [18] S. Tamboli *et al.*, "Design of the SS-TDMA Network Diagnostic System," scheduled for publication in *COMSAT Technical Review*, Vol. 22, No. 1, Spring 1992.



S. Joseph Campanella received a B.S.E.E. from the Catholic University of America in 1950, an M.S.E.E. from the University of Maryland in 1956, and a Ph.D. in electrical engineering from Catholic University in 1965. He is currently Chief Scientist and Vice President of COMSAT Laboratories. Previously, he served as Executive Director of the Communications Technology Division. He has contributed significantly to technologies for TDMA network control, satellite-switched TDMA, and TDMA terminal development, and has been responsible for the research and development of numerous other satellite communications innovations such as echo cancellers, digital speech interpolation, demand-assigned TDMA, and on-board satellite communications signal processing. Most recently, his efforts have been devoted to advanced satellite communications concepts involving on-board baseband processing, multiple hopping beams, and intersatellite links.

Dr. Campanella is a Fellow of IEEE and AAAS, an Associate Fellow of AIAA, and a member of Sigma Xi and Phi Eta Sigma. He is the recipient of the prestigious IEEE Behn award in international communications for 1990. He has authored chapters on TDMA and digital speech interpolation, and has taught courses on TDMA and satellite communications around the world. He holds numerous patents in communications technologies.

GianPiero Forcina graduated in electrical engineering from the University of Rome, Italy, in 1965, and performed postgraduate work at the George Washington University, Washington, D.C. Since 1968, he has been involved in the design of satellite systems both in Italy, at Telespazio, and in the United States, at COMSAT Laboratories, Fairchild Space and Electronics Company, and COMSAT General, where he was Manager of Systems Development. In 1978 he joined INTELSAT, Washington, D.C., where he has been largely concerned with the development of the INTELSAT TDMA System.



Benjamin A. Pontano received a B.S.E.E. from Carnegie Institute of Technology in 1965, and an M.S.E.E. and Ph.D. from the Pennsylvania State University in 1967 and 1970, respectively. He has been with COMSAT Laboratories for 10 years and is currently Executive Director of the Network Technology Division, where he directs research and development activities in the area of advanced network systems. In this capacity, he was responsible for the development of NASA's Advanced Communications Technology Satellite (ACTS) TDMA terminal equipment. He has also been involved with numerous technical and economic studies on advanced communications satellite systems.

Dr. Pontano was previously with INTELSAT for 10 years, where he was actively involved in development of the INTELSAT TDMA system and design of the INTELSAT VI spacecraft payload system. He has written more than 40 papers in the field of satellite communications, and holds patents in the area of interference measurement and cancellation. He has taught graduate-level courses in the field of communications systems at the George Washington University. Dr. Pontano is a Senior Member of IEEE and a member of AIAA and Sigma Xi.

Jack L. Dicks received a B.S. degree in Mathematics and Engineering Physics from Sir George Williams College in Montreal, Canada. He joined the Engineering Division of INTELSAT in 1978 as Manager of the Communications Engineering Department. In this position, he has been responsible for all aspects of the communications systems design and development for both the INTELSAT V and VI satellites and associated earth stations throughout the system. This involved the introduction of many new transmission techniques, both analog and digital, the most notable being development of the 120-Mbit/s TDMA system, which is now being succeeded by SS-TDMA. He has represented INTELSAT on numerous occasions at such ITU forums as the CCIR, and participated in WARC-ORB 85.

Before joining INTELSAT, Mr. Dicks was with COMSAT for 10 years where he was primarily responsible for transmission planning for the INTELSAT III, IV, IV-A, and V satellites. Prior to this, he was on the engineering staff at Teleglobe Canada, responsible for the planning, installation, and testing of submarine cable systems and the introduction of the Mill Village earth station.



INTELSAT VI transmission design and computer system models for FDMA services

M. P. BROWN, JR., R. W. DUESING, L. N. NGUYEN,
W. A. SANDRIN, AND J. A. TEHRANI

(Manuscript received June 15, 1990)

Abstract

INTELSAT employs computerized transmission system models to operate almost 10,000 communications carriers. This paper describes how these models have been prepared for use with the INTELSAT VI satellite to ensure the transmission quality necessary for a variety of frequency-division multiple access (FDMA) services, while maximizing transponder channel capacity. A general description of the modeling objectives for INTELSAT VI is given, including frequency planning, reference link budgets, co-channel interference, the transition from INTELSAT V (fourfold frequency reuse) to INTELSAT VI (sixfold reuse), and optimization of transponder channel capacity. The STRIP6 and OUTMAT6 system models and associated databases are also discussed, including mixed analog and digital operation, partial transponder optimization routines (leases), the approach used to handle hundreds of small digital carriers in a single 72-MHz transponder, and generation of antenna coverage diagrams (footprints) from measured INTELSAT VI databases.

Introduction

To date, transmission engineering and modeling have been carried out for several INTELSAT VI frequency-division multiple access (FDMA) services,

including intermediate data rate (IDR),* INTELSAT Business Services (IBS),** frequency-division multiplex (FDM)/FM, and leases. These services will account for the bulk of the traffic to be carried on these spacecraft, as depicted in Figure 1 which shows the Atlantic Primary traffic configuration for INTELSAT VI (F2) shortly after point-over of 35,728 channels of live traffic from INTELSAT V-A (F10) on April 27, 1990. This point-over involved 318 carriers and 96 earth stations.

As with each of its previous satellite series, INTELSAT has endeavored to build on past experience while introducing the new spacecraft and transmission features needed to keep pace with traffic growth and expanding services. The major transmission characteristics of INTELSAT V/V-A and VI are compared in Table 1 and briefly discussed below. Further details concerning the INTELSAT VI spacecraft communications payload specification and design are provided in companion papers [1],[2] in the *COMSAT Technical Review* INTELSAT VI series.

Sixfold frequency reuse for C-band (additional co-channel interference)

Two zone beams not on INTELSAT V/V-A have been added to INTELSAT VI in the southern hemisphere. These beams essentially increase the available bandwidth of INTELSAT VI by 648 MHz over that of INTELSAT V-A through additional reuse of the 6/4-GHz frequency band allocation. Reuse is achieved by spatial isolation of these beams from other zone beams, and by polarization isolation with the hemispheric beams. Further details on antenna tradeoff, design, and implementation are given in References 1 and 3. Although additional bandwidth is gained with this technique, more co-channel interference (CCI) is also introduced.

Higher down-link e.i.r.p. and reference link budgets

Tables 2 and 3 compare the reference transmission link budget calculations for INTELSAT VI satellites with those of INTELSAT V satellites at C- and Ku-band, respectively. Reference link budgets are used in the initial transmission design process to estimate the effect of various parameters on transponder capacity and up-link effective isotropically radiated power (e.i.r.p.). These budgets normally employ contractually specified values for

* Digital transmission using quadrature phase shift keying (QPSK) and carrier sizes from 64 kbit/s to 45 Mbit/s for public-switched network services.

** Transmission using QPSK/FDMA and carrier sizes from 64 kbit/s to 8.448 Mbit/s.

TABLE 1. COMPARISON OF MAJOR TRANSMISSION CHARACTERISTICS FOR INTELSAT V/V-A VS INTELSAT VI

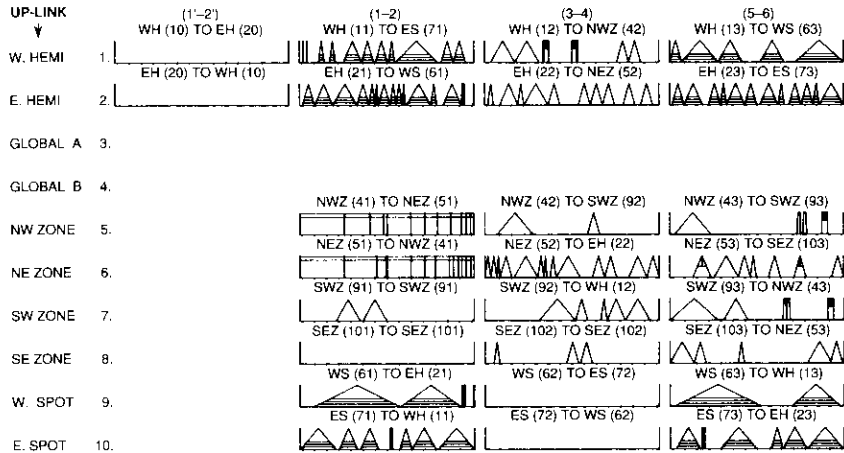
| CHARACTERISTICS | INTELSAT V/V-A | INTELSAT VI |
|--|--|---|
| C-Band Frequency Reuse (Circular Polarization) | 2x spatial 2x polarization 4x reuse | 4x spatial 2x polarization 6x reuse |
| Ku-Band Frequency Reuse (Linear Polarization) | 2x spatial | 2x spatial |
| C-Band e.i.r.p. (dBW) | | |
| • Hemi/Zone (72 MHz) | 29.0 | 31.0 |
| • Global (36 MHz) | 23.5 | 26.5 |
| Ku-Band e.i.r.p. (dBW) | | |
| • West Spot (72 MHz) | 44.4 ^a | 44.7 ^b |
| • East Spot (72 MHz) | 41.1 | 44.7 |
| Typical FDMA Carrier Modulation Technique | Analog (FM) | Analog and digital (FM and QPSK) |
| Typical No. of Carriers per Transponder | 15 to 20 (FM) | Hundreds (digital) |
| FDMA Carrier Types | FDM/FM CFDM/FM TV/FM IBS IDR SCPC Leases | Same, but predominantly digital (IBS and IDR), and more leases. |
| Atlantic Primary Satellite (335.5°E) | | |
| • Total Bandwidth (MHz) | 2,300 MHz | 3,190 MHz |
| • No. of Transponders | 32 (V-A) | 48 |
| • No. of Beams | 6 | 8 |
| • Channel Capacity ^c | 30,000 (V-A) | 48,000 (w/o DCME) 120,000 (w. DCME) |

^a Circular beam of INTELSAT V/V-A. All other INTELSAT V/V-A and VI beams are elliptical.

^b West inner beam = 44.7 dBW; West outer beam = 41.7 dBW.

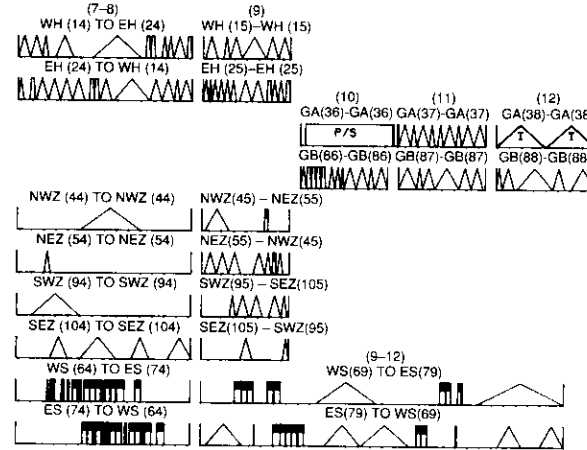
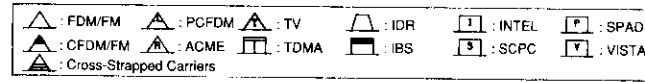
^c Equivalent 64-kbit/s bearer channels. Assuming a typical DCME gain of 2.5, the number of "derived" 64-kbit/s channels is $48,000 \times 2.5 = 120,000$. Depending on the mix of data and voice assumed, DCME gains of up to 5 are achievable.

| | | | | | | | | | | | | | |
|----------------------|--------|---------|-------|------|-----|----|-------|-----|-------|------|-------|-------|--------|
| Configured Channels: | FDM/FM | CFDM/FM | PCFDM | ACME | OCC | TV | TDMA | IDR | IBS | SCPC | SPADE | VISTA | TOTALS |
| 6/4 Direct | 16,824 | | 204 | | | 2 | 2,930 | 480 | 101 | 287 | 107 | | 20,935 |
| 14/11 Direct | 3,084 | | | | | | | | 930 | | | | 4,014 |
| Cross-Strap | 10,776 | | | | | | | | 3 | | | | 10,779 |
| Totals | 30,684 | | 204 | | | 2 | 2,930 | 480 | 1,034 | 287 | 107 | | 35,728 |



| Beam Connection | (1'-2') | | (1-2) | | (3-4) | | (5-6) | |
|-----------------|----------|-----------|----------|-----------|----------|-----------|----------|-----------|
| | BW (MHz) | No. Chan. |
| 1 | | | 53 | 1,141 | 35 | 676 | 60 | 1,260 |
| 2 | | | 64 | 1,369 | 53 | 1,212 | 65 | 1,440 |
| 3 | | | | | | | | |
| 4 | | | | | | | | |
| 5 | | | 72 | 1,459 | 20 | 468 | 20 | 384 |
| 6 | | | 72 | 1,471 | 60 | 1,320 | 40 | 720 |
| 7 | | | 20 | 384 | 40 | 936 | 35 | 696 |
| 8 | | | | | 13 | 300 | 33 | 612 |
| 9 | | | 62 | 1,585 | | | 56 | 1,404 |
| 10 | | | 61 | 1,356 | | | 56 | 1,224 |
| Total | 0 | 0 | 403 | 8,765 | 220 | 4,912 | 365 | 7,740 |
| % Used | 0 | 0 | 70 | | 38 | | 63 | |

Figure 1. INTELSAT VI (F2) Configuration After Point-Over From



| (7-8) | | (9-12) | | (9) | | (10) | | (11) | | (12) | | Grand Total | |
|----------|-----------|----------|-----------|----------|-----------|----------|-----------|----------|-----------|----------|-----------|-------------|-----------|
| BW (MHz) | No. Chan. | BW (MHz) | No. Chan. |
| 56 | 1,200 | | | 33 | 768 | | | | | | | | |
| 66 | 1,368 | | | 33 | 544 | | | | | | | | |
| 25 | 612 | | | 11 | 252 | 36 | 395 | 35 | 684 | 40 | 2TV | | |
| 3 | 36 | | | 26 | 444 | 34 | 536 | 35 | 720 | 38 | 888 | | |
| 20 | 432 | | | 20 | 396 | | | | | | | | |
| 40 | 828 | | | 8 | 192 | | | | | | | | |
| 23 | 270 | 80 | 1,791 | | | | | | | | | | |
| 25 | 269 | 88 | 1,684 | | | | | | | | | | |
| 258 | 5,015 | 168 | 3,475 | 130 | 2,596 | 70 | 931 | 70 | 1,404 | 78 | 890 | 1,763 | 35,728 |
| 45 | | 56 | | 60 | | 98 | | 97 | | 95 | | 55 | |

INTELSAT V-A (F10) (Atlantic Primary Satellite at 335.5°E, Early 1990)

TABLE 2. C-BAND TRANSPONDER REFERENCE LINK BUDGET:
REVISED STANDARD A, HEMI/ZONE
HIGH-GAIN STEP

64 kbit/s IDR PERFORMANCE ; BER = 10E-7 CLEAR SKY; FEC = 3/4

| PARAMETER | 1 | 2 | UNITS |
|---------------------------------------|----------|----------|----------|
| GENERAL | | | |
| 1 Satellite type | V-VA | V1 | |
| 2 Type of service | IDR | IDR | |
| 3 Uplink beam | H1 | H1 | |
| 4 Downlink beam | H1 | H1 | |
| 5 Frequency (up) | 6.130 | 6.130 | GHZ |
| 6 Frequency (dn) | 3.905 | 3.905 | GHZ |
| 7 Transponder bandwidth | 72.0 | 72.0 | MHZ |
| 8 Transponder amplifier type | OBTWTA02 | 16TWTA02 | |
| 9 Gain step | HIGH | HIGH | |
| 10 Transmit earth station type | A | A | |
| 11 Receive earth station type | A | A | |
| 12 Uplink eirp per carrier limit | N/A | N/A | |
| UPLINK | | | |
| 13 Combined U/L eirp of all Carriers | 78.9 | 77.4 | dBW |
| 14 Path loss (up) at 10 degrees | 200.7 | 200.7 | dB |
| 15 N/A | - | - | dB |
| 16 HPA IM Limit | N/A | N/A | dBW/4kHz |
| 17 C/T HPA IM | N/A | N/A | dBW/K |
| 18 Gain of 1m2 | 37.2 | 37.2 | dB/m2 |
| 19 Operating flux density | -84.6 | -86.1 | dBW/m2 |
| 20 Saturation flux density (B.E.) | -74.6 | -77.6 | dBW/m2 |
| 21 Antenna pattern advantage (up) | 0.0 | 0.0 | dB |
| 22 Input back-off (Total Xponder) | -10.0 | -8.5 | dB |
| LINK | | | |
| 23 Spacecraft G/T (B.E.) | -9.0 | -9.2 | dB/K |
| 24 C/T thermal (up) | -130.8 | -132.5 | dBW/K |
| 25 Spacecraft spatial beam isol. (up) | 27.0 | 27.0 | dB |
| 26 Spacecraft xpol beam isol. (up) | 24.0 | 22.2 | dB |
| 27 Earth station x-pol isol. (up) | 30.7 | 27.7 | dB |
| 28 Misalign angle (dual pol lin.)(up) | N/A | N/A | degrees |
| 29 Net isolation (up) | 21.7 | 20.1 | dB |
| 30 C/T co-channel (up) | -129.0 | -130.6 | dBW/K |
| IM | | | |
| 31 Saturated eirp (B.E.) | 29.0 | 31.0 | dBW |
| 32 Output back-off (Total Xponder) | -5.8 | -4.6 | dB |
| 33 IM power density (rel. to SCS) | -102.4 | -98.6 | dB/Hz |
| 34 Bandwidth improvement factor | 0.0 | 0.0 | dB/Hz |
| 35 C/T intermod | -132.0 | -134.5 | dBW/K |
| DOWNLINK | | | |
| 36 Spacecraft spatial beam isol. (dn) | 27.0 | 27.0 | dB |
| 37 Spacecraft xpol beam isol. (dn) | 24.0 | 22.2 | dB |
| 38 Earth station x-pol isol. (dn) | 30.7 | 30.7 | dB |
| 39 Misalign angle (dual pol lin.)(dn) | N/A | N/A | degrees |
| 40 Net isolation (dn) | 21.7 | 20.5 | dB |
| 41 C/T co-channel (dn) | -129.0 | -130.2 | dBW/K |
| LINK | | | |
| 42 Antenna pattern advantage (dn) | 2.0 | 2.0 | dB |
| 43 Path loss (dn) at 10 degrees | 196.7 | 196.7 | dB |
| 44 N/A | - | - | dB/K |
| 45 Earth station G/T | 35.0 | 35.0 | dB/K |
| 46 C/T thermal (dn) | -136.5 | -133.3 | dBW/K |
| TOTAL | | | |
| 47 C/T sum | -139.5 | -139.5 | dBW/K |
| 48 Other losses | 1.5 | 1.5 | dB |
| 49 C/T total (available) | -141.0 | -141.0 | dBW/K |
| SUMMARY | | | |
| 50 C/T thresh per 64 kbit/s (R = 3/4) | -174.8 | -174.8 | dBW/K |
| 51 System margin | 3.0 | 3.0 | dB |
| 52 C/T req per 64 kbit/s (R = 3/4) | -171.8 | -171.8 | dBW/K |
| 53 Occupied bandwidth per carrier | 51.2 | 51.2 | kHz |
| 54 U/L eirp corr. for down adv. | 0.8 | 0.4 | dB |
| 55 U/L eirp per 64 kbit/s (B.E.) | 48.9 | 47.0 | dBW |
| 56 Downlink eirp per 64 kbit/s (B.E.) | -7.6 | -4.4 | dBW |
| 57 Xponder cap (64 kbit/s info rate) | 1200 | 1200 | Channels |
| 58 Bandwidth-limited capacity | 1200 | 1200 | Channels |
| MARGIN | | | |
| 59 Uplink attenuation margin | 3.0 | 3.0 | dB |
| 60 Uplink xpol margin | 12.2 | 10.3 | dB |
| 61 Minimum uplink XPD' | 9.7 | 9.7 | dB |
| DEGRADATION | | | |
| 62 Downlink degradation margin | 5.8 | 8.4 | dB |
| 63 Downlink xpol margin | 12.2 | 11.0 | dB |
| 64 Minimum downlink XPD | 9.7 | 9.7 | dB |
| INS | | | |
| 65 Available D/L deg margin | 5.8 | 8.4 | dB |
| 66 Required D/L deg margin | 4.0 | 4.0 | dB |
| 67 Available system margin | 3.0 | 3.0 | dB |
| 68 Required system margin | 3.0 | 3.0 | dB |
| 69 Cap loss used to reduce U/L eirp | 0.0 | 0.0 | % |
| 70 Optimization method | CBWOPT8 | CBWOPT8 | |

Notes:
1. Parameter 61 = XPD' = Rain-impaired cross-pol discrimination and attenuation
2. Parameter 64 = XPD = Rain-impaired cross-pol discrimination.

TABLE 3. KU-BAND TRANSPONDER REFERENCE LINK BUDGET:
REVISED STANDARD C, WEST-TO-EAST SPOT
LOW-GAIN STEP

64 kbit/s IDR PERFORMANCE ; BER = 10E-7 (MINIMUM) CLEAR SKY; FEC = 3/4

| PARAMETER | 1 | 2 | UNITS |
|---------------------------------------|----------|----------|----------|
| GENERAL | | | |
| 1 Satellite type | V-VA | V1 | |
| 2 Type of service | IDR | IDR | |
| 3 Uplink beam | WEST | WEST | |
| 4 Downlink beam | EAST | EAST | |
| 5 Frequency (up) | 14.125 | 14.125 | GHZ |
| 6 Frequency (dn) | 11.075 | 11.075 | GHZ |
| 7 Transponder bandwidth | 72.0 | 72.0 | MHZ |
| 8 Transponder amplifier type | 10TWTA02 | 20TWTA02 | |
| 9 Gain step | LOW | LOW | |
| 10 Transmit earth station type | C | C | |
| 11 Receive earth station type | C | C | |
| 12 Uplink eirp per carrier limit | N/A | N/A | |
| UPLINK | | | |
| 13 Combined U/L eirp of all Carriers | 76.8 | 75.0 | dBW |
| 14 Path loss (up) at 10 degrees | 208.3 | 208.3 | dB |
| 15 N/A | - | - | dB |
| 16 HPA IM Limit | N/A | N/A | dBW/4kHz |
| 17 C/T HPA IM | N/A | N/A | dBW/K |
| 18 Gain of 1m2 | 44.5 | 44.5 | dB/m2 |
| 19 Operating flux density | -87.1 | -88.9 | dBW/m2 |
| 20 Saturation flux density (B.E.) | -75.3 | -73.0 | dBW/m2 |
| 21 Antenna pattern advantage (up) | 0.0 | 0.0 | dB |
| 22 Input back-off (Total Xponder) | -11.8 | -15.9 | dB |
| LINK | | | |
| 23 Spacecraft G/T (B.E.) | 3.3 | 1.7 | dB/K |
| 24 C/T thermal (up) | -128.3 | -131.7 | dBW/K |
| 25 Spacecraft spatial beam isol. (up) | 30.0 | 30.0 | dB |
| 26 Spacecraft xpol beam isol. (up) | N/A | N/A | dB |
| 27 Earth station x-pol isol. (up) | N/A | N/A | dB |
| 28 Misalign angle (dual pol lin.)(up) | N/A | N/A | degrees |
| 29 Net isolation (up) | 30.0 | 30.0 | dB |
| 30 C/T co-channel (up) | -120.7 | -120.7 | dBW/K |
| IM | | | |
| 31 Saturated eirp (B.E.) | 41.1 | 44.7 | dBW |
| 32 Output back-off (Total Xponder) | -5.8 | -9.7 | dB |
| 33 IM power density (rel. to SCS) | -102.6 | -114.4 | dB/Hz |
| 34 Bandwidth improvement factor | 0.0 | 0.0 | dB/Hz |
| 35 C/T intermod | -131.9 | -123.9 | dBW/K |
| DOWNLINK | | | |
| 36 Spacecraft spatial beam isol. (dn) | 30.0 | 30.0 | dB |
| 37 Spacecraft xpol beam isol. (dn) | N/A | N/A | dB |
| 38 Earth station x-pol isol. (dn) | N/A | N/A | dB |
| 39 Misalign angle (dual pol lin.)(dn) | N/A | N/A | degrees |
| 40 Net isolation (dn) | 30.0 | 30.0 | dB |
| 41 C/T co-channel (dn) | -120.7 | -120.7 | dBW/K |
| LINK | | | |
| 42 Antenna pattern advantage (dn) | 2.0 | 2.0 | dB |
| 43 Path loss (dn) at 10 degrees | 206.0 | 206.0 | dB |
| 44 N/A | - | - | dB/K |
| 45 Earth station G/T | 37.0 | 37.0 | dB/K |
| 46 C/T thermal (dn) | -131.8 | -132.0 | dBW/K |
| TOTAL | | | |
| 47 C/T sum | -136.0 | -135.5 | dBW/K |
| 48 Other losses | 1.5 | 1.5 | dB |
| 49 C/T total (available) | -137.5 | -137.0 | dBW/K |
| SUMMARY | | | |
| 50 C/T thresh per 64 kbit/s (R = 3/4) | -174.8 | -174.8 | dBW/K |
| 51 System margin | 7.0 | 7.0 | dB |
| 52 C/T req per 64 kbit/s (R = 3/4) | -167.8 | -167.8 | dBW/K |
| 53 Occupied bandwidth per carrier | 51.2 | 51.2 | kHz |
| 54 U/L eirp corr. for down adv. | 0.6 | 0.7 | dB |
| 55 U/L eirp per 64 kbit/s (B.E.) | 47.1 | 44.9 | dBW |
| 56 Downlink eirp per 64 kbit/s (B.E.) | 4.9 | 4.6 | dBW |
| 57 Xponder cap (64 kbit/s info rate) | 1082 | 1200 | Channels |
| 58 Bandwidth-limited capacity | 1200 | 1200 | Channels |
| MARGIN | | | |
| 59 Uplink attenuation margin | 7.0 | 7.0 | dB |
| 60 Uplink xpol margin | 22.8 | 22.3 | dB |
| 61 Minimum uplink XPD' | 7.7 | 7.7 | dB |
| DEGRADATION | | | |
| 62 Downlink degradation margin | 12.0 | 11.3 | dB |
| 63 Downlink xpol margin | 22.8 | 22.3 | dB |
| 64 Minimum downlink XPD | 7.7 | 7.7 | dB |
| INS | | | |
| 65 Available D/L deg margin | 12.0 | 11.3 | dB |
| 66 Required D/L deg margin | 11.0 | 11.0 | dB |
| 67 Available system margin | 7.0 | 7.0 | dB |
| 68 Required system margin | 7.0 | 7.0 | dB |
| 69 Cap loss used to reduce U/L eirp | 0.0 | 0.0 | % |
| 70 Optimization method | CBWOPT8 | CBWOPT8 | |

Notes:
1. Parameter 61 = XPD' = Rain-impaired cross-pol discrimination and attenuation.
2. Parameter 64 = XPD = Rain-impaired cross-pol discrimination.

such parameters as spacecraft e.i.r.p., gain-to-noise temperature ratio (G/T), and beam isolation. The link calculations assume a receive earth station with $G/T = 35.0$ dB/K (Standard A minimum value) at C-band, and $G/T = 37.0$ dB/K (Standard C minimum value) at Ku-band. Table 2 shows that, at C-band, CCI is a major contributor to the total noise budget.

To offset the increase in CCI, more down-link e.i.r.p. has been specified for the hemispheric and zone beams. As a result, the 72-MHz transponder channel capacity is about the same as for INTELSAT V/V-A (*i.e.*, 1,200 equivalent 64-kbit/s bearer channels). However, at Ku-band, the higher e.i.r.p. of an INTELSAT VI transponder results in higher capacity than INTELSAT V/V-A, since the amount of CCI is the same.

In terms of the spacecraft itself, the addition of 10 zone-beam transponders, as compared to the INTELSAT V-A baseline, is the principal channel capacity enhancer of INTELSAT VI. Other features which enhance its capacity and distinguish it from INTELSAT V-A are the addition of transponders (1'-2') occupying a new frequency band with twofold frequency reuse; better utilization of the Ku-band transponders through more narrow channelization (150 MHz vs 241 MHz); and the ability to handle satellite-switched time-division multiple access (SS-TDMA). The requirements for dual polarization operation at C-band, and the consequent need to account for rain and other transmission impairments, remain the same as for INTELSAT V/V-A [4].

Mixed modulation methods in the same transponder

The primary method of transmission used with INTELSAT V/V-A is FDM/FM/FDMA, which has been the backbone modulation and multiple-access method in the INTELSAT system for the past 25 years. However, it is INTELSAT's goal to convert the network from analog to digital modulation in the early 1990s. Digital techniques such as IDR (QPSK/FDMA) and TDMA/SS-TDMA offer the advantage of interfacing 64-kbit/s bearer channels with digital circuit multiplication equipment (DCME) for channel capacity gains of three to five. When combined with sixfold frequency reuse, digital modulation and DCME give an INTELSAT VI satellite a potential channel capacity of more than 120,000 channels.

In the transition phase, INTELSAT VI transponders will operate with a mix of analog and digital carriers sharing the same transponders. This has given rise to a new impairment—modulation transfer [5]—which must be accounted for in transmission design and is currently handled on a case-by-case basis whenever it is necessary to place large FM carriers and digital carriers in the same transponder. Eventually, INTELSAT VI will handle primarily digital modulation.

Increase in number of multiple accesses

The number of carriers and earth stations accessing a given transponder in the FDMA mode will be significantly greater on INTELSAT VI than on INTELSAT V/V-A. For example, a cross-strapped (C- to Ku-band) 72-MHz transponder on the INTELSAT V-A Primary satellite carried from 15 to 20 FDM/FM/FDMA carriers, whereas INTELSAT VI can have hundreds of QPSK/FDMA carriers. Some will be 2.048-Mbit/s IDR carriers using DCME, while many will be 64-kbit/s IBS carriers. The increase in multiple accesses has required new methods of computing intermodulation products in INTELSAT's system models, in an effort to reduce optimization time. This is discussed in more detail later. The significant increase in the number of carriers and earth stations has also required more sophisticated computer databases and output listings.

Services

Although the communications services (voice, data, fax, telex, *etc.*) to be carried on INTELSAT VI are essentially the same as those carried on the INTELSAT V/V-A series, most will be transmitted using digital modulation rather than analog modulation [6]. Another major difference will be a larger percentage of full and partial transponder leases for both domestic and international applications. The INTELSAT Board of Governors recently introduced a new type of lease known as Transponder Unrestricted Use (TUU) which recognizes, for the first time, leased bandwidth segments (and associated e.i.r.p. values) handling public-switched network voice and data for international traffic. As described later, the INTELSAT VI system models have been enhanced to permit the partial optimization of a portion of a transponder used for INTELSAT's open network services, such as IDR, while holding the remainder of the transponder "fixed" to the particular transmission design of a lease.

Transmission system models used with INTELSAT VI frequency plans

Transmission planning for INTELSAT VI has relied largely on the same engineering software developed for the INTELSAT V/V-A, but with enhancements in the following areas:

- Treatment of CCI
- Treatment of modulation transfer
- Mixed analog and digital optimization
- Partial transponder optimization

- Transponder optimization for hundreds of carriers
- Database augmentation (handling of additional beams and frequency reuse).

Each of these areas is discussed in greater detail below.

Computer system models have been developed to be used on a day-to-day basis by the INTELSAT operations staff to optimize transponder capacity through analytic study of various traffic configurations long before an agreed-upon frequency plan is actually implemented. This process ensures that a given frequency plan will deliver the appropriate quality in the presence of all transmission impairments. Once an optimized plan has been finalized, earth stations are "lined-up" on the basis of the up- and down-link c.i.r.p. values computed by these models.

STRIP6/OUTMAT6 description

Numerous software models are used at INTELSAT to support the design, analysis, evaluation, and operation of the system; however, the major transmission design models are the Satellite Transmission Impairments Program (STRIP) and the Outage Margin and Time program (OUTMAT). The versions of these programs which apply to INTELSAT VI are known as STRIP6 and OUTMAT6. The functions of this software and its major interfaces are summarized in Figure 2.

The STRIP6 software adjusts earth station c.i.r.p. levels and transponder operating points to achieve the required transmission performance for each carrier in the multiple frequency reuse satellite. The program accommodates all of the standard carrier types available via the INTELSAT network, including FDM/FM, IDR, and IBS, companded FM, single channel per carrier (SCPC), TV, and TDMA/SS-TDMA. It also has the ability to model a large number of nearly identical transmissions as single bands of carriers. In computing carrier performance and optimizing power levels, impairments resulting from up- and down-link thermal noise, up- and down-link CCI (due to frequency reuse), adjacent carrier interference (ACI), and intermodulation noise are included. The program output includes reports on the performance of the entire frequency plan in terms of picowatts for FM carriers, bit error rate (BER) for digital carriers, and signal-to-noise ratio (S/N) for TV carriers. The tabular and graphical outputs of STRIP6 provide both quick-look parameters and detailed data for in-depth analysis.

The STRIP6 calculations to meet required noise objectives are performed under clear-sky conditions. The OUTMAT6 program computes the effects of rain attenuation, depolarization, and down-link degradation (*i.e.*, the

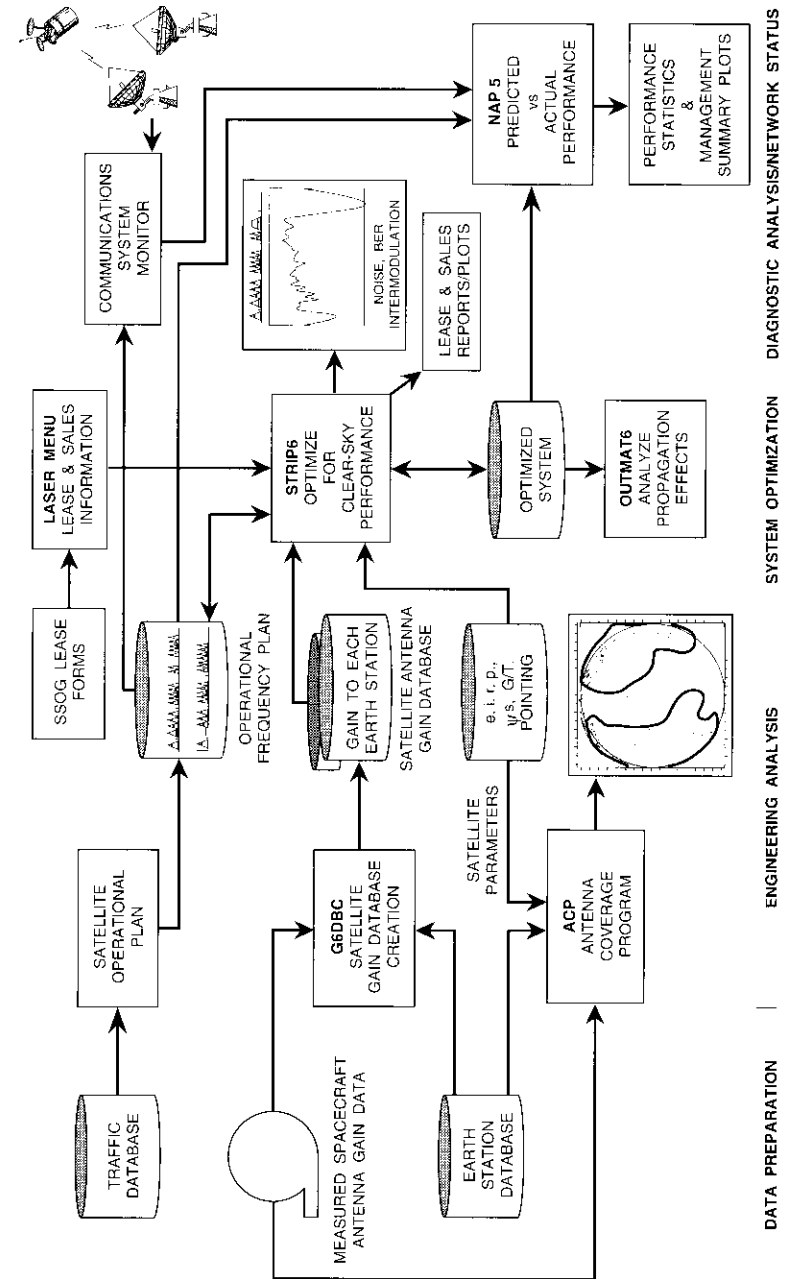


Figure 2. Overview of STRIP6/OUTMAT6 System Models and Associated Software

combined effect of attenuation and noise temperature increase) on the system. The Rice-Holmberg rain-rate model [7] is used to compute average estimates of impairments due to rain for each carrier in the system. Margin-to-threshold values are calculated to indicate the amount of protection that carriers operating in clear-sky conditions have against various rain impairments. STRIP6 and OUTMAT6 are used iteratively to ensure that carriers meet both clear-sky and rain-degraded performance criteria, with extra margin being provided to affected carriers through re-allocation of power or adjustment of required carrier performance.

As illustrated in Figure 2, the STRIP6/OUTMAT6 models interface with many applications. The major inputs to these models include frequency plan information, earth station parameters, and measured satellite data. The Lease and Sales Review model (LASER) is a menu-driven application which provides a direct user interface to the INTELSAT *Satellite System Operating Guide* (SSOG) forms submitted by lease applicants for transmission plan review. LASER assists in preparing inputs for STRIP6 and, as an adjunct to STRIP6 execution, it prints the link budget summaries and reports necessary to evaluate a transmission plan.

Once a frequency plan is optimized and implemented, carrier performance is monitored at a set of remote sites at several locations throughout the world. Automatic measurements of key parameters such as down-link e.i.r.p., center frequency, and out-of-band noise are made and transmitted back to INTELSAT headquarters. The Network Analysis Program (NAP) compares these measured quantities and earth station reported data with the predictions produced by STRIP6/OUTMAT6. Detailed reports are then produced for each transponder in the network, as well as a system summary such as that illustrated in Figure 1.

The following subsections highlight the modeled impairments and the latest techniques incorporated to support INTELSAT VI operation. Additional information regarding these system models may be found in References 8 through 10.

Co-channel interference

A major difference between INTELSAT V and INTELSAT VI satellites in the 6/4-GHz band is that INTELSAT VI employs sixfold frequency reuse, compared to fourfold frequency reuse on INTELSAT V. Sixfold reuse is accomplished by spatial isolation of the east, west, north, and south beams, together with circular polarization of opposite senses between the hemispheric and zone beams. (Design and measured antenna pattern data for spatial isolation and

orthogonal polarization isolation are provided in Reference 3.) Therefore, a carrier operating in a hemispheric or zone beam transponder can be subject to interference from five co-channel transponders in the up-link or down-link.

Among other parameters, the ratio of carrier power to CCI power for each interference is a function of the voltage axial ratio of the satellite and the earth station antennas, as well as the difference between the tilt angle, δ , of the incident wave and the antenna polarization ellipse [11]. In practice, δ can be any value between 0° and 90° . Based on experience with INTELSAT V/V-A, an average of 45° is assumed in the system models for the carrier-to-interference ratio (C/I) calculations. If 45° is assumed, the C/I reduces to

$$C/I = \text{Antenna XPD} \oplus \text{wave XPD} \quad (1)$$

where \oplus is power addition. If the worst-case condition of $\delta = 0^\circ$ is assumed, then

$$C/I = \text{Antenna XPD} \otimes \text{wave XPD} \quad (2)$$

where \otimes is voltage addition (which is 3 dB worse than power addition).

Using the power addition approach ($\delta = 45.0^\circ$), the C/I values for the INTELSAT VI and INTELSAT V/V-A satellites are compared in Table 4. It is shown that, for the up-link, the net C/I for INTELSAT VI is 1.6 dB less than for INTELSAT V/V-A. In contrast to the reference link budget calculations, the STRIP6 system model CCI calculations employ measured spacecraft co-polarization (co-pol) and cross-polarization (cross-pol) antenna gains in the direction of the desired and interfering earth stations, as well as assumed earth station polarization isolation, actual carrier levels, actual carrier modulation parameters, and actual carrier center frequencies.

Another consideration in CCI is the effect of rain attenuation and depolarization on the desired and interfering signals. At C-band, rain depolarization is a major contributor, whereas at Ku-band rain attenuation is of primary concern. Reference link budget calculations consider the need for rain margins, as shown in Tables 2 and 3. Rain margin is also provided for each carrier during the STRIP6/OUTMAT6 system model optimization process.

Modulation transfer effects

Modulation transfer occurs whenever an envelope-varying carrier shares a nonlinear amplifier (e.g., a traveling wave tube amplifier [TWT] or high-power amplifier [HPA]) with other carriers. Envelope fluctuations in one

TABLE 4. COMPARISON OF INTELSAT V AND VI CO-CHANNEL C/I: C-BAND UP-LINK*

Assumptions

- W. Hemi receive is the desired beam.
- Equal power levels for the desired and interfering carriers.
- Desired and interfering carriers are of the same type.

INTELSAT V/V-A

- C/I W. Hemi to E. Hemi = 27 dB (spatial isolation)
- C/I W. Hemi to E. Zone = 27 dB (cross-pol + spatial isolation)
- C/I W. Hemi to W. Zone = 27 dB (cross-pol isolation)
- Spacecraft beam isolation = 22.2 dB (power addition of all above)
- Interfering earth station cross-pol isolation = 30.7 dB**
- Net isolation C/I = 21.7 dB (power addition of 30.7 and 22.2 dB)

INTELSAT VI

- C/I W. Hemi to E. Hemi = 27 dB (spatial isolation)
- C/I W. Hemi to Zone 1 (NW) = 27 dB (cross-pol isolation)
- C/I W. Hemi to Zone 2 (SW) = 27 dB (cross-pol isolation)
- C/I W. Hemi to Zone 3 (NE) = 30 dB (spatial + cross-pol isolation)
- C/I W. Hemi to Zone 4 (SE) = 30 dB (spatial + cross-pol isolation)
- Spacecraft beam isolation = 21 dB (power addition of all above)
- Interfering earth station 1 cross-pol isolation = 30.7 dB**
- Interfering earth station 2 cross-pol isolation = 30.7 dB**
- Total earth station cross-pol isolation = 27.7 dB (power addition of 30.7 and 30.7 dB)
- Net isolation C/I = 20.1 dB (power addition of 21 and 27.7 dB)

* Down-link C/I can be calculated in a similar manner (see Table 2).

** An earth station cross-pol isolation of 30.7 dB has been assumed, corresponding to Standard A requirements. For other antennas such as Standard F, a value of 27.3 dB is applicable.

carrier result in phase variations in the other carriers, and therefore amplitude modulation in one carrier is transferred, as a phase modulation, to the phase of each of the other carriers.

Modulation transfer effects are analyzed for three different situations. In the first instance, when two or more FM carriers are passed through a common transponder TWTA, the modulation transfer effect manifests itself as crosstalk from other carriers in the baseband of a carrier. This is prevented by maintaining the TWTA operating point at an appropriate input backoff (IBO). In the second situation, when digital and FDM/FM carriers share a TWTA, the modula-

tion transfer effect is imparted from the former to the latter carriers due to envelope fluctuations of the digital carriers and the TWTA AM/PM conversion mechanism. In an operational environment, a few 4-kHz voice channels located at frequencies equal to the symbol rates (of the digital carriers) in the basebands of the FM carriers may receive unacceptable tonal interference and may have to be excluded from operational use. In the third situation, two or more digital carriers share a TWTA. Envelope fluctuations in one carrier become phase variations in other digital carriers and may degrade the BER performance of these carriers. Thus it is necessary to allocate sufficient system margin for these degradations.

Optimization

In a frequency reuse satellite system, it is important that up-link powers be adjusted to achieve the optimum balance among interference, intermodulation, and thermal noise so that the performance of the worst carrier in the system is optimized. If this is done, and all carriers operate above a minimum specified performance level, then system capacity can be maximized for fixed satellite resources. This is one of the principal functions of the STRIP6 program.

MIXED ANALOG AND DIGITAL OPERATION

The STRIP6 program estimates the demodulated performance for each carrier that accesses a frequency reuse transponder, and computes the optimum up-link e.i.r.p. level for each carrier in order to optimize the performance of the worst carrier. The program is primarily applicable to FDMA systems, although it can be applied to frequency plans having TDMA transponders.

The impairments computed by STRIP6 are up- and down-link intersystem interference (*i.e.*, CCI and ACI), intermodulation noise, and up- and down-link thermal noise. For the purpose of computing performance estimates and setting system up-link power levels, it is assumed that these basic impairments dominate system performance. Hence, intersystem interference, terrestrial interference, and adjacent transponder intermodulation interference are not modeled in STRIP6.

Earlier versions of STRIP6 computed impairments only for FDM/FM telephony carriers, since most of INTELSAT's traffic was of this type. However, in recent years the use of other modulation techniques has increased rapidly. Digital carriers (QPSK) are now extensively employed for TDMA, IDR, and IBS systems, as are other carrier types such as TV/FM and SCPC/FM. Hence, STRIP6 has been developed to include all carrier modulations now used by

INTELSAT, except for code-division multiple access (CDMA) carriers (*i.e.*, spread spectrum carriers). The carrier types modeled in STRIP6 include FDM/FM, TV/FM, digital, SCPC/FM, and companded single sideband (CSSB).

In STRIP6, a table lookup and interpolation technique has been implemented to compute BER based on the major impairments experienced by the carrier: thermal noise, interference, and intermodulation noise. This approach allows the use of either laboratory measurements or computer simulation results that characterize actual satellite channels and receiver implementation effects.

To address the fact that BER performance for a single strong interferer is different from an equivalent amount of thermal (Gaussian) noise, a two-dimensional interpolation scheme is employed. The data used for this scheme are the values of energy-per-bit to noise-power density ratio (E_b/N_o) vs BER for a number of different C/I 's, where the interference is that of a single interferer. These data must include an E_b/N_o vs BER relationship for $C/I = \infty$ (the all-thermal-noise case). If E_b/N_o vs BER data for additional values of C/I are omitted, the BER will be computed by treating all interference as an equivalent amount of thermal noise.

Specialized forms of the FM equation are used for FDM/FM, TV/FM, and SCPC/FM carriers. For FDM/FM carriers, multichannel loading factors, preemphasis, psophometric weighting, and companding advantage (if any) are included in a formulation that gives demodulated performance in terms of picowatts of noise. For TV/FM carriers, unified preemphasis and weighting factor improvements, with values that depend on the TV system specified, are used to compute S/N . For SCPC/FM carriers, a user-specified combined preemphasis, psophometric weighting, baseband bandwidth, and companding improvement factor is used to compute equivalent demodulated performance in terms of picowatts of noise (*i.e.*, performance judged subjectively to be equivalent to that of a voice channel with the same picowatts of noise, without the use of companders).

For FDM/FM and TV/FM carriers, the effects of interference and intermodulation noise are computed by assuming that the shape of the demodulated spectrum is the convolution of the RF spectra of the interfering and the interfered-with carriers. For SCPC/FM carriers, interference and intermodulation impairments are treated as equivalent amounts of thermal noise.

For CSSB, performance (in picowatts of noise) is computed by treating interferers and intermodulation products as equivalent amounts of thermal noise, and computing the total noise (*i.e.*, the composite of thermal, all interferer, and all intermodulation noise) at the top, middle, and bottom of the CSSB carriers' spectrum. The noise for the worst of these locations is taken as the

performance for the carrier. The CSSB performance is then computed using multichannel loading and psophometric weighting factors, as well as a user-specified companding advantage.

In addition to individually specified carriers, STRIP6 permits the specification of groups of SCPC/FM or digital carriers. This saves time in computing system performance for transponders that are loaded with a large number of similar small carriers. When such a band of carriers is specified, the effect of these carriers on the system is computed with reasonable accuracy; however, the computed performance of the carriers within the specified band is recognized to be a rough approximation. As in the case of a CSSB carrier, performance for a band of carriers is computed at the top, middle, and bottom of the band, and the worst performance of the three is selected.

In order to permit rapid computation of interference and intermodulation impairments in STRIP6, the power spectra of all carriers are assumed to have shapes that are either rectangular, Gaussian, or convolutions of rectangular and Gaussian shapes. The shape chosen for modeling the mainlobe of a digital carrier is a Gaussian shape convolved once with a rectangle. A rectangular spectrum, which serves to model the sidelobes, is added to the mainlobe spectra when the ACI that occurs within a transponder is calculated.

For FDM/FM carriers, the spectrum is a function of the ratio of the number of active telephone channels (a user-specified parameter) to the maximum number of channels in the carrier baseband. Thus, if the carrier is lightly loaded, its spectral shape is nearly rectangular, and if it is fully loaded the spectrum is close to a Gaussian shape.

For TV/FM carriers, two spectral representations are used. The first is a Gaussian spectrum which approximates the spectrum under fully loaded conditions (such as a color bar signal), while a rectangular spectrum is used for the case of an all-black picture, when the spectral shape is determined primarily by the spreading waveform. In actual interference situations, the CCI to frequency reuse carriers will be worst for an all-black picture signal, while ACI to other carriers will be worst when the carrier is fully modulated. Hence, in STRIP6, both shapes are assumed. The effect of a TV carrier's interference to another carrier is computed twice, and the worst result is kept.

Although SCPC/FM carriers have a spectrum with a significant unmodulated carrier component, the actual division between the modulated and unmodulated components is generally not critical for computing interference to other carriers. Thus, a Gaussian shape that is slightly narrower than the modulated component is used in STRIP6 as a compromise between the modulated and unmodulated components.

A rectangular spectrum is assumed for CSSB carriers and for the "band of carriers" case.

In earlier versions of the STRIP6 program, which included only FDM/FM carriers, the optimization objective was to minimize the noise (in picowatts) for each carrier, and the optimization variables were the transponder IBOs. The optimization technique used was a combination of a power-balancing algorithm described by Meyerhoff [12] and a modified Newton-Gauss optimization procedure. The power-balancing algorithm is used to adjust the relative powers of the carriers within a transponder (while maintaining a constant total operating point) so that the performance of the worst carrier is optimized—a process that tends to equalize the performance of all carriers. The modified Newton-Gauss algorithm uses as its optimization variables the operating points of individual transponders, and the two algorithms are applied alternately. This has been found to be an efficient and reliable optimization procedure.

With the incorporation of digital and other types of carriers into the STRIP6 program, the optimization procedure required modification, since the various carrier types can be specified to have different units for expressing demodulated performance (*i.e.*, picowatts for FDM/FM, SCPC/FM, and CSSB carriers; BER for digital carriers; and S/N for TV/FM carriers), although the use of predetection carrier-to-noise ratio (C/N) (or carrier-to-noise power density ratio [C/N_0] or carrier-to-noise temperature ratio [C/T]) values are also permitted. Additionally, the sensitivity of the performance of different carrier types to changes in up-link carrier power varies.

In implementing optimization in the STRIP6 program for a mix of carrier types, the optimization techniques described above for FDM/FM carriers alone were retained essentially unchanged, while the optimization objective function was modified [13]. The optimization variables (up-link powers) were unchanged.

In the modified objective function, each carrier is required to have a specified criterion (*i.e.*, minimum acceptable) performance value. Examples might be 7,500 pW for an FDM/FM carrier, a BER of 10^{-6} for a digital carrier, or a S/N of 50 dB for a TV/FM carrier. To accommodate the mix of various carrier performance measures, the difference between the actual and the specified performance for all carriers is reduced to a carrier power ratio that is approximately proportional to the change in power required for a carrier to perform at the criteria performance level. For digital carriers, the calculation of this ratio requires the conversion of BER values to approximate E_b/N_0 values.

The resulting power ratios for each carrier type are then weighted with an exponent to equalize the sensitivity of each carrier type to changes in the carrier levels. These weighted power ratios are used in an optimization objec-

tive function that is formulated to minimize them. Default values for the exponents of different carrier types are used in the program, although the user can change these and other variables that control the optimization process.

PARTIAL TRANSPONDER OPTIMIZATION

In the development of transponder loading plans carrying international carriers, STRIP6 is normally used to optimize individual carrier performance and total capacity. In this process, the total IBOs of individual transponders are used as independent variables. The optimized individual carrier IBOs are then determined from the optimum set of total transponder IBOs.

In recent years, with the introduction of transponder sales and leases, the optimization of loading plans has had to be slightly altered to address new situations. When a portion of a transponder is leased, it is necessary to reserve the leased bandwidth segment and power for the lessee while optimizing the IBOs of international carriers in the remaining portion of the transponder. In other cases, when it is necessary to introduce new carriers into a transponder already loaded with a large number of carriers, it is a practical matter to hold the IBOs of these latter carriers fixed while optimizing those of the new carriers.

In order to handle such situations, the carriers whose powers are to be fixed must be excluded from the variational part of the optimization process. Accordingly, STRIP6 has been upgraded to include a capability for partial optimization to permit evaluation of the communications performance of frequency plans loaded with international carriers, leased carriers, or a combination of these. In particular, the following four specific cases can be handled:

- *Case 1.* The IBOs (or up-link e.i.r.p.'s) of any number of carriers located anywhere in any transponder are held fixed while optimizing those of the remaining carriers.
- *Case 2.* The IBOs of any number of carriers located in any leased segment, as well as those of any number of carriers used for international traffic, are optimized while reserving the unused leased power.
- *Case 3.* The IBOs of any number of carriers located in any leased segment are held fixed, and the unused leased power reserved, while optimizing the IBOs of any number of carriers used for international traffic.
- *Case 4.* The IBOs of any number of carriers located in any leased segment are optimized, and the unused leased power reserved, while holding fixed the IBOs of any number of carriers used for international traffic.

Treatment of hundreds of carriers per transponder

When the STRIP program was first implemented, FDMA satellite transponders were loaded with a relatively small number of carriers, typically less than 20. However, FDMA transponders have recently been loaded with increasingly large numbers of smaller carriers, to the point where a single transponder may now be loaded with hundreds of carriers.

The effect of this increased number of carriers on analysis and optimization software is primarily in the increased volume of input data required to operate the programs, and in the computer resources (both time and memory) required to run the program. The primary cause of increased demand on computer resources is in the computation of intermodulation products (IMPs), since the number of third-order IMPs grows as

$$\frac{n^2(n-1)}{2} \quad (3)$$

where n is the number of carriers in the transponder.

STRIP6 has been modified in two basic ways in order to accommodate large numbers of carriers. The first technique, as noted in the above discussion on mixed carrier optimization techniques, is to treat groups of identical small carriers as "bands" of carriers. This technique allows for a simplified program input, provides a reasonable estimate of the interference and intermodulation impairments that such bands of carriers cause to other carriers, and provides a rough approximation of the performance of individual carriers within the band. However, in many instances this technique is inadequate because greater accuracy is required for the computed performance of each individual carrier.

The second technique for accommodating large numbers of carriers allows small carriers to be specified individually. This approach accelerates the computation of IMPs and reduces required computer memory size when the number of carriers in a transponder becomes large.

The method used in the STRIP6 program to compute impairments for a small number of carriers is described in References 14 and 15. Here, the approach is to compute every individual IMP and, for those IMPs creating an impairment, to compute the effect of the IMP as if it were an individual interferer.

For larger numbers of carriers where the number of IMPs grows exponentially, the IMP computation procedure has been modified to accelerate computation time. The basic premise of the accelerated technique is that, for transponders loaded with large numbers of carriers (greater than about 30), the IMP spectrum—a composite of thousands of individual IMPs—will remain

largely unchanged as long as the spectral density of the carrier plan remains approximately the same. Also, the actual carrier frequency plan is replaced by one having fewer carriers, for the purpose of computing IMP impairments when the number of actual carriers exceeds about 30. The carrier frequency plan with fewer carriers (referred to as the pseudo frequency plan) is selected so that its overall power spectrum approximates the original plan. This is done by combining clusters of carriers into single carriers. The pseudo frequency plan is used only to generate IMP products, which are then treated as interferers to the actual carriers.

The accelerated IMP computation technique has the advantage that fewer individual IMPs are generated by the pseudo frequency plan, and consequently, less computer time and memory are required to compute IMP impairments.

Databases and models

The optimization of INTELSAT VI frequency plans by using STRIP6 is based on three basic types of data: actual earth station parameters, flight-model-specific pre-launch measured data and parameters, and carrier frequency assignment and modulation parameters. The frequency planning information is derived from the traffic database, as established through a Global Traffic Meeting of all participants in the INTELSAT network, and is input to STRIP6 by system planners.

Approximately 1,600 antennas are represented in the earth station database. Key parameters include an identifying code, the station's name and country, its location (longitude and latitude), its G/T , the INTELSAT earth station standard designation, and the propagation data required by the OUTMAT6 software. The earth station database is updated regularly from a master listing of applications received from earth station operators via INTELSAT's Service Bureau. A majority of the data are automatically obtained through the use of comparison software, which extracts applicable parameters from the Service Bureau's files. The propagation information [7] includes the mean annual rainfall (M) and the fraction of M that results from thunderstorm activity, β (rain rate > 25 mm/hr). These data are acquired from worldwide weather records and are reviewed about every 12 months to ensure that the most current statistics are used.

Sixfold frequency reuse is accomplished in five frequency slots (or transponder bandwidth allocations) at C-band on INTELSAT VI satellites through the use of east and west hemispheric beams in one polarization sense, and four zone beams (northeast, northwest, southeast, and southwest) in the opposite sense. Twofold reuse is employed in four slots of global coverage at C-band

through dual-polarization beams. In Ku-band, twofold frequency reuse is accomplished via spatial isolation and cross-polarized spot beams that may be steered anywhere on the earth's surface. In order to optimize and operate the network, antenna data, measured during spacecraft construction for each beam, are employed in the STRIP6 model.

The INTELSAT VI pre-launch antenna measurements are used to determine the gain available in the direction of each earth station from each satellite in-orbit location. For each flight model, the manufacturer measures the receive and transmit co- and cross-polarization antenna patterns at the center frequency of each transponder on the satellite, as well as the saturation flux density, G/T , and e.i.r.p. These data are recorded and transferred via magnetic tape or disk through the INTELSAT Test Data Handling System, and subsequently input to the INTELSAT VI data preparation software for conversion to a format acceptable by STRIP6. This database is carefully cross-checked against in-orbit measurements taken just after launch and prior to commercial operation.

Using the pre-launch measured data, the earth station database, and the actual satellite antenna pointing information for each location, the INTELSAT VI antenna gain database creation program (G6DBC) computes the gain of each satellite antenna beam toward each station that is in view of the satellite. Both the co- and cross-polarization gains of each receive and transmit antenna are computed for each earth station for each frequency slot, and are stored in satellite antenna gain databases for input to the STRIP6 software. These files are provided for all current and planned satellite locations and are updated with each change in the earth station database.

The communications parameters (saturation flux density, G/T , e.i.r.p., and attenuator settings) are measured for each path through the satellite, including redundant receivers and transmitters. They are obtained via floppy diskette from the INTELSAT VI performance parameters program (I6PERF) and are then summarized for use in the system models by the Communications Parameter Averaging program (G6CAP). The measured amplitude and phase of each type of traveling wave tube and solid-state power amplifier on the satellite are converted to Bessel function coefficients by using the intermodulation analyzer software (CIA4) and are also stored on a STRIP6 input parameter file.

In addition to the satellite and earth station characteristics, a set of parameters for each INTELSAT-approved carrier size for all modulation techniques is maintained in a user-accessible file for input to STRIP6/OUTMAT6. Parameters are included which define the size and performance requirements of each carrier. These encompass such items as the RF allocated bandwidth, relative power, rms deviation, IF bandwidth, information rate, filter and modem curves,

and required performance parameters specified in terms of picowatts, BER, C/N , C/T , or C/N_0 .

To evaluate satellite antenna coverage areas, measured INTELSAT VI antenna patterns may be plotted on various projections of the earth's surface using the Antenna Coverage Program (ACP). Orthographic and Mercator projections from geosynchronous orbit, as well as closeup views of the earth and selected satellite antenna patterns, may be portrayed on multicolored displays or sent to various plotting devices. Figure 3 is an example of INTELSAT VI beam coverages produced by the ACP.

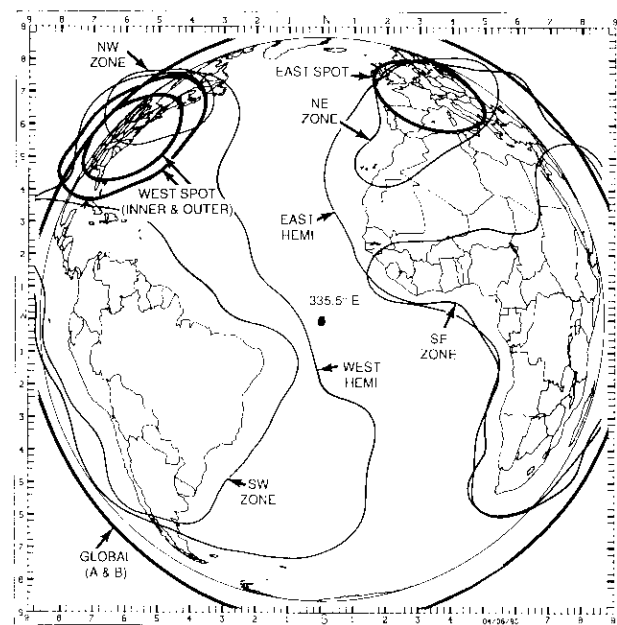


Figure 3. *INTELSAT VI Typical Measured Transmit Antenna Coverage (ACP Software)*

Conclusions

The INTELSAT VI FDMA transmission design was based on experience gained with previous INTELSAT spacecraft series. Existing computer system models were enhanced specifically for use with the INTELSAT VI series of satellites, including the need to treat mixed analog and digital operation,

partial transponder optimization for leased bandwidth, a new method of computing IMPs for hundreds of carriers per transponder, sixfold frequency reuse, and augmentation of earth station and spacecraft parameter databases. The INTELSAT VI system models are used to ensure that all of INTELSAT's FDMA services (e.g., IDR, IBS, FM, and SCPC) provide the necessary transmission quality while maximizing transponder channel capacity.

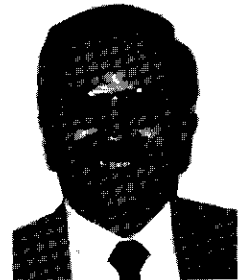
The STRIP6/OUTMAT6 system models were used as the basis for planning the successful point-over of 35,728 channels of live traffic from INTELSAT V-A (F10) to INTELSAT VI (F2) at 335.5°E on April 27, 1990. These models will continue to be used for the day-to-day operation of the INTELSAT VI satellites over their orbital life to ensure that the quality of service for each channel is satisfied in the most efficient manner. The models will also be upgraded to handle new operational requirements as they develop.

References

- [1] B. A. Pontano, A. I. Zaghoul, and C. E. Mahle, "INTELSAT VI Communications Payload Performance Specifications," *COMSAT Technical Review*, Vol. 20, No. 2, Fall 1990, pp. 271-308 (this issue).
- [2] G. Horvai *et al.*, "INTELSAT VI Communications Subsystem Design," scheduled for publication in *COMSAT Technical Review*, Vol. 21, No. 1, Spring 1991.
- [3] R. R. Persinger *et al.*, "The INTELSAT VI Antenna System," scheduled for publication in *COMSAT Technical Review*, Vol. 21, No. 1, Spring 1991.
- [4] J. L. Dicks and M. P. Brown, Jr., "INTELSAT V Satellite Transmission Design," IEEE International Conference on Communications, Toronto, June 1978, *Conf. Rec.*, Vol. 1, pp. 2.2.1-2.2.5.
- [5] O. Shimbo, L. N. Nguyen, and J. P. A. Albuquerque, "Modulation-Transfer Noise Effects among FM and Digital Signals in Memoryless Nonlinear Devices," *Proc. IEEE*, Vol. 74, No. 4, April 1986, pp. 580-599.
- [6] L. B. Perillan, W. R. Schnicke, and E. A. Faine, "INTELSAT VI System Planning," *COMSAT Technical Review*, Vol. 20, No. 2, Fall 1990, pp. 247-269 (this issue).
- [7] P. L. Rice and N. R. Holmberg, "Cumulative Time Statistics of Surface-Point Rainfall Rates," *IEEE Transactions on Communications*, Vol. COM-21, No. 10, October 1973, pp. 1131-1136.
- [8] R. W. Duesing, "Software Models for the INTELSAT System," *IEEE Computer*, Vol. 16, No. 4, April 1983, pp. 53-67.
- [9] R. W. Duesing and M. J. Kelinsky, "INTELSAT Planning and Modelling Software in Support of IDR," *International Journal of Satellite Communications*, Vol. 6, No. 4, October-December 1988, pp. 407-417.
- [10] M. J. Robusto, "INTELSAT V Transmission System Models Used for Analysis, Optimization, and Operational Control," AIAA 9th Communications Satellite Systems Conference, San Diego, California, March 1982, *Proc.*, pp. 282-293.
- [11] D. F. DiFonzo and W. S. Trachtman, "Antenna Depolarization Measurements Using Satellite Signals," *COMSAT Technical Review*, Vol. 8, No. 1, Spring 1978, pp. 155-185.
- [12] H. J. Meyerhoff, "Power Balancing in Multibeam Satellites," AIAA 5th Communications Satellite Systems Conference, Los Angeles, California, April 1974, *Proc.*, Paper No. 74-470.
- [13] W. A. Sandrin and L. N. Nguyen, "Computing the Performance of Digital Satellite Links on a System-Wide Basis," 8th International Conference on Digital Satellite Communications, Guadeloupe, FWI, April 1989, *Proc.*, pp. 747-754.
- [14] J. C. Fuenzalida, O. Shimbo, and W. L. Cook, "Time-Domain Analysis of Intermodulation Effects Caused by Nonlinear Amplifiers," *COMSAT Technical Review*, Vol. 3, No. 1, Spring 1973, pp. 89-143.
- [15] N. K. M. Chitre and J. C. Fuenzalida, "Baseband Distortion Caused by Intermodulation in Multicarrier FM Systems," *COMSAT Technical Review*, Vol. 2, No. 1, Spring 1972, pp. 147-172.

Martin P. Brown, Jr., received a B.E.E. from the Georgia Institute of Technology in 1966. Before entering military service, he was employed by IBM at Cape Kennedy where he was involved in construction of the first Saturn V launch vehicle. From 1967 to 1971, he served as an engineering communications officer with the U.S. Air Force. He worked for COMSAT Laboratories, beginning in 1971, where he was primarily involved in transmission design for INTELSAT IV, IV-A, and V. Leaving COMSAT in August 1978, he joined INTELSAT to become Manager of the Satellite Transmission Engineering and Modeling Section, where he has been responsible for FDMA transmission design for the INTELSAT VI, VII, and K satellites, and for preparing the required earth station performance characteristics associated with each of these spacecraft series. He has also been involved in the design of most of the analog and digital modulation techniques employed by INTELSAT, and in the development of computer system models for satellite communications.

Mr. Brown is a past Chairman of the IEEE Communications and Broadcast Satellite Systems Committee and a Registered Professional Engineer.





Richard W. Duesing received a B.S. in mathematics from Youngstown University in 1962. He joined INTELSAT in 1979, and is currently a Principal Engineer in the Transmission Engineering and Modeling Section, where he is responsible for the management and implementation of computer system models pertaining to communications engineering and transmission analysis. He has been involved in the transmission planning and development of satellite characteristics modules for the INTELSAT V, VI, VII, and K series satellites. He was employed by Computer Sciences Corporation in 1969 as a Department Manager and participated in developing models in support of the defense communications satellite system; orbit determination applications for the NASA/JPL deep space probes; and real-time message switching and scientific systems. He also worked at McDonnell-Douglas Astronautics, beginning in 1962, where he developed software models for digital filtering, telemetry data reduction, acoustic and vibration analysis, and weight control applications.

Lan N. Nguyen received a B.S.E.E. from the University of Florida, Gainesville, in 1967; an M.S.E. in electrical engineering from the University of Pennsylvania, Philadelphia, in 1968; and became a Ph.D. candidate at the same school in January 1969. From October 1969 to April 1975, he worked in Saigon, Viet Nam. Following this, he was a Transmission Analyst and a Systems Project Engineer at COMSAT General Corporation, Washington, D.C., and later a Staff Engineer at Satellite Business Systems, McLean, Virginia.

Mr. Nguyen joined INTELSAT, Washington, D.C., as a Member of the Technical Staff in the Communications Analysis and Design Section of the Engineering Division in April 1979. In his current capacity as a Principal Engineer, he has been responsible for the technical management of major activities related to digital services. His interests include system studies, performance analysis, and implementation of efficient communications systems techniques in satellite systems. He is a Member of IEEE.



William A. Sandrin received a B.S.E.E. from the University of Vermont in 1963, and an M.E.E. from Rensselaer Polytechnic Institute in 1966. From 1966 to 1971, he worked for the Boeing Company, Aerospace Group, where he was involved in space communications system design and in the development of phased-array antennas. In 1971, he joined COMSAT Laboratories, where he has been engaged in multibeam antenna studies; transponder linearizer development; transmission impairments analysis; studies of domestic, maritime, and aeronautical satellite systems; studies of adaptive phased-array antennas for spacecraft and small-terminal applications; frequency planning studies; and transmission software development. He is currently Manager of the Systems Modeling and Analysis Department of the Communications Technology Division. Mr. Sandrin is a member of IEEE.

Jahangir Anvari Tehrani received a B.S.E.E. from Oklahoma State University in 1977, and an M.S. from George Washington University in 1979. He joined INTELSAT in 1979 and is currently a Senior Engineer in the Satellite Transmission Engineering and Modeling Section. He has worked in the areas of transmission planning for INTELSAT VI, VII, and K; design of the digital modulation techniques employed with these spacecraft; and evaluation of the transmission plans for the leased transponders. In 1978 he worked at COMSAT, where he was involved in the intersystem coordination efforts between INTELSAT and the USSR. He is a member of IEEE.



CTR Note

Offset-QPSK modulation for maritime satellite communications

L-N. LEE AND S. A. RHODES

(Manuscript received November 27, 1990)

Introduction

In maritime mobile communications, RF power is always at a premium because of the physical constraints and costs of mobile terminals. Designers of mobile communications systems must therefore consider every possible means of maximizing the power efficiency of the transmission system. Maritime mobile satellite systems typically employ frequency modulation (FM), which trades bandwidth for power [1]. However, the thresholding effect of FM reception results in a limit beyond which the bandwidth/power tradeoff no longer applies. Furthermore, as traffic grows, systems gradually become bandwidth-limited, as well as power-limited.

Recent technical advances in mobile satellite communications systems design include significant progress in digital speech coding and digital transmission techniques that are both power- and bandwidth-efficient. Typically, good communications-quality speech is being achieved with 4.8-kbit/s encoders [2], and near-toll-quality speech with 16-kbit/s encoders [3]. Coherent detection of phase shift keying (PSK) modulated signals that employ forward error correction (FEC) codes is routinely combined with soft-decision decoding to achieve extremely good power efficiency [4]. In particular, quadrature PSK (QPSK) with efficient filtering is frequently the modulation of choice, as it often achieves a bandwidth efficiency of 1.4 to 1.5 bit/s/Hz without degrading power efficiency in additive white Gaussian noise (AWGN) channels [5].

Lin-Nan Lee, formerly a Principal Scientist in the Communications Technology Division at COMSAT Laboratories, is currently Chief Scientist with COMSAT Systems Division.

Smith A. Rhodes, formerly a Senior Scientist in the Communications Technology Division at COMSAT Laboratories, is currently a Member of the Technical Staff at TASC, McLean, Virginia.

To take full advantage of the total amplifier output power, high-power amplifiers (HPAs) often are operated in the highly nonlinear class-C mode. However, conventional QPSK signals experience sidelobe regrowth when transmitted through nonlinear amplifiers. The distortion introduced by the nonlinearity causes energy dispersion, filter mismatch, and adjacent channel interference (ACI), all of which degrade performance. By staggering the timing of data transitions between in-phase and quadrature channels, offset-QPSK (O-QPSK) has less amplitude fluctuation than QPSK, and is therefore less susceptible to nonlinear distortion [6]. In order to understand the design trade-offs and performance limitations of O-QPSK modulation in a power- and bandwidth-limited nonlinear channel in a mobile environment, a computer and hardware simulation study was conducted using Inmarsat-B parameters. This note discusses the computer simulation and laboratory measurement results.

Channel model

In maritime mobile satellite communications, satellites are typically operated in the single-carrier-per-channel (SCPC) mode, with sufficient backoff to provide a quasi-linear channel and thereby allow frequency-division multiple access (FDMA) of multiple simultaneous carriers. However, the characteristics of the communications channels differ somewhat between the mobile-to-fixed-station link and fixed-station-to-mobile link. Since fixed stations have less stringent power limitations than mobile terminals, HPA nonlinearity is generally a problem only in the mobile-to-fixed-station link. Also, the impairments of the mobile-to-fixed-station link are dominated by the mobile-to-satellite portion (up-link) of the link.

The channel model developed for this study assumes that the mobile terminals use a nonlinear HPA with certain amplitude and phase characteristics. The transmission may experience multipath signal fades before reaching the satellite. At the satellite, the signal is further corrupted by AWGN and ACI. The signal is then translated to a higher frequency band and repeated without processing. The satellite transponder is sufficiently backed off in power to a quasi-linear region such that effects of intermodulation and modulation transfer are negligible. The majority of the frequency error due to satellite motion and frequency translation is pre-corrected by a network-wide frequency control scheme. Thus, the residual frequency error is much smaller than the data symbol rate, and can be removed completely by the data demodulator once the signal is acquired.

To gain insight into the effects of nonlinearity on the reliability of data transmission in the mobile-to-fixed-station link, and on the filter design in such a link, the performance of QPSK and O-QPSK were evaluated using com-

puter simulations to estimate the bit error rates (BERs) under the modeled channel conditions. The channel conditions studied included AWGN in combination with the following:

- a. A single channel.
- b. Two adjacent channels in addition to the channel of interest.
- c. Two adjacent channels in addition to the channel of interest, with the channel of interest faded by 5 dB.
- d. Four adjacent channels in addition to the channel of interest.
- e. Four adjacent channels in addition to the channel of interest faded by 5 dB.

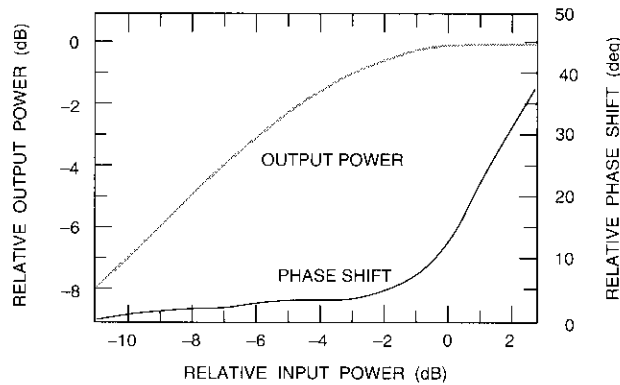
Case (a) establishes the baseline; cases (b) and (d) are used to examine the effect of ACI; and cases (c) and (e) are intended to examine the effect of up-link fading of the desired channel, which usually creates the most severe operating condition in the presence of adjacent channels.

It should be mentioned that a constant or quasi-static fade, instead of Ricean fade, is applied to cases (c) and (e). When mobile terminals are moving rapidly, fading dynamics must be included in the fading model. Such dynamics result in some decorrelation of the carrier phase for the modulation symbol that is being "coherently" demodulated.

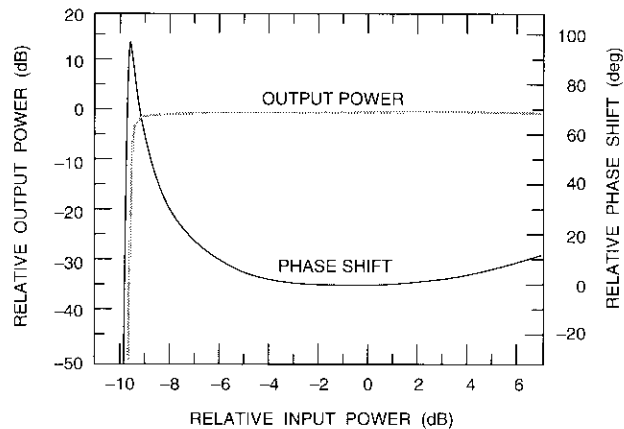
Compared with the case of quasi-static fading, the problem of time-varying carrier phase causes some additional performance loss. However, the use of powerful FEC codes and soft-decision decoding result in acceptable decoded BERs, with a raw channel BER greater than 10^{-2} . The effect of time-varying carrier phase at this BER range ($>10^{-2}$) is negligible. This is particularly true for maritime mobile stations because vehicle motion is relatively small. Hence, quasi-static fade is employed to reduce the time required for the computer simulation. The 5-dB fade margin is selected to restrict the outage probability to less than 0.02 for the Inmarsat channel, with an assumed Ricean ratio of 10 dB for the direct signal power relative to the average power of the diffuse multipath interference.

In order to evaluate cases (b) through (e), certain channel spacing between the signal of interest and the adjacent channel must be assumed. The example of Inmarsat-B [7] was used, which employs a 20-kHz channelization for the transmission of 24-kbit/s coded data. Two types of HPAs are assumed, with amplitude and phase characteristics as shown in Figure 1. The class-A HPA is operated at 2-dB output backoff, while the class-C HPA is operated at saturation.

Since the transmit filter shapes the spectrum of the signal, it has significant impact on the overall performance of the transmission system. The family of



(a) Class-A HPA



(b) Class-C HPA

Figure 1. Amplitude and Phase Characteristics of L-Band HPAs

square-root Nyquist filters was selected for use throughout the computer simulations. With square-root Nyquist filters at both the transmit and receive sides, the overall response is Nyquist, which has no intersymbol interference at detection sampling instants. Since the transmit and receive filters are identical, the pair yields optimal performance in an AWGN channel. Furthermore, the bandwidth of the filtered signal can easily be controlled by the rolloff factor of the filter. Thus, a large number of modulation/filtering/HPA combinations (refer to Table 1) were considered for each condition.

TABLE I. MODULATION/FILTERING/HPA COMBINATIONS USED IN COMPUTER SIMULATIONS

| MODULATION | ROLLOFF FACTOR (%) | HPA TYPE | LEGEND (FIGS. 2-6) |
|------------|--------------------|----------|--------------------|
| QPSK | 40 | A | QA40 |
| QPSK | 60 | A | QA60 |
| QPSK | 40 | C | QC40 |
| QPSK | 60 | C | QC60 |
| O-QPSK | 40 | A | OA40 |
| O-QPSK | 40 | C | OC40 |
| O-QPSK | 50 | C | OC50 |
| O-QPSK | 60 | C | OC60 |

The results of the computer simulations for cases (a) through (e) are shown in Figures 2 through 6, respectively. From Figure 2 it can be seen that the performance of QPSK and O-QPSK for AWGN channels is very close, except for the case of O-QPSK with 40-percent rolloff and class-C HPA, which is noticeably worse than the other cases. This was expected, as the main lobe of O-QPSK is somewhat wider than QPSK, and 40-percent rolloff may be too restrictive for the O-QPSK signal. When the adjacent channels are present, the performance of O-QPSK with 60-percent rolloff and a class-C HPA is still slightly worse than that of QPSK with a class-A HPA. However, since a channel-coded system with efficient soft decoding typically operates at a very low ratio of energy-per-modulation-bit to noise-power-density (E_{mb}/N_o), the performance of all modulation/filtering/HPA combinations under the above operating conditions is practically the same. When a 5-dB up-link fade is applied to the desired channel, QPSK and O-QPSK with a 40-percent rolloff factor behave poorly with the class-C HPA. However, as the rolloff factor is increased to 60 percent for O-QPSK, the BER performance with a class-C HPA approaches that of QPSK with 40-percent rolloff and a class-A HPA.

The five channel cases of Figures 5 and 6 are quite similar to those of the three channels discussed above, indicating that conclusions drawn from cases (b) and (c) will not be significantly affected by additional adjacent channels. QPSK with 60-percent rolloff and a class-C HPA was also simulated with four adjacent channels. It can be seen that while the rolloff factor significantly impacts O-QPSK performance, it has very little influence on QPSK performance using a class-C HPA. This indicates that the amplitude fluctuation of QPSK is the major source of degradation.

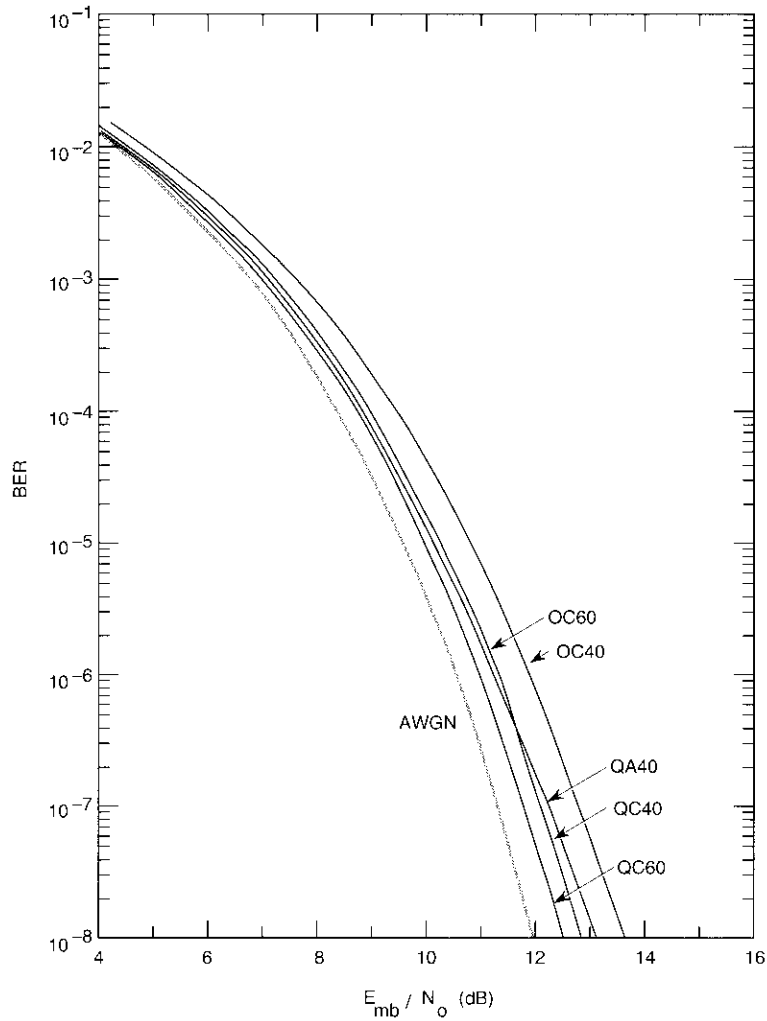


Figure 2. BER Performance for Various Modulation/Filtering/HPA Combinations in the AWGN Channel (Case a)

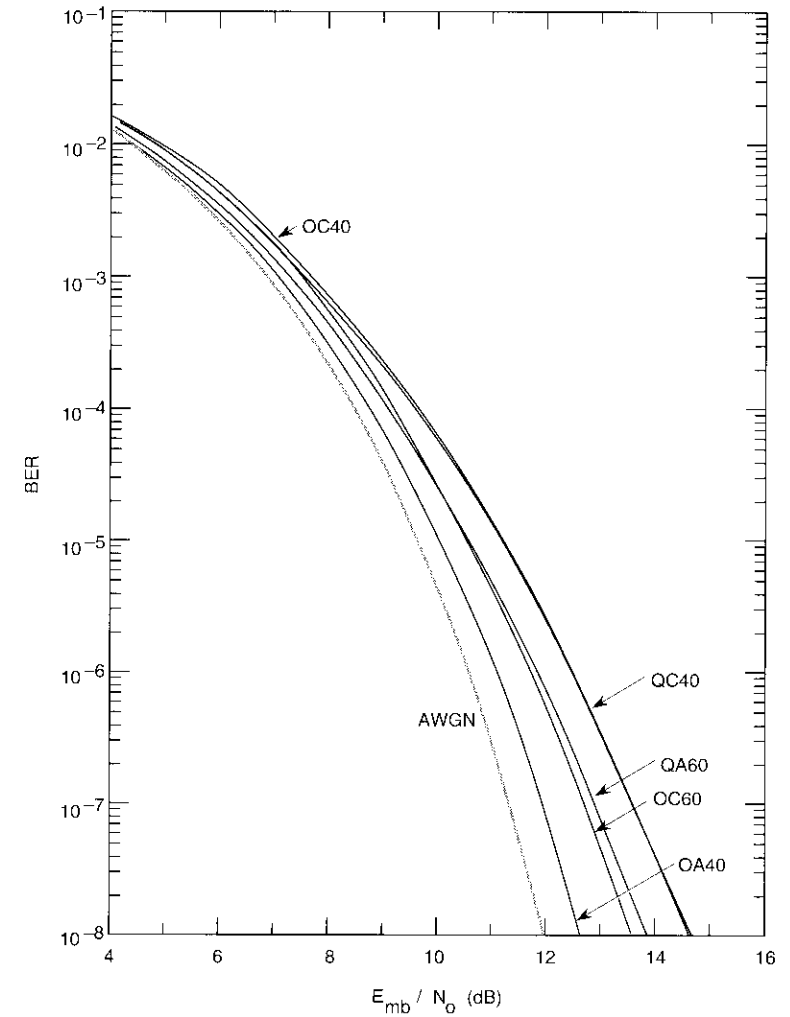


Figure 3. BER Performance of Modulation/Filtering/HPA Combination in the Desired Channel With Adjacent Channels on Both Sides (Case b)

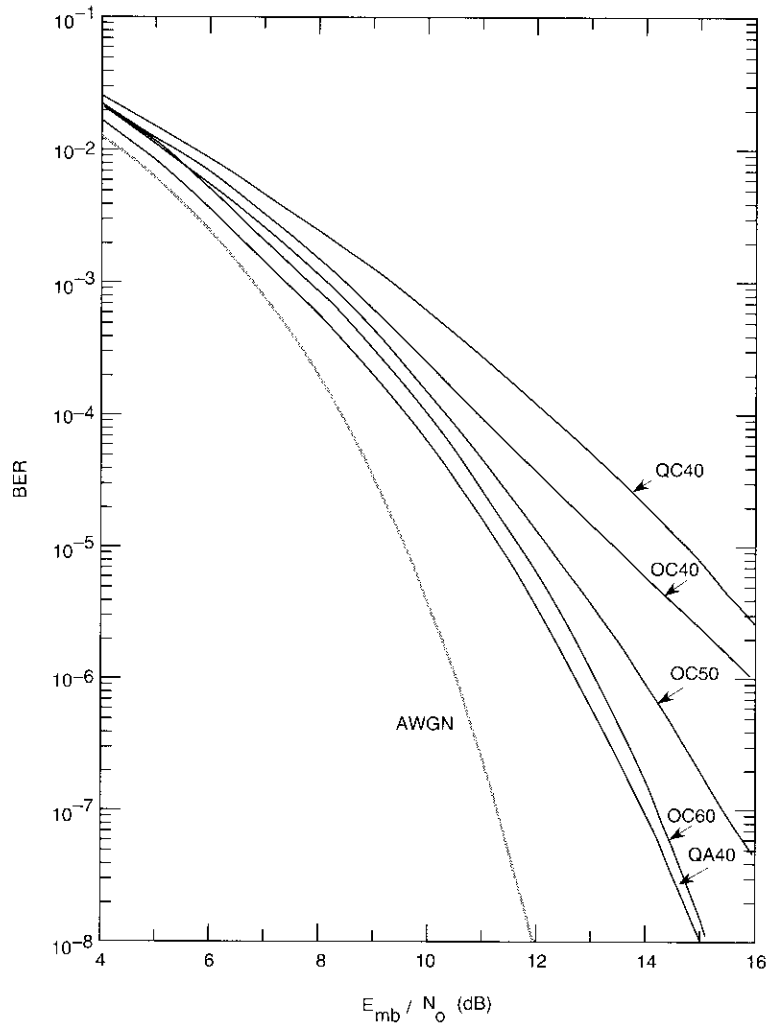


Figure 4. BER Performance of Modulation/Filtering/HPA Combination in the Desired Channel With 5-dB Fading and One Adjacent Channel on Each Side (Case c)

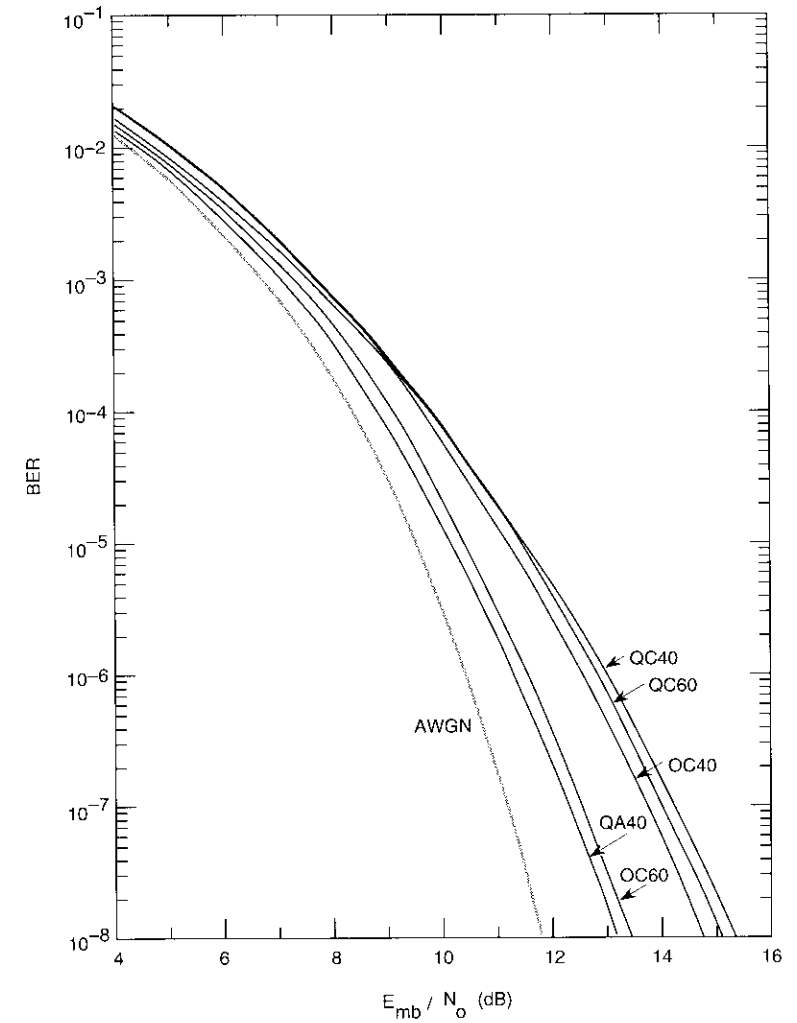


Figure 5. BER Performance of Modulation/Filtering Combination With Class-C HPA and Four Adjacent Channels, Two on Each Side (Case d)

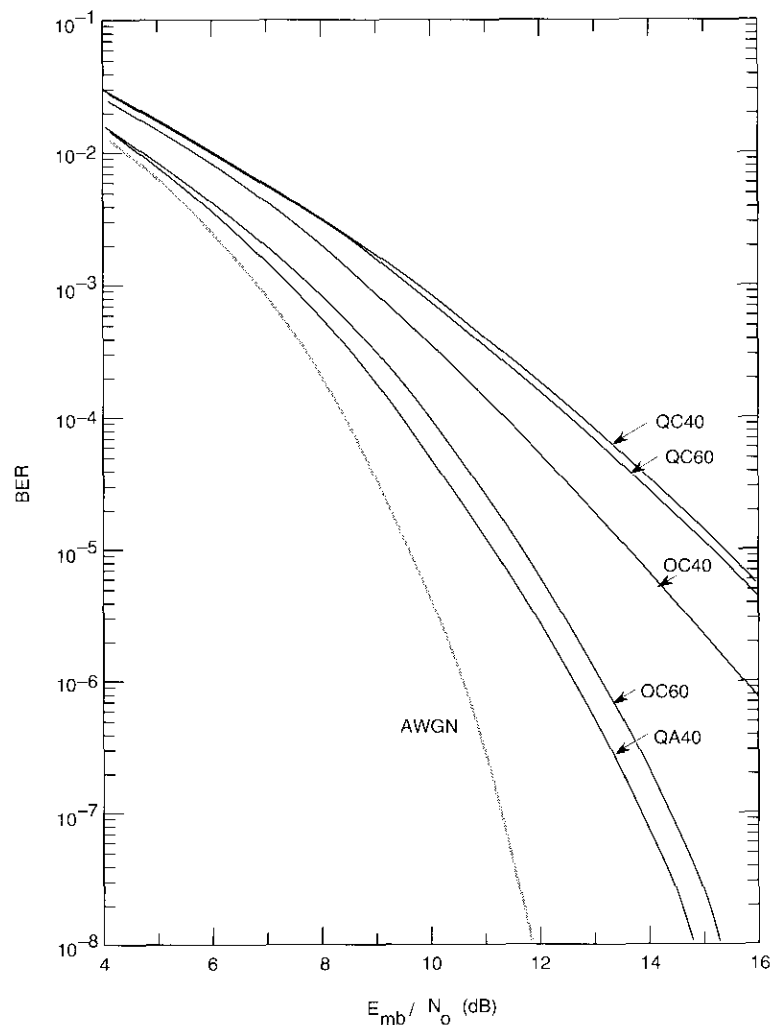


Figure 6. BER Performance of Modulation/Filtering Combinations Using Class-C HPA, With a 5-dB Fade of the Desired Channel and Four Unfaded Adjacent Channels, Two on Each Side (Case e)

Based on the data obtained using the channel model, it was concluded that the performance of O-QPSK with a class-C HPA and 60-percent rolloff is very close to that of QPSK with a class-A HPA and 40-percent rolloff with or without up-link fade. Therefore, use of O-QPSK modulation and a class-C HPA is a viable alternative for mobile applications.

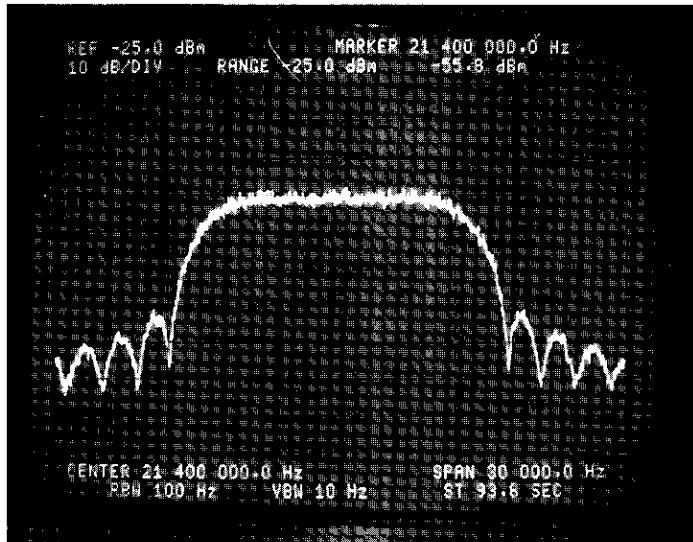
The results are generally consistent with those of Reference 8, in which a TDMA channel for fixed service is modeled by a moderately nonlinear TWTA and a nonlinear HPA with some backoff. Here, the robust performance of O-QPSK in the presence of up-link fade is demonstrated for the case where the HPA is highly nonlinear and the TWTA is almost linear.

Hardware tests

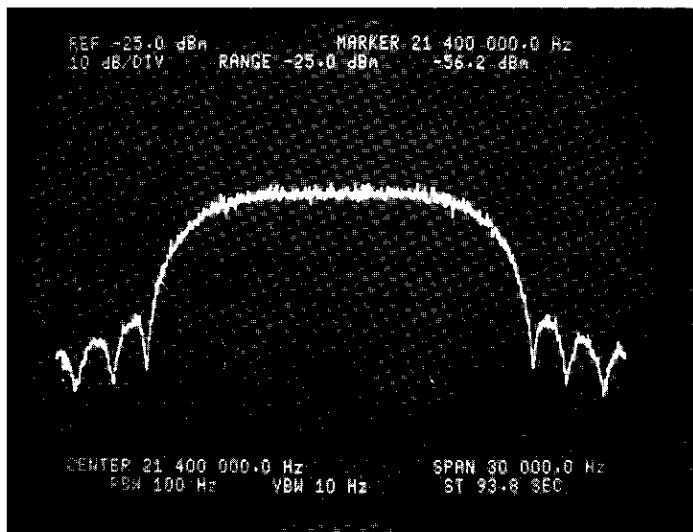
In order to evaluate the performance of QPSK and O-QPSK in a more realistic environment, a programmable modem based on digital signal processors was developed. The modem can be operated in either QPSK or O-QPSK mode. Since square-root Nyquist filters with rolloff factors of 40 to 60 percent typically have an impulse response overlapping about seven symbols, the modulator is implemented with lookup tables that generate the impulse response as a function of these seven symbols. The response is converted to analog form in a low IF equal to 16 times the symbol rate, which is then up-converted to a 21.4-MHz IF for interfacing with the standard test equipment. Two sets of tables are stored, one for 40-percent rolloff and the other for 60-percent rolloff. Figure 7 shows the spectral shapes for the QPSK signal with 40-percent rolloff and the O-QPSK signal with 60-percent rolloff. Digital implementation provides a signal with a highly accurate spectral shape.

The demodulator first down-converts the received signal to a very low IF, equal to the symbol rate. This signal is then sampled at four times the symbol rate. Two Texas Instruments TMS 32020 processors are used to perform the quadrature mixing and matched filtering operations, and two 29-tap finite impulse response (FIR) digital filters are employed to implement the square-root Nyquist filters. Two sets of coefficients (one for 40-percent rolloff factor and the other for 60 percent) are maintained in the firmware, and the appropriate filter can be selected as needed. The carrier and clock recovery loops are implemented in software based on decision feedback algorithms. The bandwidth of both loops can be changed for optimal performance in very noisy channels.

The BER performance of the modem has been measured in an IF loopback configuration with AWGN introduced at 21.4 MHz. For both QPSK and O-QPSK, the performance is indistinguishable from ideal detection theory because of



(a) QPSK With 40% Filtering



(b) O-QPSK With 60% Filtering

Figure 7. Modulated Spectra of QPSK and O-QPSK With Square-Root Nyquist Filtering

the precise implementation of the matched filters. Figure 8 shows the measured performance for O-QPSK modulation. To verify the results from computer simulations, Inmarsat provided two class-C HPAs, and tests were performed in the following configurations:

- Test 1. Single channel L-band loopback with one of the two class-C HPAs operated at saturation.
- Test 2. Adjacent channel added, with a second modulator and with the second class-C HPA at equal output power.
- Test 3. Main channel faded by 5 dB.
- Test 4. Main channel faded by 8 dB.

Test 1 establishes the baseline performance with the class-C amplifier. As shown in Figure 9, a slight degradation of about 0.4 dB (at 10^{-3} BER) from the IF loopback is observed—exactly the same as for the computer simulation. Test 2 is intended to show the effect of ACI under a normal environment. A slight degradation of about 0.4 dB from test 1 is observed, resulting in a total degradation of about 0.8 dB from the ideal AWGN channel. Comparison with Figure 3, which shows a 0.7-dB degradation from the AWGN case, demonstrates that the software and hardware test results are consistent.

Test 3 is intended to evaluate the effect of an up-link fade in the presence of ACI, while test 4 is intended to simulate the effect of two adjacent channels in the presence of an up-link fade of the desired channel. The BERs measured in tests 3 and 4 are virtually the same, both exhibiting an additional loss of about 0.4 dB from that obtained in test 2. (Note that the measured data points for tests 3 and 4 are superimposed on the graph in Figure 9.) The total degradation from the AWGN case is approximately 1.2 dB at 10^{-3} BER, which is also consistent with the 1.1-dB degradation shown in Figure 4 for the computer simulation. Also included in Figure 9 is the BER performance of coded O-QPSK using a rate 3/4 code with soft-decision Viterbi decoding.

Since the results of hardware measurements and computer simulations for O-QPSK agree to within 0.1 dB in the regions of interest, it was unnecessary to test the QPSK modem with the hardware, as the computer simulation results should provide a good indication of its performance.

Conclusions

Computer simulations and hardware tests have shown that O-QPSK with a class-C HPA is a viable alternative to QPSK with a class-A HPA for mobile applications, if filters are properly selected. In the particular example of

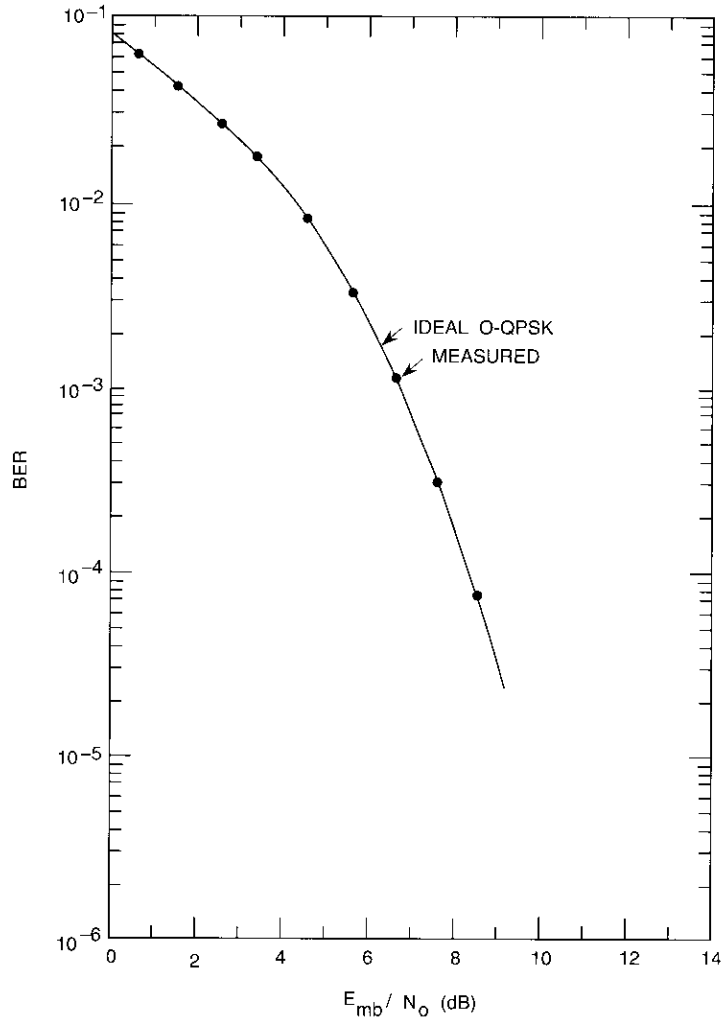


Figure 8. Measured BER Performance for a Modem With Continuous O-QPSK Modulation, 60% Square-Root Nyquist Filtering, and a Linear AWGN Channel

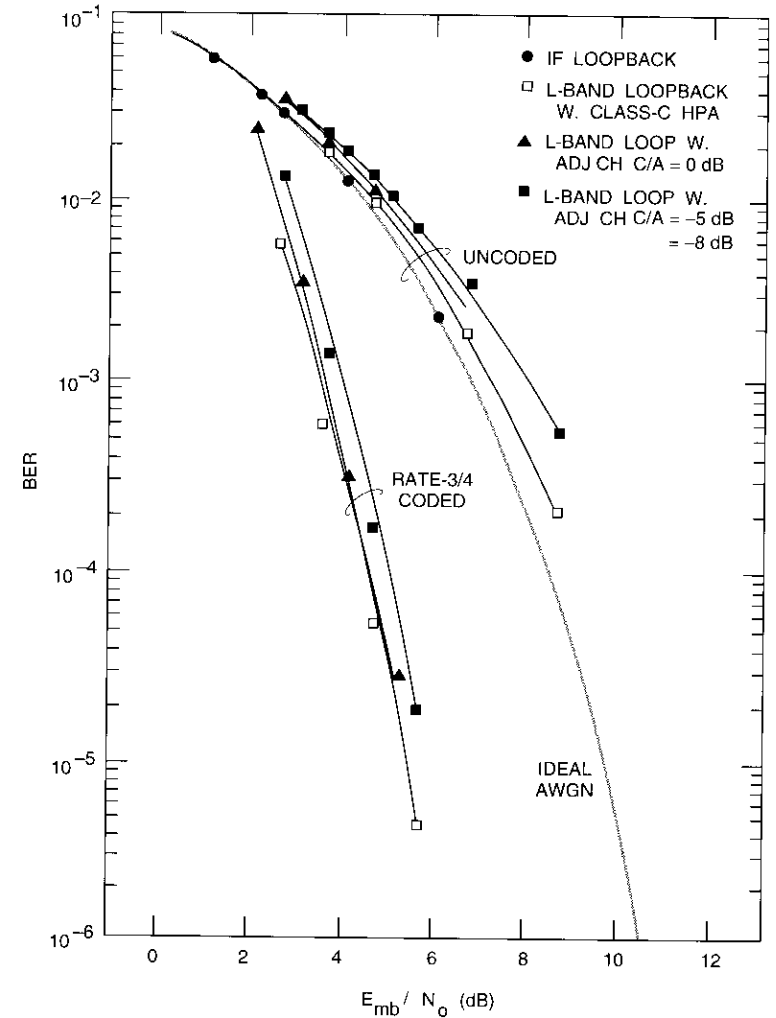


Figure 9. Measured BER Performance for Continuous O-QPSK Modulation in the Standard-B Mode With Class-C HPA and ACI

the Inmarsat-B channel, it appears that a square-root Nyquist filter with 60-percent rolloff factor is appropriate. The results are also applicable to the high-rate voice channel for aeronautical mobile communications, where coded data of 21 kbit/s will be transmitted in a 17.5-kHz SCPC channel. In both cases, the degradation due to use of a class-C HPA rather than a class-A HPA is only about 0.3 to 0.6 dB. This seems to be a good tradeoff for the substantial cost saving which may be obtained by using a class-C HPA.

Generalization of these results to other mobile applications will depend on the bandwidth efficiency of the system. For example, because the 5-kHz channel in the Inmarsat-C system is very wide considering the coded data rate of 1,200 bit/s, efficient filtering is not needed. Since the data rate is very low, the benefits of using a class-C HPA with O-QPSK modulation are probably outweighed by the robust performance of binary PSK in severe phase noise conditions. For the 4.8-kbit/s voice channels for land and aeronautical mobile applications currently under development, the allowable coded data rate and frequency uncertainty are still to be determined. However, since some frequency guard band must be allocated for the 5-kHz channel, these channels will appear to be very bandwidth-limited. A rolloff factor of less than 60 percent may be applicable for O-QPSK, and further studies are therefore required.

Acknowledgments

The authors wish to express their sincere appreciation to their colleagues P. Chang (who conducted the computer simulation) and M. Eng (who implemented the programmable modems used to obtain the above results). Appreciation is also due to D. V. Ramana of Inmarsat, who provided the two class-C amplifiers used during the hardware tests and participated in some of the measurements.

References

- [1] D. W. Lipke *et al.*, "MARISAT—A Maritime Satellite Communications System," *COMSAT Technical Review*, Vol. 7, No. 2, Fall 1977, pp. 351–391.
- [2] F. F. Tzeng, "Multipulse Excitation Codebook Design and Fast Search Methods for CELP Speech Coding," IEEE Global Telecommunications Conference, Hollywood, Florida, November 1988, *Conf. Rec.*, Vol. 1, pp. 18.6.1–18.6.5.
- [3] T. E. Tremain and J. S. Collura, "A Comparison of Five 16 Kbps Voice Coding Algorithms," IEEE International Conference on Acoustics, Speech and Signal Processing, New York, N.Y., April 1988, *Proc.*, pp. 695–698.

- [4] A. J. Viterbi, "Convolutional Codes and Their Performance in Communication Systems," *IEEE Transactions on Communications Technology*, Vol. COM-19, No. 5, October 1971, pp. 751–772.
- [5] B. I. Edelson and A. M. Werth, "SPADE System Progress and Application," *COMSAT Technical Review*, Vol. 2, No. 1, Spring 1972, pp. 221–242.
- [6] S. A. Rhodes, "Effects of Hardlimiting of Bandlimited Transmissions With Conventional and Offset QPSK Modulation," IEEE National Telecommunications Conference, Houston, Texas, December 1972, *Conf. Rec.*, pp. 20F-1–20F-7.
- [7] *Inmarsat Standard-B System Definition Manual*, Inmarsat, 40 Melton Street, London, NW1 2EQ England.
- [8] R. J. F. Fang, "Quaternary Transmission Over Satellite Channels With Cascaded Nonlinear Elements and Adjacent Channel Interference," *IEEE Transactions on Communications*, Vol. COM-29, No. 5, May 1981, pp. 567–581.

Diseño de transmisión de los INTELSAT VI y modelos computadorizados de sistemas para los servicios FDMA

M. P. BROWN, JR., R. W. DUESING, L. N. NGUYEN, W. A. SANDRIN
Y J. A. TEHRANI

Abstracto

INTELSAT utiliza modelos computadorizados de sistemas de transmisión para operar casi 10.000 portadoras de comunicaciones. Se describe cómo se prepararon estos modelos para usarlos con los satélites INTELSAT VI y asegurar la calidad de transmisión necesaria para una variedad de servicios con acceso múltiple por distribución de frecuencia (FDMA), a la par que se maximiza la capacidad de canales de los transpondedores. Se explican a grandes rasgos los objetivos de modelado para los INTELSAT VI, incluida la planificación de frecuencias, los cómputos de referencia del enlace, la interferencia cocanal, la transición del INTELSAT V (reutilización cuádruple de frecuencias) al INTELSAT VI (reutilización séxtuple de frecuencias), y la optimización de la capacidad de canales de los transpondedores. También se discuten los modelos de sistemas STRIP6 y OUTMAT6, con sus bases de datos conexas, así como la operación analógica y digital combinadas, rutinas para la optimización parcial de transpondedores (alquileres), el método empleado para cursar cientos de portadoras digitales de poca capacidad por un solo transpondedor de 72-MHz, y la generación de diagramas de cobertura de antenas partiendo de bases de datos medidos del INTELSAT VI.

Papers Scheduled for Publication in the CTR INTELSAT VI Series

COMSAT TECHNICAL REVIEW

Volume 20 Number 2, Fall 1990 (this issue)

FOREWORD

J. D. Hampton AND I. Goldstein

EDITORIAL NOTE

S. B. Bennett AND G. Hyde

INTELSAT VI: The Communications System

THE PROCESS FOR SUCCESS—INTELSAT VI

E. I. Podraczky AND W. R. Schnicke

INTELSAT VI SYSTEM PLANNING

L. B. Perillan, W. R. Schnicke AND E. A. Faine

INTELSAT VI COMMUNICATIONS PAYLOAD PERFORMANCE SPECIFICATIONS

B. A. Pontano, A. I. Zaghloul AND C. E. Mable

SPECIFYING THE SPACECRAFT BUS

G. P. Cantarella AND G. Porcelli

SS-TDMA SYSTEM CONSIDERATIONS

**S. J. Campanella, G-P. Forcina, B. A. Pontano AND
J. L. Dicks**

INTELSAT VI TRANSMISSION DESIGN AND ASSOCIATED COMPUTER SYSTEM MODELS FOR FDMA SERVICES

**M. P. Brown, Jr., R. W. Duesing, L. N. Nguyen,
W. A. Sandrin AND J. A. Tehrani**

COMSAT TECHNICAL REVIEW

Volume 21 Number 1, Spring 1991

EDITORIAL NOTE

S. B. Bennett AND **G. Hyde***INTELSAT VI: Spacecraft Design*

INTELSAT VI SPACECRAFT BUS DESIGN

L. R. Dest, **J-P. Bouchez**, **A. F. Dunnet**, **V. R. Serafini**,
M. Schavietello AND **K. J. Volkert**ATTITUDE AND PAYLOAD CONTROL SYSTEM FOR THE INTELSAT VI
COMMUNICATIONS SATELLITE**L. I. Slafer** AND **V. L. Seidenstucker**

INTELSAT VI COMMUNICATIONS SUBSYSTEM DESIGN

G. Horvai, **L. Argyle**, **T. Ellena**, **R. R. Persinger** AND
C. E. Mable

THE INTELSAT VI ANTENNA SYSTEM

R. R. Persinger, **S. O. Lane**, **M. F. Caulfield** AND
A. I. Zaghoul

SS-TDMA ON-BOARD SUBSYSTEM DESIGN

R. K. Gupta, **J. N. Narayanan**, **A. M. Nakamura**, **F. T. Assal**
AND **B. Gibson**

COMSAT TECHNICAL REVIEW

Volume 21 Number 2, Fall 1991

FOREWORD: MAKING A REALITY OUT OF A VISION

P. Madon

EDITORIAL NOTE

S. B. Bennett AND **G. Hyde***INTELSAT VI: From Spacecraft to Satellite Operation*

ENSURING A RELIABLE SATELLITE

C. Johnson, **R. R. Persinger**, **J. Lemon** AND **K. J. Volkert**INTELSAT VI LAUNCH OPERATIONS, DEPLOYMENT, AND BUS
IN-ORBIT TESTING**L. Virdee**, **T. L. Edwards**, **A. Corio** AND **T. Rush**

IN-ORBIT RF TEST OF AN INTELSAT VI SPACECRAFT

G. Rosell, **B. Teixeira**, **A. Olimpiew**, **B. A. Pettersson** AND
S. Sanders

TT&C EARTH STATION OPERATIONS

R. J. Skroban AND **D. J. Belanger**

INTELSAT COMMUNICATIONS OPERATIONS

M. Wheeler

INTELSAT SATELLITE OPERATIONS

G. Smith

COMSAT TECHNICAL REVIEW

Volume 22 Number 1, Spring 1992

EDITORIAL NOTE

S. B. Bennett AND **G. Hyde***INTELSAT VI: System and Applications*

EARTH STATION CONSIDERATIONS FOR INTELSAT VI

M. P. Brown, Jr., **F. A. S. Loureiro** AND **M. Stojkovic**

DCME IN THE INTELSAT VI ERA

M. Onufry, **G-P. Forcina**, **W. S. Oei**, **T. Oishi**, **J. F. Phiel**
AND **J. H. Rieser**

VIDEO TRANSMISSION AND PROCESSING IN THE INTELSAT VI ERA

L-N. Lee AND **A. K. Sinha**

MODULATION AND CODING TECHNIQUES IN THE INTELSAT VI ERA

L-N. Lee AND **G. Hyde**

COMSAT TECHNICAL REVIEW

Volume 22 Number 2, Fall 1992

EDITORIAL NOTE

S. B. Bennett, **G. Hyde** AND **J. A. Lunsford***SS-TDMA in the INTELSAT VI System*

SS-TDMA SYSTEM DESIGN

J. A. Lunsford, **J. F. Phiel**, **R. Bedford** AND **S. Tamboli**

GENERATION OF BURST TIME PLANS FOR THE INTELSAT VI

SS-TDMA SYSTEM

T. Mizuike, **L. N. Nguyen**, **K. P. Chaudhry**, **J. A. Lunsford**
AND **P. A. Trusty**

INTELSAT SS-TDMA HEADQUARTERS SUBSYSTEM

F. H. Luz, **D. Sinkfield** AND **N. Engelberg**THE SATELLITE CONTROL CENTER AND ITS ROLE IN THE TESTING
AND OPERATION OF THE INTELSAT VI SS-TDMA PAYLOAD**B. A. Pettersson**, **A. K. C. Kwan**, **S. Sanders**, **L. Khoo**,
AND **T. Duffy**

DESIGN OF THE SS-TDMA NETWORK DIAGNOSTIC SYSTEM

S. Tamboli, **X. Zhu**, **K. N. Wilkins** AND **R. K. Gupta**

TIMING SOURCE OSCILLATOR CONTROL

C. L. Maranon, **J. A. Lunsford**, **T. Inukai**, **F. H. Luz** AND
S. J. Campanella

SS-TDMA REFERENCE TERMINAL

R. Bedford, **A. Berntzen**, **J. A. Lunsford**, **Y. Ishi**,
T. Nakamura AND **T. Khimura**DEPLOYMENT, TEST, AND TRANSITION TO OPERATION OF THE
INTELSAT SS-TDMA SYSTEM**C. Kullman**, **S. J. Smith**, **R. Bedford**, **J. A. Lunsford**,
P. Nethersole, **G. Burns**, **P. Roach** AND **K. P. Chaudhry**